Mechanisms Underlying Postnatal Development of Primary Somatosensory Cortex

Thesis submitted for the degree of Doctor of Philosophy

Mark James Philip Hillen
University of Edinburgh
2006

Declaration

I, Mark James Philip Hillen, candidate for a PhD in Neuroscience, declare that this thesis has been composed solely by myself, that the work herein described is my own, except for Figure 4.14 where sectioning was carried out by Anne Ellwood half of the Nissl staining, and Figure 4.15 where mGluR5 and α-5-HTT immunochemistry were performed by Lasani Wijetunge, and that this work has not been submitted for any other degree or professional qualification.

Mark J.P. Hillen, BSc (Hons).

Acknowledgements

I'd like to thank everyone in "Team Kind" for the moral support and helping me in my quest to drink as much coffee as is possible. Specifically, Mark Barnett, Ruth Watson and Patrick Stoney for their input over the years, and the newbies to the lab, Anne "Jake" Ellwood, Lasani "Lasagne" Wijetunge and Sally "Sally" Till for brightening the place up and bringing some youthful exuberance and enthusiasm to the lab. I bet it won't last. I'd like to thank the boss, Pete, for his support and encouragement over the years. I don't think I'll ever have a boss that is as relaxed and cool as he is ever again. My second supervisor, John West, I'd like to thank for his time and effort in training me in making mouse chimeras (although, because of genotyping issues, none of that is in the thesis—and the same goes for Phil Larkman and electrophysiology, which worked, but we lost use of the rig!).

A big thanks to those in the MBG that helped me drink coffee—Steve MacDonald (to whom I also owe him thanks for helping me achieve my karate black belt), Karen Smillie, Angela MacDonald, Gareth Evans and all the rest. I'd like to thank Mark Bryars, who is a genius with PHP and regexon, and without whose help I'd have a broken database and no hair left, as I'd have pulled it all out in despair.

I'd like to thank the Wellcome Trust for funding my PhD, and members of DBUG for inviting me over for cake when it was someone's birthday over the years, but most of all, John Mason for all of those handy tips in performing all of those mystical molecular biology techniques and for being the engine of Wnt discussion; Dennis McCaffery for being a fellow *Wnt in-situ* prisoner, and Tom Pratt and Katie Gillies for making DBUG run smoothly.

Most of all, I'd like to thank my girlfriend, Lucy for providing easy distraction from the stress of writing up, and motivation to carry on and get it finished.

Abbreviations

°C	Degrees Celsius
µg	Microgram
µM	Micromolar
5-HT	5-hydroxytryptamine
5-HTT	5-hydroxytryptamine transporter
AC	Adenylyl cyclase
AMPA	alpha-amino-3-hydroxy-5-methyl-4-isoxazolepropionic acid
ANOVA	Analysis of variance
APC	Adenomatous polyposis coli protein
ATP	Adenosine triphosphate
BF	Bright field
Bp	Base pairs
BSTC	Brainstem trigeminal complex
CaMKII	Calcium/Calmodulin-dependent kinase II
cAMP	Cyclic adenosine monophosphate
Cdh	Cadherin
cDNA	Complimentary deoxyribonucleic acid
CKI	Casein kinase I
CNS	Central nervous system
DAG	Diacylglycerol
DIC	Diffuse interference contrast
Dkk	Dickkopf
DNA	Deoxyribonucleic acid
dNTP	Deoxynucleoside triphosphates
Dvl	Dishevelled
E	Embryonic day
EGL	External granular layer
ER	Endoplasmic reticulum
ERK	Extracellular signal-related kinase
Fz	Frizzled
G	Gram

g	Gravitational force
GAPDH	Glyceraldehyde-3-phosphate dehydrogenase
GC	Granule cell
GR	Glomerular rosette
GSK	Glycogen synthase kinase
IGL	Internal granular layer
ION	Infra-orbital Nerve
IP_3	Inositol 1,4,5-triphosphate
ISH	In-situ hybridisation
JNK	c-Jun N-terminal kinase
LB	Luria Broth
LGIC	Ligand gated ion channel
LRP	Low-density lipoprotein receptor
LTD	Long term depression
LTP	Long term potentiation
M	Molar
mA	Milliamperes
MAGUK	Membrane-associated guanylate kinase
MAO	Monoamine oxidase
MF	Mossy fibre
Mg	Milligram
mGluR	Metabotropic glutamate receptor
ML	Molecular layer
ml	Millilitre
mM	Millimolar
MMLV	Moloney murine leukaemia virus
Mol.	Mole
mRNA	Messenger ribonucleic acid
NBT/BCIP	nitro blue tetrazolium and 5-bromo-4-chloro-3-indolyl phosphate
NMDA	N-methyl-D-aspartate
NMDAR	N-methyl-D-aspartate receptor
nNOS	Neuronal nitric oxide synthase
NR	N-methyl-D-aspartate receptor subunit
NRC	NMDA-receptor complex
nVc	Nucleus caudalis

nVi	Nucleus interpolaris
nVo	Nucleus oralis
nVp	Nucleus principalis
P	Postnatal day
PBS	Phosphate buffered saline
PCL	Purkinje cell layer
PCP	Planar cell polarity
PCPA	Parachlorophenylalanine
PCR	Polymerase chain reaction
PFA	Paraformaldehyde
PIP2	Phosphatidyl inositol 4,5-bisphosphate
PKA	Protein kinase A
PKC	Protein kinase C
PLC	Phospholipase C
PMBSF	Posteromedial barrel subfield
PP	Protein phosphatase
PrV	Principal trigeminal nucleus
PSD	Postsynaptic density
RNA	Ribonucleic acid
rpm	Revolutions per minute
RT-PCR	Reverse transcriptase polymerase chain reaction
RYK	Receptor-like tyrosine kinase
S1	Primary somatosensory
SERT	Serotonin Transporter
sFRP	Secreted frizzled related protein
TCA	Thalamocortical axons
TCF	T-cell specific transcription factor
TG	Trigeminal ganglion
V	Volts
VMAT	Vesicular Monoamine Transporter
VpM	Ventral posterior medial
WIF	Wnt inhibitory factor
Wnt	Wingless-type mouse mammary tumour virus integration site family

Abstract of thesis

Layer IV of the mouse somatosensory cortex contains discrete cytoarchitectonic units called 'barrels', formed in response to thalamocortical axon invasion by two processes: translocation of cortical cells to form a cell-dense barrel wall and cell-sparse barrel hollow, and selective dendritic elaboration toward thalamocortical afferents to form oriented dendritic branch patterns. Interestingly gene knockout of several members of the N-Methyl-D-Aspartate (NMDA) receptor -complex (NRC) disrupts barrel formation, indicating that synaptic activity is critical for barrel formation. Little is known of the cellular processes initiated by glutamate receptor activation; however, recent evidence suggests an interaction between neuronal activity and Wnt signalling. Wnts are secreted glycoproteins, are powerful regulators of cell proliferation and differentiation, and their signalling pathway involves proteins that directly participate in both gene transcription and cell adhesion. Wnt7a and Dvl1 knockout mice exhibit delays in glomerular rosette formation; a cerebellar structure similar to barrels whose development involves granule cell migration and dendritic rearrangement. Furthermore activity dependent Wnt release can regulate the enhancement of dendrite arborisation, raising the possibility that NRC components and Wnts may interact to regulate barrel development.

Recent findings suggest that membrane association guanylyl kinases (MAGUKs) may be the key scaffolding molecules that mediate the interaction between glutamate receptor and Wnt signalling pathways. The MAGUK family includes Postsynaptic Density (PSD)-95 and Synapse Associated Protein (SAP)-102, two key molecules of the NRC during barrel formation. These MAGUKs also bind the Wnt receptor family Frizzled and SAP-102 binds to APC, a key Frizzled-signalling protein. As a first step in examining a role for Wnts in barrel formation, the gene expression patterns of members of the Wnt, Frizzleds and secreted Frizzled related protein (sFRPs) families during barrel cortex development were measured using degenerate primer RT-PCR, quantitative real-time PCR and in-situ hybridization. *Wnts*

2b, 3, 4, 5a, 7a, 7b, 9a, 11, 16 were found in the barrel cortex, suggesting that these members of the Wnt family may play a role in barrel development, and *Wnt7b, Frizzled 4, Frizzled 9,* and *Frizzled 3* were conspicuously downregulated in mutant mice that lack barrels, namely *Plc-β1*$^{-/-}$, *Pkar2β*$^{-/-}$ and *Mglur5*$^{-/-}$ mice.

In order to determine whether Wnts, members of the Wnt signaling machinery and MAGUKs associated with Wnt signaling are essential for barrel formation, the barrel phenotype of all available postnatally viable Wnt gene knockouts, *Wnt2b*$^{-/-}$, *Wnt7a*$^{-/-}$, *Wnt8b*$^{-/-}$, Wnt signaling component knockouts *Dvl*$^{-/-}$, MAGUK knockouts *Sap-102*$^{-/-}$, *Psd-95*$^{-/-}$ and double knockouts of *Wnt7a*$^{-/-}$*Dvl*$^{-/-}$ and of *Sap-102*$^{-/-}$*Psd-95*$^{+/-}$ were examined. Barrels appeared normal in all mutants, apart from compound *Sap-102*$^{+/-}$*Psd-95*$^{+/-}$ and *Sap-102*$^{-/-}$*Psd-95*$^{+/-}$ mice, which exhibited poorer barrel segregation compared to wild type.

In order to achieve a detailed understanding of the mechanisms by which neuronal activity regulates barrel development, we need a detailed understanding of the intracellular pathways activated by NMDA receptors during development. In searching the literature, data concerning the developmental expression patterns of NRC components can be difficult to locate, as the prevailing database tools used either search only title, author and keyword abstract text (NCBI PubMed) potentially missing desired information, or as in the unique case of Google Scholar, search the full text of electronically published papers, but yield overwhelming numbers of results in the process.

The Jackson Laboratories MGI suite offers an impressive way of mining the literature for such data, but the content is sparse, relying on author submission and attempting to map expression throughout the whole mouse. For example, the only gene present in MGI for postnatal layer IV cerebral cortex is *Apc2*.

In order to bring together the data in the literature and from the mouse genome projects into a usable and accessible way, we decided to create a web-based centralised resource for the developmental neuroscience community, containing expression profiles of NRC components

within mouse somatosensory cortex. By performing exhaustive literature searches utilising Google Scholar and PubMed, and linking to sequence and mutant mouse availability information elsewhere, BGI offers a portal for such information and also offers a forum for the notification of unpublished observations of transgenic animals displaying normal barrel formation, preventing duplication of experiments. Barrelgene.info should provide a key resource for any researcher interested in the molecular basis of cortical development.

Table of Contents

1 Introduction

1.1 Society's need for developmental neurobiology research.

With the demographics of an aging population, the incidence and social impact of neurodegenerative disorders is immense: in the case of Alzheimer's disease, 5% of 65 year olds rising to 95% of 90 year olds are afflicted (Brookmeyer et al., 1998). The chronic and highly debilitating illness schizophrenia affects about 1% of the population (Jablensky, 1997) and often begins in childhood. The closure of long-stay mental hospitals in Britain and the introduction of "care in the community" programmes now accounts for many of society's outcasts (Andrews and Phillips, 2000). Injury leading to neural trauma is almost always permanent, debilitating and distressing. Childhood learning disabilities can be immensely stressful to all involved in caring for the child, yet no truly effective treatment is available for any of these disorders or disabilities.

In order to develop effective therapies the problem must be approached from two sides:

1. Understanding the basic pathologies involved in the disease.
2. Understanding the processes involved in generating the normal neurophysiology, including growth, development and plasticity, enabling the development of new and improved treatments for diseased or injured neural tissue.

Much is known about the basic pathologies, and recent technical and conceptual advances now permit in-depth investigation of the development and plasticity of the brain.

Study of the molecular mechanisms underlying developmental plasticity gives insight into the mechanisms implicated in neural growth, damage, and disease— either with a neurodevelopmental component, like schizophrenia (Harrison, 1997; Murray et al., 2004; Eastwood, 2004; Arnold et al., 2005) or environmental, where the disease state comes from exposure to hazardous chemicals or infection, such as herpes simplex encephalitis (Schlitt et al., 1985; Howard, 1996). This research has strong potential to yield medical treatments in the long term.

1.1.1 The Cerebral Cortex, a paradigm for the examination of neural development and plasticity.

In 1909 Korbinian Brodmann published the classic neurological textbook "*Vergleichende Lokalisationslehre der Grosshirnrinde in ihren Prinzipien dargestellt auf Grund des Zellenbaues*" (Study of comparative localisations of the cerebral cortex shown in its principles based on cellular structure). Brodmann defined the primate cerebral cortex as containing 52 distinct regions from their cytoarchitectonic characteristics (Figure 1.1), and proposed that each cortical (now referred to as Brodmann) area served a unique and specific set of functions. Subsequent research has validated and advanced his results; for example, the function of Brodmann areas 1, 2 and 3 in the postcentral gyrus of the parietal lobe concern the somatosensory region, and areas 17 and 18 in the occipital lobe represent the primary visual areas. Furthermore, advances in histological techniques, microscopy and the development of new methods of imaging the brain, such as magnetic resonance imaging (MRI), have enabled in-depth characterisation of these areas of the cortex. For example, sensory and motor areas of the cortex were mapped to distinct areas in the brain using electrical stimulation during neurosurgery (Penfield and Boldrey, 1937; Penfield and Rasmussen, 1950), work recently reconfirmed by Magnetoencephalography and MRI studies (Rothemund et al., 2005). The adult cerebral cortex develops from a small swelling of cells at the rostral end of the embryonic neural tube, yet eventually becomes an immensely complex and intricately connected organ, with many functionally distinct regions. The development of these characteristics has been the focus of intense investigation for over a century.

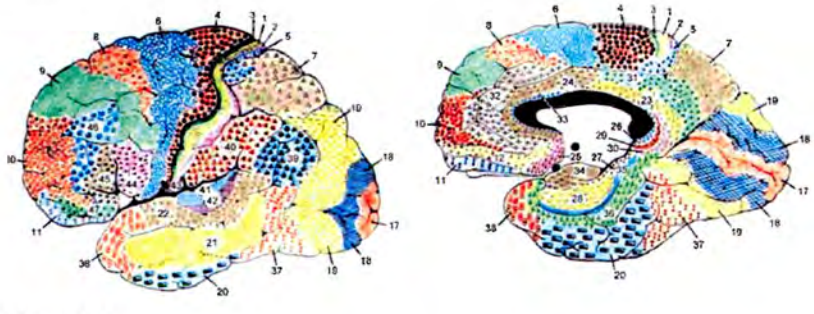

Figure 1.1
Areas of the neocortex as defined by their cytoarchitecture. Korbinian Brodmann defined the primate cerebral cortex into 52 different regions based on the histology of each area. Diagram adapted from Spires (2003), which is a colourised version of a translation of Brodmann's work published in Garey (1994).

1.1.2 Development of the Cerebral Cortex and Cortical Lamination

The mammalian cerebral cortex is composed of six layers that in primary sensory cortices are distinguishable by variation of cell density and cell type (Figure 1.2). Within the cortex, discrete regions exist that are defined by the origin of their afferent axons and by the same token, their function. In rodents, the vast majority of cortical afferents originate in the thalamus (Caviness, 1988). In the somatosensory system, all sensory organs send their information to the cortex via at least one thalamic nucleus specific to that system, except the olfactory system, which can also project directly to the cortex (Krettek and Price, 1977a; Krettek and Price, 1977b). Each thalamic nucleus receives well-defined reciprocal connections with specific cortical areas and there is a precise isomorphic correspondence between the topography of the thalamic nuclei and the organisation of cortical areas (Caviness, 1988; Molnár et al., 1998) and reviewed in López-Bendito and Molnàr, 2003). This topography is most apparent in the whisker-barrel pathway (section 1.4.1, below).

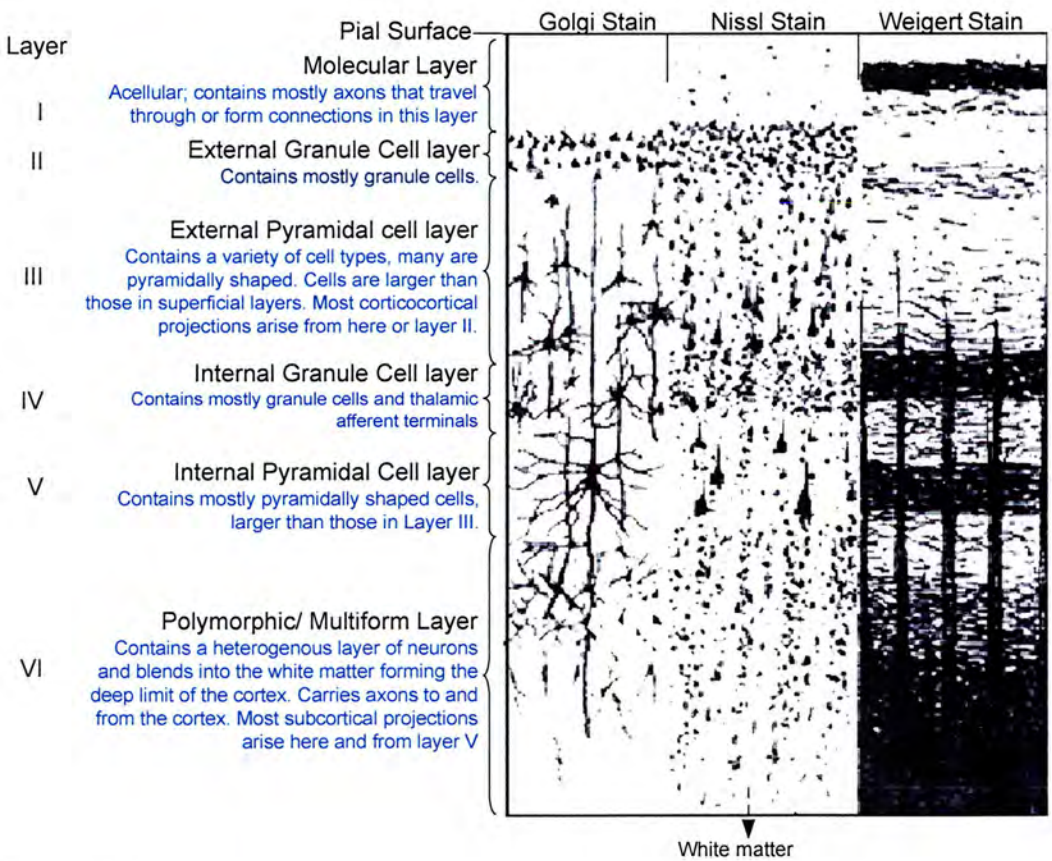

Figure 1.2
The neurons of the Cerebral Cortex are arranged in distinctive layers, distinguishable by variations in cell density and cell type. The appearance of the cortex depends on the compound used to stain it. Golgi stain reveals neuronal cell bodies and dendritic trees; Nissl method shows cell bodies and proximal dendrites; a Weigert stain for myelinated fibres reveals the pattern of axonal distribution. Cell types and neuronal projections to different brain regions (including other regions of the neocortex) are outlined in blue text. Figure adapted from Heimer (1994) and Kandel et al., (2000

1.2 Mechanisms of Corticogenesis

The formation of the neocortex has been described in detail by Price and Willshaw (2000) and the lineage of its formation is illustrated in Figure 1.3. Cells destined to become the cerebral cortex originate at neurulation, where an inductive signal causes ectodermal cells to thicken, forming the neural plate. The neural plate then folds forming the neural tube, which will give rise to the entire Central Nervous System (CNS). The rostral end of the neural tube balloons, forming three primary vesicles: forebrain (prosencephalon), midbrain (mesencephalon) and hindbrain (rhombencephalon). The rostral end of the prosencephalon enlarges and divides, generating the anterior telencephalon and the more caudal diencephalon. The diencephalon will form the thalamic and hypothalamic brain regions and the epithelial lining of the telencephalon will eventually form the cerebral cortex, hippocampus, basal ganglia, basal forebrain nuclei, and olfactory bulbs. The most dorsal part of telencephalon forms the neocortex (Bayer and Altman, 1991; Price and Willshaw, 2000).

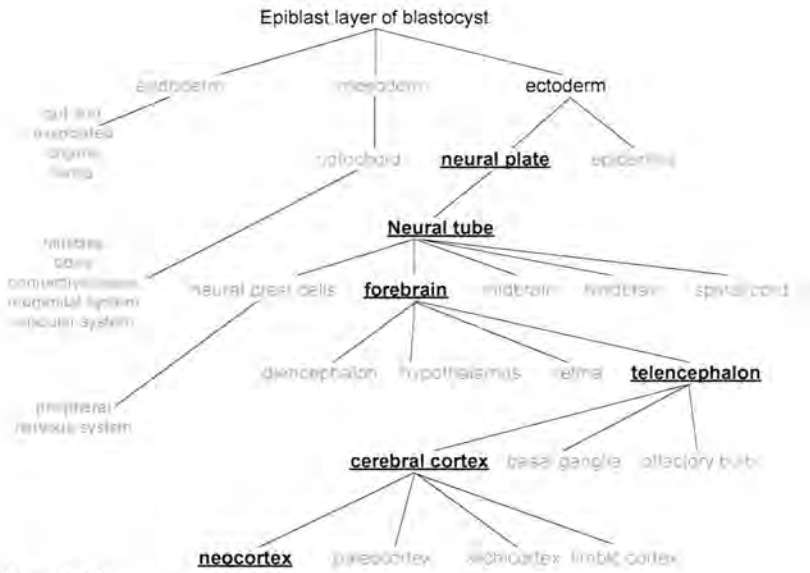

Figure 1.3
Lineage diagram showing the development of the neocortex from the blastocyst.
Each stage in the development of the epiblast layer of the blastocyst into the neocortex is represented as underlined black text, whilst other structures that arise are depicted as grey text. Adapted from Price and Willshaw (2000); see text for details.

At embryonic day 12 (E12) in rat, the cortex is divided into an inner layer of rapidly proliferating cells termed the ventricular zone, and an outer layer of cells called the preplate (or primordial plexiform layer). Preplate neurons play an important role in neurogenesis; they are the first to express many different types of neurotransmitter receptors (Chun and

Shatz, 1989) and the first to send axons out of the cortex. Cells from the ventricular zone accumulate between the ventricular zone and preplate. This accumulation of cells splits the preplate— the outer layer is termed the medial zone and the new layer, which is called the subplate, exists only transiently and is removed by programmed cell death early in postnatal life after thalamocortical innervation (Allendoerfer and Shatz, 1994). At approximately E15, cells migrating from the ventricular zone split the medial zone and subplate, forming the cortical plate which in turn forms layers VI and V. Subsequent cells arriving from the ventricular zone form the remaining layers IV, III, II in that order, and the medial zone cells form layer I. These cells arrive at their final destination by climbing radial glial cells, which are expressed transiently during cortical development (Rakic, 1972) and have processes that span from the ventricular zone along the full thickness of the cortex, providing a scaffold for migrating neurons (Rakic, 1974; Lund and Mustari, 1977; Rakic and Nowakowski, 1981; Gillies and Price, 1993, Figure 1.4 and Figure 1.5).

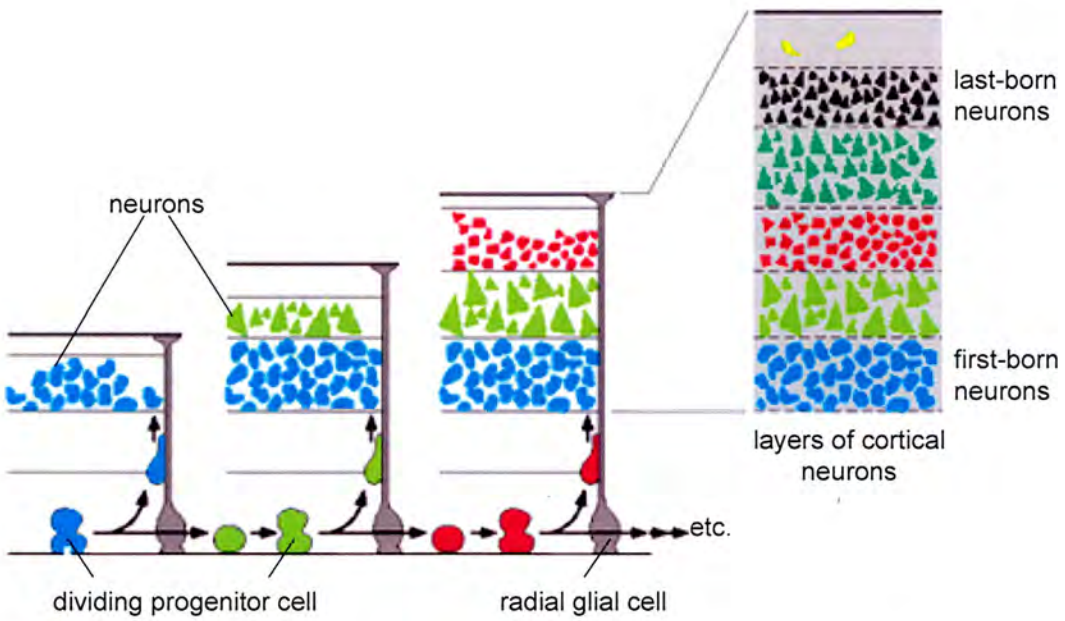

Figure 1.4
Inside-out production of the cerebral cortex. **Different types of neurons are programmed to be made at different times by dividing progenitor cells. Close to one face of the cortical neuroepithelium, neuronal progenitor cells divide repeatedly, in stem-cell like fashion, producing neurons. The neurons migrate out towards the opposite face of the epithelium by crawling along the surfaces of radial glial cells. The first-born neurons settle closest to their birthplace, while later-born neurons crawl past them to settle further out. Successive generations of neurons thus occupy different layers in the cortex and have different intrinsic characters according to their birth dates. Based on Alberts et al. (2002).**

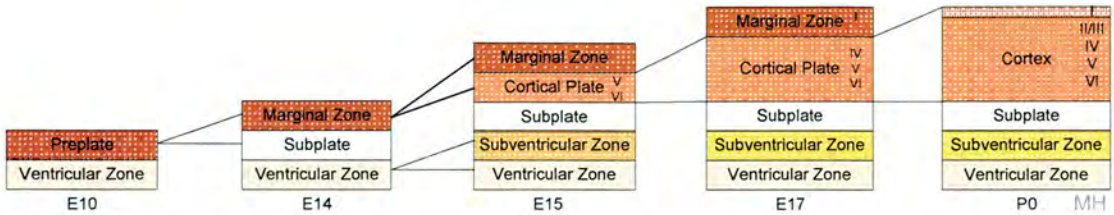

Figure 1.5
Schematic view of the development of cortical layers. At E10 the neuroepithelium of the cortex is composed of the proliferative inner layer of the developing brain, called the ventricular zone, which is only a few cells thick at this age. Cells born in the ventricular zone migrate to expand outwards, forming the cortical plate subsequently the cortical layers. Abbreviations: PP, pre-plate; VZ, ventricular zone; MZ, marginal zone; SP, subplate; CP, cortical plate; SVZ, sub ventricular zone. Dates from Price and Willshaw (2000), see text for further details.

1.3 Cortical area specification

What specifies the cortical areas? In embryonic development, the cortical area map is guided by at least two types of molecular effectors; gradients of locally secreted molecules such as Wnts 2b, 3a, 5a and 7a, FGF8 and BMPs, and graded expression of transcription factors such as Emx2 and Pax6 (Warren and Price, 1997; Warren et al., 1999; Pratt et al., 2000; Bishop et al., 2000; Fukuchi-Shimogori and Grove, 2001; Hevner et al., 2002; Bishop et al., 2002; Talamillo et al., 2003; Grove and Fukuchi-Shimogori, 2003; Bishop et al., 2003; Polleux, 2004; Hamasaki et al., 2004). One stark example of neocortex area specification is that of FGF8, the transcription factor Emx2 and barrel field location. *FGF8* and *Emx2* regulate the expression of each other (Fukuchi-Shimogori and Grove, 2003; Garel et al., 2003) and interaction between the two molecules sets up a developmental cascade that leads to the differentiation of area-specific features (Fukuchi-Shimogori and Grove, 2001; Huffman et al., 2004; Hamasaki et al., 2004; Shimogori and Grove, 2005). Fukuchi-Shimogori and Grove (2001) used electroporation-mediated gene transfer in mouse embryos to express FGF8 in embryonic cortex. Augmentation of anterior FGF8 expression in the mouse cortical primordium can shift the barrel field posteriorly; reducing the FGF8 signal shifts the barrel field anteriorly, and introducing a posterior source of FGF8 causes partial area duplication, with ectopic barrels that are innervated by properly segregated thalamocortical axons (see Figure 1.6).

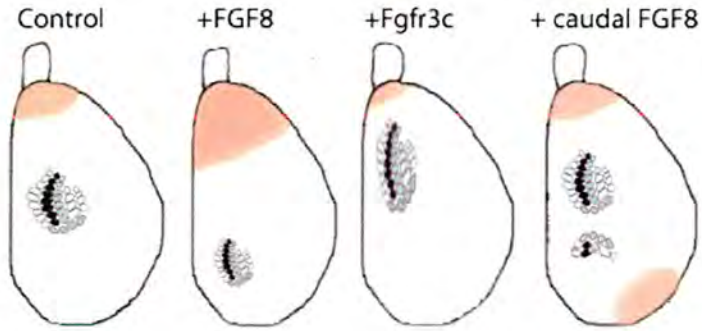

Figure 1.6
FGF8 electroporation shifts the barrel field. Site of FGF8 (or a soluble, truncated form of a high-affinity FGF8 receptor, sFgfr3, which antagonises FGF8 signalling) electroporation is shown in pink. Augmenting FGF8 signalling shifts the barrel field posteriorly; reducing FGF8 signalling with sFgfr3c shifts the barrel field anteriorly, and adding a posterior source of FGF8 causes partial duplication of the barrel field. Based on Grove and Fuckuchi-Shimogori (2003).

Some studies suggest that the cytoarchitectonic characteristics of specific cortical areas are predetermined in the ventricular zone (Reznikov et al., 1984; Rakic and Lyubimov, 1988), yet others (O'Leary, 1989) suggest that the cortical plate is not predetermined and the determination of specific cortical areas are due to external signals. For example, the arrival of topographically organised thalamocortical axons in the sensory cortices would determine the characteristics of primary somatosensory cortex (O'Leary et al., 1994). O'Leary's hypothesis is supported by the observation that the organisational development of sensory cortical areas appear to be governed by the distribution of thalamocortical axons, such as the development of the primary visual cortex into ocular dominance columns in the monkey (Hubel et al., 1977) and barrels in the primary somatosensory cortex in rodents (Van der Loos and Woolsey, 1973b). These structural specialisations only appear after the arrival of thalamocortical axons in the cortical plate (Jhaveri et al., 1991). Further experimental evidence to support this hypothesis was provided when presumptive embryonic rat visual cortex was grafted into P0 somatosensory cortex, causing it to develop the cytoarchitectonic characteristics of somatosensory cortex (Schlaggar and O'Leary, 1991). Barrels, which are stereotypical structures found only in rodent somatosensory cortex, were observed to form within the transplanted region. If this same region was grafted into a rostral, non-somatosensory cortex region, it adopted the characteristics of that region (Schlaggar and O'Leary, 1991, Figure 1.7). However, when the experiment was repeated in mice this transformation only occurred in three out of one-hundred and twenty four (2.4%) of transplants that exhibited good graft integration (Katsnelson, 2002) suggesting that in mice there is very limited potential for re-specification of the identity of the transplanted tissue. However, the work of Schlaggar and O'Leary on the timing of these events disagree somewhat from the results of similar transplantation experiments performed by the

laboratory of Michel Roger (Garnier et al., 1995; Ebrahimi-Gaillard and Roger, 1996; Letang et al., 1998; Frappe et al., 1999; Gaillard and Roger, 2000; Frappe et al., 2001). Roger and colleagues demonstrated that at E16, embryonic tissue that has been heterotopically transplanted into neonatal animals maintained the characteristics of its site of origin, as determined by the projections to and from the transplant. Their results suggest that at E16 some specification of cortical areas already exists, even within mediolateral versus lateromedial orientation inside a single cortical area (Garnier et al., 1995). However, cortical progenitors can change their fate upon heterotopic transplantation when these experiments are performed at E12 (Gaillard et al., 2003).

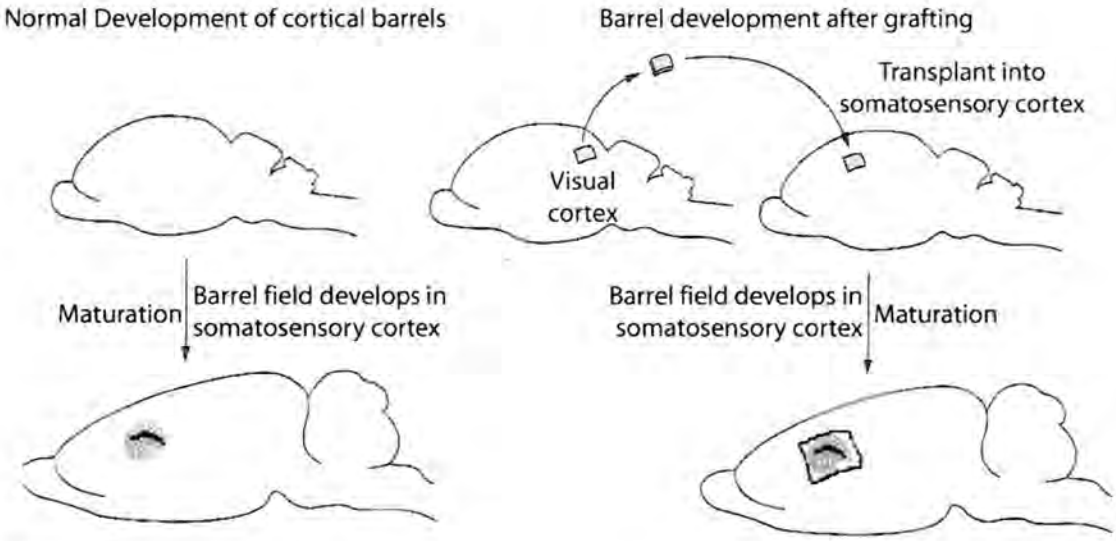

Figure 1.7
Thalamic input influences the organisation of barrels in the somatosensory cortex
Barrel field organisation is induced when a region of the developing visual cortex is grafted into the site normally occupied by somatosensory cortex. The grafted region of visual cortex then acquires a barrel-like organisation. Redrawn and adapted from Schlaggar and O'Leary (1991).

Recently, evidence from genetic knockout mice has shown that the areas of cortex are pre-specified to a certain extent, and that proper cortical lamination is independent of thalamic input. *Gastrulation Brain Homeobox 2* (*Gbx-2*) knockout mice have disrupted thalamic differentiation and lack thalamocortical axons (Hevner et al., 2002) and these mutants die at birth (Wassarman et al., 1997). However, neocortex lamination appears normal, as neocortical region-specific gene expressions develop normally (as measured by *cadherin-6*, *Ephrin receptor A-7* (*EphA-7*) and the transcription factors *Inhibitor of DNA Binding, 2* (*Id-2*) and *Rar-Related Orphan Receptor B* (*RORβ/RZRβ*); Rubenstein et al., 2002; Hevner et al., 2002). These results indicate that lamination of the cortex does not require thalamic influence. However it is likely that lateral regional specialisation of the

cortex, i.e. the formation and function of neocortical columns such as barrels, needs thalamocortical input.

1.4 The somatosensory system

1.4.1 Organisation of the somatosensory cortex

The rodent primary somatosensory (S1) cortex is organized as a topographic map that reproduces the pattern of peripheral sensory receptors. The primary somatosensory cortex is divided into topographic regions, each representing a specific part of the body. In rodents, the pattern of whiskers on the snout is isomorphically represented in the primary somatosensory cortex as structures termed "barrels", in a topographic map known as the "barrel field". Barrels that receive input from the large mystacial vibrissae are located in a region termed the posteromedial barrel subfield (PMBSF, Woolsey and Van der Loos, 1970; Erzurumlu and Kind, 2001; Barnett et al., 2006b, Figure 1.8, Figure 1.9). In rodent and murine somatosensory cortex, the whisker representation accounts for about one-third of the S1 region; other areas of the sensory periphery are also represented with barrel-like structures (Welker and Woolsey, 1974). The smaller barrels in rodent S1 represent input from the hindlimb, forelimb and smaller whiskers on the anterior snout. However, the topographic mapping of these structures with the periphery is not as precise as the large vibrissae-to-barrel mapping, with the cortical representation of these structures lacking clearly defines segregation into individual barrel-like structures (Welker and Woolsey, 1974). However, other areas of the periphery do not have any representation as cellular aggregations in the cortex, and the reasons why are unknown, as are the reasons for this somatotopic representation in mice and rats. The one-to-one mapping of the main facial whiskers and their proportionally large representation in the cortex may be an evolutionary outcome of the functional significance of whiskers for these animals.

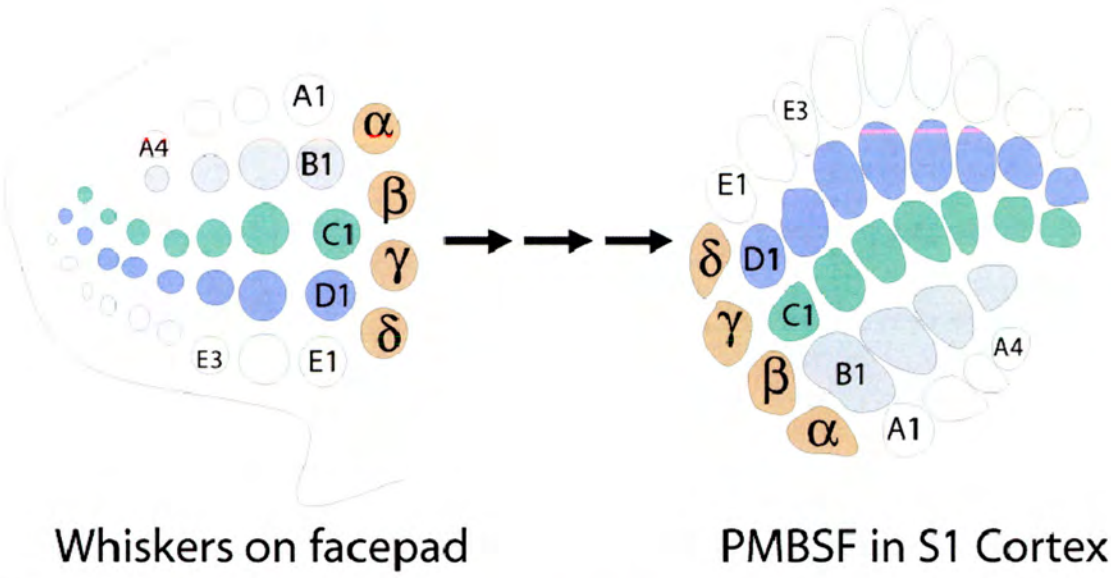

Figure 1.8
There is a precise isomorphic correspondence between the layout of whiskers on the whiskers on the mouse or rat facepad and the mapping of barrels in the Posteromedial Barrel Subfield (PMBSF). The whiskers are arranged in five principal rows on the face, labelled A-E in the dorsal-ventral axis. Arcs are labelled 1 to n in the posterior to anterior directions. Four caudal whiskers "straddle" the rows and are labelled α, β, γ, δ.

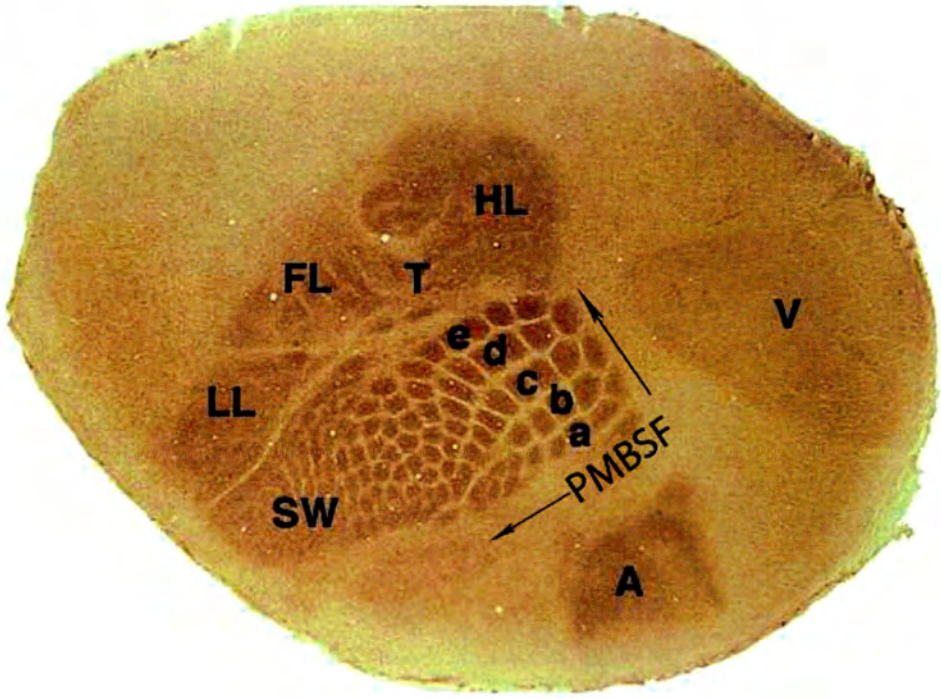

Figure 1.9
The PMBSF: the area consisting of large barrels. Flattened left hemisphere section of layer IV of a wild-type P7 mouse cortex immunostained with GAP-43 transporter antibody, staining TCAs. The TCAs are labelled to show the sensory origin of each region: V: visual A: auditory, a-e: input from large whiskers, SW: input from small whiskers, LL: lower lip, FL: forelimb, T: trunk, HL: hindlimb, Posteromedial Barrel Subfield (PMBSF). Original image from Maier et al., 1999.

1.4.2 Neuroanatomy from whisker to barrel

Whisker follicle receptor cells are found at the base of each whisker and these cells detect deflection of the whisker caused by brushing against an object (Figure 1.10). By E12 the follicle receptor cells of each whisker are supplied by a single afferent from a group of anatomically segregated fibres ascending from a peripheral branch of the infraorbital nerve (ION) of the maxilliary division of the of the trigeminal ganglion (Van der Loos and Dörfl, 1978). Projections from this branch of the ION also progress toward the brainstem (Erzurumlu and Jhaveri, 1992). On entering the brainstem the trigeminal ganglion nerves give off collaterals to four distinct subnuclei in the brainstem trigeminal complex (BSTC): principalis (nVp), interpolaris (nVi), caudalis (nVc) and in rats but not mice, oralis (nVo, Hayashi et al., 1984; Ma, 1991) of which only nVp, nVi and nVc receive anatomically segregated inputs from whiskers (Bates and Killackey, 1985). The structures formed in each of these three nuclei recapitulate the ipsilateral whisker pattern and are called "barrelettes". They are first visible by postnatal day (P)0 using cytochrome oxidase histochemistry (Ma, 1991) and are well segregated by P1 (Ma, 1993). Neurons in the nVp and nVi nuclei (and to a lesser extent in nVo and nVc) project axons across the midline of the brain to VpM of the thalamus, arriving by P2. Axon terminals and cell bodies in the contralateral thalamus replicate the whisker pattern in cytoarchitectonic arrangements termed "barreloids" (Van der Loos, 1976) although only nVp input is required for barreloid formation (Killackey and Belford, 1979). Barreloids begin to form at P3 and can be visualised by cytochrome oxidase histochemistry (Yamakado, 1985; Agmon et al., 1995), see Figure 1.10. Thalamocortical axons (TCAs) project from VpM thalamus to the cortex and invade the cortical plate by E16 (Molnár et al., 1998; Molnar and Hannan, 2000).

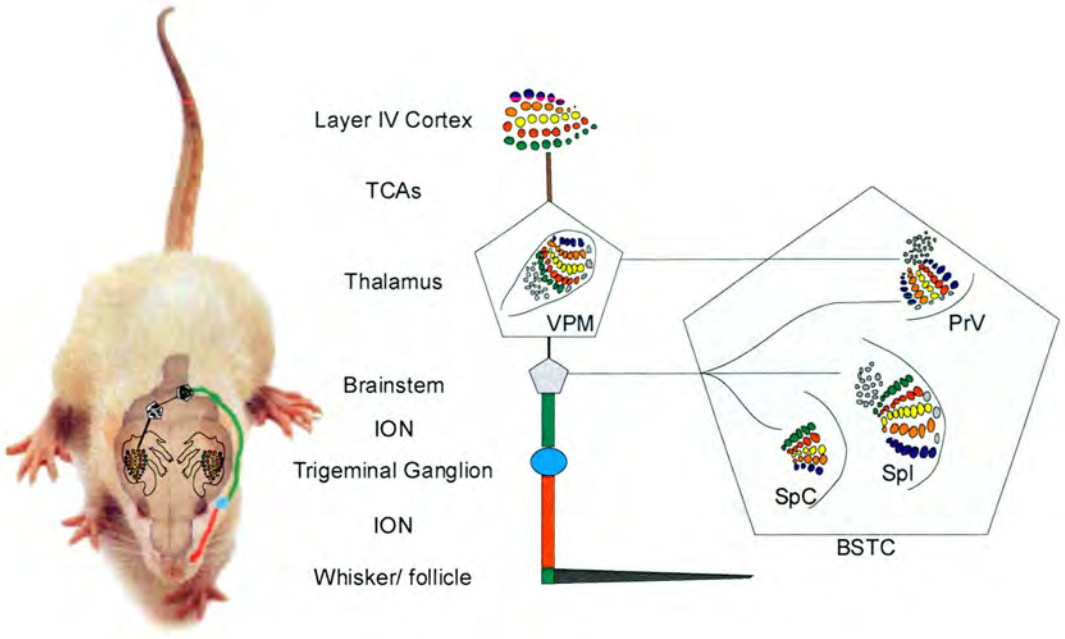

Figure 1.10
The whisker-barrel pathway of mice. The infraorbital (ION) branch of the trigeminal ganglion (TG) innervates the whiskerpad on the snout. Central counterparts of these axons deliver the patterns to the brainstem trigeminal complex (BSTC), where whisker-related patches are called "barrelettes". Barrelette neurons of the PrV carry these patterns to the ventroposteromedial nucleus (VPM) of the contralateral dorsal thalamus. In VPM, whisker-related patterns are referred to as 'barreloids'. Barreloid or VPM neurons form the final relay to the layer IV somatosensory "barrel" cortex. At each level there is a topographically aligned map of the face (and the body) and whisker-specific patterning of axonal and cellular elements within the face map. In mice, a mature cortical barrel consists of a cell-dense barrel wall with asymmetrically projecting dendrites oriented into cell-sparse barrel hollows where incoming thalamocortical axon terminals (TCAs) segregate. These patterns are established during a sensitive period in development under the guidance of signals coming from the sensory periphery (Woolsey and Van der Loos, 1970; O'Leary et al., 1994; Killackey et al., 1995; Erzurumlu and Kind, 2001).

1.4.3 Thalamocortical axon growth and guidance

Each region of the neocortex is characterised by the patterning of innervation from the thalamus. If TCAs do not grow to reach and terminate in layer IV of the cortex and segregate into whisker-related patches, barrels do not form.

Relatively little is known about the molecules that guide TCA growth towards the cortex. However, variety of molecules have been implicated both TCA growth and guidance, including neurotrophins, cadherins, ephrins, Eph receptors, limbic-associated membrane protein (LAMP), *semaphorin 6A* (Leighton et al., 2001), *GAP-43* (Maier et al., 1999) and netrin 1 (reviewed in Lopez-Bendito and Molnár, 2003). TCA pathfinding defects in most of

these mice are subtle, suggesting that these molecules are either playing minor roles in TCA development, or that they act in concert to generate correctly guided thalamocortical axons.

GAP-43 is selectively expressed within TCAs during barrel formation (Erzurumlu et al., 1990). *Gap-43*$^{-/-}$ mice have enlarged barrels and there is also a TCA patterning defect within cortex, with TCAs exhibiting widespread, sparsely branched terminal arbors in layer IV, reflecting the large-barrel phenotype (McIlvain et al., 2003). Barrels appear one day later than wild-type mice, likely due to a two-day delay in differentiation of radial glial cells from monopolar to multipolar phenotypes which should occur at P5 (McIlvain and McCasland, 2006). Radial glial cells represent many of the neuronal progenitors in developing cortex and aid in cell migration and as such the delay in radial glial differentiation may contribute to the delay in *Gap-43*$^{+/-}$ barrel segregation. *Gap-43*$^{-/-}$ mice have normal barrelettes and barreloids, but thalamocortical afferent projection is distributed to widely separated cortical targets (Maier et al., 1999), and TCAs originating from VpM thalamus have abnormal somatotopy and hence cortical cells fail to form barrels.

Ephrin/Eph interactions are important molecular cues for TCA guidance within the primary somatosensory cortex. *Ephrina5* is expressed in a mediolateral gradient in primary somatosensory cortex, whilst VpM thalamus is expressed in a ventromedial-dorsolateral gradient during the perinatal stage. Recent studies on *Ephrina5*$^{-/-}$ mice demonstrated that cortical EphrinA5 is an important molecular cue for the topographic projection of EphA4-expressing TCAs (Vanderhaeghen et al., 2000; Egea et al., 2005). Notably *Ephrina5*$^{-/-}$ mice have distorted barrels and barrel fields.

Mice that are mutant for two Wnt/PCP signalling pathway members (Section 1.10.3), the Wnt receptor *Frizzled 3* (Wang et al., 2002) and the protocadherin *Celsr3* (Tissir and Goffinet, 2006; Tissir et al., 2005; Tissir et al., 2002; reviewed in Price et al., 2006) have drastic defects in TCA formation and guidance. Frizzled 3 and Celsr3 are both essential for the formation and guidance of thalamocortical and corticofugal axons. Mice mutant for either of these genes die perinatally, lack the anterior commissure and the internal capsule and have neocorticies that are entirely disconnected from other structures (Wang et al., 2002; Tissir et al., 2002; Tissir et al., 2005; Tissir and Goffinet, 2006).

Finally, TCAs from VpM thalamus that are incorrectly guided can still form barrels. In *reeler* mutant embryos, TCAs penetrate the cortical plate and grow directly to the roof of the

cortex (which in these mutants is an unsplit preplate). TCAs then turn and descend and arborise within the cortical plate and assume an almost normal periphery-related pattern, forming a near-normal barrel field (Caviness, Jr., 1982; O'Brien et al., 1987). TCAs incorrectly routed to other regions of the cortex, as generated by perturbation of FGF8 signalling (Fukuchi-Shimogori and Grove, 2001; Shimogori and Grove, 2005, Figure 1.6) can still form barrels. The work by Shimogori and colleagues demonstrates dissociation between TCA guidance and subsequent patterning in the cortex as TCAs misguided to the wrong cortical area still segregate and cortical patterning into barrels still form.

Of the genetic mutants of members of the NMDA receptor complex (NRC, Section 1.7) that have been generated that result in the failure of barrel formation, none have defects in whisker-to-barrel topography (Barnett et al., 2006a). It is therefore thought that the topographically organised projections from whisker to barrel are established via activity-dependent mechanisms, whilst the patterning of neural connections within these topographic maps in cortex is determined by neural activity, mainly through NMDA receptors and members of the NMDA-receptor complex (Erzurumlu and Kind, 2001; Dickson and Kind, 2003).

1.4.4 TCA terminal segregation into a barrel-like pattern

TCAs reach layer IV by P0, beginning the process of barrel formation that occurs when TCA afferents synapse onto layer IV granule cells, where the neurons subsequently form a "barrel" (Killackey and Leshin, 1975; Erzurumlu and Jhaveri, 1992; Killackey et al., 1995). Current opinion is that TCAs reach layer IV at P0 with an initially diffuse distribution, with each axon occupying one to two prospective barrel diameters; a tangential aggregation of the axons then occurs, with emergence of whisker rows in PMBSF at P2 and segregation into the characteristic barrel-like pattern (Figure 1.9, Figure 1.11) between P2 and P5 (Rebsam et al., 2002). This involves the retraction of inappropriately located arbors and elaboration of appropriately placed arbors, and by P7 each TCA arborises exclusively in a single barrel.

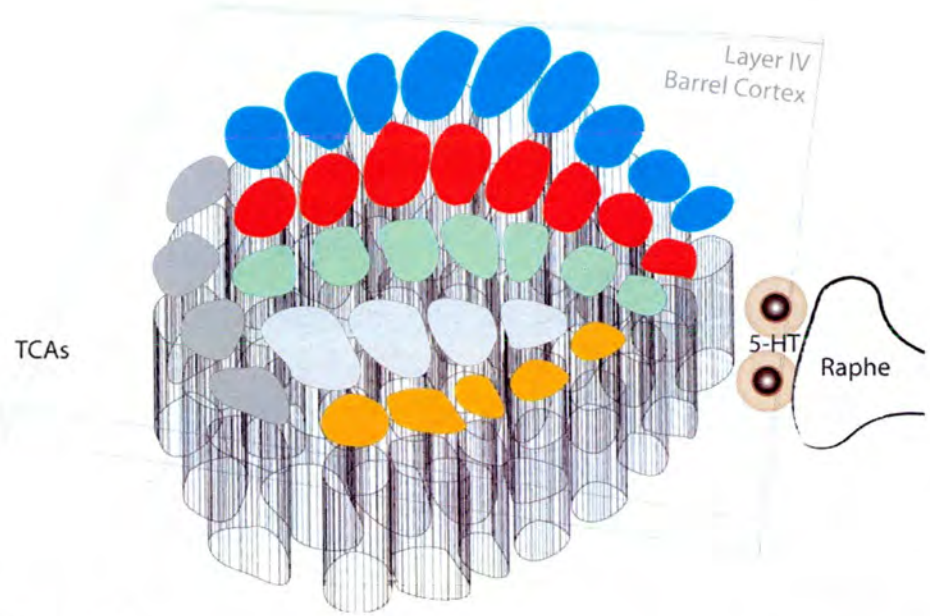

Figure 1.11
Thalamocortical Axon terminals segregate into a barrel-like pattern. TCAs in PMBSF region. By P4, the TCAs have finished segregating into a barrel-like pattern. The pattern of barrels is represented by the coloured shapes; TCAs are represented by the columnar structures. Patch size and formation is heavily influenced by serotonin/ 5-HT released by Raphe terminals in layer IV of the cortex.

1.4.5 Forming a barrel.

The term "barrel" has been used differently by different laboratories. In some laboratories, a barrel is the highly stereotyped group of cellular aggregates that recapitulate the pattern of whisker arrangement on the facepad. By this definition, the TCA segregation is not part of the barrel but forms a "barrel-like" pattern. In other laboratories, the term barrel includes the TCA terminals. For the purpose of this thesis, the term barrel only refers to the cellular aggregates not the TCA patches. In both cases the relatively acellular areas that separate individual barrels are called "septae".

Three processes are currently thought to be key to barrel formation: proper axon guidance, aggregation and termination of TCAs in the correct location (Rebsam et al., 2002; Vitalis et al., 2002); selective segregation of cortical cells to form a barrel wall, leaving a barrel hollow (Rice and Van der Loos, 1977); and dendritic elaboration within the barrel hollow (Woolsey et al., 1975).

When TCAs reach layer IV on the day of birth, they encounter a homogenous population of cortical granule cells that have just started to elaborate dendrites. By P3 the TCA pattern has been refined into individual clusters, yielding a barrel-like pattern (Figure 1.9). The presence

of segregated TCAs induces the clustering of cortical cells around the TCA patches, forming the barrel. By P5, cellular clustering is observed for the first time and a full barrel field is visibly by P7 (Figure 1.12). Dendrites of barrel wall cells selectively elaborate within the TCA terminals in the barrel hollow over the next fortnight, although the precise timing of this process in not clear (Greenough and Chang, 1988), but by P14 (the peak of dendritogenesis) layer IV cell dendrites are restricted to barrel hollows and few remaining barrel wall cells demonstrate a symmetric distribution of dendrites (Erzurumlu and Kind, 2001), see Figure 1.7, Figure 1.13.

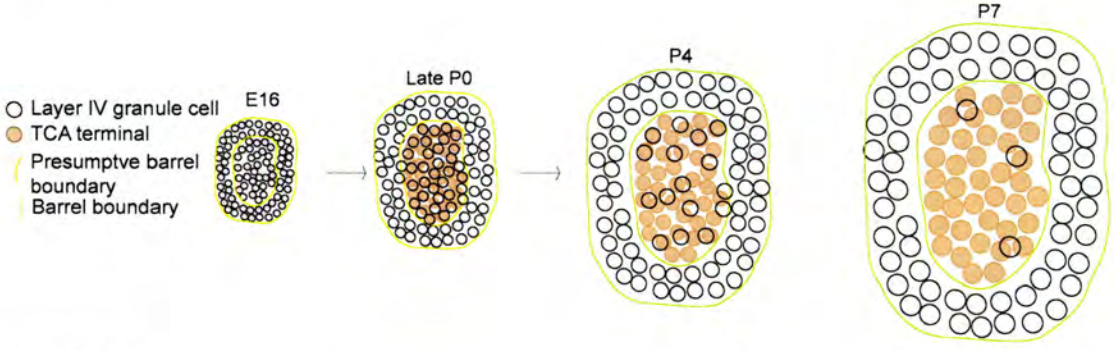

Figure 1.12
Cellular segregation of cortical cells to form barrels in response to TCA invasion. At E16, TCAs have not yet arrived in presumptive laver IV cortex in the cortical plate; by late P0, TCAs have arrived and terminated in Layer IV and are segregated into a barrel-like pattern. By P4, segregation of cortical cells forming a cell-dense barrel wall and a cell-sparse barrel hollow is visible, and by P7 barrel walls are anatomically well-defined and a full barrel field is visible.

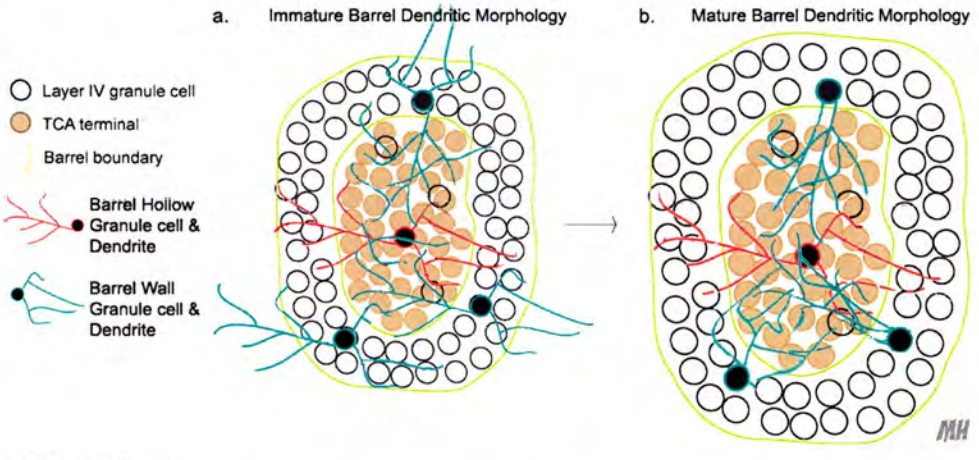

Figure 1.13
Barrel dendritic morphology. **Immature dendritic morphology (a): Dendrites in the barrel wall have no specific orientation, but once mature (b), dendrites of cortical cells in the barrel wall (light blue lines) have undergone selective elaboration towards the TCA plexus but the dendrites of cortical cells that are not located in the barrel wall show no specific orientation.**

Although the actual cellular mechanisms underlying barrel wall formation are unknown, several theories exist, as described in Figure 1.14. Potential mechanisms include: 1) the massive elaboration neuropil within the TCA patch— both axons and dendrites, causing passive displacement of cortical neuronal soma, forming the cell-dense barrel wall; 2) selective cell death in the region of TCA innervation, although no such selective cell death within TCA patches has been observed (Miller, 1995) and knockout mice with reduced segregation show no change in overall cell density (Barnett et al., 2006b); 3) active migration of layer IV neurons away from the incoming TCA; and 4) differential cell adhesion induced by TCA innervation concurrent with tangential cortical growth. It is unknown whether one or more of these processes are responsible for barrel formation (for a review see Barnett et al, 2006b).

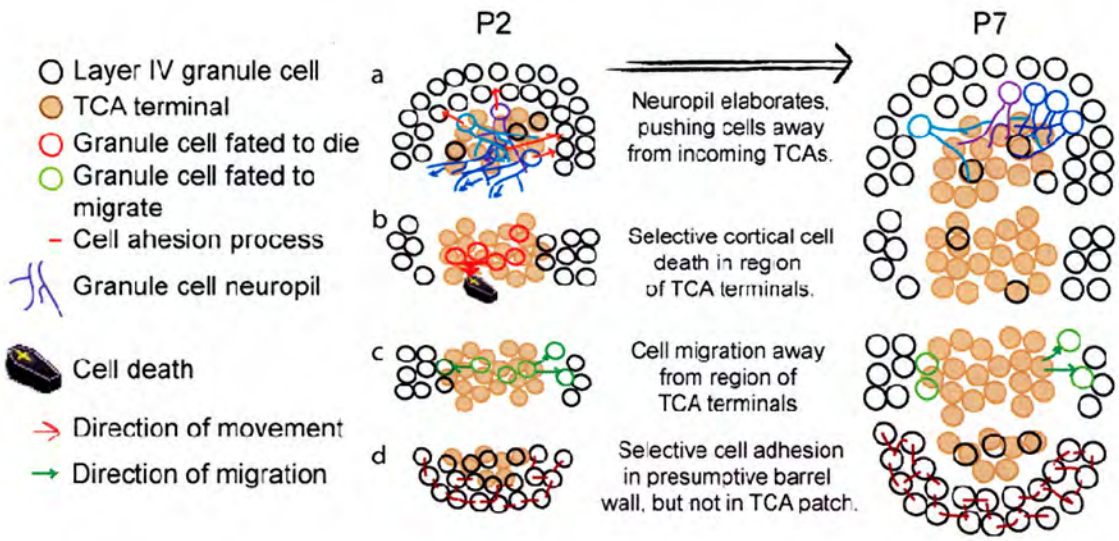

Figure 1.14
Cellular mechanisms of barrel formation. Potential mechanisms that might generate a cell-dense barrel wall and cell-sparse barrel hollow include: (a) The massive elaboration of both axons and dendrites causing a passive displacement of cortical neurons to form the barrel-dense cell wall, as denoted by the purple and blue cells and their corresponding neuropil, arrows represent the direction that the neuropil is pushing against. (b) Selective cell death in the region of TCA innervation, as denoted by the red circles with the arrow to the coffin. (c) Migration of layer IV neurons away from the incoming TCA as denoted by the green circles, and (d) Selective cell adhesion in the region around the TCA, as denoted by the dark red lines, generating a tethered, cell-dense barrel wall as the cortex grows and leaving the untethered cells remaining within the barrel hollow representing proportionately less of the area of a single barrel as the cortex grows.

The molecules that underlie the dendritic shape change in developing barrels are unclear. *Plc-$\beta_1^{-/-}$* mice have normally segregated TCAs (Hannan et al., 2001) and cortical cell dendrites that orient normally into the TCA plexus despite the absence of barrels (Upton et al., in preparation, Section 1.4.9) and as such is a good example of a molecule crucial for

barrel formation that is unimportant for dendritic orientation; the two processes can be genetically dissociated. However, in both P16 cortex-specific NMDA receptor *NR1* subunit knockout (*CxNr1*$^{-/-}$) and P14 *Pkar2β*$^{-/-}$ mice, a lack specific dendrite orientation in barrel cortices has been reported, although both of these mutants lack barrels (Datwani et al., 2002b; Inan et al., 2006), discussed in Section 1.4.9 and Figure 1.19). However, any mechanisms downstream of these molecules have not yet been elucidated. A concern in both these studies however, is that analysis of dendritic orientation was done in coronal sections and did not control for the changes in the tangential distribution of cells in layer IV. Instead the authors simply reported on a decrease in the proportion of layer IV cells with oriented dendrites. Since both of these mice lack barrels, the percentage of cells located at the edge of a TCA patch, and hence would be expected to have oriented dendrites into the patch, would be greatly reduced. In wild type animals the ratio of cell soma in a wall compared to a hollow is approximately 1.75:1 (Watson et al., 2006a). Datwani et al. (2002), reported a drop from 63% to 17% of cells with oriented dendrites in the *CxNr1*$^{-/-}$ animals. However, since the position of the soma relative to the TCA patch is not known, these changes could simply be due to the reduced number of cell soma located at the edge of a TCA patch. The work of Upton et al. on *Plc-β*$_1^{-/-}$ mice was completed on tangential sections through layer IV and all dendritic orientation was performed with taking into account soma position relative to TCA patch. Soma located at the edge of a TCA patch displayed oriented dendrites into a patch. Those soma located with a TCA patch showed little preference for dendrite orientation, however, their dendrites remained restricted to the patch boundaries indicating that the ability of the layer IV cells to restrict their dendrites to the location of TCA terminals is unaltered in *Plc-β*$_1^{-/-}$ mice. A similar analysis would be prudent for other mutants that alter barrel formation including the *CxNr1*$^{-/-}$ and *Pkar2β*$^{-/-}$ mice.

Dendrite growth and orientation in the developing cortex include neurotrophins, which regulate layer-specific dendritic growth and branching in an glutamate receptor-dependent manner (McAllister et al., 1996; McAllister et al., 1997). In general neurotrophins increase the length of dendrites and increase dendritic complexity, but the effects differ by cortical layer and by whether the dendrites are apical or basal dendrites (Scott and Luo, 2001). Semaphorins have been shown to regulate apical dendrite orientation in pyramidal neurons in the cerebral cortex. Semaphorin 3A, a chemorepellant for cortical axons, is a chemoattractant for dendrites and this effect is dependent on asymmetric localization of soluble guanylate cyclase to the developing apical dendrite (Polleux et al., 2000). Slit genes are important regulators of guidance of corticofugal, callosal, thalamocortical, serotonergic,

and dopaminergic projections in the embryonic forebrain (Plump et al., 2002) and Slit-1 increases dendritic growth and branching (Whitford et al., 2002b). The Notch1 receptor restricts dendritic growth and can cause dendrite retraction in cortical neurons; neurons with low notch signalling readily extend neurites, whereas mature neurons that have stopped growing exhibit high notch activity (Sestan et al., 1999; Redmond et al., 2000; Redmond and Ghosh, 2001). Classical cadherins and their interaction partner β-catenin play a role in the stabilization of dendrites (Yu and Malenka, 2003; Yu and Malenka, 2004) and dendritic spines (Togashi et al., 2002; Abe et al., 2004). These, in addition to the role Wnts play in determining dendritic shape are discussed further below.

RhoGTPases have shown to be key to regulating activity-dependent dendrite development (Threadgill et al., 1997), reviewed in Van Aelst and Cline, 2004) and play roles in initiation, dendritic branching and spine formation (Luo, 2000; Whitford et al., 2002a). In early dendrite development in Xenopus Laevis tectal neurons and Drosophila Melanogaster mushroom body neurons, RhoA activation reduces dendritic growth and branching, while Rac1 activation increases dendritic branching (Ruchhoeft et al., 1999; Li et al., 2000; Lee et al., 2000b). RhoGTPases have been shown to act in mature hippocampal neurons to maintain dendritic arbors (Nakayama et al., 2000). Rho and Rac have been implicated in sense-induced NMDA-dependent dendritic shape change. In Xenopus tadpole visual tectum, light stimulus driving visual activity promotes dendritic arbour growth and this process requires NMDA receptors, decreased RhoA, increased Rac and Cdc42 activity (Sin et al., 2002; Van Aelst and Cline, 2004). It has been hypothesised that Rho-GTPases integrate signals from neurotrophins signalling through trk-family receptors, Ephrin-Bs signalling through EphB receptor kinases. Although it remains to be investigated, RhoGTPases could mediate this function in cortical cell dendrites in barrel cortex.

1.5 Plasticity of the somatosensory system

Somatosensory system organisation is dependent on the integrity of the peripheral receptors during development (Van der Loos and Woolsey, 1973b; Woolsey and Wann, 1976). Each synaptic level from the periphery to the cortex can be altered in neonates by whisker follicle ablation during a "sensitive period" (Killackey and Leshin, 1975; Killackey et al., 1976; Belford and Killackey, 1979a; Belford and Killackey, 1979b; Belford and Killackey, 1980; Bates et al., 1982). Cauterisation of the whisker follicles from P0 to P3 leads to considerable

overlapping of TCAs and permanent alteration of the barrel field (Belford and Killackey, 1980; Jeanmonod et al., 1981; Jensen and Killackey, 1987); patterning of whisker topography is no longer transferred. Thalamic lesions and infraorbital nerve lesion reduce the thickness of layer IV and prevent TCA segregation in PMBSF (Wise and Jones, 1978; Jensen and Killackey, 1987; Rhoades et al., 1997). Postnatal whisker follicle lesion before P4/ P5 leads to a reduction in the area occupied by the cortical representation of the barrel associated with the lesioned whisker and a simultaneous increase in the size of adjacent barrels (Figure 1.15). The ability of cortical cells to respond to whisker ablation is limited by age; the earlier the lesion, the more pronounced the effect. After P5, no effect is seen (Woolsey and Wann, 1976). Lesion of an entire whisker row leads to the formation of a megabarrel, a barrel spanning the entire cortical representation of the ablated whisker row (Van der Loos and Woolsey, 1973). This forms despite the lack of any sensory input, suggesting that spontaneous activity is sufficient for megabarrel formation (Van der Loos and Woolsey, 1973).

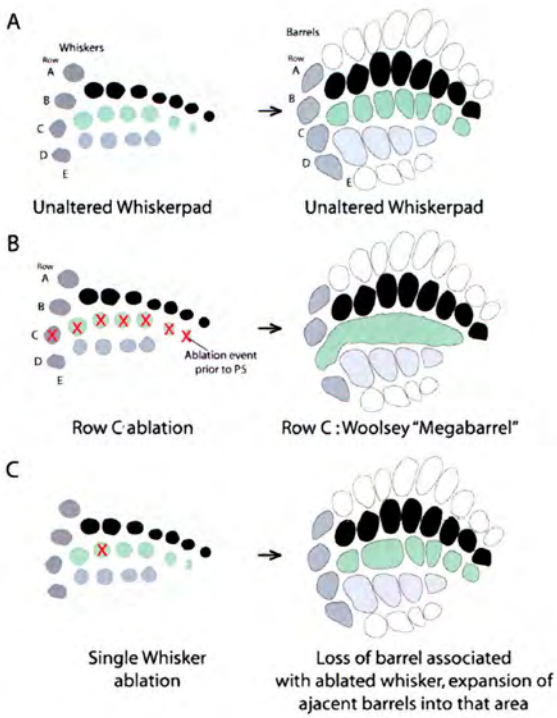

Figure 1.15
Cortical plasticity in response to whisker ablation in PMBSF. A. Normal, uninterfered environment. Single barrels exist which represent each whisker associated with it on the facepad. B. Cauterisation of whiskers row C of whiskers results in the fusion of the row C barrels into a "megabarrel". C. Cauterisation of a single whisker results in the expansion of the cortical area occupied by adjacent barrels into the area ordinarily occupied by the ablated whisker.

1.6 Molecular and biochemical mechanisms of barrel formation

1.6.1 Presynaptic events

During barrel field formation, there are not only TCAs projecting from VpM of the thalamus to layer IV, but also serotonergic afferents from the raphe nuclei that arrive in layer IV one day after TCA arrival (Fujimiya et al., 1986; Rhoades et al., 1990; Blue et al., 1991; Fujiyama and Masuko, 1996). Strong serotonin immunolabelling in TCAs is observable in the murine somatosensory cortex during the first ten days of postnatal life although it peaks at P5 when the initially diffuse pattern of serotonin labelling observed at birth is organised into the barrel pattern (Fujimiya et al., 1986; D'Amato et al., 1987). This transitory uptake of serotonin by TCAs (Lebrand et al., 1996; Cases et al., 1996) results from a transient expression of serotonin transporter (5-hydroxytryptamine (5-HT) transporter, 5-HTT) and vesicular monoamine transporter in TCAs (VMAT, Lebrand et al., 1996; Lebrand et al., 1998).

Lesion of the raphe-cortical axons deletes serotonin input to the cortex and this causes smaller than normal TCA patches, (Killackey, 1973; Bennett-Clarke et al., 1997) showing that serotonin is not required for TCA segregation, but serotonin plays a role in the fine-tuning of TCA segregation (Gaspar et al., 2003). Finally, mice lacking the *Adenylate Cyclase 1* (*Adcy1*) gene lack barrels and have barreloids in the thalamus that are poorly formed (Welker et al., 1996). The pre- and post-synaptic roles of *Adcy1*, cAMP production and Protein Kinase A (PKA) are discussed in Section 1.6.9.

1.6.2 Postsynaptic events

1.6.2.1 Glutamate receptors

Glutamate is the main excitatory neurotransmitter in the vertebrate CNS, and the functions of glutamate are mediated by two groups of glutamate receptors; ionotropic and metabotropic receptors. There are three types of ligand gated ion channels (LGICs) that respond to glutamate in CNS; α-amino-3-hydroxy-5-methyl-4-isoxazolepropionic acid (AMPA), N-Methyl-D-Aspartate (NMDA) and kainate receptors (Figure 1.16, Hollmann and Heinemann, 1994; Dingledine et al., 1999). NMDA receptor signalling requires depolarisation of the membrane of the cell in which it resides; AMPA and kainate receptors perform this action, as their channels swiftly open to glutamate binding of the receptor, and rapidly pass mostly Na^+ but also Ca^{2+} and K^+ (Dingledine et al., 1999). In addition, there are metabotropic

glutamate receptors, which have no ion channel, but instead couple to G proteins that activate the Phospholipase C-β (PLCβ) family of proteins and also regulate Adenylyl Cyclase (AC) intracellular messenger pathways, depending on the G-protein to which it couples (Figure 1.16).

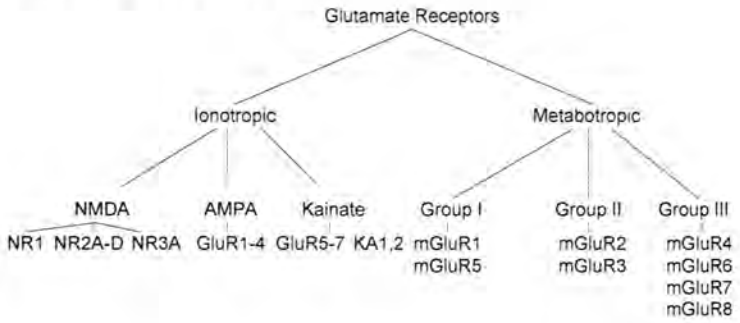

Figure 1.16
Classification of the different types of Glutamate Receptors, adapted from the MRC Centre for Synaptic Plasticity website, http://www.bris.ac.uk/synaptic/. The classification of each type of ionotropic receptor was originally determined by pharmacology activity to different agonists; metabotropic receptors were originally grouped by what second messenger pathway was utilised by the activated receptor. Subsequently, the availability of genetic sequences for these receptors has refined these classifications.

1.6.3 Glutamate signalling and the NMDA Receptor

Donald Hebb postulated a mechanism for synaptic plasticity, wherein an increase in synaptic efficacy arises from repeated and persistent stimulation of a postsynaptic cell by a presynaptic cell (Hebb, 1949), often simplified to "cells that fire together, wire together". The phenomenon of LTP was discovered in 1973, where long-lasting Hebbian modification of synapses occurred in response to an *in vitro* electrophysiological brain slice stimulation paradigm. The postsynaptic response to a uniform presynaptic stimulation is termed the excitatory postsynaptic potential (EPSP), and the EPSP was greater after application of the LTP paradigm than before (Bliss and Lomo, 1973).

1.6.4 Composition and opening of NMDARs.

There are seven NMDAR subunits (NR1, NR2A-D and NR3A-B); the NMDAR consists of at least one obligatory NR1 subunit, at least two NR2(A-D) subunits. It is believed to be tetrameric in structure (Clements and Westbrook, 1991). The combination of NR1 with different NR2 subunits causes variation in pharmacological and electrophysiological properties (Moyner et al., 1999). NMDA receptors contain an integral cationic channel that is normally Ca^{2+} selective, although Na^{+} and K^{+} ions can pass depending on the subunit

composition of the receptor. Under normal conditions, a voltage-dependent Mg^{2+} block restricts channel opening; only after a large number of co-ordinated synaptic inputs does the membrane containing the NMDAR become depolarised sufficiently to lift the Mg^{2+} block and permit ions to flow through the NMDAR in response to glutamate ligand binding. Ca^{2+} influx into the cell following NMDAR activation mediates activation of the signal transduction pathways within the cell and the plastic changes seen at the synapse (Hollmann and Heinemann, 1994; McBain and Mayer, 1994; Dingledine et al., 1999). Different NMDAR subunits are able to signal through different intracellular signalling cascades mainly because of sequence differences in the C-terminal tails between each subunit. For example, NR2A subunits preferentially bind PSD-95 (Kornau et al., 1995), which binds neuronal Nitric Oxide Synthase (nNOS, Brenman et al., 1996b), whereas NR2B preferentially binds SAP-102 (Lim et al., 2002), which binds SynGAP (Kim et al., 1998).

1.6.5 NMDARs and plasticity.

The involvement of the NMDAR in most forms of LTP (Collingridge, 1987; Bliss and Collingridge, 1993) lead to the concept that the NMDAR is the most important molecule in synaptic plasticity. The majority of NMDA receptors (NMDARs) are found at postsynaptic sites (but also can exist presynaptically (DeBiasi et al., 1996) and play a major role in behaviour, learning (Morris, 1984) and in *in vitro* paradigms of learning and plasticity (Morris et al., 2003). NMDARs mediate not only LTP but also LTD (Wilson and Racine, 1983; Artola and Singer, 1987; Hardingham et al., 2003; Malenka and Bear, 2004) and NMDAR activation leads to activation of almost all of the molecules thus far implicated in synaptic plasticity (Bear and Malenka, 1994; Bear, 1996; Dickson and Kind, 2003).

The role of NMDAR-dependent pathways in cortical development has been established using pharmacological blockade of NMDAR and production of transgenic mice carrying mutations for NMDAR subunits. These studies have revealed several NMDAR-dependent pathways involved in cortical development and plasticity, including the cyclic adenosine monophosphate (cAMP) dependent-Protein Kinase A (PKA) pathway (Abdel-Majid et al., 1998; Beaver et al., 2001; Liu et al., 2003), Calcium/Calmodulin-dependent kinase II (CaMKII) pathway (Glazewski et al., 1996; Taha et al., 2002), Extracellular signal-related kinase (ERK) pathways (Di Cristo et al., 2001; Cancedda et al., 2003a), Calcineurin (Yang et al., 2005) and Phospholipase C-β1 (Hannan et al., 2001). All of these pathways play crucial

roles in various types of hippocampal LTP and LTD (Malenka and Nicoll, 1993; Bear and Malenka, 1994; Bear, 1996; Malenka and Nicoll, 1999; Grant and O'Dell, 2001; Malenka and Bear, 2004) indicating conservation of signalling pathways between different brain structures. Furthermore, glutamate signalling though NMDAR, along with γ-amino-butyric acid (GABA) acting on GABA receptors determine the timing and extent of visual plasticity during development (Kleinschmidt et al., 1987; Bear et al., 1988; Daw et al., 1995; Hensch et al., 1998; Hensch and Fagiolini, 2005).

1.6.5.1 Loss of NMDAR function

Pharmacological blockade of the NMDA receptor prevents the anatomical barrel field plasticity seen in rodent somatosensory cortex in response to whisker removal (Fox et al., 1996; Mitrovic et al., 1996). The complete knockout of the NR1 subunit of the NMDA receptor (*Nr1*$^{-/-}$ mice) results in the topography of somatosensory brainstem projections being unaltered, yet whisker and digit-related neural patterns fail to form in the first relay stations in the somatosensory pathway (Forrest et al., 1994; Li et al., 1994; Kutsuwada et al., 1996; Rudhard et al., 2003a). The structure of the thalamus and cortex could not be studied since *Nr1*$^{-/-}$ mice die of respiratory failure within twenty-four hours of birth. Nevertheless, pharmacological intervention can be made to delay the birth of *Nr1*$^{-/-}$ mice by an extra twenty-four hours, after which respiratory assistance can prolong their survival to the equivalent of P2 in normal mice; no whisker-related patterns were present in BSTC in such "P2" *Nr1*$^{-/-}$ mice (Li et al., 1994). Since these mice die at an age equivalent to P2 in wild-type mice, the structure of higher trigeminal centres could not be studied. *NR2B*$^{-/-}$ mice exhibit the same phenotype of perinatal death due to respiratory failure, and even after the same pharmacological and respiratory interventions, have the same brainstem phenotype as the *Nr1*$^{-/-}$ mice (Kutsuwada et al., 1996). *NR2D*$^{-/-}$ mice have normal barrelettes, barreloids and barrels (Ikeda et al., 1995).

An experiment whereby *NR1* knockout mice were "rescued" by transgenic expression of the *NR1-1a* splice variant was performed (Iwasato et al., 1997). *Nr1*$^{-/-}$ mice that had high levels of *NR1-1a* transgene expression survived to adulthood and had normal sensory related patterns in their trigeminal pathway. *Nr1*$^{-/-}$ mice that had low levels of *NR1-1a* transgene expression (*NR1KD*) had a reduction of approximately 70% of *NR1* expression and lost all sensory-related patterns throughout the trigeminal pathway. Mice with mutation of the

asparagine 598 amino acid in the *NR1* protein sequence to arginine (N598R) generate receptors that do not permit Ca^{2+} to flow and are insensitive to Mg^{2+} (Single et al., 2000; Rudhard et al., 2003b). Mice that are $NR1^{N598R/N598R}$ die at birth with the same respiratory phenotype as the $Nr1^{-/-}$ mice. $NR1^{+/N598R}$ have approximately 25% of NMDARs containing wild-type *NR1* and the rest are Ca^{2+} impermeable, and $NR1^{-/N598R}$ mice have normal barrels, as determined by cytochrome oxidase histochemistry (Single et al., 2000; Rudhard et al., 2003b). This, along with the *NR1KD* mice suggests that a threshold level of NMDAR function is required for normal whisker-barrel pathway formation, although the threshold has yet to be determined for any of the different somatosensory relay stations within this pathway.

1.6.5.2 Cortex-specific NR1 mutant mice

Iwasato et al., (2000) generated a cortex-specific deletion of the *NR1* gene using the Cre/LoxP system (Sauer and Henderson, 1988; Kanegae et al., 1995; Tsien et al., 1996). They utilised the *Emx1* promoter which is expressed exclusively in the dorsal telencephalon from embryonic stages to adulthood (Gulisano et al., 1996) to drive *Cre recombinase* expression. This caused a deletion of *NR1* in virtually all of the excitatory neurons of the cerebral cortex, hippocampus and olfactory bulb, although *NR1* expression is left intact in the thalamus, brainstem, striatum and cerebellum. These mice survive to adulthood and barrelettes and barreloids appear normal in the brainstem and thalamus. However, in primary somatosensory cortex, cortical barrels were absent, despite segregation of TCAs in PMBSF (albeit into smaller, more rudimentary patches that correspond to the larger whiskers; smaller whisker representations are absent). This rudimentary TCA patterning could be due to activation of NMDARs present in cortical GABAergic cells that escaped the *NR1* deletion, which represent 15-20% of the total number of cells in the cortex (Iwasato et al., 2000). Whisker follicle lesion-induced TCA plasticity in $CxNr1^{-/-}$ mice aged between P0 and P3 is no different to that observed in wild-type mice, suggesting that TCA plasticity in the cortex occurs via mechanisms independent of postsynaptic NMDAR activity (Datwani et al., 2002a). This contrasts with the observation that pharmacological blockade of the NMDA receptor prevents anatomical barrel field plasticity (Fox et al., 1996; Mitrovic et al., 1996). The most likely explanation for the difference between the two results is that the NMDAR antagonist impregnated into an elvax and placed on the cortex escapes into the cerebrospinal fluid (CSF) and reaches the thalamus, preventing lesion-induced thalamic cell death.

Alternatively, when the NMDAR is knocked out, it is possible that the whole complex associated with the NMDAR is disrupted. However, pharmacological intervention may block the function of the NMDAR, but is unlikely to disrupt the protein complex associated with the NMDAR.

CxNr1$^{-/-}$ mice have layer IV cortical cells that exhibit profusely branched dendrites that have increases spine density (Datwani et al., 2002a). The Datwani *et al.* (2002a) paper reports that layer IV cortical cells in *CxNr1*$^{-/-}$ mice do not exhibit the selective dendritic elaboration towards TCA terminals seen in wild type mice, and based on this result they hypothesised that activation of NMDAR in dendrites by TCAs could cause preferential stabilisation of dendrites in barrel hollows. However, the method employed to investigate the dendritic phenotype in this paper was flawed. In wild type mice, only cells in the barrel wall exhibit selective dendritic orientation. However, up to thirty percent of cells in layer IV of PMBSF exist in the barrel hollow, and these cells do not exhibit any selective dendritic reorientation. The Datwani *et al.* (2002) paper sampled cells from layer IV, but since TCA patterning was not examined, they could not demonstrate that the cells chosen to examine dendrite orientation were from the region where the barrel wall should be. Since there is no selective cellular aggregation to form barrels in these mice; fewer cells are present in the cell wall region. This means that fewer cells are likely to exhibit selective dendritic orientation, and the investigators are less likely to choose a cell from the barrel wall region in that experiment. As such, the evidence from *CxNr1*$^{-/-}$ mice shows NMDARs play a crucial postsynaptic role in cortical cell movement, as barrels fail to form, but it cannot be concluded that NMDARs are required for selective dendritic elaboration towards TCA patches.

1.6.6 Metabotropic glutamate receptors, Phospholipase C-β1 and barrel formation

The metabotropic glutamate receptor (mGluR) family consists of eight single polypeptide chain receptors that function by coupling to G-proteins. In common with other G protein coupled receptors (GPCRs), mGluRs possess a seven-pass transmembrane domain motif and an extracellular N-terminus and intracellular C-terminus. mGluRs have been divided into three groups based on sequence similarities, signal transduction systems and pharmacology (Pin and Duvoisin, 1995, Figure 0.17).

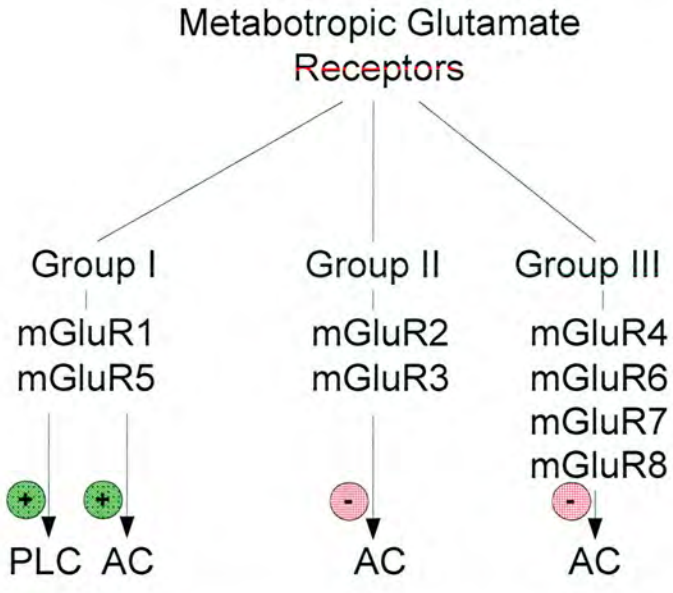

Figure 1.17
Classification of the different types of metabotropic glutamate Receptors. Group I mGluRs positively couple to PLC, whereas Group II and III mGluRs negatively couple to Adenylate Cyclase. Adapted from the MRC Centre for Synaptic Plasticity website, http://www.bris.ac.uk/synaptic/

mGluRs have also been implicated in cortical plasticity (reviewed in Maiese et al., 2005); phosphoinositide (PI) turnover initiated by mGluR stimulation correlates with the critical period in cat visual cortex, and Group I mGluRs (mGluR1 and mGluR5) have been implicated in hippocampal and cortical plasticity (Bortolotto et al., 1999), are essential for hippocampal LTD (Huber et al., 2000) and are present throughout the developing somatosensory pathway during the sensitive period (Blue et al., 1991; Romano et al., 1996; Munoz et al., 1999). *Mglur5*$^{-/-}$ mice display segregation of large whisker TCAs into rows but not individual patches within rows, and lack barrels (Hannan et al., 2001). This total loss of barrels, despite partial segregation of TCAs into whisker rows in PMBSF, signifies that mGluR5 signalling is crucial for the normal transfer of patterns from TCAs to their postsynaptic partners during barrel development, since no megabarrel is formed (Van der Loos H. and Woolsey, 1973). However, mGluR5 protein is found not only in cortex but also somatosensory thalamus and brainstem during barrel formation (Munoz et al., 1999). Genetic deletion in the *Mglur5*$^{-/-}$ mice occurs throughout the brain, so the position of the defect in barrel patterning within the somatosensory pathways cannot be determined, although barreloids are normal (Hannan et al., 2001) suggesting that the site of mGluR5 action during barrel formation is cortical.

Although presynaptic mGluRs that couple to PLC have been found in cortex (Sanchez-Prieto et al., 1996), the precise subtype thus far remains undetermined; mGluR5 immunoreactivity in adult mice appears to be entirely postsynaptic (Romano et al., 1996). If the barrel phenotype observed in *Mglur5*$^{-/-}$ mice is cortical, it could be that retrograde signalling is crucial for TCA pattern maintenance. Since the *Mglur5*$^{-/-}$ defect is different to that of *CxNr1*$^{-/-}$, this might indicate that more than one retrograde signal is required for proper TCA patterning (Erzurumlu and Kind, 2001).

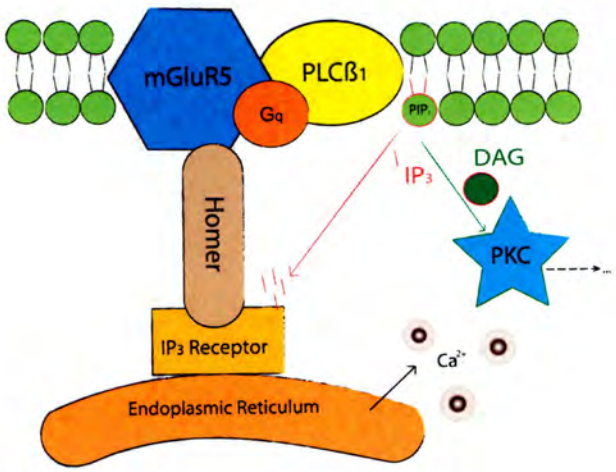

Figure 1.18
mGluR5 signals through PLCβ1 to form barrels. PLCβ1 hydrolyses phosphatidyl inositol 4,5 bisphosphate (PIP_2) into Diacylglycerol (DAG) and Inositol 1,4,5 triphosphate (IP_3); DAG can activate Protein Kinase C (PKC) and IP_3 causes the release of Ca^{2+} from the endoplasmic reticululm (ER) by activating the IP_3 receptor. mGluR5 binds Homer proteins that bind directly to the IP_3 receptor

1.6.7 PLCβ1 and barrel formation

In barrel cortex, mGluR5 has been shown to signal through PLCβ1 (Figure 1.18), as Phosphoinositide (PI) hydrolysis is drastically reduced in *Plc-β1*$^{-/-}$ mice following type I mGluR stimulation (Hannan et al., 2001). Furthermore *Plc-β1*$^{-/-}$ mice also lack barrels; cortical cell segregation does not occur, but TCAs do segregate into a barrel-like pattern (Section 1.3.2, Hannan et al, 2001). PLCβ1 is a postsynaptic G-protein-coupled phosphodiesterase that, on activation, hydrolyses phosphatidyl inositol 4,5-bisphosphate (PIP_2) into Diacylglycerol (DAG) and Inositol 1,4,5-triphosphate (IP_3); DAG can activate Protein Kinase C (PKC) and IP_3 causes the release of Ca^{2+} from the endoplasmic reticululm (ER) by activating the IP_3 receptor (Figure 1.18).

PLCβ$_1$ is highly expressed in layer II-IV of rodent S1 cortex during the first two postnatal weeks, with a periodicity and spatial location matching that of barrel formation (Hannan et al., 1998; Hannan et al., 2001). Interestingly, *Plc-β$_1^{-/-}$* mice demonstrated normal patterning, distribution and size of TCA patches in contrast to *Mglur5$^{-/-}$* mice where partial whisker row segregation of TCAs is observable only in PMBSF (Hannan et al., 2001). The difference in the TCA phenotypes between these two mutant mice indicates that mGluR5 regulation of TCA segregation occurs in a PLCβ$_1$-independent manner. Furthermore, mGluR5 is expressed at high levels in somatosensory thalamus but PLCβ$_1$ is not (Watanabe et al., 1998; Munoz et al., 1999) suggesting that mGluR5 in VpM in neurons may regulate TCA segregation. However, this defect seems not to result from a loss of segregation at lower levels in the trigeminal pathway; barreloids, as visualised by CO histochemistry appear normal in both *Mglur5$^{-/-}$* and *Plc-β$_1^{-/-}$* mice. This suggests that TCA segregation may be regulated by retrograde signals from layer IV under the control of mGluR5 in a similar manner to NMDARs (Iwasato et al., 2000), although a direct role of mGluR5 in the TCAs cannot be excluded. As mentioned above, studies using Rapid Golgi staining show that dendrites of *Plc-β$_1^{-/-}$* layer IV neurons are orientated toward TCA patches as normal (Upton et al., in preparation). This suggests that either dendritic reorientation does not require PLCβ$_1$ and selective dendritic reorientation within TCA patches is insufficient (although possibly necessary) to form barrels. Dendritic spine density is unaltered in *Plc-β$_1^{-/-}$* mice compared to wild-type, but a reduced symmetric/asymmetric synaptic ratio has been observed in layers II-IV of P5 *Plc-β$_1^{-/-}$* mutants, which may result in an imbalance in excitatory and inhibitory circuitry (Spires et al., in preparation). Furthermore, Spires et al. found that *Plc-β$_1^{-/-}$* mutants display a reduction in the number of mushroom-type dendritic spines that are present on layer V pyramidal neurons that pass through layer IV compared to age-matched wild-type mice. This is consistent with observations in the hippocampus that stimulation of group I mGluRs results in spine elongation (Vanderklish and Edelman, 2002) and that spine morphology is altered in response to Ca^{2+} release from intracellular stores. *Plc-β$_1^{-/-}$* signalling appears to be influential in the development of cortical connectivity by regulating dendritic spine shape and synapse formation, but not dendritic complexity or spine number, (Barnett et al., 2006a).

1.6.8 Potential mechanisms of mGluR5/ PLCβ$_1$ leading to barrel formation

The mechanism by which mGluR5 activates PLCβ_1 and regulates these cellular processes is unknown. One hypothesis is that PLCβ_1 effects changes to spine morphology via Homer proteins (Spires et al., 2005). Homers are multi-domain scaffolding molecules, three of which exist in the mouse genome, and can bind mGluR5/PLCβ_1 linking them to the IP_3R. Homers can link mGluR5 with the NRC by binding Shank, another scaffolding molecule that can associate with the GKAP/PSD-95 complex (Naisbitt et al., 1999; Tu et al., 1999), and Homers have been implicated in dendritic spine morphology changes (Sala et al., 2003). Mice that are null mutants for each individual or all *Homer* genes display normal cell segregation into barrels; barrel walls and septa appear normal (Barnett et al., 2006b). This suggests that the mechanism by which PLCβ_1 controls barrel development is Homer-independent and that IP_3 stimulated Ca^{2+} release from the ER is not crucial to barrel development. Another hypotheses is that DAG activation of PKC or a direct regulation of PIP_2 hydrolysis by PLCβ_1, plays the crucial step in barrel development (Barnett et al., 2006b). PKC has been shown to have a role in dendritic spine plasticity via its interaction with the Rho GTPases, Rac and Rho (Pilpel and Segal, 2004) and therefore is a good candidate molecule for further investigation into the biochemical pathways involved in barrel formation.

1.6.9 Adenylate Cyclase I and Protein Kinase A

The discovery that the gene *Adcy1* (Adenylate Cyclase I, AC1) was defective in the spontaneously occurring *barrelless* mouse strain (Welker et al., 1996; Abdel-Majid et al., 1998) gave the first clue to the signal transduction pathways involved in barrel formation. AC1 is a component of the NRC (Husi et al., 2000) and is present in mouse somatosensory cortex during barrel formation (Nicol et al., 2005). *Barrelless* mice do not exhibit segregation of TCAs into a barrel-related pattern, nor do layer IV cortical cells segregate into barrels and the overall thalamocortical projection field is reduced (Welker et al., 1996; Abdel-Majid et al., 1998). As such AC1 seems to be playing roles in both pre- and post-synaptic events required to form barrels. In the visual system, AC1 is required for the refinement of the retinotopic map (Ravary et al., 2003; Nicol et al., 2006) and is also required for EphrinA5-dependent retraction of exuberant retinal axons (Nicol et al., 2006). *Ephrina5*$^{-/-}$ mice have distinct barrels, but display both a distorted face map and distorted alignment of TCAs in this region, although any requirement of AC1 in TCA mapping has not yet been investigated.

AC1 is a Ca^{2+} and Calmodulin-sensitive adenylyl cyclase. On stimulation of NMDAR, Ca^{2+} entry and Calmodulin binding activates AC1, converting adenosine triphosphate (ATP) to cAMP, a ubiquitous second messenger found in all cells. cAMP opens cyclic mononucleotide gated channels (Wei et al., 1998) but its best characterised role is activation of PKA. In the absence of cAMP, PKA is found as heterodimer comprising of paired catalytic (C, either Cα or Cβ) and regulatory (R, RIα, RIβ, RIIα or RIIβ) subunits. R subunits bind and inactivate the C subunits. When cAMP binds the regulatory subunits (with a stoichiometry of 2 cAMP : 1R), a conformational change occurs, causing a 10^{-3} to 10^{-5}-fold reduction in affinity for the catalytic units, whereupon the PKA tetramer dissociates, freeing the catalytic subunits and allowing protein phosphorylation at serine or threonine residues contained in a –RRxSX- motif on the target protein (Stryer, 1995). Phosphorylation of proteins by PKA (and other kinases) and dephosphorylation by protein phosphatases play key regulatory roles in LTP and LTD (Malenka and Bear, 2004).

Disrupted gene knockout mice are available for all PKA subunit isoforms, except PKARIα, which is embryonic lethal. Our laboratory has recently demonstrated barrel morphology is affected in *Pkar2β*$^{-/-}$ mice (Watson et al., 2006b). These mice have a 40% reduction in PKA activity in cortex, have poorly defined barrels and the septa and barrel hollows do not display the reduction in number of cells seen in wild-type animals (Inan et al., 2006; Watson et al., 2006b). The ratio of cells in the barrel wall to barrel hollow in wild-type mice is 1.8:1, yet in *Pkar2β*$^{-/-}$ mice this ratio is 1.3:1 (Watson et al., 2006b). However, *Pkar2β*$^{-/-}$ mice show good segregation of TCAs in PMBSF, whilst *barrelless* (*Adcy1*$^{-/-}$) mice segregate extremely poorly. Recently PKARIIβ has been shown to be expressed exclusively postsynaptically in layer IV post-synaptic densities (Watson et al., 2006b) and *Pkar2β*$^{-/-}$ mice exhibit a significant reduction in phosphorylation of postsynaptic but not presynaptic PKA targets (Inan et al., 2006). In addition, the dendrites of layer IV spiny stellate cells do not exhibit selective orientation in towards the TCA plexus that occurs in wild-type mice (Figure 1.19). However, the same defect in the interpretation of the *CxNr1*$^{-/-}$ layer IV cortical cell phenotype (Datwani et al., 2002b) is evident in the Inan et al., (2006) paper. No attempt was made to determine the localisation of TCA terminals in layer IV cortex, and therefore determining the location of cells that are in the area where the barrel wall should be (i.e. the only cells that would normally orient their dendrites into the TCA plexus) cannot be performed. Cells that are not in the barrel wall region will not exhibit selective dendritic orientation, and since no cellular segregation has occurred, fewer cells are to be found in the

barrel wall region. Thus, most *Pkar2β*$^{-/-}$ cells chosen for dendritic analysis in the Inan et al., (2006) paper are bound to exhibit a dendritic phenotype of no selective orientation.

Adcy1$^{-/-}$ mice have defects in LTP, seemingly due to a defect in PKA-dependent phosphorylation of AMPA receptors (AMPAR) and trafficking to the synapse. *Pkar2β*$^{-/-}$ mice also have impaired LTP (Lu et al., 2003) and exhibit reduced incorporation of GluR1 AMAPR subunits into layer IV postsynaptic densities. Cortex-specific knockouts of *Adcy1* have normal barrels (Iwasato et al., 2006, Society for Neuroscience 2006 Meeting abstract). Taken together, these results suggest that the effects of AC1 are presynaptic, that cAMP has a presynaptic effect which would occlude, but not preclude, any postsynaptic effect involving PKA containing the PKARIIβ subunit, and that the *Pkar2β*$^{-/-}$ defect is postsynaptic.

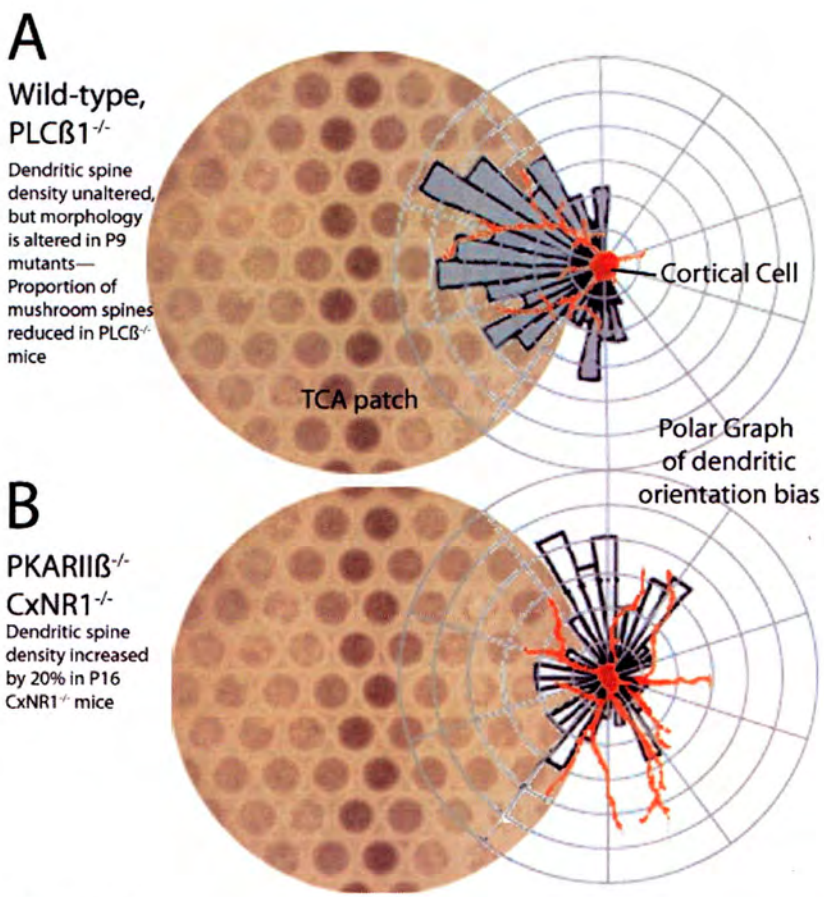

Figure 1.19
Known dendritic orientation in barrels in wild-type and mutant mice. A. Wild-type and *Plc-β*$_1$$^{-/-}$ mice. Dendrites of layer IV spiny stellate cells orient towards the TCA patch plexus. B. No specific orientation of layer IV cortical cell dendrites is observable in *Pkar2β*$^{-/-}$ mutants. The polar graphs and dendrites (red) are adapted from Inan et al., (2006) and are only present to illustrate dendritic orientation bias.

1.7 The NMDA Receptor complex

The traditional view of the NMDA receptor was that depolarisation of the membrane surrounding the NMDAR (usually by sustained activation of AMPA receptors) removes the Mg^{2+} block of the NMAR channel and allows ions (mostly Ca^{2+}) to flow following NMDA receptor activation by glutamate (Nowak et al., 1984; Kleckner and Dingledine, 1991). Ca^{2+} entry to the cell then causes Ca^{2+}-dependent signalling events to occur (MacDermott et al., 1986; Kleckner and Dingledine, 1991; Xia et al., 1996; Rang et al., 1997; Zhang et al., 1998). Subsequent discoveries (outlined below) have demonstrated that the composition of the proteins that associate with the postsynaptic NMDAR (which can determine the response of the cell to glutamate) can change dynamically in response to activity, other developmental cues and the molecular history of the cell.

The cytoplasmic tails of NMDA receptor subunits interact with postsynaptic proteins, such as the scaffolding molecules PSD-95 (Kornau et al., 1995; Wyszynski et al., 1997; Allison et al., 1998; Hughes et al., 2001; Rutter et al., 2002; Lim et al., 2002; Papadakis et al., 2004; Ying et al., 2004) and SAP-102 (Kim et al., 1998; Cai et al., 2002; Lim et al., 2002). The cluster of proteins that the C-termini of the NR-subunits bind to is often referred to as the NMDA Receptor Complex (NRC). The identification of NRC components has been attempted by two main methods: initially, yeast two-hybrid screening (Kornau et al., 1995; Kim et al., 1995) and more recently a mass spectrometery method (Walikonis et al., 2000; Husi et al., 2000). The latter method involves immunoprecipitation of NR1 or NR2A subunits that are still bound to their associated proteins, proteolytic digestion of the components, Matrix-Assisted Laser Desorption Ionization Time of Flight (MALDI-TOF) mass spectrometry of the fragments and computer-based reconstruction of the PSD components from the patterns of peaks generated (Walikonis et al., 2000; Husi et al., 2000). To date, the PSD has been shown to contain mostly receptors, scaffolding proteins, signalling enzymes, cytoskeletal components and adhesion molecules (Walikonis et al., 2000; Husi et al., 2000).

Over 200 proteins have been shown to bind to NMDAR subunits and their scaffolding partners (Walikonis et al., 2000; Husi et al., 2000; Sheng, 2001), as illustrated in Appendices A and B. The NRC has been shown to be a dynamic complex; the proteins bound change throughout development and in response to synaptic input (Petralia et al., 2005) and this dynamic structure is an attractive model for the organisation of postsynaptic signalling. One can envisage the appropriate enzymes and substrates being held in place, ready to respond to

the entry of Ca^{2+} through the NMDAR, allowing specific and local intracellular signalling. For example, the PKARIIβ–AKAP–PSD-95 complex has been shown to associate with the NRC in a Ca^{2+}-dependent manner (Colledge et al., 2000; Snyder et al., 2005) Ca^{2+}-entry has been shown to cause the dissociation of PKARIIβ from the NRC in S1 cortex (Watson et al., 2006b). In essence, the specificity in signalling arises from the proteins that have been incorporated into the NRC that supports and surrounds that particular NMDAR (this is sometimes termed "the memory of the synapse").

1.7.1 NRC scaffolding molecules

The frame on which the NRC is built is composed of groups of scaffolding molecules, such as A-Kinase anchoring proteins (AKAPs), homers, shanks, citron, guanylate kinase-associated proteins (GKAPs), synapse associated protein(SAP)90/PSD-95-associated Protein (SAPAPs) and the Membrane Associated Guanylate Kinases (MAGUKs). MAGUKs interact with both membrane bound proteins (such as NR subunits of the NMDA receptor and cytoplasmic proteins) and help form multi-protein complexes at sites of epithelium cell-cell contact (Makino et al., 1997; Hanada et al., 2000) and at synaptic junctions of neuronal cells (Makino et al., 1997).

MAGUKs contain three distinct domains:

1. **PDZ** (PSD-95/Dlg/ZO-1) that bind the consensus sequence: `T/SXV` on target proteins. PDZ domains consist of 80-90 amino. Different PDZs possess different binding specificities.
2. **SH3** (Src homology 3) that bind to target proteins through sequences containing proline and hydrophobic amino acids.
3. **GK** (Guanylate Kinase-like) that are inactive as a kinase but bind other scaffolder molecules such as GKAPs and SAPAPs at excitatory synapses and also importantly AKAP150, which binds PKARIIβ.

Each domain can interact with various proteins giving dynamic multiprotein complexes, and each MAGUK can perform distinct cellular functions and associate with different molecules, depending on its temporal and spatial expression (reviewed in Dimitratos et al., 1999; Kim and Sheng, 2004). PSD-95 is widely expressed in the postsynaptic densities throughout the developing and adult brain (Fukaya and Watanabe, 2000), Wijetunge et al, 2006) and binds NR2A and NR2B subunits (Kornau et al., 1995; Niethammer et al., 1996).

1.7.2 MAGUKs during barrel formation

Levels of PSD-95 and SAP-102 in barrel cortex vary during the first postnatal week. PSD-95 levels are initially low and SAP-102 levels are relatively high when barrels are forming (Wijetunge et al, 2006), but levels of PSD-95 steadily rise over the next fortnight becoming the major MAGUK present in barrel cortex, whereas SAP-102 levels remain constant (Barnett et al., 2006a), see Figure 1.20.

1.7.3 Differential binding of SAP-102 and PSD-95 by NR2 subunits

Martha Constantine-Paton and colleagues note that in developing visual cortex the predominant NR2 subunit in the NMDAR is NR2B in immature synapses (Quinlan et al., 1999; Philpot et al., 2001a; Philpot et al., 2001b; van Zundert et al., 2004). As the synapse matures, the predominant NMDAR subunit becomes NR2A (van Zundert et al., 2004). NR2B-containing NMDARs have longer open-probabilities and longer-lasting series of channel opening and closing events than NR2A-containing NMDARs (Hollmann and Heinemann, 1994; McBain and Mayer, 1994; Dingledine et al., 1999), and it is thought that NR2B is preferentially bound by the MAGUK SAP-102, whereas NR2A is preferentially bound by PSD-95 (Shi et al., 1997; Sans et al., 2000; Yoshii et al., 2003). Constantine-Paton and colleagues suggest that since the neonate NRC is rich in the NR2B subunit, which binds the whole receptor to SAP-102, and that this complex is constitutively inserted into the synaptic membrane (Sans et al., 2003). Increases in afferent activity leads to postsynaptic neurons responding by synthesizing PSD-95 and inserting it into the centre of the postsynaptic density, whereupon PSD-95 binds the C-terminal of the NR2A subunit (van Zundert et al., 2004). NMDARs can exist that contain NR2A and NR2B (in addition to the obligatory NR1 subunit). Such NMDARs will bind both MAGUKs, before expression of NR2A overwhelms NR2B levels. PSD-95 is thought to stabilize GluR1 AMPA receptors (AMPAR) by binding, recruiting and stabilizing the stargazin-GluR1 complex to the NRC (Chen et al., 2000; van Zundert et al., 2004). Furthermore, NR2B containing NMDARs have been shown in hippocampal neuron cultures to inhibit the surface expression of GluR1 by regulation of insertion into the synapse, and this is mediated by SynGAP inhibition of the Ras-ERK pathway (see below; Kim et al., 2005).

Notably, the Husi *et al.*, 2000 screen of NRC components did not find AMPAR in the NRC, although this may have been due to technical considerations. Since NMDARs can be linked to AMPAR via two protein interactions (NMDAR-PSD-95-Stargazin-AMPAR; Kornau et

al., 1997) this suggests that the interactions between AMPAR and NMDAR are too weak to survive the immunoprecipitation and MALDI-TOF experimental conditions used in the Husi et al., 2000 paper.

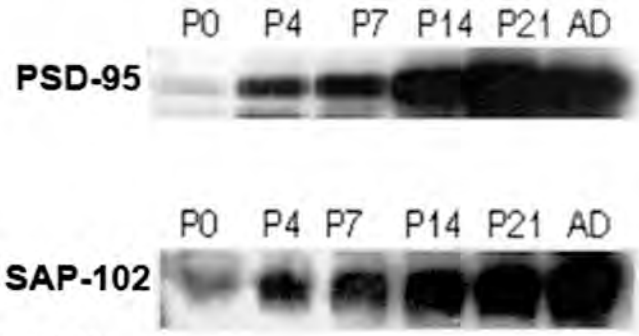

Figure 1.20
Western Blot showing SAP-102 and PSD-95 protein levels in barrel cortex homogenate over the timecourse of barrel development. PSD-95 is expressed in lowest amounts at P0 (the period when TCAs arrive in layer IV), and expression levels increase over development. SAP-102 protein is highly abundant during the first postnatal week, especially after P0, at P4 and P7; after that expression remains uniformly high (Barnett et al., 2006a).

In addition to binding NMDAR subunits and AMPAR, PSD-95 can bind shaker-type potassium channel subunits and many other scaffolding molecules, enzymes and receptors, such as other PSD-95 or SAP-102 molecules, nNOS (Brenman et al., 1996a) and certain Frizzleds (Hering and Sheng, 2002). A list of molecules that interact with PSD-95 and are pertinent to this thesis is presented in Table 1.1 and a full list of PSD-95 interaction partners is presented in Appendix C.

Table 1.1
List of names of interaction partners of PSD-95 in the literature. For full list of interaction partners, types of interaction and references, see Appendix D.

Name of Interactor	Experiment Type	Reference
Frizzled 1	*In vivo*, Yeast 2 Hybrid	Hering and Sheng, 2002
Frizzled 2	*In vivo*, Yeast 2 Hybrid	Hering and Sheng, 2002
Frizzled 4	*In vivo*, Yeast 2 Hybrid	Hering and Sheng, 2002
Frizzled 7	*In vivo*, Yeast 2 Hybrid	Hering and Sheng, 2002
APC	*In vivo, In vitro*, Yeast 2 Hybrid	Kiyono et al., 1997, Yanai et al., 2000
SynGAP	*In vivo, In vitro*, Yeast 2 Hybrid	Kim et al., 1998
SAP-102	*In vivo, In vitro*, Yeast 2 Hybrid	Masuko et al., 1999
PSD-95	*In vivo*	Hsueh et al., 1997
NR1	*In vivo, In vitro*	Rutter et al., 2002, Allison et al., 1998, Hughes et al., 2001, Papadakis et al., 2004, Ying et al., 2004, Wyszynski et al., 1997
NR2A	*In vivo, In vitro*, Yeast 2 Hybrid	Kornau et al., 1995,
NR2B	*In vivo, In vitro*, Yeast 2 Hybrid	Kornau et al., 1995, Niethammer et al., 1998, Lim et al., 2002
NR2C	*In vivo, In vitro*, Yeast 2 Hybrid	Kornau et al., 1995, Lim et al., 2002
NR2D	*In vivo, In vitro*, Yeast 2 Hybrid	Kornau et al., 1995
NR3A	*In vivo, In vitro*, Yeast 2 Hybrid	Kornau et al., 1995
NR3B	*In vivo, In vitro*, Yeast 2 Hybrid	Kornau et al., 1995
Nitric oxide synthase 1	*In vivo*, Yeast 2 Hybrid	Brenman et al., 1996a
Guanylate cyclase1 soluble α2	*In vivo, In vitro*	Russwirm et al., 2001
MAP1A	*In vivo, In vitro*, Yeast 2 Hybrid	Brenman et al., 1996b
5-HT-2A & 2C receptor	*In vivo, In vitro*	Xia et al., 2003, Becamel et al., 2002
Chapsyn110	*In vivo*	Hsueh et al., 1997
A kinase anchor protein 5	*In vivo, In vitro*	Colledge et al., 2000

SAP-102 is widely expressed throughout the brain, throughout development and into adulthood, and notably SAP-102 is present in the postsynaptic densities of somatodendritic bodies and dendritic spines of the cortex, hippocampal dendritic shafts, spines of asymmetric type I synapses (Makino et al., 1997; Fukaya and Watanabe, 2000), and is enriched in synaptosome preparations (Muller et al., 1996). Like PSD-95, it is promiscuous in the molecules it binds, as listed in Table 1.2.

Table 1.2.
Interaction partners of SAP-102 in the literature

Name Of Interactor	Experiment Type	Type	Reference
NR1 (via SynGAP)	In vivo	Complex	(Kim et al., 1998)
NR2A	In vivo, In vitro	Direct	(Choi et al., 2002; Cai et al., 2002)
NR2B	In vitro, In vivo	Direct	(Lim et al., 2002)
NR2C	In vitro, In vivo	Direct	(Lim et al., 2002)
PSD-95	In vitro, In vivo, Yeast 2 Hybrid	Direct	(Masuko et al., 1999)
Calmodulin	In vitro, In vivo, Yeast 2 Hybrid	Direct	(Masuko et al., 1999)
SynGAP	In vitro, In vivo, Yeast 2 Hybrid	Direct	(Kim et al., 1998)
PSD-95	In vivo, In vitro	Direct	(Karnak et al., 2002)
Discs large associated protein 4	Yeast 2 Hybrid	Direct	(Takeuchi et al., 1997)
Synaptic Ras GTPase activating protein 1	Yeast 2 Hybrid	Direct	(Kim et al., 1998)
Kainate 2	In vitro	Direct	(Cai et al., 2002; Lim et al., 2002)
Low density lipoprotein related protein 2	In vitro, Yeast 2 Hybrid	Direct	(Larsson et al., 2003)
ErbB4	In vivo, In vitro, Yeast 2 Hybrid	Direct	(Garcia et al., 2000; Huang et al., 2002)
Postsynaptic protein CRIPT	In vivo, In vitro, Yeast 2 Hybrid	Direct	(Lim et al., 2002)
Guanylate cyclase 1 soluble alpha 2	In vitro	Direct	(Russwurm et al., 2001)
Veli 1	In vitro	Direct	(Butz et al., 1998)
Plasma membrane Ca2+ ATPase type 4	In vitro, In vivo, Yeast 2 Hybrid	Direct	(DeMarco and Strehler, 2001)
SEC8 like 1	In vivo	Complex	(Sans et al., 2003)
Focal adhesion kinase 2	In vivo, In vitro	Direct	(Seabold et al., 2003)
Cypin	In vivo, In vitro	Direct	(Kuwahara et al., 1999)
SEC8 like 1	In vitro, Yeast 2 Hybrid	Direct	(Sans et al., 2003)
Neuroligin 3	Yeast 2 Hybrid	Direct	(Irie et al., 1997)
Semaphorin 4C	In vitro, Yeast 2 Hybrid	Direct	(Inagaki et al., 2001)

An up-to-date schematic of interactions of NRC components identified in the Husi *et al.*, (2000) paper is presented in Appendix B.

1.8 NMDAR signalling pathways and barrel formation

Many of the molecules involved in barrel formation are members of the NRC. Genetic knockouts of certain NRC components (including *Plc-β1*, which is discussed above) results in altered barrel phenotypes, as detailed below.

1.8.1 PSD-95 and SAP-102 mutants

Psd-95 mutants do not exhibit an altered barrel phenotype, (Barnett et al., 2006a) although these mice have altered hippocampal LTP, defects in their ability to complete spatial memory tasks (Migaud et al., 1998) and impaired NMDA-mediated plasticity in the visual cortex (Fagiolini et al., 2003). However, PSD-95 mutant mice have normal synaptic localisation of NMDAR and no alterations in NMDA-evoked currents (Migaud et al., 1998). Two possible explanations for the normal barrel phenotype in *Psd-95* mutants are: NMDA receptor complexes are not required for barrel formation or alternatively, compensatory upregulation of other MAGUKs such as SAP-102 occurs. In support of this latter interpretation, Migaud and colleagues found that NMDARs and other proteins are still trafficked to the postsynaptic density in *Psd-95*$^{-/-}$ mice; i.e. the postsynaptic density remains intact.

SAP-102 is most highly expressed in barrel cortex between P0 and P4 (Barnett et al., 2006a; see Figure 1.20), which is the period encompassing TCA arrival in layer IV of the cortex and the initial cellular segregation events to form barrels occurs. Furthermore, SAP-102 binds preferentially to SynGAP (Kim et al., 1998; Kim et al., 2005), and Synaptic Ras-GTPase Activating Protein (SynGAP) plays a role in barrel formation (Barnett et al., 2006a). No *Sap-102*$^{-/-}$ phenotype has yet been published, but these mice would be good candidates to have an altered barrel phenotype.

1.8.2 SynGAP and barrel formation

SynGAP (Chen et al., 1998) is an NRC component (Husi et al., 2000) that interacts directly with the PDZ domains of PSD-95 (Kim et al., 1998; Chen et al., 1998) and regulates levels of phosphorylated ERK (Komiyama et al., 2002), most likely by regulating levels of Ras-GTP (Chen et al., 1998, Figure 1.21). Interestingly, SynGAP is still present in barrel cortex in PSD preparations made from *Psd-95*$^{-/-}$ mice, suggesting that either SynGAP is binding other MAGUKs, such as SAP-102 (Kim et al., 1998) to tether it to the PSD. *Syngap* mRNA and SynGAP protein are expressed in developing primary somatosensory cortex and at highest levels in layer IV during barrel formation (Barnett et al., 2006a). *Syngap*$^{-/-}$ mice have lack barrels—no cellular segregation occurs, and TCAs segregate into rows but not into barrel-associated patches; and barreloids in VpM thalamus are poorly segregated (Barnett et al., 2006a). *Syngap*$^{+/-}$ mice exhibit reduced barrel segregation compared to wild-type mice, yet have normally segregated TCAs and normal barreloids (Barnett et al., 2006a).

Syngap is a heteromeric mRNA consisting of three known N-terminal (a, b, c) and seven known C-terminal (α1, 2, β1–4, γ) isoforms (Li et al., 2001). *Syngapα1* was the first *Syngap* isoform to be discovered and characterised (Kim et al., 1998; Chen et al., 1998). *Syngapα2* localises to axons in cultured cerebellar neurons (Tomoda et al., 2004). Barnett and colleagues used primers that amplified all 3' isoforms of Syngap and performed RT-PCR, sequenced and cloned *Syngap* mRNAs from VpM thalamus, and found 17 *Syngap* splice variants, but could not detect the axon-associated isoform *Syngapα2*. This result suggests that SynGAP expression is not present in TCAs.

Since TCAs in *Syngap*$^{-/-}$ mice form rows but not individual patches suggests that the cortical defect in *Syngap*$^{-/-}$ mice is secondary to thalamic defects. However, a cortical role for SynGAP in barrel formation is indicated, as *Syngap*$^{+/-}$ animals exhibit a significant reduction in barrel segregation, despite normal segregation of TCAs into whisker-related patches. Furthermore, in *Syngap*$^{-/-}$ mice, TCAs segregate into rows, but no megabarrel forms around these rows (Van der Loos and Woolsey, 1973b), as would have been expected if barrel formation is independent of cortically expressed Syngap.

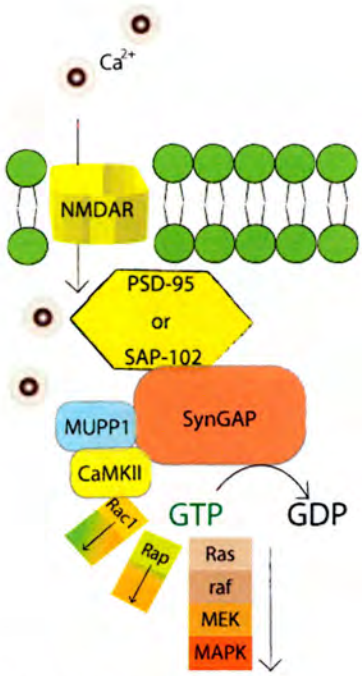

Figure 1.21
SynGAP is a Ras-, Rac- and Rap-GTPase that regulates barrel and barreloid formation. SynGAP is directly bound by the PDZ domains of PSD-95 or SAP-102, which directly bind the NMDAR. Thus SynGAP activation is likely to result from NMDAR activation. SynGAP can act as a Ras-, Rac- or Rap-GTPase. When SynGAP is phosphorylated, it can form a complex with MUPP1 and CaMKII and act as a Rac1-GTPase.

The SynGAP substrate in barrel formation was thought to be the small G-protein H-Ras, however *h-ras*$^{-/-}$ mice have normal barrels. There are many other Ras isoforms that could be the substrate of SynGAP during barrel development. SynGAP can also act as a Rab-GTPase (Tomoda et al., 2004) or Rap-GTPase (Krapivinsky et al., 2004), and when phosphorylated, forms a complex with MUPP1 and CaMKII (Krapivinsky et al., 2004). When SynGAP is dephosphorylated, it dissociates from the complex with MUPP1 and CaMKII and causes an inactivation of Rap and subsequent increase in p38MAPK activity. p38MAPK is therefore another potential signalling cascade by which SynGAP could be regulating barrel formation. SynGAP also regulates Rab5 activity; Rab5 has been shown to regulate vesicle trafficking (Miaczynska et al., 2004) and actin cytoskeleton dynamics (Lanzetti et al., 2004), so it is possible that other small non-Ras G-proteins are crucial effectors of SynGAP during barrel development.

The main signalling pathways involved in barrel formation are summarised in Figure 1.22.

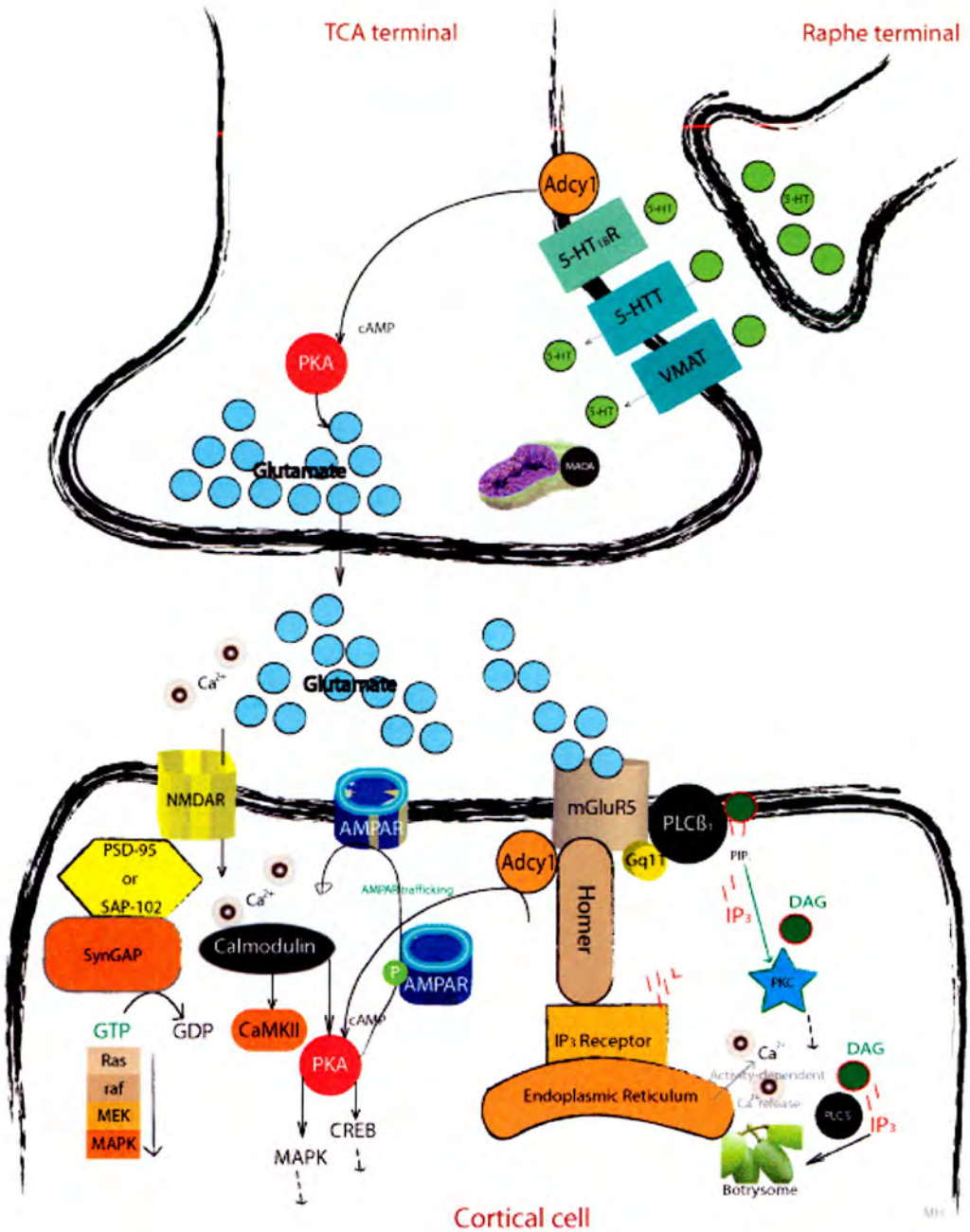

Figure 1.22
Putative intracellular signalling pathways involved in barrel differentiation. Research on transgenic mice suggests two gross subdivisions of neurotransmitter systems that are crucial for normal barrel development: presynaptic serotonergic receptor activity and postsynaptic glutamatergic receptor activity. Furthermore, the intracellular pathways downstream of these receptors are beginning to be elucidated. Abbreviations: AdCyl, adenylyl cyclase; BDNF, brain-derived neurotrophic factor; CaMKII, Ca^{2+}–calmodulin kinase type II; CREB, cAMP response element binding protein; DAG, diacylglycerol; IP_3, inositol (1,4,5)-trisphospate; MAPK, mitogen activated protein kinase; MGLUR5; metabotropic glutamate receptor 5; NMDAR, NMDA receptor; AMPAR, AMPA receptor, PIP_2, phosphatidylinositol (4,5)-bisphosphate; PKA, protein kinase A; PKC, protein kinase C; $PLC\beta_1$, phospholipase C-β1; TCA, thalamocortical axon terminals; VMAT, vesicular monoamine transporter. Text from Erzurumlu and Kind, 2001.

1.8.3 ERK and barrel development

The discovery of a role for SynGAP in barrel development agrees with previous findings that the ERK pathway is involved in many forms of NMDAR-dependent synaptic plasticity (Sweatt, 2001), including monocular deprivation (MD) induced shifts in ocular dominance in visual cortex (Di Cristo et al., 2001). NMDAR activation increases levels of pERK, and one way of achieving this rise is by inhibiting the activity of SynGAP, which would increase Ras-GTP levels and therefore ERK phosphorylation (Chen et al., 1998; Kim et al., 2003b). However, NMDAR stimulation activates CaMKII, and SynGAP phosphorylation by CaMKII increases the RasGAP activity of SynGAP by 70-95% (Oh et al., 2004). Therefore SynGAP activity would be expected to increase following NMDAR stimulation and reducing levels of pERK. However, in *Syngap*$^{+/-}$ hippocampal slices, basal pERK and NMDAR-mediated pERK levels are increased, supporting the hypothesis that SynGAP regulates the ERK pathway. These findings indicate that ERK can still be phosphorylated in an NMDAR-dependent manner in the absence of SynGAP, perhaps via PKA or PKC-dependent pathways. Perhaps NMDAR stimulation causes simultaneous activation of SynGAP-dependent and SynGAP-independent pathways to regulate the precise levels of Ras-GTP and pERK, with the SynGAP/CaMKII pathway negatively regulating ERK phosphorylation and the SynGAP-independent pathway modulating ERK phosphorylation. Reduction or removal of SynGAP would therefore result in an increase in NMDAR stimulated pERK levels, as less or no SynGAP-mediated inhibition of NMDAR/CaMKII-activated ERK phosphorylation would occur.

It is thought that ERK can function as an integrator of signals that originate from a variety of sources to produce coordinated cellular events (as reviewed in Adams and Sweatt, 2002). In order to form barrels, the activation of many receptors (NMDA and mGluR5), which activate numerous intracellular signalling pathways (PLCβ_1, PKA, SynGAP) are required to form barrels (Barnett et al., 2006b). It is therefore an attractive hypothesis that ERK is acting to integrate these signals to mediate barrel formation. Indeed, the ERK pathway can be activated by mGluR5 (Choe and Wang, 2001; Berkeley and Levey, 2003; Gallagher et al., 2004), PKA (Cancedda et al., 2003b), and PKC (Sweatt, 2004) activity. Disruption of any of these signalling pathways may sufficiently alter ERK activity to disrupt barrel formation, in a similar manner to blocking ERK activation using MEK inhibitors prevents ocular dominance plasticity to MD in visual cortex (Di Cristo et al., 2001) and LTP in hippocampus (Sweatt, 2001).

1.9 Conclusions

It is thirty-six years since Thomas Woolsey and Henrik Van der Loos published their description of barrels in layer IV of S1 cortex (Woolsey and Van der Loos, 1970) and in this time, the role of neuronal activity and the key neurotransmitters involved in TCA and cortical cell pattering have been identified (serotonin and glutamate, respectively). The development of genetic knockout mice has enabled the dissection of the biochemical signalling pathways that play roles in barrel formation. However, many aspects of barrel development remain uninvestigated, such as the dendritic structure of cortical cells in barrel walls in mice younger than P7, or proper investigation of the dendritic phenotypes of all mouse mutants with barrel defects other than *Plc-$\beta_1^{-/-}$* (Upton et al., in preparation). The advent of conditional mouse mutants has enabled the examination of barrels in mice that only lack expression of the conditionally deleted gene in cortex; this permits not only examination of the effects of genes that would ordinarily be embryonically or perinatally lethal in cortex, but also enables dissection of whether a molecule is acting presynaptically (i.e. expressed in TCAs) or postsynaptically (in cortical cells), such as the cortex-specific knockout of *Adcy1* (Iwasato et al., 2006) which has helped confirm that AC1 mediates its effects presynaptically. Research into barrel cortex development will be immensely aided by this technique in the near future.

1.10 Wnts

The Wnt signalling pathway is highly conserved throughout evolution and plays a critical role in normal development in diverse species from *Caenorhabditis elegans* to human. The first Wnt gene to be discovered was *Wingless/Int1* (Wnt1; Nusse and Varmus, 1982). *Wnt1* was first characterized as a proto-oncogene as inappropriate expression caused mammary tumours in mice. Since then, nineteen Wnt genes have been discovered in the mouse genome (reviewed in Miller, 2002 and Roel Nusse's Wnt gene homepage, http://www.stanford.edu/~rnusse/wntwindow.html). Wnt proteins have a conserved pattern of 23-24 cysteine residues, are between 350 and 380 amino acids in length and almost all are cysteine-rich, secreted signalling molecules that tend to associate with the extracellular

matrix. Wnt proteins play roles in regulating embryonic patterning, cell proliferation and cell fate determination (reviewed in Wodarz and Nusse, 1998; Nusse, 2005; Logan and Nusse, 2004; Ciani and Salinas, 2005).

Inappropriate activation of Wnt signalling is implicated in many cancers, including mammary and colorectal cancers and retinoblastoma (reviewed in Polakis, 2000; van Es et al., 2003). Recently, it has been hypothesised that Wnt signalling may be dysregulated in people with schizophrenia. It has been shown that levels of a Wnt-signalling pathway kinase, GSK-3β are reduced in the prefrontal cortex in schizophrenic patients (Kozlovsky et al., 2001; Beasley et al., 2001; Kozlovsky et al., 2005). In addition, alterations of *Wnt-1* and β-catenin levels have been found in the hippocampus of schizophrenic patients (Cotter et al., 1998; Miyaoka et al., 1999), suggesting that defects in schizophrenic brains might be related to dysregulation of Wnt signalling.

1.10.1 The mouse Wnt signalling pathways

Wnt proteins bind with high affinity to the Frizzled (Fz) family of seven pass transmembrane proteins, of which ten are known in the mouse genome (Hsieh et al., 1999b). Wnt access to Fz receptors can be blocked by various secreted proteins, such as WIF-1, cerberus and the secreted Frizzled-related protein (sFRP) family (Hsieh et al., 1999a; Hsieh et al., 1999b). Depending on the combination of Wnt, Frizzled and both intra- and extra-cellular environments, the transduction of the Wnt signal can proceed by the following mechanisms, summarised in Figure 1.23.

1.10.2 Canonical/ β-catenin pathway

The canonical signalling pathway was originally characterised as: Wnt protein binds a Frizzled receptor (Bhanot et al., 1996), to signal through the cytoplasmic scaffold protein, Dishevelled (Dvl; Wharton, Jr., 2003). Dvl causes the inhibition of GSK-3β mediated phosphorylation and subsequent degradation of β-catenin, which then accumulates, translocates to the nucleus, binds T-cell specific transcription factor (TCF) and the β-catenin-TCF complex causes transcription of target genes (reviewed in Logan and Nusse, 2004). Notably, in BAT-gal mice, where β-galactosidase is provided as an artificial substrate

for the TCF/LEF factors activated by Wnt/β-catenin pathway signalling, strong staining is observed throughout the neocortex (Maretto et al., 2003).

Further complexities within this pathway have been discovered. Within the canonical Wnt signalling pathway there is an absolute requirement for members of the low-density lipoprotein-related receptor family, LRP5 or LRP6 to be present at the membrane with Frizzled (Wehrli et al., 2000; Pinson et al., 2000; Tamai et al., 2000a; Tamai et al., 2000b; Mao et al., 2001); reviewed in Miller, 2002; Ciani and Salinas, 2005; Bafico et al., 2001; Nusse, 2005). LRP5/6 receptors are antagonised by members of the Dickkopf (Dkk) family (Bafico et al., 2001), which are potent secreted Wnt antagonists that bind with high affinity to Kringle-containing transmembrane protein (Kremen)-1 or Kremen-2 receptors (Mao et al., 2002). Dkk antagonises Wnt signalling by forming a ternary complex with Dkk1 and LRP6, which induces rapid endocytosis and removal of the Wnt coreceptor LRP6 from the plasma membrane. Wnt signal transduced through Frizzled causes the scaffold protein Dishevelled (Dvl) to be shuttled to the β-catenin destruction complex (Wharton, Jr., 2003) and reviewed extensively in Logan and Nusse, (2004).

Mammalian RYK functions as a co-receptor along with Frizzled for Wnt ligands (Lu et al., 2004; Inoue et al., 2004). RYK binds Dishevelled, activating the canonical Wnt pathway, providing a link between Wnt and Dvl that does not require Frizzled. Transgenic mice expressing RYK small interfering RNA (siRNA) exhibit defects in axon guidance and RYK was required for Wnt3a-induced neurite outgrowth and in Wnt1-induces the activation of TCF (Lu et al., 2004).

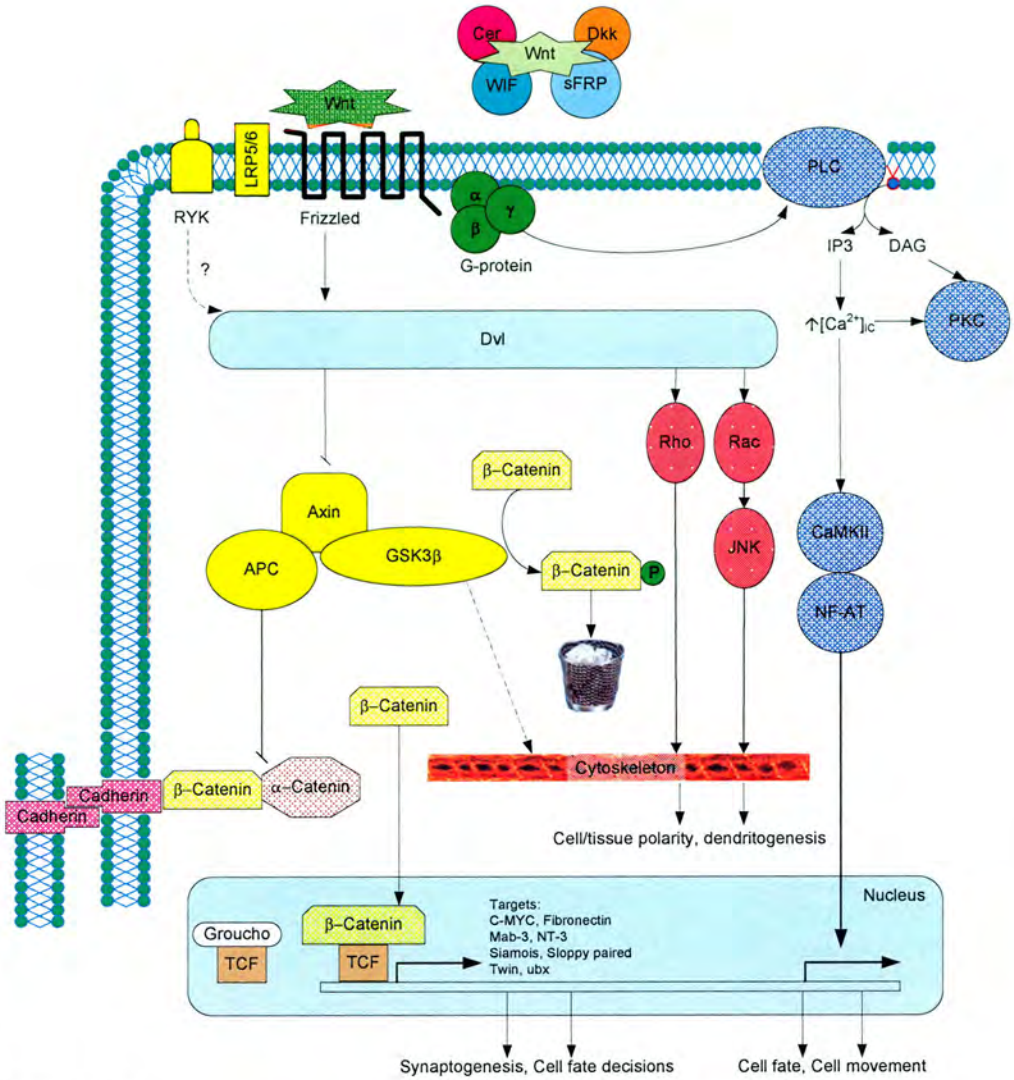

Figure 1.23

Wnt signalling pathways. Canonical/β-catenin pathway (Yellow). Wnt activation of Frizzled causes signalling through Dishevelled, resulting in inhibition of GSK-3β mediated phosphorylation (and subsequent degradation of β-catenin). β-catenin accumulates, translocates to the nucleus, binds TCF and the complex causes transcription of target genes. The Wnt/Ca^{2+} pathway (Blue). Activation of the Wnt/Ca^{2+} pathway results in intracellular Ca^{2+} release and activation of CaMKII and PKC in a β-catenin-independent manner, with a potential requirement for G proteins in this pathway. The PCP pathway (red). Wnt activation of Frizzled causes signalling through Dishevelled, which then signals to Rac and/ or Rho; Rac activation can signal through JNK, and activation of either Rac or Rho can result in cytoskeletal shape change.

β-catenin Destruction Complex

When no Wnt signal is present, free cytosolic β-catenin protein is degraded by a destruction complex (Figure 1.24), which is built around the scaffold protein Axin (either as a homodimer or a heterodimer with Axin2). Bound to Axin/ Axin2 are APC, casein kinase Iα (CKIα) diversin, GSK-3β, PP2A (reviewed in Logan and Nusse, 2004; Huelsken and

Behrens, 2002). CKIα and/or CKIε phosphorylates ser45, priming β-catenin for phosphorylation of residues Thr41, Ser37 and Ser33 by GSK-3β. Phosphorylation of Ser33 and Ser37 causes ubiquitination by β-transducin repeat-containing protein (βTrCP) and subsequent proteasomal degradation of β-catenin (Huelsken and Behrens, 2002; Logan and Nusse, 2004). The rate of β-catenin degradation can be modulated by the serine/threonine phosphatase PP2A acting to phosphorylate Axin and APC. Phosphorylation of GSK-3β by kinases such as PKC and Akt result in a decrease in GSK-3β activity (Woodgett, 2001; Logan and Nusse, 2004) and hence accumulation of β-catenin. It is thought that once Wnt ligand binds Frizzled, Dvl inhibits GSK-3β-mediated destruction of β-catenin by recruiting GBP/Frat-1, displacing GSK-3β from Axin. β-catenin then accumulates, translocates to the nucleus and associates with members of the TCF/LEF-1 transcription factor family, causing transcription of Wnt target genes, such as *Cyclin D1*, *En-2*, *MMP7*, *Myc*, *PPARdelta* and *TCF-1* (reviewed in Logan and Nusse, 2004; Huelsken and Behrens, 2002).

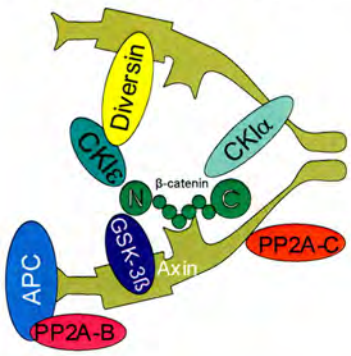

Figure 1.24
The β-catenin destruction complex. Axin holds together the β-catenin destruction complex components together, permitting CKI phosphorylation of β-catenin, priming β-catenin for GSK-3β phosphorylation. Adapted from Huelsken and Behrens, 2002.

GSK-3β inhibition leading to microtubule reorganisation

Microtubules are cytoskeletal components that are necessary for fundamental cellular processes such as cell division, cell polarity and vesicle transport. Microtubules are also responsible for the formation of axons and dendrites in neurons and maintenance of their structure (Baas, 1999). Microtubules exist in highly dynamic state, and have a half-life in the region of seconds to minutes, reviewed in (Desai and Mitchison, 1997). One protein family that colocalises with microtubules are the microtubule-associated proteins (MAPs, Maccioni and Cambiazo, 1995) and MAPs regulate microtubule organisation (Drewes et al., 1998; Gordon-Weeks and Fischer, 2000). The microtubule associated proteins Tau and MAP-1B are phosphorylated by GSK-3β (Mandelkow et al., 1992; Guidato et al., 1996) and

alterations in GSK-3β-mediated Tau and MAP-1B phosphorylation are associated with changes in microtubule stability and organization (Wagner et al., 1996; Goold et al., 1999), Figure 1.25).

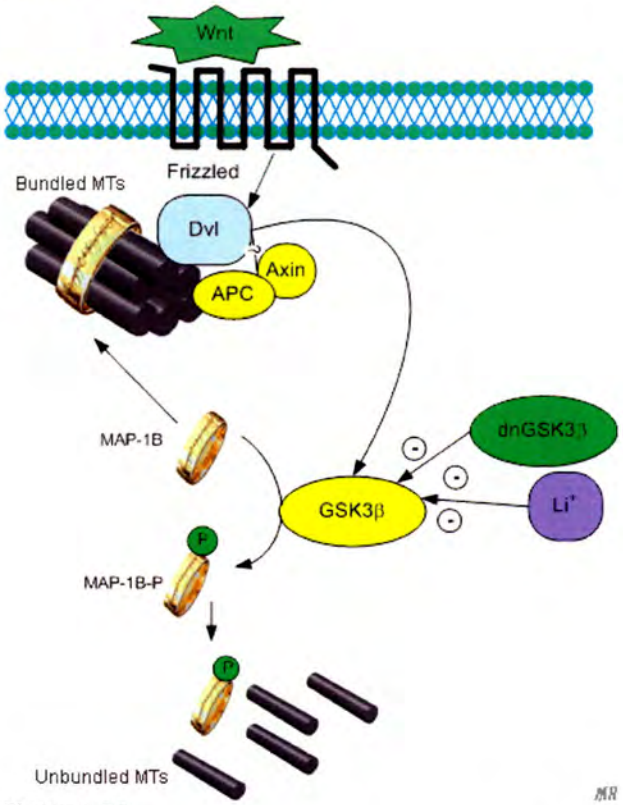

Figure 1.25
Wnt/Fz/Dvl mediated inhibition of GSK-3β can alter MAP-1B phosphorylation states and therefore microtubule stability and organisation. Phosphorylation of MAPs cause MAP dissociation from microtubules and destabilisation of the microtubule occurs, causing it to fall apart.

1.10.3 Non-canonical pathways

The first Wnt signalling pathway to be discovered became the "canonical" Wnt-1 pathway, which functions to stabilise cytoplasmic β-catenin, as described above. Subsequent research into Wnt signalling showed that other Wnts could, for example, stimulate intracellular Ca^{2+} release and activate CaMKII and PKC in a G-protein-dependent manner. This was then termed the "Wnt/ Ca^{2+} pathway" (Sheldahl et al., 1999; Kuhl et al., 2000b; Sheldahl et al., 2003). Wnt signalling through Frizzled was discovered to alter levels of Rho and Rac (Strutt et al., 1997) and this was initially discovered to regulate the orthogonal polarity of epithelium through regulation of cytoskeletal organization, and so was termed the Planar Cell Polarity pathway (PCP).

Planar Cell Polarity Pathway

PCP signalling is thought to control polarized cell movements during gastrulation and neurulation in vertebrates (Strutt et al., 1997; Wallingford et al., 2000; Tada and Smith, 2000; Marsden and DeSimone, 2001; Wallingford and Harland, 2001; Strutt, 2001; Dabdoub et al., 2003). Since modification of cytoskeletal structure within the context of postnatal brain is a component in almost all aspects of neuronal development and plasticity, there may be a role for the PCP that is unrelated to cell polarity (reviewed in Ciani and Salinas, 2005).

In common with the β-catenin/canonical pathway, in the PCP pathway Wnts signal through Frizzleds and act through Dvl, but it is at the level of Dvl where the pathways diverge (Wallingford and Habas, 2005). In *Drosophila*, Dvl has been shown to activate RhoA and JNK, alter levels of myosin II, myosin VIIA and levels of the products of the novel genes *flamingo*, *fuzzy*, *inturned* and *strabismus/van gogh* (Adler and Lee, 2001; Strutt, 2001). Furthermore, in mammalian cells and *Xenopus laevis* embryos, both Rho and Rac are signalling targets of Dvl (Strutt et al., 1997; Habas et al., 2003). Rho and Rac alter the cytoskeletal structure and have been implicated in sense-induced NMDA-dependent dendritic shape change; in *Xenopus* tadpole visual tectum, light stimulus driving visual activity promotes dendritic arbour growth and this process requires NMDA receptors and decreased RhoA and increased Rac and Cdc42 activity (Sin et al., 2002; Van Aelst and Cline, 2004). Constitutively active RhoA has been shown to reduce dendritic length in rat hippocampal slices (Nakayama et al., 2000) and loss of function analysis for RhoA in Drosophila mushroom body results in neurons overshooting their normal dendritic boundaries (Lee et al., 2000b). In *Drosophila*, the gene *flamingo* has been shown to act in the PCP pathway, encoding a protein with multiple cadherin domains as well as seven transmembrane domains (Usui et al., 1999; Chae et al., 1999). *Flamingo* has been shown to be important for limiting dendrites to their territories in *Drosophila* multiple dendritic neurons (Usui et al., 1999) which is a key process involved in correct barrel formation (Section 1.4.5). Additionally, a mouse homologue of flamingo, *Celsr3* has drastic defects in TCA formation and guidance when genetically knocked out in mice (see section 1.4.3, above).

Wnt/Ca^{2+} pathway

The Wnt/Ca^{2+} pathway has been implicated in cell fate determination in *Xenopus Laevis* embryos (Saneyoshi et al., 2002), movement during gastrulation and heart development (Sheldahl et al., 2003; Veeman et al., 2003). The binding of certain Wnts (Wnt5a, Wnt11) to specific Frizzleds (Fz2) causes signalling through Dvl and this activates PLC, yielding IP_3 and DAG (Kuhl et al., 2000b; Ishitani et al., 2003). IP_3 causes Ca^{2+} release and both DAG and Ca^{2+} cause activation of CaMKII and PKC; this PKC activation is also G-protein dependent (Sheldahl et al., 1999; Kuhl et al., 2000b). Whilst the downstream targets of CaMKII and PKC within this pathway are currently unknown, it has been shown in *Xenopus laevis* that Wnt/Ca^{2+} signalling can lead to antagonism of the Wnt/ β-catenin pathway, although it is unclear at what level this interaction occurs (Torres et al., 1996). It is of note that Wnts can signal through PLC, as *Plc-*$\beta_1^{-/-}$ mice fail to form cortical barrels (Hannan et al., 2001). PLCβ$_1$ hydrolyses phosphatidyl inositol 4,5 bisphosphate (PIP_2) into Diacylglycerol (DAG) and inositol 1,4,5 triphosphate (IP_3); DAG can activate Protein Kinase C (PKC) and IP_3 causes the release of Ca^{2+} from the endoplasmic reticululm (ER) by activating the IP_3 receptor. mGluR5 has been shown to signal through PLCβ$_1$ in barrel formation (Hannan et al., 2001) and mGluR5 binds Homer proteins which bind directly to the IP_3 receptor, Section 1.4.5). As mentioned above, PKC has been shown to have a role in dendritic spine plasticity via its interaction with Rac and Rho (Pilpel and Segal, 2004) which are also members of the Wnt/PCP pathway. PLC could be a point of interaction between the Wnt signalling and NRC-dependent pathways, and this raises the possibility that the defects in *Plc-*$\beta_1^{-/-}$ mice could be due to defects in Wnt signalling.

β-catenin and cadherins

Over 100 members of the cadherin family exist and most can be classified into six subfamilies (Nollet et al., 2000) of which the type I family are the most characterized and are implicated in synapse development (reviewed in Salinas and Price, 2005). Type I family cadherins are characterized as mediating Ca^{2+}-dependent cell adhesion between the cadherin expressing cell and a neighbouring cell which is usually expressing the same cadherin (Nose et al., 1988). These cadherins bind armadillo-family catenins (either β- or γ-catenin) by conserved peptide sequences on their cytoplasmic tails. These catenins also bind α-catenin, linking them to the actin cytoskeleton (Shapiro et al., 1995), see Figure 1.23.

Cadherins and catenins have also been shown to bring pre- and post- synaptic membranes in close proximity, physically attaching the two membranes together and restricting the size of the synaptic cleft (Uchida et al., 1996; Tamura et al., 1998; Shapiro and Colman, 1999; Boggon et al., 2002). Cadherin complexes have been implicated in initiating synapse assembly (Bamji et al., 2003; Salinas and Price, 2005; Rubio et al., 2005; Bamji, 2005). N-cadherin is found in all newly formed synapses, yet only remains present in mature excitatory synapses and not inhibitory synapses (Benson and Tanaka, 1998). Dominant-negative mutants of N-cadherin disrupt synapse formation, both presynaptically, as measured by a reduction in Synapsin I immunolabelling and postsynaptically, as measured by PSD-95 immunolabelling (Togashi et al., 2002).

Studies performed in hippocampal neuronal cell culture have suggested a Wnt-induced non-canonical role for β-catenin interacting with cadherins in dendritic shape change (Yu and Malenka, 2003; Yu and Malenka, 2004). GFP-labelled β-catenin expression (GFP-β-cat*) causes dendritic arborisation. Furthermore, K^+ neuron depolarization results in Wnt release (Yu and Malenka, 2003). The Wnt then acts through Frizzled to raise local levels of β-catenin, which can interact with members of the cadherin family, and that these effects are independent of TCF/LEF transcription. Overexpression of N-cadherin also results in dendritic branching, and Malenka and Yu hypothesise that since β-catenin links cadherins at the cell membrane to the actin cytoskeleton, increasing the availability of β-catenin could permit the anchoring of motile actin to the plasma membrane of developing neural processes, thus stabilizing new dendritic processes (Yu and Malenka, 2003). Notably this work was performed in hippocampal neuron cultures at nine days *in vitro* (d.i.v). The authors continued this work to look at overexpression of GFP-β-cat* in this system over the first twelve d.i.v cell culture (Yu and Malenka, 2004). Overexpression of GFP-β-cat* on the first d.i.v. increases axonal length and complexity, whereas sequestering endogenous β-catenin with the intracellular domain of N-cadherin has the opposite effect (Yu and Malenka, 2004). GFP-β-cat* overexpression over the first three d.i.v. enhances dendritic arborisation, but this effect is reduced in magnitude as neurons mature from 3-12 d.i.v. By 12 d.i.v. the overexpression of GFP-β-cat* has increased dendritic spine density, but has no effect on the relative proportion of different subtypes of spines, suggesting that the role that cadherins and catenins play in the development of neuronal morphology change as neurons mature (Yu and Malenka, 2004).

Cadherins and barrels

Cadherin-8 is expressed throughout the barrel cortex before the TCA invasion (Gil et al., 2002). When TCAs invade layer IV of the cortex at P3/ P4 and segregate into their barrel like pattern, they release glutamate, and this inhibits cadherin-8 expression in presumptive barrel hollows, but not in the barrel wall region. Thus, as the brain grows and the cortex expands tangentially, there is only cell adhesion in the now cell-dense barrel wall, leaving a cell-sparse barrel hollow (Gil et al., 2002).

β-catenin can function to link cadherins at the cell membrane to the actin cytoskeleton and β-catenin is the only catenin so far shown to bind Caherin-8 (Kido et al., 1998). Wnt/β-catenin pathway activation causes β-catenin accumulation, and it is possible that Cadherin-8 expressed in the barrel walls binds the actin cytoskeleton via β-catenin, and that this tethering of cells together causes retention of barrel structure, once formed, throughout brain development and cortex growth.

Frizzled as a GPCR

Frizzleds are seven-pass transmembrane receptors; most proteins of this type are able to signal through heterotrimeric G-proteins, and there is evidence to suggest that Frizzled can signal in this manner. Wnt proteins are difficult to isolate and use as ligands for Fz, so an alternative approach in studying Fz signalling has been taken, the creation of chimeric Fz receptors that contain the β-adrenoceptor ligand-binding domain and hence respond to β-adrenergic ligands. The chimeric receptors can regulate Go, G_q and G_i classes of heterotrimeric G-proteins (Liu et al., 1999b; Liu et al., 2001). Recently, loss- and gain-of function studies in *Drosophila* have demonstrated that the G_o subunit is immediately downstream of Frizzled, and is necessary for canonical/β-catenin and PCP signalling pathways (Katanaev et al., 2005). Finally, all Frizzled genes contain GPCR domains, as determined by protein motif prediction algorithms provided by the Swissprot/ Interpro project at the European Bioinformatics Institute (http://www.ebi.ac.uk/interpro/ISearch?query=frizzled&mode=all and Okazaki et al., 2002).

1.10.4 Wnts in other systems

In the nervous system of the developing embryo, Wnts and endogenous Wnt antagonists are involved in a wide range of processes as diverse as neural tube closure (Wallingford and Harland, 2002 and reviewed in Ciani and Salinas, 2005), specification of early anterior posterior axis patterning (reviewed in Yamaguchi, 2001b) and regionalisation and specification of forebrain areas such as the neocortex and hippocampus (reviewed in (Grove and Fukuchi-Shimogori, 2003). Wnts play a role in maintaining the pluripotency of embryonic stem (ES) cells (Sato et al., 2004) and antagonism of Wnt signalling can promote ES cell differentiation into neural progenitors in some cases (Aubert et al., 2002; Haegele et al., 2003), whilst Wnt3a signalling can direct differentiation of ES cells into dorsal interneurons (Murashov et al., 2005).

Wnts and embryonic nervous system patterning

Wnts and Wnt antagonists are involved in embryonic nervous system patterning. For example Wnt signalling is crucial for the correct anterior-posterior patterning of the vertebrate neural tube. Wnts are posteriorising factors (Kiecker and Niehrs, 2001; Nordstrom et al., 2002, reviewed in Yamaguchi, 2001) and inhibition of Wnt signalling is required in order for normal formation of the neural tube. During this period Wnts also play a role in the dorsoventral patterning of the emerging forebrain with Wnts acting as dorsalising factors and antagonism of Wnt signalling is required to form the telencephalon (Houart et al., 2002; Braun et al., 2003), reviewed in (Wilson and Houart, 2004; Ciani and Salinas, 2005). Wnts also play a role in the regionalisation of the forebrain; inhibition of Wnt signalling is required to divide the embryonic forebrain dorsally into the telencephalon and eye field, ventrally into the hypothalamus and most posteriorly, giving rise to the telencephalon (Heisenberg et al., 2001).

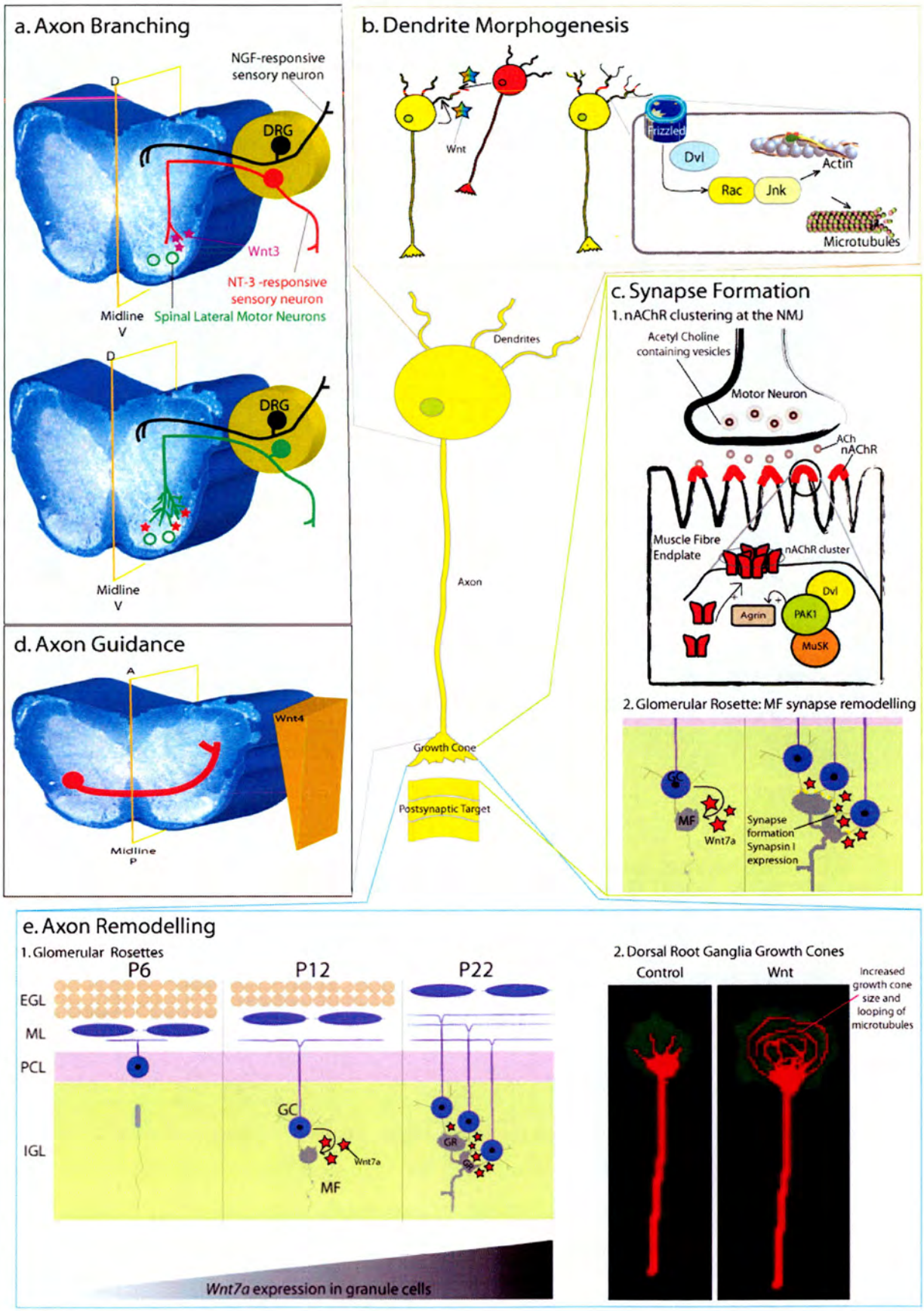
a. Axon Branching
NGF-responsive sensory neuron
D
DRG
Wnt3
NT-3 -responsive sensory neuron
Midline
V
Spinal Lateral Motor Neurons
D
DRG
Midline
V
b. Dendrite Morphogenesis
Wnt
Frizzled
Dvl
Actin
Rac
Jnk
Microtubules
Dendrites
Axon
Growth Cone
Postsynaptic Target
c. Synapse Formation
1. nAChR clustering at the NMJ
Acetyl Choline containing vesicles
Motor Neuron
ACh
nAChR
Muscle Fibre Endplate
nAChR cluster
Agrin
Dvl
PAK1
MuSK
2. Glomerular Rosette: MF synapse remodelling
GC
MF
Wnt7a
Synapse formation
Synapsin I expression
d. Axon Guidance
A
Wnt4
Midline
P
e. Axon Remodelling
1. Glomerular Rosettes
P6
P12
P22
EGL
ML
PCL
IGL
GC
Wnt7a
MF
GR
Wnt7a expression in granule cells
2. Dorsal Root Ganglia Growth Cones
Control
Wnt
Increased growth cone size and looping of microtubules

Figure 1.26

Wnt signalling in other systems. Wnt signalling has been shown to play roles in axon branching, guidance and remodelling; synapse formation and dendritic morphogenesis. A. Axon branching. Wnt3 released by spinal lateral motor neurons regulates the arborisation and differentiation of NT-3-responsive (but not NGF-responsive) sensory neurons. B. Dendrite Morphogenesis. The expression of Dvl in hippocampal neurons increases the length and branching of neurons compared to control neurons. The planar cell polarity pathway, which requires Dvl to function, and Rac and Jnk to stimulate the growth and branching of dendrites. Wnts might stimulate the development of dendrites by acting in a paracrine fashion, after being released by incoming axons (red) or in an autocrine manner, having been released by responding neurons (yellow). C. Synapse Formation. 1. Dvl has been shown to be an essential component of a ternary complex that requires MuSK and PAK1 to induce Agrin-mediated clustering of nicotinic Acetylcholine receptors (nAChRs) at the muscle fibre endplate synapse with motor neurons. 2. Wnt7a, expressed in granule cells (purple) has been shown to be an essential part of normal, timely glomerular rosette (GR) formation. Wnt7a addition to mossy fibre (grey) explants increases Synapsin I (a presynaptic protein involved in synapse formation and function) expression, and *Wnt7a*$^{-/-}$ mice exhibit delays in delays in Synapsin I accumulation, synapse formation and GR formation. See (e). D. Axon guidance. Wnts can function to guide axons in transit to their targets. In the spinal cord, a gradient of Wnt4 attracts commissural axons (red) anteriorly once they have crossed the midline. E. Axon Remodelling. 1. Glomerular Rosettes. Wnt7a is expressed during the formation of MF-GC synapses. At P6, GC progenitors in the EGL begin to differentiate into postmitotic cells (purple). These GCs become bipolar and the cell body migrates to the IGL. MFs (light grey), originating outside the cerebellum, wait in the IGL to make synaptic contacts with GCs. At P12, GCs have begun to contact MFs in the IGL. The MF morphology becomes more complex and spread areas develop along the axon shaft. By P22, most GCs have migrated to the IGL and formed synapses with MFs. Multisynaptic structures, the glomerular rosettes (GR) mentioned in part (c2), form between one MF and numerous GCs. GC dendrites interdigitate with MFs to form multilobulated glomeruli. Wnt7a is expressed at low levels in GCs as they extend processes and migrate from the EGL to the IGL at P6. Wnt7a expression reaches a peak as most GCs make synapses with MFs at P22. EGL, external granular layer. Abbreviations ML, molecular layer; PCL, Purkinje cell layer; IGL, internal granular layer; MF, mossy fibre; GC, granule cell; GR, glomerular rosette; A, anterior; D, dorsal; ML, midline; P, posterior; V, ventral; NGF, Nerve growth factor; NT-3, neurotrophin-3; MuSK, muscle-specific kinase; p21/CDC42/RAC1-activated kinase 1, PAK1. Parts adapted and redrawn from Ciani and Salinas (2005) and Hall *et al.*, (2000)

Wnts and embryonic hippocampus formation

Wnts are involved in hippocampus development. The expression of *Wnts 2b*, *3a*, *5a*, *7a*, *7b* and *8b* have been described in the telencephalon in the region surrounding the cortical hem, (Grove et al., 1998; Lee et al., 2000a) and *Wnt3a* expression marks the cortical hem from E9.75 (Roelink and Nusse, 1991; Parr et al., 1993; Grove et al., 1998) and is the only Wnt gene expressed exclusively in this structure at this age. Wnt3a appears to be required for the development of the hippocampus, since *Wnt3a*$^{-/-}$ mice lack hippocampi (Lee et al., 2000a). An almost identical phenotype is observed in *Lef1*$^{-/-}$ mice (Galceran et al., 2000) and in dorsal telencephalon-specific β-catenin knockout mice (Machon et al., 2003). It appears that in each of these mutants, the pool of precursor cells that generate the hippocampus proliferate at a much reduced rate than in wild-type mice: cell survival and differentiation are not affected in these mutants, suggesting that Wnt signalling through the Wnt/β-catenin pathway regulates hippocampus formation, possibly through controlling determination of cell fate and cell proliferation rates.

Wnts and postnatal hippocampus dendrite morphogenesis.

It has been shown recently that *Wnt7b* expressed in cultured hippocampal neurons increases dendritic arborisation of hippocampal neurons during dendritogenesis, and expression of Dishevelled mimics this effect (Rosso et al., 2005 and Figure 1.26b). Perturbations in GSK3β levels, either by inhibition or overexpression, have no effect on dendritogenesis, and the role of Dvl in dendritogenesis is not blocked by dominant-negative β-catenin, suggesting that canonical Wnt signalling is not involved. The authors demonstrated in this system that Wnt7b and Dvl signal by activating Rac, but not Rho; Dvl signalling also leads to activation of JNK, and the dendrite arborising function of Dvl can be blocked by either expression of dominant-negative Rac or inhibition of JNK and pharmacological activation of JNK enhances dendrite development. Notably, hippocampal neurons in *Dvl1*$^{-/-}$ mice exhibit shorter and less complex dendritic morphology than wild-type mice (Rosso et al., 2005). This paper demonstrates a non canonical role of Wnt7b, Dvl and JNK in hippocampal dendrite morphogenesis.

Wnts and Dorsal Root Ganglion axon branching in the spinal cord

Wnt3 has been shown to be selectively expressed in the subset of spinal cord lateral motor neurons that innervate limb muscles, during the period when spinal neurons receive contact from proprioceptive sensory neurons (Krylova et al., 2002). Wnt3 regulates the terminal arborisation of NT-3 responsive sensory neurons in vitro, increasing growth cone size and axon branching (Figure 1.26a), although Wnt3 has no such effects on NGF-responsive sensory neurons. Similar Wnt3-mediated axon remodelling activity has been observed in ventral spinal cord explants, and is observed at limb levels, but not thoracic levels of the spinal cord and this axon remodelling can be blocked by the introduction of sFRP-1. In this system, Wnt3 is acting as a target-derived retrograde signal that regulates the terminal arborisation of a class of sensory neurons.

Dishevelled at the neuromuscular junction

The neuromuscular junction (NMJ) is the synapse of a motor neuron with the motor end plate of a muscle fibre (reviewed in Zaimis and Head, 1976; Bowman et al., 1990). Motor neuron axons originate in the spinal cord; the motor endplate is a specialised and highly

electrically excitable region of a muscle fibre which contains high concentrations of nicotinic Acetyl Choline (ACh) receptors (nAChR). ACh ligand released from the motor neuron binds nAChRs, causing the nAChR channel to open and causing an influx of Na^+ and an efflux of K^+ from the cell, resulting in depolarisation of the endplate. Depolarisation of the endplate causes release of Ca^{2+} from internal stores in the sarcoplasmic reticulum, initiating muscle contraction.

During NMJ development, the growing end of the motor neuron releases agrin which binds a tyrosine kinase class receptor called muscle-specific kinase (MuSK). MuSK has been shown to signal through rapsyn to cause nAChR clustering in the endplate (Apel et al., 1995). Recently a yeast-two-hybrid study has shown that MuSK can interact with Dishevelled (Luo et al., 2002). Dvl interacts with the serine/threonine kinase PAK1, and the formation of a ternary complex containing Dvl, MuSK and PAK1 leads to PAK1 activation, which is necessary for the formation and stabilisation of nAChR clusters (Luo et al., 2002, Figure 1.26c). Although no Wnt has so far been identified in this process, if it is assumed that Dvl is functions as part of a Wnt signalling cascade, then Wnts can play a role in regulating synapse formation in the peripheral nervous system.

Wnts and commissural axon guidance in the spinal cord

Wnt4 signalling through Frizzed 3 in the spinal cord regulates the axon guidance of commissural axons (Lyuksyutova et al., 2003). Wnt4 is expressed in an anterior-posterior gradient in the floor plate and acts in a chemorepulsant manner to stimulate the turning and outgrowth of commissural axons (Figure 1.26d). *Frizzled 3*$^{-/-}$ mice (in addition to their defects in TCA formation discussed in Section 1.4.3) have defects in normal anterior turning of commissural axons; they project normally to the floor plate, but stall or extend in a random manner once they cross the midline. However, in *Drosophila Melanogaster*, DWnt5 signalling (through the *D. Melanogaster* homologue of Ryk, Derailed) has been shown to be a chemoattractive signal for commissural axons in *D. Melanogaster* embryos (Yoshikawa et al., 2003).

Wnts, axon remodelling and synapse formation

Wnts are required for proper formation of structures in the cerebellum known as glomerular rosettes (GR, Hall et al., 2000, Figure 1.26e). These are formed by the interaction of the dendrites from cerebellar granule cell (GC) neurons and mossy fibre axons (MF). MFs originate from the pontine nuclei and other sources and invade the cerebellum by P6, reaching the granule cells by P6. At P12, GCs make contact with MFs and MF growth cones increase in size, generating folds and with it many synaptic sites, whilst GC dendrites extend and synapse in the MF folds, generating the GR structure, (Hall *et al.*, 2000). The processes occurring are similar to that of barrel formation; both are postnatal manifestations of synaptic plasticity, both involve axon invasion and the requirement to stop in the correct layer and both involve interaction with cells resulting in dendritic shape change and elaboration. Removal of a specific Wnt signal can severely disrupt GR formation. *Wnt7a*$^{-/-}$ mice exhibit delays in formation of GR, and the eventual structure has less complex MF morphology; GC do not extend as deeply into the MF folds compared to the wild-type mouse (Hall et al., 2000). These processes can be mimicked in *in vitro* neuronal culture and GC-MF interactions are caused by incorporating Wnt7a in the culture medium and this effect (characterized by increased growth cone size, increased spreading along the axon shaft, and axonal branching) is blocked by adding sFRP-1 but is mimicked by addition of Lithium Chloride or valproic acid (which are both inhibitors of GSK-3β, Lucas and Salinas, 1997; Hall et al., 2000). Wnt7a mediates its effects via GSK-3β inhibition to alter the morphology of mossy fibre axons. In cerebellar granule cell culture, Wnt7a and the GSK-3β inhibitors lithium can all induce axonal remodelling which is characterized by increased growth cone size, increased spreading along the axon shaft, and axonal branching (Hall et al., 2000; Hall et al., 2002), and these events correlate with the loss of GSK-3β-phosphorylated MAP-1B (Lucas et al., 1998; Goold et al., 1999; Hall et al., 2002). As such, the effect of Wnt7a on axonal remodelling in cerebellar granule cells is mediated through the inhibition of GSK-3β.

Synapsin I is a presynaptic protein involved in the formation and function of synapses (Li et al., 1995; Rosahl et al., 1995; Hilfiker et al., 1999). Wnt7a induces Synapsin I expression and clustering in GC at GR synapses and expression is mediated through GSK-3β activity (Hall et al., 2000; Hall et al., 2002), thus Wnt7a plays an important role in Synapse formation; *Wnt7a*$^{-/-}$ mice have reduced levels of Synapsin I in GR compared to wild-type between P8 and P12, however no significant difference exists at P15, demonstrating that the lack of Wnt7a causes a transient delay in both Synapsin I clustering and GR formation (Figure 1.26c).

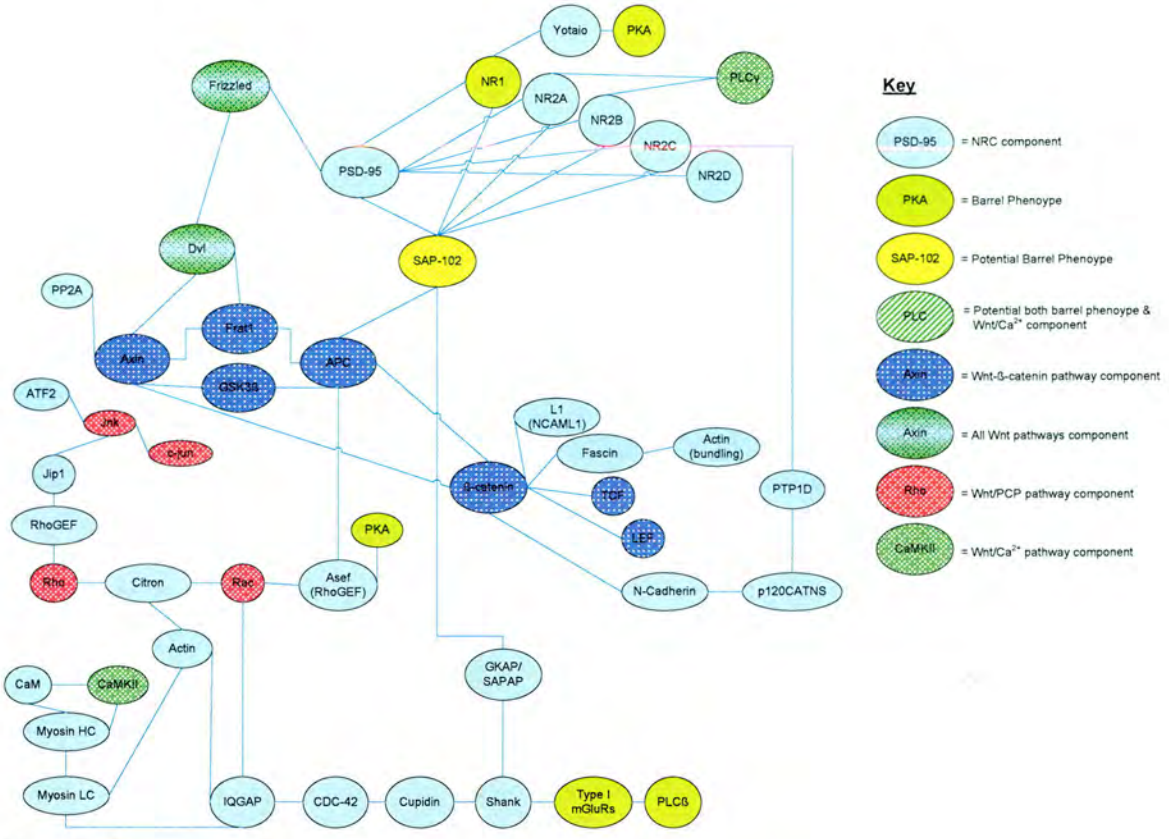

Figure 1.27
Schema of known interactions of NRC proteins with Wnt signalling pathway components. Dark yellow ovals represent genes when knocked out, affect barrel formation. Bright yellow ovals represent candidate NRC genes that may have a barrel phenotype. Light blue ovals represent NRC components; light purple ovals represent Wnt-β-catenin pathway components. Green ovals represent Wnt/Ca^{2+} signalling components and pink ovals represent Wnt/PCP pathway components. Dark green ovals with grey in the centre represent components common to all Wnt pathways; crosshatched green ovals represent molecules that are common to barrel formation and Wnt/Ca^{2+} signalling pathways.

1.10.5 Summary of Wnts and Barrel Formation

Since numerous NRC components are crucial for normal barrel formation, it is notable that many components of all three Wnt signalling pathways are also found in the NRC (Figure 1.27). Many of the NRC molecules identified in dendritic shape change are members of the PCP pathway—Rho, Rac, JNK. The NRC also contains Axin and β-catenin from the Wnt/β-catenin pathway (Husi et al., 2000). The major MAGUKs in the NRC bind vital components for Wnt signalling—PSD-95 can bind Frizzleds 1, 2, 4 and 7 (Hering and Sheng, 2002) and since all mouse Frizzled receptors contain the QT/SRV consensus binding motif for PDZ domain binding, there is the potential for binding of other MAGUKs to Frizzleds. SAP-102 has been shown to downregulate β-catenin levels, can bind adenomatous polyposis coli protein (APC) and application of SAP-102 cells in cell culture can cause changes in the

cytoskeleton, altering cell shape in gut epithelial cells (Makino *et al.*, 1997). Furthermore, the NRC contains APC (Yanai et al., 2000; Husi et al., 2000) and Yanai *et al.*, 2002 suggest that APC, like PSD-95, might be involved in ion channel clustering and/or organising of signalling molecules.

The processes involved in barrel formation have been mentioned above; correct TCA guidance, segregation and termination, cell movement and selective dendrite elaboration towards the TCA terminal. Wnts are involved in all of these processes in other systems (for review, see Ciani and Salinas, 2005) so it is conceivable that Wnts could play a role in any of the events in barrel formation. Furthermore, Rob Malenka and Xiang Yu have linked NMDA receptor activity and activity-dependent Wnt release leading to dendritic shape change (Yu and Malenka, 2003; Yu and Malenka, 2004), a process that is key to normal barrel formation (Section 1.4.5). Recently, it has been shown that Wnt release can occur in hippocampal slices via an NMDAR- and Ca^{2+}-dependent pathway (Wayman et al., 2006). Moreover, proteomic data has revealed many proteins in the NRC that are involved in barrel formation and are also present in Wnt signalling pathways and many NRC proteins have the potential to bind Wnt signalling components, discussed below and outlined in Figure 1.27 (Yanai et al., 2000; Walikonis et al., 2000; Husi et al., 2000; Hering and Sheng, 2002; Husi, 2005).

1.11 Hypotheses and aims

Hypothesis 1: *Wnts, Frizzleds* and *sFRPs* are required to form barrels.

We hypothesised that *Wnts*, *Frizzleds* and *sFRPs* are required to form barrels based on many published descriptions of the roles Wnts can play in modulating cell adhesion, movement, death and migration in the developing embryo (Moon et al., 1993; Peifer and Polakis, 2000; Schmidt and Patel, 2005; Nakamura and Akiyama, 2005). All of these processes have been hypothesised to regulate barrel formation (Figure 1.14; Barnett et al., 2006b). In mature barrels, the dendrites of barrel wall cells selectively orient their dendrites into the TCA plexus; Wnts have been shown to alter dendritic morphology in the hippocampus (Rosso et al., 2005). In addition, neuronal activity has been shown to induce Wnt release and alterations dendritic branching in cultured hippocampal cells (Yu and Malenka, 2003; Yu and Malenka, 2004) and preliminary studies suggest that application of NMDA or glutamate to this system can also induce these effects (X. Yu, personal communication). Glutamate signalling through NMDARs is crucial for barrel formation and the Wnt/ β-catenin pathway signalling components, APC, Axin and β-catenin are present in the NRC providing a possible route for crosstalk between these two signalling complexes. Additionally, NRC scaffolding molecules PSD-95 and SAP-102 interact with Wnt signalling pathway components; Frizzleds 1, 2, 4 and 7 have been shown to bind PSD-95 (Hering and Sheng, 2002), and APC binds SAP-102 *in vitro*, (Makino *et al.*, 1997). Finally, Wnt7a is crucial for normal formation complex of multi-synaptic structures in postnatal cerebellum called Glomerular Rosettes, and proper synaptogenesis in these structures is also dependent on Wnt7a (Hall et al., 2000).

To begin testing this hypothesis, we formed three specific aims, outlined below.

Aim 1: To determine the Wnts, Frizzleds and sFRP genes present in developing barrel cortex and the expression profiles of these genes at crucial ages for barrel formation.

Because of the similarities between the roles Wnts play in other parts of the brain and the mechanisms of barrel formation outlined above, we decided to determine the complement of Wnt, Frizzled and sFRP genes expressed in barrel cortex. Initial screens for the presence of

Wnts were performed using degenerate primers that amplify almost all *Wnt* genes, followed by sequencing of the PCR products. The next step in the characterisation of these expression profiles was to examine each *Wnt* gene using individual primer RT-PCR, and expanding the age range to examine Wnt gene expression at significant ages in barrel development. In order to quantify the differences in expression between each age group, SYBRgreen qRT-PCR was performed and the study was expanded to include the expression profiles of *Frizzleds* and the *sFRP* genes. Finally, the expression of selected *Wnt* genes was examined by *in situ* hybridisation, in order to determine in which cortical layers these *Wnts* are expressed. This work is presented in Chapter 3.

Aim 2: To determine if Wnt, Frizzled and sFRP expression is dysregulated in barrel cortices of mice with barrel defects, namely: *Pkar2β*$^{-/-}$, *Plc-β1*$^{-/-}$ and *Mglur5*$^{-/-}$ mice.

Since *Pkar2β*$^{-/-}$, *Plc-β1*$^{-/-}$ and *Mglur5*$^{-/-}$ mice lack barrels, we reasoned that any Wnts involved in barrel formation may be mis-regulated in these mutants. Each mutant mouse has similar, but slightly different barrel and TCA patterning phenotypes. By looking at common Wnt changes *versus* those specific to a given mutant might give insight into the processes regulated by each Wnt. Therefore, I examined the expression of *Wnt*, *sFRP* and *Frizzled* genes in these mutants to determine if expression if these genes is perturbed in mice that lack barrels. This work is presented in Chapter 3.

Aim 3: To determine the barrel phenotype of all available *Wnt* and *Dvl* knockout mice.

Examination of the barrel phenotype of genetic mutant mice has been the traditional method in trying to determine whether a certain gene is necessary for normal barrel formation. Although many *Wnt* mutant mice die embryonically, and some *Wnt* genes have not yet been knocked out in mice, we examined the barrel phenotype of all available *Wnt* mutant mice that live long enough to form barrels. Dishevelled proteins are thought to be crucial transducers of most forms of Wnt signalling, acting as a cytoplasmic shuttle between Frizzled receptors and downstream signalling components. P7 *Wnt7a*$^{-/-}$, *Dvl1*$^{-/-}$ and *Wnt7a*$^{-/-}$ *Dvl1*$^{-/-}$ mutants were kindly gifted by Prof. Patricia Salinas (University College London, UK), *Wnt2b*$^{-/-}$ mice were a kind gift of Prof. Terry Yamaguchi (NIH Bethesda, MD, USA) and *Wnt8b*$^{-/-}$ mice were examined in collaboration with Dr. John Mason (Edinburgh University, UK)

In addition, two other lines of related work were followed:

Aim 4: To determine whether the scaffolding molecules SAP-102 and PSD-95 that are found in both the NMDAR and Wnt signalling complexes are required for barrel formation.

SAP-102 and PSD-95 are present in barrel cortex (Barnett et al., 2006a) and both proteins can act as bridges between the NMDAR and molecules known to be essential to barrel formation. Furthermore, both molecules can interact with Wnt signalling pathway components, and potentially provide a link between the Wnt and NMDAR signalling pathways (Li et al., 2001; Colledge et al, 2000, Hering and Sheng, 2002).

Mutant mice were bred that carried one allele of *Psd-95* and none of *Sap-102*, and also one allele of *Sap-102* and none of *Psd-95* in order to assess the contribution of each allele of each MAGUK in barrel formation. This aim was pursued by examination of the barrel phenotypes in the same manner as in Aim 3. This work is presented in Chapter 4.

Aim 5: To make a web-accessible database cataloguing the gene and protein expression profiles of NRC components in barrel cortex that would be useful to a researcher in the barrel cortex community.

Researchers today have available an abundance of genetic and protein sequence information in addition to many e-journal articles. In order to plan an experiment to demonstrate an expression profile of a certain gene in barrel cortex, multiple databases must be consulted to obtain the relevant sequence information and to examine the literature to ensure this work is novel. This is time consuming and often poorly indexed papers that contain this information will not be presented by valid queries of the NCBI PubMed archives.

We decided to develop a highly curated web-accessible database that enables a user to search for a gene, and all available nucleotide and protein sequences, information on the availability of mutant mice, and published expression patterns of that gene would be presented back to the user. This was achieved by exhaustive literature searches of all papers that contained the name of the gene of interest, then inspection of the full text and figures of that paper to determine if any appropriate content should be entered into the database. This work is presented in Chapter 5.

2 Materials and methods

2.1 Dissection and tissue preparation

2.1.1 Barrel Cortex Dissection

Mice aged P7 and older were sacrificed by cervical dislocation and mice aged less than P7 decapitated. Brains were dissected out of the skull and placed in a Petri dish containing ice-cold phosphate buffered saline (PBS, NaCl 137mM, KCl 2.7mM, NaH_2PO_4 1.4mM, Na_2HPO_4 4.3mM, pH 7.4) and the cerebral hemispheres were divided using a sharp razor blade. Each hemisphere was dissected as follows: The medial side was laid down on the Petri dish and a coronal cut was made at a point just posterior to the point where the olfactory tubercle becomes continuous with the piriform cortex on the ventral surface of the brain and another cut was made just forward from the cerebellum (Figure 2.1). The central section of the brain was laid on its anterior surface. The hippocampus should be at the point of maximum medial-lateral length but before it begins to curve ventrally. An additional thin slice may be required to be removed from the posterior side of the tissue obtain the correct profile of the hippocampus. One cut is made just ventral to the small bump landmark that is present at the divide between the archicortex and neocortex. The second cut is made at a 40° angle from the previous cut (Figure 2.1). The cortex was laid pial surface down; striatum and sub-cortical white matter was pinched off was with curved forceps and hippocampus falls away. Striatum removal is crucial, as it can provide a major source of contamination, since many NRC component genes are expressed earlier in striatum than in cortex, such as SynGAP (Porter et al., 2005). The resultant tissue will contain all six cortical layers, should measure 2.5-3mm wide and long and be between 1 and 1.5mm thick, depending on age. The tissue was placed on aluminium foil, under which was dry ice. Once the tissue was frozen, it was placed in an Eppendorf tube that was pre-chilled on dry ice, then the tube and tissue were kept in dry ice until all dissections were complete, then placed in a -80°C freezer.

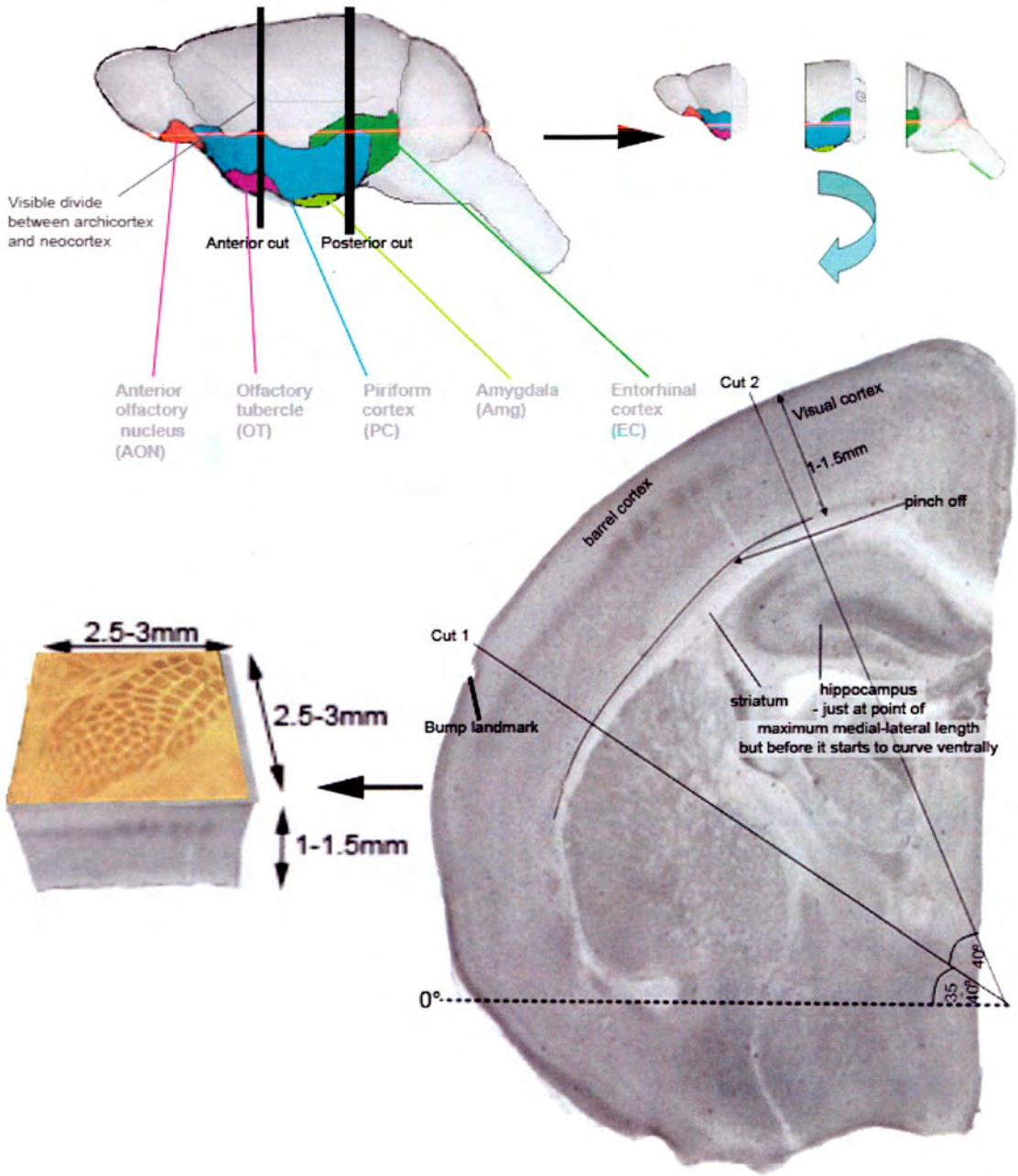

Figure 2.1
Barrel cortex dissection.
After bisection of the cerebral hemispheres, a coronal cut was made at a point just posterior to the point where the olfactory tubercle becomes continuous with the piriform cortex on the ventral surface of the brain. A second cut was made just forward from the cerebellum. The central section of the brain was laid on its anterior surface and the hippocampus should be at the point of maximum medial-lateral length but before it begins to curve ventrally. One cut is made just ventral to the small bump landmark that is present at the divide between the archicortex and neocortex. The second cut is made at a 40° angle from the previous cut The cortex was laid pial surface down; striatum and sub-cortical white matter was pinched off was with curved forceps and hippocampus falls away, leaving tissue containing all six layers of the barrel cortex.

2.1.2 Isolation of mRNA from barrel cortices.

Barrel cortices were homogenised in Qiagen RLT Lysis buffer containing 10µl β-mercaptoethanol (BME) per 1ml buffer. Homogenisation was performed by repeatedly drawing and expelling the thawed tissue and buffer through a 0.2mm diameter syringe needle. After approximately fifteen iterations, the tissue was sufficiently homogenised to proceed using the Qiagen RNeasy Mini Kit according to the manufacturer's instructions to extract total RNA. This included the optional fifteen minute RNase-free DNase (Qiagen) digestion step.

2.1.3 RNA quality assessment

The quality of mRNA was ascertained by running 1µl samples in a 1% agarose gel made with 1x TBE buffer (100 mM Tris, 90 mM boric acid and 1 mM EDTA, made with DEPC-treated water) containing 0.002% Ethidium Bromide in a gel tank specifically reserved for RNA sample running. The samples were run at 100V for ten minutes and the resultant gel was imaged. Undegraded mRNA should have distinct bands for 60S and 40S RNA. Smeared RNA or RNA where the 60S band did not exhibit approximately double the signal intensity of the 40S band after band signal intensities were optically quantified; samples were re-run on a fresh gel. If the mRNA exhibited these characteristics on the second run, it was more likely that the RNA was degraded rather than RNase contamination of the gel so that sample would then be discarded.

2.1.4 Quantification of DNA/ RNA

A 1:200 dilution of the DNA or RNA sample was prepared and its absorbance at 260 and 280nm was measured by UV spectrophotometery. Purity was assessed examining the ratio of UV light absorbance at 260 and 280nm, using calculation: A_{260}/A_{280}. A ratio of 1.8 indicates pure dsDNA and a ratio of 2 indicates pure RNA. Lower ratios are indicative of contamination with other nucleic acids or protein, and such samples would be discarded. To calculate the concentration, where an optical density at 260nm (OD_{260}) of 1 equals DNA at a concentration of 50µg/ml, the following formula was applied:

OD_{260} x 50μg/ml x dilution factor = [DNA] (μg/ml)

whilst an OD_{260} of 1 for RNA indicates 40μg/ml:

OD_{260} x 40μg/ml x dilution factor = [RNA] (μg/ml)

2.1.5 Reverse Transcription of messenger RNA

1μg of mRNA, made up to 21.1μl with 18.2MΩ double distilled water (ddH_2O) was added into a RNase-free 0.5ml PCR Eppendorf tube, heated to 75°C in a PCR block for five minutes and immediately cooled and stored on ice until use.

A cDNA synthesis mastermix solution was prepared, containing 3.3μM random hexamers (Amersham Pharmacia Biotech, St. Albans, UK), 3mM $MgCl_2$ (Invitrogen), 500μM of dNTPs (Promega), 1 unit/μl RNase inhibitor (Invitrogen) and a final concentration of 1x PCR buffer (Invitrogen). A volume of 7.9μl was added to each tube containing diluted mRNA previously made and placed in a PCR block at 42°C for five minutes, after which 2μl MMLV-RT (Invitrogen, 200u/μl) was added to each tube and incubated at 42°C for one hour, then heated to 95°C for five minutes, then stored at -20°C until use.

2.1.6 Polymerase Chain Reaction

A stock reaction mixture was made up in a 1.5ml Eppendorf tube for the required number of samples in order to minimise pipetting errors. PCR took place in 25μl reactions. Each reaction contained 10mM Tris-HCl pH9.0, 50mM KCl, Thermophilic DNA polymerase Mg^{2+}-free 10x buffer (Promega), 2.5mM $MgCl_2$ (Promega), 0.2pmol. forward primer, 0.2pmol. reverse primer and 0.2mM of each dNTP, 1μl of 5u/μl Platinum Taq polymerase (Invitrogen), then made up to 24μl with ddH_2O. This mixture was added to each PCR tube, and then 1μl RT product added. Tubes were then incubated at 95°C for 15 minutes to initiate the hot-start processes and tubes were thermocycled using an appropriate program for the primers used. PCR product was stored at -20°C.

2.1.7 SYBRgreen PCR Protocol

Primers (obtained from MWG, Ebersberg, Germany) were designed to span introns and provide an amplicon of 80-200bp. A mixture of whole body embryo cDNA taken from E10.5, E11.5 and E12.5 embryos was used as a positive control to ensure the validity of the primers. The amplified DNA fragment was cloned and sequenced to ensure amplification of the correct gene occurred. Each primer pair was tested so that they produce the same unique melting curve in both embryonic and postnatal cDNA PCR reaction runs. This confirms that a unique replicon species is being generated by each primer pair at all ages. Duplicate serial dilution series (consisting of stock concentration cDNA, and three iterations of 1:10 dilutions) of P14 cDNA were performed for each primer pair in each qRT-PCR run in order to test the linearity of each PCR reaction. Linear regression analysis was performed on the data. PCR reactions where the R^2 values ≥ 0.95 were included in the developmental analysis of *Wnt* expression. The regression line equation was used to calculate the relative amount of each species present in the logarithmic phase of DNA amplification. 18S was chosen as the housekeeping gene; all *Wnt* expression values are relative to 18S expression levels. To compare *Wnt* levels between PCR runs, all ages were normalised to P14 values, which was the age chosen to perform the linear regression on as P14 was the crucial age of interest and normalised to Adult values, allowing comparison of the relative expression levels throughout earlier ages in barrel development to be performed. One way Analysis of Variance (ANOVA) analysis was performed and Student-Newman-Kuels multiple comparisons test were performed *post-hoc* if the ANOVA yielded a p-value of less than 0.05. Bar charts were then plotted, error bars were defined as the Standard Error of the mean (SEM).

2.1.8 Primer Sequences

Wnt1 Forward	*Wnt3* Forward	*Wnt5a* Forward
TGCACCTGCGACTACCGGCG	GCCGACTTCGGGGTGCTGGT	TCCTATGAGAGCGCACGCAT
Wnt1 Reverse	*Wnt3* Reverse	*Wnt5a* Reverse
GTGCGCGGGGTCTTCGGGCT	CTTGAAGAGCGCGTACTTAG	CAGCTTGCCCCGGCTGTTGA
Wnt2 Forward	*Wnt3a* Forward	*Wnt5b* Forward
CGGCCTTTGTTTACGCCATC	ATTGAATTTGGAGGAATGGT	TCGGAGGAGCAGGGCCGAGC
Wnt2 Reverse	*Wnt3a* Reverse	*Wnt5b* Reverse
TGAATACAGTAGTCTGGAGAA	CTTGAAGTACGTGTAACGTG	CAGCTTGCCCTGGCGGGTGA
Wnt2b Forward	*Wnt4* Forward	*Wnt6* Forward
GCCAAAGAGAAGAGGCTTAA	GGCGTAGCCTTCTCACAGTC	ATGGATGCGCAGCACAAGCG
Wnt2b Reverse	*Wnt4* Reverse	*Wnt6* Reverse
TCAGTCCGGGTGGCGTGGCG	TGCATTCCGAGGCACCAGCG	TTTGCCGTCGTTGGTGCCCA

Wnt7a Forward
CAAGGCCAGTACCACTGGGA
Wnt7a Reverse
GGCTCCACGTGGACGGCCTC
Wnt7b Forward
CAAGGCTACTACAACCAGGC
Wnt7b Reverse
CACCTCCACCTGCACCGCTG
Wnt8a Forward
AACGTGGAGTTCGGGGAAAA
Wnt8a Reverse
GTTGCCAGCCCTTAGCTGGC
Wnt8b Forward
AACGTGGGCTTCGGAGAGGC
Wnt8b Reverse
GCCCGCGCCCTGCAGCAGGT
Wnt10a Forward
AAAGTCCCCTACGAGAGCCC
Wnt10a Reverse
CAGCTTCCGACGGAAAGCTT
Wnt10b Forward
CGGCTGCCGCACCACAGCGC
Wnt10b Reverse
CAGCTTGGCTCTAAGCCGGT
Wnt11 Forward
GCCATGAAGGCCTGCCGTAG
Wnt11 Reverse
GATGGTGTGACTGATGGTGG
Wnt14 Forward
CGGCAAGATGCTGGATGGGTC
Wnt14 Reverse
GTCAGCCCTTGCAGGTATAGAC
Wnt15 Forward
CTACGCTATGACACGGCTGT
Wnt15 Forward
GTACTTGCTGGGCCGGCAGA
Wnt16 Forward
CAGGGACACAAGGCAGAGAATG
Wnt16 Reverse
GCTGGATGGAGTGGTTACTT
β-actin Reverse
CCTGTCAGCAATGCCTGGGT
β-actin Reverse
CCAGCCTTCCTTCTTGGGTA
GAPDH Forward
TGGTGAAGCAGGCATCTGAG
GAPDH Reverse
TAGGCCATGAGGTCCACCAC
18S Forward
GTGGAGCGATTTGTCTGGTT
18S Reverse
CAAGCTTATGACCCGCACTT
sFRP1 Forward
GGCCAGTTCAAAAGCTGAAG
sFRP2 Reverse
ACGACAACGACATCATGGAA
sFRP2 Forward
CAGCACGGATTTCTTCAGGT
sFRP3 Reverse
ACGTGGGGACTGTTCTTTTG
sFRP3 Forward
TGGCCAAACAGGTACAAACA
sFRP4 Forward
ATCATCCTTGAACGCCACTC
sFRP4 Reverse
ACCCTGGCAACATACCTGAG
Frizzled1 Left
CAAGGTTTACGGGCTCATGT
Frizzled1 Right
GAGAAAGCCAGCGATGTAGG
Frizzled2 Left
CCGACGGCTCTATGTTCTTC
Frizzled2 Right
TAGCAGCCGGACAGAAAGAT
Frizzled3 Left
TGGGTTGGAAGCAAAAAGAC
Frizzled3 Right
CCTGCTTTGCTTCTTTGGTC
Frizzled4 Left
ACTGGGTGGGATTTCAACTG
Frizzled4 Right
GGGAGTGCGCTACAGAGTTC
Frizzled5 Left
ACATGGAACGATTCCGCTAC
Frizzled5 Right
GGCCATGCCAAAGAAATAGA
Frizzled6 Left
TCTGTGCCTCTGCGTATTTG
Frizzled6 Right
TCTCCCAGGTGATCCTGTTC
Frizzled7 Left
GCTTCCTAGGTGAGCGTGAC
Frizzled7 Right
AACCCGACAGGAAGATGATG
Frizzled8 Left
CCGCCTAGAGAAGGAGGACT
Frizzled8 Right
TGAACTGGTTGGGCATGTAA
Frizzled9 Left
TGAACTGACTGGGCTCTGCTATG
Frizzled9 Right
GGCACTGTGTAAAGGATGGAAAAG
Frizzled10 Left
TGGTACGCATAGGGGTCTTC
Frizzled10 Right
TCAGGCAGTCAGGTGTCTTG

2.1.9 Transformation of chemically competent E. coli

50µl aliquots of chemically competent *E. coli* JM-109 cells were thawed on ice. 10ng of plasmid DNA was added and the mixture was incubated on ice for 20 min. Subsequently, cells were heat-shocked at 42°C for 45 seconds, placed back on ice for two minutes and 500µl of SOC medium (0.5% Yeast extract, 2.0% tryptone, 10mM NaCl, 2.5mM KCl, 10mM $MgCl_2$, 20mM $MgSO_4$, 20mM glucose) was added. The mixture was incubated for 30-45 min at 37°C with 200rpm shaking, and then 200µl of cells were plated onto agar containing the appropriate antibiotic for the plasmid (either Ampicillin at 10µl/ml or kanamycin at 5µl/ml) and incubated overnight at 37°C.

2.1.10 Selection of bacterial colonies for production of plasmid DNA

LB (170 mM NaCl, 10 g/L bactotryptone, 5 g/L yeast extract)-Agar plates were supplemented with (final concentrations) 0.5mM IPTG (isopropyl-beta-D-thiogalactopyranoside) and 80µl/ml X-gal (5-bromo-4-chloro-3-indolyl-beta-D-galactopyranoside) which facilitated blue/white colony screening, where white colonies contain an insert. Only plasmid vectors that facilitated blue/white screening were used. The selected colonies were grown overnight and those that were shown by PCR to contain the correct insert were again picked using a sterile pipette tip and inoculated into 50ml of selective medium. This was incubated overnight at 37°C with 200rpm shaking.

2.1.11 Incubation and centrifugation of plasmid-containing bacteria

5ml of sterile LB Medium containing appropriate selective antibiotic were inoculated from single colonies of bacteria harbouring the plasmid of interest. The bacteria were left to grow at 37°C for 16 hours, shaking at 200 rpm. This culture was then centrifuged at 13,000 x *g* for 15 minutes and the supernatant disposed of in bleach

2.1.12 Alkaline Lysis Miniprep procedure

Plasmid DNA was extracted from bacteria using Qiagen Plasmid Mini kits, following the manufacturer's instructions.

2.1.13 Restriction digest

20µl reactions were prepared, each containing 2-10U of an appropriate restriction enzyme Promega, Roche) in the appropriate buffer (Promega, Roche) diluted to 1x with ddH_2O and 0.2-1µg of DNA sample. These were then incubated at the optimum temperature (usually 37°C) for 1-4 hours.

2.1.14 DNA extraction

The tails of embryos were removed and digested overnight in 500µl tail-tip lysis buffer (TTLB) with Proteinase K (10mg/ml) at 55°C in a shaking water bath. An equal volume of phenol chloroform was added and mixed for at least ten minutes. The mixture was centrifuged at 13,000 x *g* for two minutes and the aqueous phase retained. 1ml of 100% ethanol and $^{1}/_{10}^{th}$ volume NaOAc (pH5.5) was added to precipitate the DNA. This was extracted, dipped in 70% EtOH and transferred to a fresh Eppendorf. The DNA was air dried for ten minutes and re-suspended in 50µl Tris EDTA buffer by shaking overnight at 37°C, yielding an approximate DNA concentration of 0.5µg/µl, suitable for genotyping by PCR.

2.1.15 Colony Screening

Bacterial colonies that contained fragments amplified by degenerate primers were inserted into pGEM-T easy plasmid (Promega), spread onto LB-Agar plates containing Ampicillin and incubated at 37°C overnight. Individual colonies were picked by sterilised toothpick and pasted onto a fresh LB-Agar-Ampicillin plate in a grid array pattern and incubated at 37°C overnight. A nylon membrane was then placed on top of the bacteria and immediately lifted off. The plate containing the array of bacteria was placed in a fridge until later use. The membrane was wrapped in Seranwrap and placed under an ultra-violet crosslinker (Spectrolinker XL-1000, Spectroline, NY, USA) set to "cross-link", with the bacteria side directed toward the ultraviolet light source. The membrane was unwrapped and left for 12-24 hours at room temperature. Afterwards, the membrane was air dried and baked for 30 minutes to two hours at 120°C.

2.1.16 *Wnt7a* DNA probe production and hybridisation

A *Wnt7a* fragment was excised from pGEM-T Easy vector by digestion with BstZI enzyme and purified by ethanol precipitation (as outlined in Section 2.1.14). The probe was labelled with ^{32}P radiolabelled dCTP (Amersham) using a High Prime kit from Roche, as per manufacturers instructions. The probe was added to the membrane and left to hybridise overnight at 65°C. After hybridisation, the membrane was washed with Church Wash solution (2% Sodium dodecyl Sulphate (SDS), 100mM $NaPO_4$, 1mM EDTA), wrapped in cling film to retain moisture and exposed to X-ray film for visualisation of radioactivity (Kodak X-OMAT XAR-5).

2.2 Histological techniques

2.2.1 Perfusion

Mice were sacrificed by lethal overdose injection of 0.1ml Sodium Pentobarbitone (60 mg/ml, Sagatal/Pentoject, Animal Care Ltd, Dunnington, York, UK) and once the pedal withdrawal reflex ceased, perfused transcardially with cold Phosphate Buffered Saline (PBS, 137mM NaCl, 2.7mM KCl, 4.3mM $Na_2HPO_4 \cdot 7H_2O$, 1.4 mM KH_2PO_4) then immediately followed by perfusion of ice-chilled 4% Paraformaldehyde in pH 7.2 Phosphate Buffer solution (0.1M KH_2PO_4, pH to 7.2 by addition of 1M NaOH and autoclaved; PFA). Brains were harvested and post-fixed in 4% PFA overnight. If the brains were to be used for immunohistochemistry on sections cut by freezing microtome, then the brains were transferred from PFA into 30% sucrose solution and left overnight at 4°C, or until the brains sank into the sucrose solution. The tail tip was removed after sacrifice, but before perfusion and stored at -20°C for subsequent genotyping.

2.2.2 Embedding sections for cryostat sectioning

After perfusion, brains were placed in a Disposomould (RA Lamb, Eastbourne, UK) containing Sakura Tissue-Tek OCT Compound (RA Lamb) then placed in a pre-chilled weigh boat on dry-ice, containing chilled Pentan-2-ol (BDH). Once the OCT compound was thoroughly frozen, the tissue was placed in a -80°C freezer. The brains were sectioned at 10μm in a coronal plane on a Leica Cryostat CM 3050S (Leica Microsystems (UK) Ltd.,

Milton Keynes, UK) and mounted onto TESPA (3-aminopropyl-triethoxysilane) coated slides.

2.2.3 Embedding and tissue processing for wax sectioning

Brains were embedded in paraffin wax using an automated tissue processor (Leica ASP-200, Leica Microsystems Nussloch GmbH, Nussloch, Germany), consisting of a 17 hour cycle in which the brains were dehydrated through an ethanol series from 50% to 100% concentration in 10% increments, followed by four and a half hours in xylene. The brains were sectioned at 10μm in a coronal plane and mounted onto TESPA coated slides.

2.2.4 Freezing microtome sectioning

30% sucrose cryoprotected brains (Section 2.2.1) were bisected along the midline and for each half, the cerebellum was removed and this cut formed the base of the tissue to be sectioned. The tissue was placed on a piece of Postlip blotting paper (RA Lamb) which was pre-positioned on top of the freezing microtome platform. A small amount of 30% sucrose solution was placed onto the Postlip paper and base of the brain and the freezing microtome platform was cooled to -40°C. After the sucrose and brain had frozen, the platform was set to -20°C and the temperature was left to equilibrate for fifteen minutes. For cortical flats, cerebellum and area anterior of archicortex were removed, followed by removal of hippocampus and striatum. The resulting curved cortex was placed on the Postlip paper and a microscope slide was placed on top of the cortex, flattening it. The freezing microtome platform was cooled to -40°C and the process of freezing described above was followed. The microscope slide held on top of the tissue during the freezing process, and carefully removed just before the tissue was completely frozen.

2.3 In-situ hybridisation

2.3.1 Production of plasmid DNA

50mls of L-Broth were inoculated from single colonies of bacteria harbouring the plasmid of interest. The bacteria were left to grow at 37°C for 16 hours, shaking at 200rpm. This culture was then centrifuged at 13,000 x *g* for 15 minutes and the supernatant disposed of in bleach.

Plasmid DNA was purified by alkaline lysis using a midiprep kit, following the manufacturer's instructions (Qiagen Plasmid Midi kit).

2.3.2 Probe linearisation

10μg plasmid DNA, 5μl of appropriate buffer, 38μl ddH_2O and 4 units of restriction enzyme were added into a 1.5ml Eppendorf tube and incubated at 37°C for four hours. The digest was applied to a DEPC-H_2O Chromaspin column (K-1332-2, BD Biosciences, California, USA) and the probe stored in RNase-free 0.5ml Eppendorf tubes.

2.3.3 Probe transcription

The linearised plasmids were transcribed using the Roche DIG RNA labelling kit (Manufacturer's code: 11175025910). Transcription reactions were carried out in a final volume of 20μl. For both sense and antisense reactions, 2μg linearised plasmid DNA, 2μl 10X digoxygenin NTP labelling mix and 2μl 10X transcription buffer were added into a 1.5ml Eppendorf and the volume made up to 18μl with ddH_2O. Two units of the appropriate RNA polymerase were added and the reactants mixed and placed at 37°C for two hours. 2μl of 0.2M EDTA was added to stop the reaction and RNA was precipitated with 2x volume of 100% EtOH and $^1/_{10}{}^{th}$ volume of 3M NaOAc, then placed in a -70°C freezer for one hour. After centrifugation at 13,000 x *g* for fifteen minutes, the supernatant was removed and the pellet washed with 50μl of 70% EtOH and centrifuged again at 13,000 x *g* for five minutes. The supernatant was removed and the pellet air dried for ten minutes and the RNA was re-suspended in 100μl DEPC-treated water. The yield of DIG labelled RNA was estimated after running a sample of the probe on a 1% agarose gel at 100V for ten minutes.

2.4 Wax section in situ hybridisation

2.4.1 Pre-hybridisation washes

Washes were performed in baked, RNase free glass slide dishes. Slides were places in: fresh Histoclear for ten minutes, then another fresh Histoclear for ten minutes, 100% Ethanol for five minutes, then another 100% Ethanol for five minutes, 2xSSC for five minutes, then a fresh 2xSSC for five minutes, then in 10mg/ml Proteinase K for between one to seven and a half minutes (and in some cases omitted, depending on the protocol), followed by two thirty

minute incubations in 2 x SSC, fifteen minutes fixation in 4% PFA, fifteen minutes in 0.1M HCl, followed by thirty seconds in 1 x TEA and ten minutes in 0.003125% Acetic Anhydride. Slides were returned to the 1 x TEA until pre-hybridisation.

2.4.2 Pre-hybridisation

For every ten slides, 1ml of prehybridisation mix was made, which consisted of:

Reagent	Volume (µl)
Deionised Formamide	500
20 x SSC	100
50 x Denhardt's Solution	100
50% Dextran	200
Yeast tRNA (10mg/ml)	20
20% SDS	25
dH_2O	75
Total:	1000

The prehybridisation mix was vortexed thoroughly before use and 75µl was applied per slide onto the hydrophobic side of a GelBond coverslip (Flowgen #53745, Nottingham, UK), and the coverslip and mixture was placed onto the slide containing the sections, so that mixture was in contact with the section. The slides were then placed in a pre-warmed box, humidified with 5x SSC and incubated in an oven set to an appropriate temperature for thirty minutes. The coverslips were removed immediately prior to application of the hybridisation mix.

2.4.3 Hybridisation

For every ten slides, 1ml of hybridisation mix was made, which consisted of:

Reagent	Volume (µl)
Deionised Formamide	500
20 x SSC	100
50 x Denhardt's Solution	100
50% Dextran	200
20% SDS	25
dH_2O	x
Total:	1000

The appropriate volume of DIG-labelled probe (approximately 100ng per slide) was added to 20µl yeast tRNA (10mg/ml) for each slide and heated to 80°C for three minutes, then

immediately cooled on ice. A volume of 75µl hybridisation mix per slide was added to the probe/ yeast tRNA mix, vortexed thoroughly and applied to the hydrophobic side of a GelBond coverslip and applied in the same manner as the prehybridisation mix. The slides were returned to the pre-humidified box, sealed with electrician's tape and incubated at the appropriate temperature overnight.

2.4.4 Post-hybridisation

Slides were washed in staining buffer (0.1 M Tris-HCl, 0.15 M NaCl, pH 7.5) twice for fifteen minutes, then placed in a coplin jar that was covered in aluminium foil and contained 20µl NBT/BCIP (Roche, 18.75 mg/ml NBT (Nitro blue tetrazolium chloride) and 9.4 mg/ml BCIP (5-Bromo-4-chloro-3-indolyl phosphate, toluidine salt) in 67% DMSO (v/v)) diluted in 10ml staining buffer. Staining levels were checked quickly by eye every fifteen minutes. Once staining was complete, slides were washed in PBS for fifteen minutes and coverslipped and mounted using one drop of Aquamount (BDH Ltd, Poole, UK).

2.4.5 Cryostat section *in-situ* hybridisation

Cryostat sections were cut at -20°C and TESPA-coated slides pressed onto the sections, affixing them to the slide. Sections were stored in sealed slide boxes, containing bags of silica gel to absorb water. Before use, slides were thawed and briefly dried using a hairdryer set to "cool". Slides were placed in ice-cold 4% PFA in PBS for ten minutes, followed by two washes in PBS. Slides were incubated for ten minutes in 0.1M TEA containing 0.003125% Acetic Anhydride for ten minutes, then rinsed twice in PBS for three minutes each. Latterly, sides were sectioned and then fixed in ice-cold 4% PFA in PBS for ten minutes, followed by two washes in PBS, then used immediately.

The tissue was dehydrated by placing the tissue in three consecutive ethanols diluted in DEPC-treated water for two minutes apiece; 70%, 80%, 95% and then air dried for thirty minutes. The subsequent steps were identical to the wax section protocol above, starting from the Prehybridisation step.

2.5 MRCT In-Situ Hybridisation

Cryostat sections were cut at -20°C and TESPA-coated slides pressed onto the sections, affixing them to the slide. Originally slides were stored in 70% Ethanol 30% DEPC treated water at 4°C prior to use, but latterly sides were sectioned and, then used immediately.

Sections were air dried for one hour before use, then fixed for five minutes in 4% PFA in PBS, then washed twice in PBS for two and a half minutes each. The slides were then placed in 70% Ethanol: 30% DEPC-treated water for five minutes, then 95% Ethanol: 5% DEPC-treated water for another five minutes. Sections were placed in 70% Ethanol: 30% DEPC-treated water at 4°C until use.

Slides were rehydrated through 70%, 50% and 30% ethanols for two minutes a time, washed twice for ten minutes in PBS, followed by ten minutes in Proteinase K (15µg/ml in Proteinase K buffer; 50mMM Tris HCl, 20mM EDTA, pH 7.5), followed by two rinses in PBS for two minutes. The slides were placed in 0.1M TEA containing 0.003125% Acetic Anhydride which was added immediately to the TEA immediately prior to slide introduction and was mixed with a small magnetic flea throughout. This was left for five minutes, then repeated again with fresh reagents, then was washed for two minutes in 1X SSC.

2.5.1 Pre-hybridisation and hybridisation

The hybridisation mix consisted of:

Reagent	Volume (µl)
Deionised Formamide	500
20 x SSC	100
50 x Denhardt's Solution	100
50% Dextran	200
20% SDS	25
dH_2O	x
Total:	1000

Hybridisation mix was mixed thoroughly by pipetting up and down within the Eppendorf tube in which it was stored. 100µl of hybridisation mix was spread onto the slide and covered with a GelBond coverslip. The slides were placed in a sealed box, humidified with tissue soaked in 50% formamide, 1x SSC mixture. The box was placed in a waterproof bag and placed in a circulating water bath for one hour, submerged by placing a 1L Pyrex bottle containing water on top.

DIG labelled probe was diluted in hybridisation buffer at the required concentration and vortexed. The hybridisation mixture was heated to 80°C for five minutes, placed on ice to cool, and then 100µl of hybridisation mix was spread onto the slide and covered with a GelBond coverslip. The slides were placed in a sealed box, humidified with tissue soaked in 50% formamide, 1x SSC. The box was placed in a waterproof bag and submerged in a circulating water bath overnight set to the hybridisation temperature required.

2.5.2 Post Hybridisation Washes

Slides were washed in Solution A (1:1 ratio of Formamide: 2x SSC plus 0.1% Tween-20) at hybridisation temperature for fifteen minutes to allow GelBond coverslips to fall off, followed by two thirty minute washes in Hybridisation-temperature TBS-0.1% Tween (TBST).

2.5.3 Blocking and antibody staining

Slides were placed in 10% Heat-inactivated sheep serum/1 x TBST (HISST) at room temperature for one hour. Anti-DIG AP-fab fragments (Roche) were diluted 1:2000 in HISST. Slides were quickly removed from HISST and 100µl of the diluted antibody applied to the slide and covered with a glass coverslip as fast as possible to ensure the slide did not dry out. The slides were once again placed in box humidified with TBST, sealed and left at 4°C overnight. The slides were washed four times, for twenty minutes in TBST, then two ten minute washes in 1x NTMT (Alkaline phosphate buffer; 0.1M NaCl, 0.05M $MgCl_2$, 0.1M Tris Base, 0.01% Tween-20, 1 drop/ 5ml Levamisole) at room temperature, followed by staining of the sections in coplin jars wrapped in Aluminium foil containing 40ml NTMT, 180µl NBT and 140µl BCIP. Staining was checked every hour. The reaction was halted by washing twice in tapwater, and then the slides were fixed in 4% PFA in PBS for twenty minutes. Slides with strong staining were counterstained with Nuclear Fast Red for two minutes and washed in water, and then the slides were dehydrated of thirty seconds apiece through an ethanol series of 30%, 50%, 70%, and 90%, followed by two 100% ethanol steps for five minutes each. The slides were placed in Histoclear twice for five minutes, Histomount was applied to the sections on the slide and a glass coverslip mounted on top.

2.6 DAB Immunohistochemistry on Wax sections

Wax embedded sections were dewaxed in two consecutive seven minute incubations in Xylene, followed by five minutes in: 100%, 90% and then 70% ethanol, then rinsed in ddH_2O. The following steps were performed with a DAKO (Carpinteria, California, UK) Envision Kit, K-4000. For each slide, 150µl peroxidase block was applied for five minutes, followed by a brief rinse in ddH_2O, and then placed in TBS for five minutes. 350µl immuno media (Foetal Calf Serum containing 0.1% Triton X-100) was applied to each slide for ten minutes, followed by 200µl primary antibody diluted to the appropriate concentration in immuno media was applied and left at room temperature for forty-five minutes, then rinsed with ddH_2O, then placed in TBS for five minutes. 150µl Horseradish Peroxidase (HRP) anti mouse (or anti-rabbit, as appropriate in relation to the primary antibody used) reagent was applied and left for thirty minutes, then the slides were washed twice for five minutes each in TBS. 150µl of pre-prepared diaminobenzene (DAB) reagent was applied to each slide and colour development noted. Once enough colour was generated, the slides were washed twice in ddH_2O, dehydrated for two minutes in each of 70%, 80%, 90%, 95% and 100% Ethanols, then were placed for twice for ten minutes in Xylene then distrene plasticiser xylene, (DPX, obtained from BDH) applied to the sections and coverslips mounted on top.

2.6.1 Nissl Substance and Cytochrome Oxidase Staining

48µm frozen sections stored in PBS were mounted onto poly-L-lysine coated slides and left to dry at room temperature overnight.

Slides to be stained for Nissl substance were stained with 0.025% Thionine stain in acetate buffer (0.037M Sodium acetate anhydrous, 0.063M Acetic Acid, pH 4.4) until sections were appropriately coloured, then were placed in 95% ethanol for five minutes, followed by two five minute steps in 100% ethanol, then two Xylene steps for seven minutes each, then mounted with DPX and coverslipped.

Slides to be stained for Cytochrome Oxidase (CO) presence were placed in CO staining solution— 0.1M Phosphate Buffer containing 0.05% DAB, 0.2mg/ml Cytochrome c (Sigma C-2506), 0.4mg/ml Sucrose (Sigma S-1174) in an oven set to 37°C for three to seven hours, checking for colour development regularly. The slides were washed three times, for ten minutes each, then dehydrated through a series of Ethanols and defatted in Xylenes, in the same manner as slides stained with Thionine above.

2.7 Serotonin and 5-HTT immunohistochemistry

Monoclonal anti-5-HT antibody from Harlan-Seralab (Cambridge, UK) was diluted 1:5 (or monoclonal anti-5-HTT (Calbiochem, CA, USA) was diluted 1:2000) in immuno media, then free-floating frozen sections were exposed to the antibody overnight, then washed in 0.1% Triton X-100 in PBS (PBST) three times at five minutes apiece. Sections were then incubated for two hours in 1:200 biotinylated secondary antibody (DAKO) diluted in immuno media, rinsed three times for five minutes in PBST, then incubated for two hours in 1:400 Streptavidin peroxidase complex (Amersham), rinsed in PBST three times for five minutes per wash and revealed in 0.02% diaminobenzidine, 0.003% H_2O_2 solution, washed three times in PBS and mounted on a poly-L-lysine subbed microscope slide, left overnight at room temperature to dry, then dehydrated through a series of Ethanols and defatted in Xylenes, in the same manner as slides stained with Thionine above (Section 2.6.1).

2.7.1 Genetic Backgrounds of mouse mutants

The genetic backgrounds of the mice used in this thesis are outlined in Table 2.1. The *Sap-102-Psd-95* compound mutants and heterozygotes were generated by breeding together of homozygous mutants from the two mouse colonies. Since *Wnt7a*$^{-/-}$ mice are infertile but *Wnt7a*$^{+/-}$ are not (Parr and McMahon, 1998), *Wnt7a*$^{-/-}$*Dvl1*$^{-/-}$ double mutants must be generated by breeding together of the two colonies, and then breeding together either *Wnt7a*$^{+/-}$*Dvl1*$^{+/-}$ (where Mendelian law dictates that on average, 1 in 16 of the offspring will be *Wnt7a*$^{-/-}$*Dvl1*$^{-/-}$) or *Wnt7a*$^{+/-}$*Dvl1*$^{-/-}$ mice (where 1 in 4 offspring should be *Wnt7a*$^{-/-}$*Dvl1*$^{-/-}$).

Table 2.1 Genetic backgrounds of the mice used in this thesis.

Mutant Name	Genetic Background	References
Dvl1$^{-/-}$	C57BL/6	Ahmad-Annuar et al., 2006
Dvl2$^{-/-}$	129S/SvEvTac	Hamblet et al., 2002
Psd-95$^{-/-}$	MF1/BL6 mixed background	Migaud et al., 1998
Psd-95GK$^{-/-}$	MF1/BL6 mixed background	Personal communication, Prof. Seth Grant
Sap-102$^{-/-}$	MF1/BL6 mixed background	" "
Plc-β1$^{-/-}$ and "wild-type"	B6/129	Hannan et al., 2001
Mglur5$^{-/-}$	B6/129	Hannan et al., 2001
Pkar2b$^{-/-}$	C57BL/6	Dr. Stanley McKnight, personal communication
Wnt2b$^{-/-}$	129S1/Sv	Personal communication, Prof. T.P. Yamaguchi
Wnt7a$^{-/-}$	C57BL/6	Ahmad-Annuar et al., 2006
Wnt8b$^{-/-}$	CBA	Personal communication, Dr. J.O. Mason

3 Characterisation of *Wnt, Frizzled and sFRP* mRNA expression in postnatal barrel cortex.

3.1 Introduction

There are four processes involved in barrel formation; cell adhesion, movement, death and migration (Barnett et al., 2006b), and Wnts can regulate all of these processes. Yu and Malenka demonstrated that Wnt release is activity-dependent (Yu and Malenka, 2003), raising the possibility that NMDARs regulate barrel formation by regulating Wnt release. Furthermore, NMDAR activation and Wnt signalling regulate similar developmental events, including axon and dendrite remodelling, cell death and cell migration (reviewed in Gould and Cameron, 1996; Patapoutian and Reichardt, 2000; Contestabile, 2000; Marin and Rubenstein, 2003; Ciani and Salinas, 2005; Waxman and Lynch, 2005; Erzurumlu and Iwasato, 2006). It is clear that certain NRC components are essential for normal barrel cortex development (reviewed in Erzurumlu and Kind, 2001; Barnett et al., 2006b) and that Wnt signalling components are present in, and have the potential to interact with the NRC (Makino et al., 1997; Masuko et al., 1999; Husi et al., 2000; Hanada et al., 2000; Hering and Sheng, 2002).

A role for Wnts in thalamocortical axon (TCA) development was revealed when it was discovered that *Frizzled 3*$^{-/-}$ and *Celsr3*$^{-/-}$ mice exhibit a total loss of thalamocortical and corticothalamic axons (Wang et al., 2002). It is conceivable that localised expression of Wnt proteins could lead to TCA termination in layer IV and segregation into the characteristic barrel-like pattern that is a prerequisite to barrel formation. Most mouse Wnt proteins are highly glycosylated, rarely travel more than three cell diameters from the cell that produces it (Sanson, 2000) and it is therefore possible that localised *Wnt* expression in layer IV cortical cells could specify the appropriate regions for normal TCA termination and segregation.

As a first step in examining the role of Wnt signalling in barrel development, we examined the developmental expression profile of Wnt mRNA with qRT-PCR. We chose P4, P7, P14, P21 and Adult as time points to examine Wnt expression because barrels form between P4 and P7; P14 is the peak of dendritic elaboration, P21 marks the end of dendritic elaboration, and in Adult mice, cell maintenance events and layer II/III synaptic plasticity are occurring.

3.1.1 Screening of Wnt, Frizzled and sFRP expression in mouse mutants that lack barrels

Since the cell aggregations that comprise the barrel structure are not maintained in cortical slice culture, there are few options available to study the effects of certain proteins on barrel formation. One way of investigating the role of Wnts in barrel formation was to compare the differences in mRNA expression levels of *Wnt*, *Frizzled* and *sFRP* genes between wild-type mice and mutants that lack barrels by qRT-PCR. This would identify candidate genes for further investigation, and should also help build a hypothesis about the functions of each gene in barrel cortex during the development and maturation of barrels. We chose to examine for differences in Wnt, Frizzled and sFRP expression in *Mglur5*$^{-/-}$, *Plc-*$\beta_1^{-/-}$ and *Pkar2*$\beta^{-/-}$ mice, since these mice lack barrels. We chose to examine at the age of P14, as this was the period of peak dendritogenesis, a process that was thought to be essential for the formation of a normal, mature barrel (Datwani et al., 2002b). However, it is now known that selective elaboration of layer IV cortical cell dendrites into TCA patch plexus is not required for the cellular aggregation events that form barrels to occur (Upton et al., 2006).

Mglur5$^{-/-}$ mice lack barrels and display segregation of TCAs in PMBSF into rows but not individual patches (Hannan et al., 2001; Spires et al., 2004). This total loss of barrels, despite partial segregation of TCAs into rows strongly suggests that mGluR5 signalling is crucial for the normal transfer of patterns from TCAs to their postsynaptic partners during barrel development. mGluR5 has been shown to signal through PLCβ_1 to form barrels (Hannan et al., 2001) and *Plc-*$\beta_1^{-/-}$ mice lack cortical barrels, although the patterning, distribution and size of TCA patches are unaffected. *Plc-*β_1 mutant mice were of particular interest, as PLCs have been shown to be part of the Wnt/Ca^{2+} pathway (Miller et al., 1999; Kuhl et al., 2000a; Kuhl et al., 2000b). *Pkar2*$\beta^{-/-}$ mice have poorly defined barrels; the septa and barrel hollows do not display the reduction in number of cells seen in wild-type animals, although good TCA segregation in PMBSF is observed (Inan et al., 2006; Watson et al., 2006a). If Wnt signalling is perturbed in these mutants, it would support the hypothesis that Wnts are involved in the processes of barrel formation. In addition, by comparing animals with slightly different barrel phenotypes we hoped to identify Wnts involved in specific aspects of barrel development.

3.1.2 Chosen methodology for determining the presence and location of *Wnt*, *Frizzled* and *sFRP* genes

As a first step in determining whether Wnt signalling is involved in barrel cortex development, I identified the *Wnts*, *sFRPs* and *Frizzleds* that are present in the barrel cortex during the period of barrel formation. As mentioned in the introduction chapter, Wnt proteins are highly glycosylated, difficult to purify and problematic for antibody generation. For these reasons, few anti-Wnt antibodies were available at the beginning of this project, although antibodies to mouse Wnts 1, 3a, 4, 5a, 8a, 10b and 11 are now commercially available. Nevertheless, studies characterising the presence, relative levels and localisation of *Wnt* genes have focused on mRNA expression. Although RNase Protection assays (RPA) are considered to be "gold standards" in quantification of RNA (Bustin, 2000; Dheda et al., 2004; Wong and Medrano, 2005), they do have their limitations. Often large numbers of samples have to be pooled together to allow the extraction of sufficient amounts of RNA. Our barrel cortex dissections have a volume of approximately 2.5mm^3 (Barnett et al., 2006a, see Materials and Methods chapter). However, Reverse Transcriptase Polymerase Chain reaction (RT-PCR) can amplify from femtomoles of target DNA sequence generated from reverse transcription of mRNA. Therefore, RT-PCR was chosen to examine for the presence of *Wnt*, *Frizzled* and *sFRP* genes, although initial screens were restricted to identifying *Wnts* present in P0 and P7 cortex. However, we subsequently used quantitative real-time RT-PCR (qRT-PCR) to amplify all *Wnt*, *Frizzled* and *sFRP* genes and expanded the number ages examined. Further descriptions of these techniques, including their strengths and limitations follow.

3.1.3 Degenerate primer *Wnt* gene PCR

A degenerate primer RT-PCR strategy has been described that amplifies DNA at two conserved sites common to almost all Wnts (Figure 3.2) yielding a PCR product of approximately 400bp (Gavin et al., 1990). These degenerate primers detect all *Wnts* other than *Wnts 9a*, *9b* and *11* (Figure 3.1). Any PCR product of the appropriate size of approximately 400bp would be identified by subsequent cloning and sequencing. Degenerate *Wnt* primer RT-PCR was performed on barrel cortex dissections taken at two ages, P0 and P7 as a preliminary test of *Wnt* gene expression in primary somatosensory cortex. The advantage of degenerate primer RT-PCR is that this technique would quickly establish if *Wnt* genes were present in barrel cortex. The disadvantages of this technique are that certain *Wnts*

are not amplified, it is impossible to ascertain whether certain *Wnts* have been missed by this method and so an exhaustive list of *Wnt* genes present in barrel cortex is not revealed. Finally, no insight is given about expression levels of each gene.

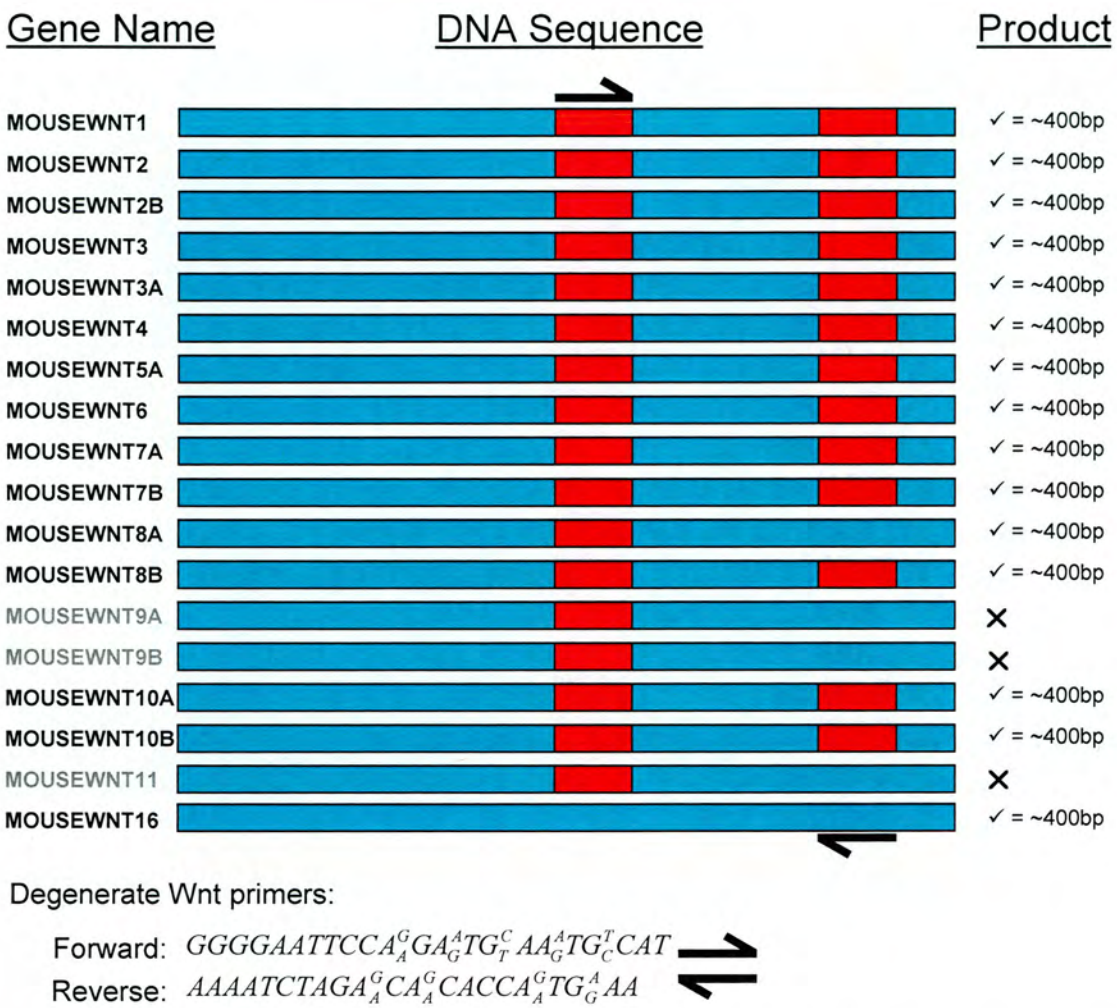

Figure 3.1
Degenerate Wnt primer strategy. Wnt genes (blue bars) showing the consensus binding sites (red bars) for the degenerate primers (half arrows). Note: *Wnts 9a*, *9b* and *11* do not contain the 3' consensus binding site, and therefore will not be amplified. PCR product size should be approximately 400bp.
The PCR product bands were cut from the gel, purified on Qiaspin Gel Extraction columns (Qiagen), cloned into pGEM-T Easy (Promega), transformed into competent JM-109 cells (Promega), cultured in 2XTY medium, miniprepped (Qiagen) and sequenced (MWG Biotech AG, Figure 3.11).

```
MOUSEWNT1     MRQECKCHGMSGSCTVR..<>..FHWCCHVSCRNCTHTRVLHECL----------------
MOUSEWNT2     LKQECKCHGVSGSCTLR..<>..FHWCCAVRCQDCLEALDVHTCKAPKSADWATPT------
MOUSEWNT2B    LKLECKCHGVSGSCTLR..<>..FHWCCAVRCKECRNTVDVHTCKAPKKAEWLDQT------
MOUSEWNT3     MHLKCKCHGLSGSCEVK..<>..FHWCCYVSCQECIRIYDVHTCK----------------
MOUSEWNT3A    MHLKCKCHGLSGSCEVK..<>..FHWCCYVSCQECTRVYDVHTCK----------------
MOUSEWNT4     MRVECKCHGVSGSCEVK..<>..FHWCCFVKCRQCQRLVEMHTCR----------------
MOUSEWNT5A    ADVACKCHGVSGSCSLK..<>..FHWCCYVKCKKCTEIVDQFVCK----------------
MOUSEWNT5B    ADVACKCHGVSGSCSLK..<>..FHWCCFVRCKKCTEVVDQYVCK----------------
MOUSEWNT6     TRTECKCHGLSGSCALS..<>..FHWCCVVQCHRCRVRKELSLCL----------------
MOUSEWNT7A    MKLECKCHGVSGSCTTK..<>..FHWCCYVKCNTCSERTEMYTCK----------------
MOUSEWNT7B    MKLECKCHGVSGSCTTK..<>..FHWCCFVKCNTCSERTEVFTCK----------------
MOUSEWNT8A    TKRTCKCHGISGSCSIQ..<>..FQWCCTVKCGQCRRVVSRYYCTRPVGSARPRGRGKDSAW
MOUSEWNT8B    MKRTCKCHGVSGSCTTQ..<>..FHWCCAVRCEQCRRRVTKYFCSRAERPPRGAAHKPGKNS
MOUSEWNT9A    VETTCKCHGVSGSCTVR..<>..VRWCCYVECRQCTQREEVYTCKG----------------
MOUSEWNT9B    LRTTCKCHGVSGSCAVR..<>..VQWCCYVECQQCAQQELVYTCKR----------------
MOUSEWNT10A   MRRKCKCHGTSGSCQLK..<>..FHWCCFVVCEECRITEWVSVCK----------------
MOUSEWNT10B   LKRKCKCHGTSGSCQFK..<>..FHWCCYVLCDECKVTEWVNVCK----------------
MOUSEWNT11    LETKCKCHGVSGSCSIR..<>..YHWCCYVTCRRCERTVERYVCK----------------
MOUSEWNT16    MSVDCRCHGVSGSCAVK..<>..FIWCCYVRCRRCESMTDVHTCK----------------

PrositePattern Wnt-1 Family: PAC-[KR]-C-H-G-[LIVMT]-S-G-x-C.
```

Figure 3.2
Mouse Wnt protein sequence alignment.
Degenerate primers were designed previously (Gavin et al., 1990) to the conserved CKCHG and FHWCC sequences (Gavin et al., 1990). Note that these primers miss Wnt8a, Wnt9a, Wnt9b, Wnt11 and Wnt16. The current consensus Wnt protein sequence from Prosite service is also shown. Adapted from Roel Nusse's Wnt Gene Homepage Website. (http://www.stanford.edu/~rnusse/wntwindow.html).

3.1.4 Individual primer *Wnt* gene PCR

An experiment utilising a RT-PCR method has been published that describes primer pairs designed to amplify each *Wnt* gene individually (Lako et al., 2001). The primer sequences and the PCR reaction conditions published in that paper were used to determine the complement of *Wnts* present in the barrel cortex of mice taken at different ages throughout barrel cortex development. An important modification was made to the experiment described in the Lako et al., (2001) paper. In order to obtain a general picture of relative expression levels of *Wnt* genes over development, the amounts of mRNA loaded into the cDNA

synthesis reaction were normalised by quantification of mRNA on an ultraviolet (UV) spectrophotometer, i.e. mRNA volumes were adjusted so that equal amounts were loaded into each cDNA synthesis reaction. However, there are significant limitations of RT-PCR with products run on agarose gel—the technique is not an ideal way of determining relative amounts of mRNA species because of two major problems in quantifying PCR product amounts with this method, namely PCR reaction kinetics, and visualising and quantifying the amount of DNA product in agarose gels.

3.1.4.1 PCR reaction kinetics

The log-linear phase of the PCR reaction (Figure 3.3) is the point in the PCR reaction where the rate of production of PCR product is constant. This is the only stage in the PCR reaction where the amount of DNA product made relates to the starting amount of cDNA. During this phase, virtually every molecule of primer interacts with a molecule of template DNA (as primers are in vast excess at this stage). This kinetic environment exists only between (approximately) the tenth and the twentieth cycle of the PCR reaction, although this varies according to the starting amount of cDNA present. Genes expressed in low abundance often enter the log-linear phase of the PCR reaction at around 30 cycles. As greater amounts of PCR product are made, the efficiency of the PCR reaction is reduced, and log-linear production of product ceases to occur. Standard RT-PCR protocols often have cycle numbers in the mid thirties to forty in order to generate enough PCR product to visualise on an agarose gel stained with Ethidium bromide (EtBr) and as such the amount of product visualised after 35-40 PCR reaction cycles may not correlate to the amount of cDNA at the start of the reaction. Variation of the concentration of any PCR reaction component can alter the rate of (or eliminate) production of PCR product. However, only annealing temperature and $MgCl_2$ concentration changes were required to optimise the PCR reaction for this study. By reducing the number of cycles to be within the log-linear phase and running dilution controls, these problems can be overcome. However, this is a very time-consuming technique that is inappropriate for analysing large numbers of genes. Furthermore the problem of visualisation and quantification of DNA product remain.

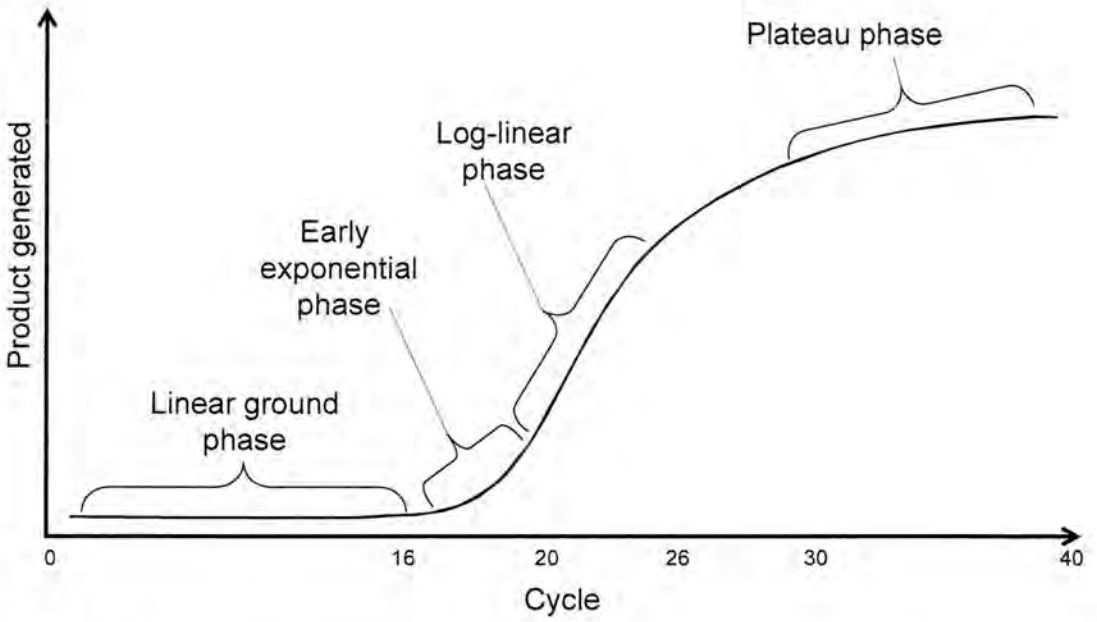

Figure 3.3
Phases of the PCR amplification curve.
The PCR amplification curve charts the accumulation of fluorescent emission at each reaction cycle. The curve can be broken into four different phases: the linear ground, early exponential, log-linear, and plateau phases. Data gathered from these phases are important for calculating background signal, cycle threshold (C_T), and amplification efficiency, discussed in text.

Quantification of RT-PCR product which has been run out on an agarose gel and visualised under ultraviolet (UV) illumination can introduce further variability in results. If the template *Wnt* cDNA species are in extremely low abundance, it is possible that PCR product is being generated during the PCR reaction, but in insufficient amounts to be visualised on the gel and this assumes that no PCR product is lost during gel loading. Finally, EtBr has a poor affinity for DNA, and when incorporated into agarose gel is 1,000 times less sensitive than SYBRgreen when used to visualise DNA (Wong and Medrano, 2005). When making the agarose gel, it can be difficult to obtain even EtBr staining throughout. One can quantify the amount of DNA present in a band by comparing the brightness of the band of interest against a corresponding band of DNA of known concentration, normally from quantitative molecular weight ladder. If EtBr gel staining varies between the ladder and the band of interest, quantification will be inaccurate.

3.1.5 *Wnt, Frizzled* and *sFRP* gene SYBRgreen qRT-PCR

3.1.5.1 *Principles of SYBRgreen RT-PCR*

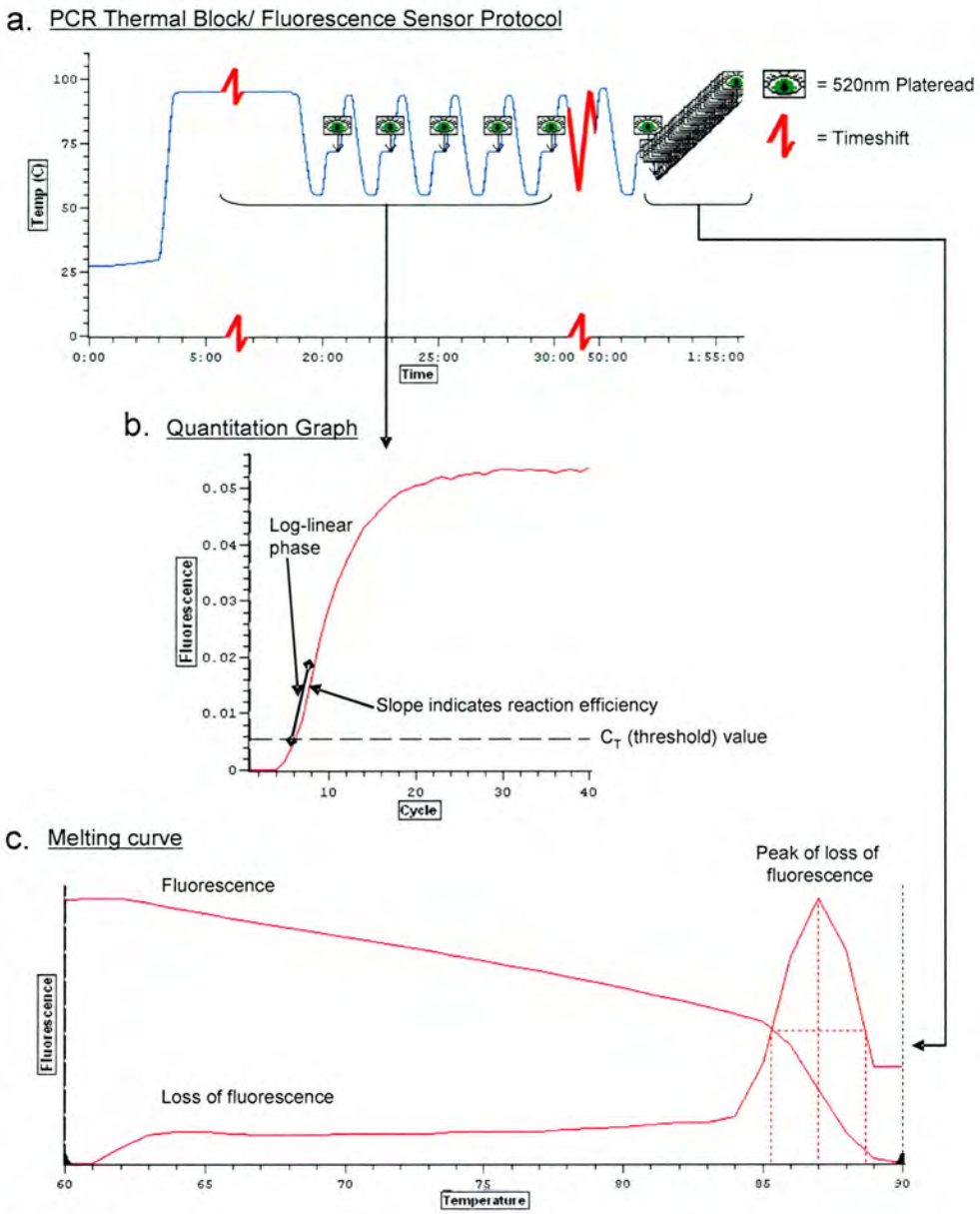

Figure 3.4
Opticon Monitor software analysis tools.
A: Thermal cycler sensor. The PCR machine illuminates the reaction mixture at 497nm (the peak absorption wavelength of SYBRgreen) and reads the resultant fluorescence at 520nm (the peak emission wavelength of SYBRgreen) which should directly correlate with the amount of SYBRgreen bound double-stranded DNA (dsDNA) in the well. B: Quantification graph. The data collected in (a) is graphed by cycle number. The log-linear phase is the time where the PCR reaction is at peak efficiency, rates are not limited by a surfeit of cDNA, dNTPs or primers, nor inhibited by excess product; the efficiency is revealed by the slope of the reaction. The C_T value is a user-defined point on the graph where all (background) fluorescence below that level is ignored, and should be defined within the log-linear phase. C: Melting curve profile showing loss of fluorescence, and 1/loss of fluorescence. The melting curve profile should give a single defined peak if only one product has been generated in the PCR reaction; as the head breaks the hydrogen bonding of dsDNA. The SYBRgreen dissociates and fluorescence is lost. Each amplicon exhibits a unique melting profile.

Real-time quantitative RT-PCR (qRT-PCR) overcomes some of the limitations of measuring the amount of product made during the linear phase of the PCR reaction and subsequent

quantification on an agarose gel. SYBRgreen I binds the minor groove of double stranded DNA and once bound, fluoresces strongly with a maximum absorbance at 497nm, and an emission maximum at 520nm (Morrison et al., 1998). Using a specialised PCR machine (DNA Engine Opticon I System, PTC-200 Cycler coupled to CFD-3200 Detector, Bio-Rad, California, USA) it is possible to detect the amount of fluorescence produced after each PCR cycle, as the PCR machine illuminates the sample with 497nm light and reads light emitted at 520nm (Figure 3.4) By assaying fluorescence, one can determine the amount of cDNA species in the reaction after each cycle, and generate a graph showing amplification rates, permitting quantification of the original amount of cDNA in the reaction (Figure 3.4).

3.1.5.2 Background fluorescence

There will always be a low level of background fluorescence in the PCR reaction; this is disregarded in quantification by manually specifying a threshold level (called C_T; cycle number threshold (Figure 3.4), which is placed at the beginning of the log-linear phase; below which all fluorescence is ignored. The slope of the log-linear phase reflects the PCR reaction efficiency and is assumed to be the same in all PCR reactions. The C_T value is crucial for quantification. Genes that are represented in greater amounts in the cDNA accumulate detectable fluorescent product sooner (and therefore cross the C_T threshold at a lower cycle number) than lower abundance species.

3.1.5.3 Managing potential problems of performing SYBRgreen RT-PCR.

SYBRgreen qRT-PCR has problems that need to be managed by careful experimental design. Since SYBRgreen binds all double stranded DNA, including non-specific amplification products, primer dimers *et cetera*, primers have to be designed carefully and reactions optimised to eliminate this problem. A key feature of the Opticon I qRT-PCR system is that it performs a melting curve analysis on any PCR product produced (Figure 3.4). Melting curve analysis can identify specific sequence fragments, thereby determining the homogeneity of the sample. At the end of a PCR reaction run, the Opticon I machine raises the temperature of the reaction mixture and records fluorescence levels. As the temperature increases, the hydrogen bonds in the dsDNA are broken, dsDNA is denatured and consequently the SYBRgreen fluorescence is lost. The denaturation temperature depends on the size and G+C content of the amplicon, and is unique to the sequence of each sample.

Thus a unique melting curve for each primer pair/ product is observed, and can be used as measure of the quality of the reaction. If more than one curve is seen, then it is likely due to amplification of multiple PCR products. Accordingly, if a melting curve profile is incorrect compared to a positive control, or two peaks are seen, primer redesign and/ or PCR reaction condition optimisation are required. As a further step to ensure amplification of the gene of interest, the DNA generated by all primer pairs was cloned and sequenced.

3.1.6 *In situ* hybridisation

Since many *Wnts*, *sFRPs* and all *Frizzled* genes are expressed throughout barrel cortex, the next step in characterising any role for *Wnts* in barrel formation is to examine the laminar distribution of the expression of these genes in the cortex. During my time spent performing *in situ* hybridisations (ISH), the laboratory of Elizabeth Grove published a paper containing *in situ* hybridisations for all of these genes in postnatal cerebral cortex (Shimogori et al., 2004). The genes they found to be expressed exclusively in barrel cortex were *Wnt2b* and *Frizzled 3*—both are observed in barrel walls at P20. Prior to the publication of this paper, ISH for *Wnts 2b, 3, 4, 5a, 7a, 7b, 8b* and *11* in barrel cortex at P4, P7, P14, P21 and Adult were attempted unsuccessfully in collaboration with a commercial *in situ* hybridisation service run by MRC Technologies (MRCT) at the Western General Hospital, Edinburgh. In order to focus on one gene to validate use of this method, *Wnt7a* was chosen and pursued, as the laboratory of Patricia Salinas had observed low levels of *Wnt7a* expression in postnatal cortex (P. Salinas, personal communication). However, the *in situ* hybridisation runs performed at MRCT failed to work properly for the reasons discussed below.

After the Shimogori *et al.*, 2004 paper was published, much effort was spent trying to replicate the *Wnt2b* expression data shown in the barrel cortex and expand the ages examined (P4, P7, P14, P21 and Adult) to cover various key points in barrel development. We used a different *Wnt2b in situ* probe to the one used by the Grove Laboratory as their probe was not made available and it was impossible to generate their probe *de novo* from their published information (Grove et al., 1998). Instead we used an alternative probe (Zakin et al., 1998) that was designed to hybridise to a 384bp cDNA fragment located over the fourth and fifth exons of *Wnt2b*. Additionally, we used mice with the genetic background of B6/129, whereas the mice used in the Shimogori *et al.*, 2004 paper had a CD-1 genetic background.

3.2 Methods

3.2.1 RNA extraction and cDNA synthesis

Barrel cortices were dissected from wild-type mice and from mice from the following genotypes: *Pkar2β*$^{-/-}$, *Plc-β*$_1^{-/-}$ and *Mglur5*$^{-/-}$ at the following ages: P4 (barrels begin to form), P7 (barrels fully formed), P14 (peak of dendritogenesis), P21 (near end of dendritogenesis) and Adult mice (two months of age, Erzurumlu and Kind, 2001). Genetic backgrounds are specified in the Materials and Methods chapter. Total RNA was extracted from two different barrel cortices, each from a different animal of the same age and genotype, using a Qiagen RNeasy mini kit. cDNA was made using a dithiothreitol-free, MMLV based synthesis reaction which is outlined in detail in the Materials and Methods chapter.

3.2.2 Non-quantitative PCR

Primers, thermocycler timings, annealing temperatures and reaction conditions were performed as described previously (Lako et al., 2001). 1µl PCR product was added to 3µl double distilled water and 1µl 5x gel loading buffer (Bioline, Cambridge, UK), mixed and loaded and run on a 1% agarose gel containing $2x10^{-5}$% Ethidium bromide. See Materials and Methods chapter for greater detail.

3.2.3 Cloning and sequencing of PCR product

PCR product-containing bands were identified and excised from agarose gel and the DNA was extracted from the agarose using a Qiagen Quickspin Gel extraction kit. 1µl product was ligated into pGEM-T easy plasmid vector (Promega). Subsequently the cloned plasmids were heat shocked into JM-109 competent *E. coli* cells (Promega) and plated onto LB-Ampicillin IPTG X-Gal plates at 37°C overnight. Since the pGEM-T Easy plasmid permits blue/white colony screening as inserts disrupt the β-galactosidase gene, three white colonies were picked, grown in 5ml LB, miniprepped using an alkaline lysis method (Qiagen plasmid Minikit) and 1µg was vacuum dried and sent for commercial sequencing by MWG Biotech AG. See Materials and Methods chapter and Figure 3.11 for further details.

3.2.4 SYBRgreen RT-PCR

1µl of cDNA was placed into each well of an 8-well optical PCR strip (MJ Research, UK) along with 24µl of a mastermix containing: 0.5µl of each appropriate primer, 10.5µl double distilled water and 12.5µl of Qiagen 2x SYBRgreen RT-PCR mix. Repetitions of PCRs were performed for P4, P7, P14, P21 and Adult cDNAs, and were placed in adjacent reaction wells; blank controls used 1µl of no reverse transcriptase cDNA synthesis product, and dual serial dilution series of P14 cDNA were performed (discussed below). The Opticon Monitor thermocycler machine was programmed with an initial 95.0°C incubation for 15 minutes, followed by a loop of 94.0°C for 15 seconds, 55.0°C for 30 seconds, 72.0°C for 30 seconds, which repeated 35 times. Following this, a melting curve analysis from 60.0°C to 90.0°C was performed. See the Materials and Methods chapter for greater details.

3.2.5 SYBRgreen RT-PCR Primer Design.

Each primer pair used in the PCR reaction had to fulfil five criteria;

1 Amplicon size must be between 80-200bp.
2 The primers must span an intron.
3 The primer sequences must pass a BLAST test so that primers have homology to only the gene of interest.
4 The primers must produce a single specific DNA product, initially testable by standard agarose gel PCR (on positive control cDNA, a mixture of cDNA taken from E10.5, E11.5, and E12.5 mouse embryos) then performing a qRT-PCR run on the same cDNAs.
5 The sequence of PCR product, once cloned and sequenced must pass another BLAST test.

These processes are illustrated in a flowchart diagram in Figure 3.5.

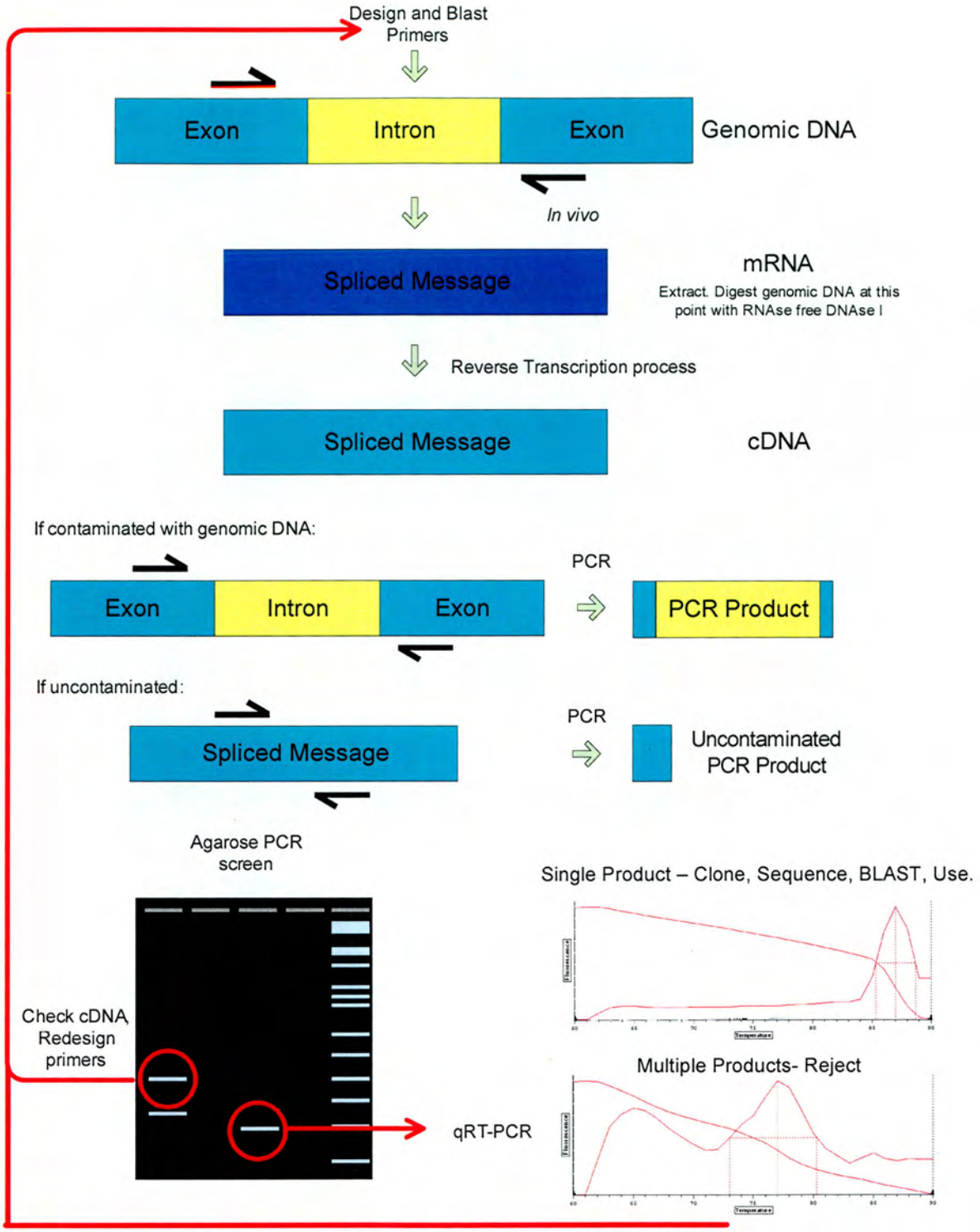

Figure 3.5
Flowchart of the primer design process. Intron spanning primers are designed, and a BLAST search is performed to determine what the primer sequences will bind. If the primers bind only the intended sequences, they are used to amplify cDNA fragments. Primers are tested for quality on agarose gel (to determine if the product is at the correct molecular weight) and by SYBRgreen melting curve profiles (see text).

3.2.6 Relative Gene Expression Quantification

In order to compare the data generated by qRT-PCR between different ages, primer pairs and repetitions of each run, it is necessary to normalise the data against a "housekeeping gene". The ideal housekeeping gene would be expressed at a level that would remain in a constant proportion to total RNA amongst all samples (allowing normalisation of variation in amount of total RNA added to each cDNA synthesis reaction) and not exhibit any increase or decrease in expression over age or genotype (Suzuki et al., 2000). Common housekeeping genes used to normalise qRT-PCR data against include Glyceraldehyde-3-phosphate dehydrogenase (GAPDH), ß-actin, 18S RNA (if a total RNA extraction method is used, Suzuki et al., 2000). All three housekeeping genes were tested (Figure 3.9), and 18S was selected as our control gene as it showed the least variability between cDNA samples from tissue taken at different ages (Figure 3.9, Barnett et al., 2006a). We have observed developmental regulation in ß-actin and GAPDH expression in barrel cortex (Figure 3.9). This could be due to the high metabolic rates that occur in TCAs and elaborating cortical neuron dendrites (Sharp et al., 1988). There are potential problems in using 18S as the housekeeping gene; it is a ribosomal, not cellular RNA, and in poor RNA extractions may not represent the total cellular mRNA pool (Aerts et al., 2004). When 18S is used as the housekeeping gene, it is assumed that the ratio of 18S to mRNA does not vary from sample to sample. If a poor RNA extraction alters this ratio, this distorts the 18S:mRNA ratio, and will result in inaccurate quantification of all data from this sample. To overcome this problem, all RNA extracted from barrel cortex was tested for its quality by running out on an RNase free 1% agarose gel and quantifying the difference in fluorescence under UV illumination (see Materials and Methods chapter for more details).

3.2.7 SYBRgreen qRT-PCR linearity tests

Once the primers were satisfactorily optimised and cloning and sequencing confirmed the identity of the amplicon, we started to examine *Wnt*, *Frizzled* and *sFRP* expression levels in cDNA made from RNA extracted from barrel cortices aged P4, P7, P14, P21 and Adult. Duplicate serial dilution series of P14 cDNA (were performed for every primer pair in every qRT-PCR run, in order to test the linearity of each PCR reaction, as a test of cDNA quality and pipetting accuracy (Figure 3.6). The dilution series also served to test that the rate of amplification of DNA does not vary by sample concentration and allows comparison of the DNA amplification rates between different primer pairs.

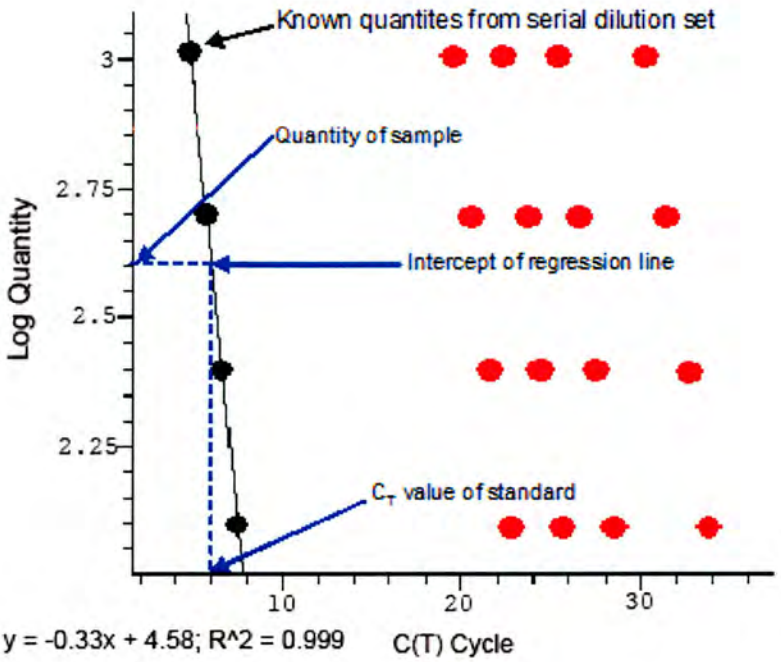

Figure 3.6
Linear regression analysis for each set of primers used per run. Linear regression analysis was performed on the dilution series, allowing quantification (see text and Figure 3.7). Runs that yielded r^2 values of ≥ 0.95 were included for further analysis; otherwise they were discarded and redesigned (see Figure 3.5).

3.2.8 Normalisation of data

To compare *Wnt* levels between PCR runs, all ages were normalised to both P14 and Adult values, generating two datasets, presented below. Since the data is normalised to 100% of one age (Figure 3.7), every data point at that age will automatically be 100% (Figure 3.8). This means that meaningful statistics cannot be performed at that age, and any variability within that age point will be masked. To ensure statistical analysis included all ages, data was normalised to P14 (the age at which all of the linearity dilution series were performed) and Adult (to allow comparison of all of the earlier ages). One-way analysis of variance (ANOVA) statistical tests were performed, followed by Student-Newman-Keuls post-hoc tests for all ages with significance on the ANOVA.

$$\text{Value on bar chart} = \left[\frac{\text{Units in 1ul ageX cDNA with wntY primers}}{\text{Units in 1ul ageX cDNA with 18S primers}} \div \frac{\text{Units in 1ul P14 cDNA with wntY primers}}{\text{Units in 1ul P14 cDNA with 18S primers}} \right] \times 100\%$$

Figure 3.7
Equation used to normalize data against P14 18S housekeeping gene cDNA standard. AgeX = the age of the mouse from which the cDNA was extracted, WntY = the gene of interest. Values are expressed as a percentage.

a.

Normalisation of genes to Adult allows direct comparison of all earlier ages by ANOVA

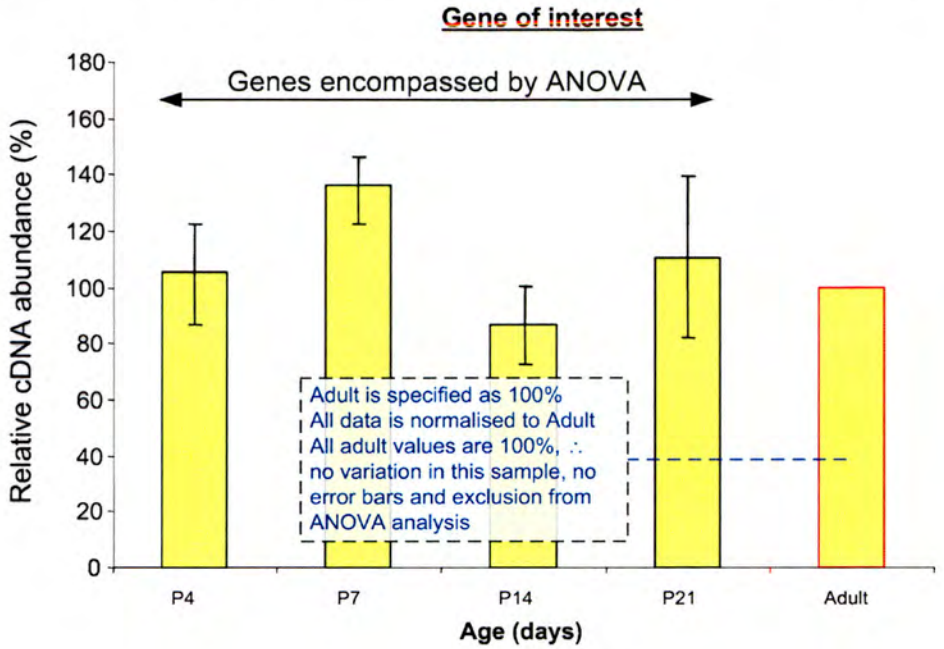

b.

Normalisation of genes to P14 allows direct comparison of all other ages by ANOVA

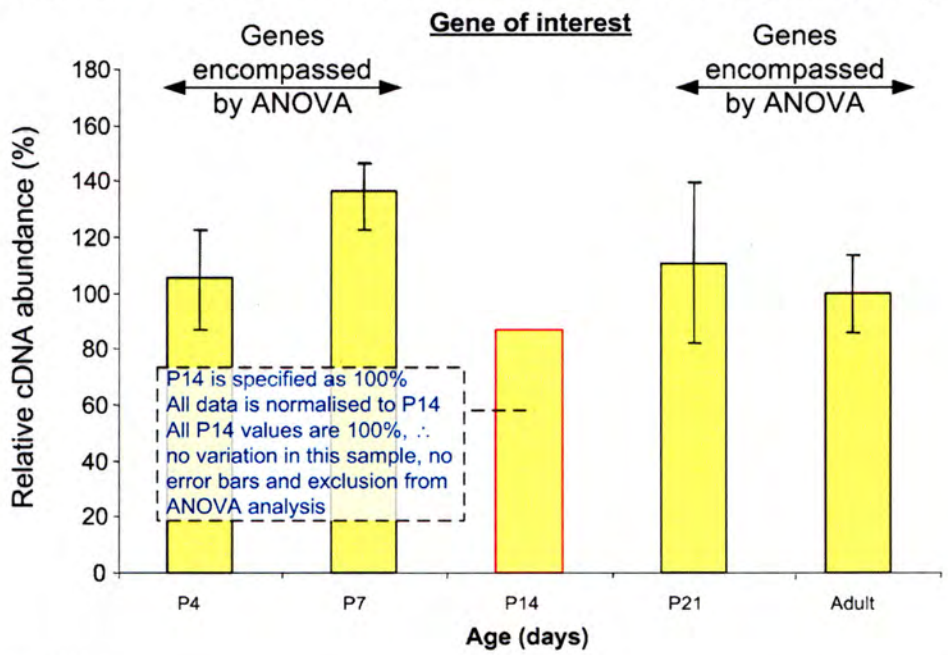

Figure 3.8

The genes are normalised against Adult (a) and P14 (b) ages. Since Adult in (a) and P14 in (b) are defined as 100%, no variation is seen at those ages, and therefore it is inappropriate to include them in a one-way ANOVA test (as no measure of the variability in that age can be made). As such, the two normalisations shown above were performed, allowing comparison of all of the ages prior to Adult to be performed (a) and all of the ages except P14 (b). P14 was chosen in (b) as this was the age at which all of the linearity analyses were performed in Figure 3.6.

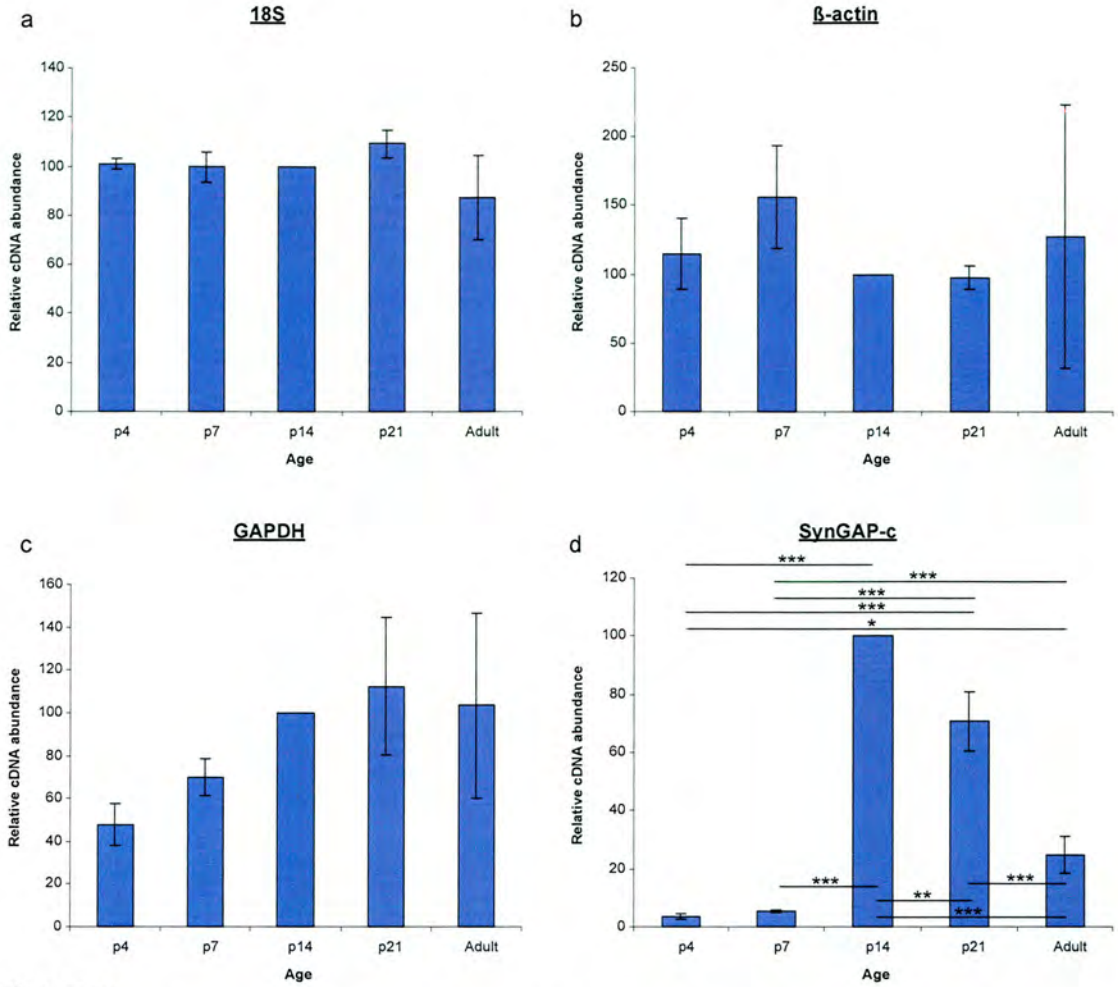

Figure 3.9
Assay of developmental regulation of housekeeping genes and recapitulation of published expression profiles using the same qRT-PCR method.
Graphs a-c, raw expression data normalised to P14 values; 18S appears to be expressed in similar amounts throughout development, β-actin and GAPDH appear to show developmental regulation. Graph d shows *Syngap-c* expression on the same cDNA. The standardised age range of P4, P7, P14, P21 and Adult was used throughout all developmental qRT-PCR studies. * = $p < 0.05$; ** = $p < 0.01$; *** = $p < 0.001$, n=6.

3.2.9 ΔΔCT method for comparison of gene expression levels between wild-type and mutant mice

In order to reduce the number of samples required to compare *Wnt* expression between genotypes, we changed the methodology to remove the dilution series from each qRT-PCR run. Linear regression analysis on dilution series were preformed for every run when examining changes in gene expression through development (Figure 3.6). In total just under 1,500 individual qRT-PCR reactions had to be performed. However, the $\Delta\Delta C_T$ method (Figure 3.10) does not require linearity regression analysis to be performed for each primer pair per run. This method makes assumptions about the nature of the kinetics of the PCR reaction, specifically that the amount of DNA produced in the log-linear phase doubles each

cycle (i.e. the PCR reaction efficiency is 100% within the log-linear phase). Variations in PCR reaction efficiency between different primer pairs are almost always negligible (Pfaffl, 2001). Furthermore, since each primer pair had already had linear regression analyses done in previous experiments, the regression equations were assessed for big variations in the gradients generated; little variation was observed between primer pairs (<5%). The $\Delta\Delta C_T$ method is a widely used technique (Gibson et al., 1996; Pfaffl, 2001; Terada et al., 2003) and is suitable as a preliminary screen for potential genes for further investigation. Briefly, a threshold value is set just above background levels within the linear phase of the PCR reaction, as before (Figure 3.4). Individual reactions to amplify 18S and each gene of interest were performed on P14 cDNA extracted from both wild-type and knockout barrel cortices. C_T values for 18S and the gene of interest, in wild type and mutant mice were recorded. Relative induction levels (i.e. differences in expression levels between wild-type and knockout mice) were calculated thus:

$$\frac{2^{(C_T\,(Gene X\,Wildtype) - C_T(Gene X\,knockout))}}{2^{(C_T(18S\,Wildtype) - C_T(18S\,knockout))}}$$

Figure 3.10
The $\Delta\Delta C_T$ method equation, which enables calculation of relative gene expression levels between two samples based on the difference in CT values between wild-type and knockout samples, and assumes that the amount of DNA present after each cycle examined is doubled.

This extra assumption using the $\Delta\Delta C_T$ method is that the PCR reaction efficiency is 100% when in the linear phase (i.e. each PCR reaction doubles the amount of DNA produced each cycle in this phase), whereas performing Three repetitions of each run were performed using cDNA from a different animal, and bar charts were plotted showing the mean values for each gene, and error bars were standard errors of the mean.

3.2.10 *In situ* hybridisations

In situ hybridisations were performed in order to determine the location of *Wnt* gene expression within the cortex. When the experiments were commenced, there was no description of *Wnt* gene expression in postnatal cerebral cortex. However, mid-way through the experiments, the laboratory of Elizabeth Grove published *in situ* hybridisation expression patterns for certain members of the Wnt, Frizzled and sFRP families (Shimogori et al., 2004) which are summarised in Table 3.1.

Table 3.1
Summary of in situ hybridisation expression patterns in neocortex, described in Shimogori et al., (2004). Wnt2b and Frizzled 3 exhibit particularly interesting expression profiles, since both genes are expressed in barrel walls. n.d., not described; +, detectable signal; -, not described.

Gene/Age	P0	P7	P20	P70	Comments
Wnt2b	+	+	+	+	Specific expression in layers 4 and 6. Expressed in barrel walls but not hollows; similar expression pattern to *Frizzled 3*. Only described at P20.
Wnt3a	+	+	+	+	Homogenously expressed throughout cortex.
Wnt5a	+	+	+	+	" "
Wnt7a	+	+	-	-	Not detected at P20 or later ages.
Wnt7b	+	+	+	+	Low expression in neocortex, but stronger expression in more caudal regions
Frizzled 3					Specific expression in layers 4 and 6; Expressed in barrel walls but not hollows; similar expression pattern to *Wnt2b*. Only described at P20.
Frizzled 7	+	-	-	-	Found in neocortex at P0 only.
Frizzled 8	+	+	+	+	Homogenously expressed throughout cortex.
Frizzled 9	+	+	+	+	" "
Frizzled 10	+	+	+	+	" "
sFRP-1	++	+	+	n.d.	Much stronger expression at P0 than at later ages.
sFRP-2	++	+	+	n.d.	" "
sFRP-3	+	+	+	n.d.	Specific expression observed in layers 2/3 and 6 (in lateral neocortex) at P20.

3.3 Results

3.3.1 Degenerate primer RT-PCR

Utilisation of the degenerate primer strategy to amplify most Wnt genes (Figure 3.5) revealed that *Wnt7a*, *Wnt5* and *Wnt3* were expressed at P0, and *Wnt7a*, *Wnt2b* and *Wnt4* were expressed at P7 (Figure 3.11). Of the sequences obtained, 80% of P0 and 70% of P7 sequences were *Wnt7a*, and *Wnt2b*. *Wnt3*, *Wnt4* and *Wnt5a* were also discovered, although less frequently (Figure 3.12). Notably, *Wnt3* was expressed at P0 but was not detected at P7, whereas *Wnt4* and *Wnt2b* were found to be expressed at P7 but not P0. However, since *Wnt7a* was by far the most prominent gene found by this technique, one had to address the question whether *Wnt7a* expression is actually the most abundant *Wnt* at this age in barrel cortex, or whether it is amplified preferentially by the degenerate primers due to some kinetic affinity for this gene? If the latter scenario is true, then many other *Wnt* genes might have be present in barrel cortex, but missed by the sheer number of *Wnt7a* clones generated.

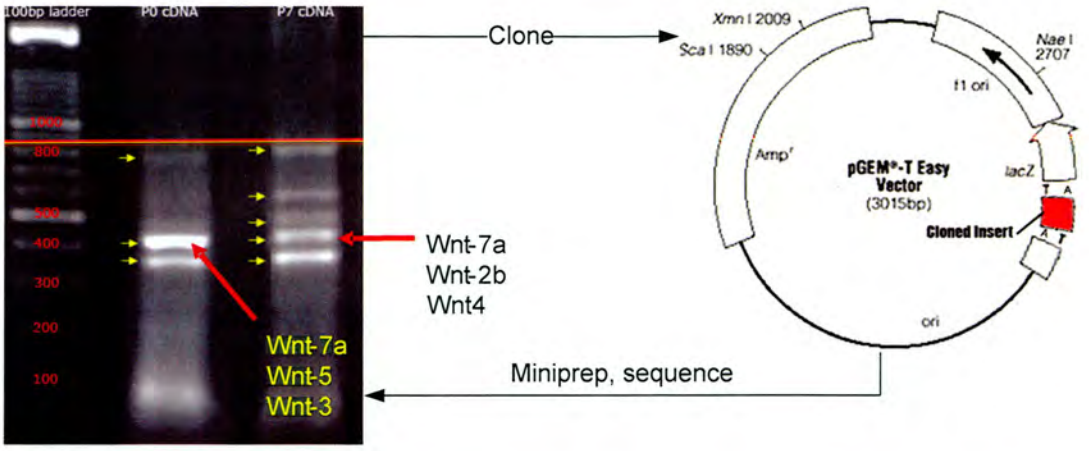

Figure 3.11
Results of Wnt degenerate primer PCR. Bands excised from the gel (yellow arrows) underwent DNA extraction. The DNA was cloned and sequenced and the bands that contained Wnt genes are indicated with red arrows. At P0, Wnt7a, Wnt5 and Wnt3 were found to be present, and at P7 Wnt7a, Wnt2b, and Wnt4 were present.

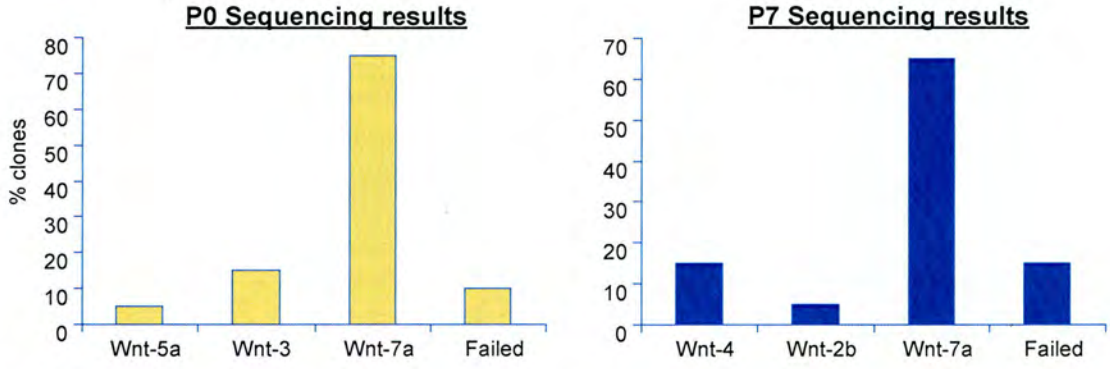

Figure 3.12
Bar chart of Wnts yielded by degenerate primer RT-PCR. At P0, *Wnt3*, *Wnt5a* and *Wnt7a* were present and at P7, *Wnt2b*, *Wnt4* and *Wnt7a* were discovered. Wnt7a saturates the results with over Data is displayed as a percentage of the total number of clones sequenced.

3.3.2 Colony Screen

To determine which colonies contained fragments other than *Wnt7a*, a colony screen was performed using a radiolabelled probe to the *Wnt7a* fragment that was amplified by the degenerate primer PCR (Figure 3.13, see Materials and Methods chapter for methodological details). Colonies that bound most radiolabelled probe were strongly radioactive and caused greater exposure of the photographic film. The colonies that corresponded to the most highly exposed spots on the photographic film were more likely to contain *Wnt7a*. Apart from five control samples, any colony that strongly exposed the photographic film was not chosen and the remainder picked for growth, miniprepping and sequencing.

The colony screen was a partial success, yielding *Wnt2b* at P0, but conspicuously failed to eliminate *Wnt7a* from the sequencing results—the vast majority of colonies that were

sequenced were still *Wnt7a*-containing. Perhaps the vast majority of colonies contained *Wnt7a* fragments, but unequal radiolabelling of the DNA on the membrane occurred, leaving the bottom left of the membrane poorly labelled, yet holding *Wnt7a* containing colonies. Another method was required to determine if other Wnts are expressed in barrel cortex during the period of barrel formation.

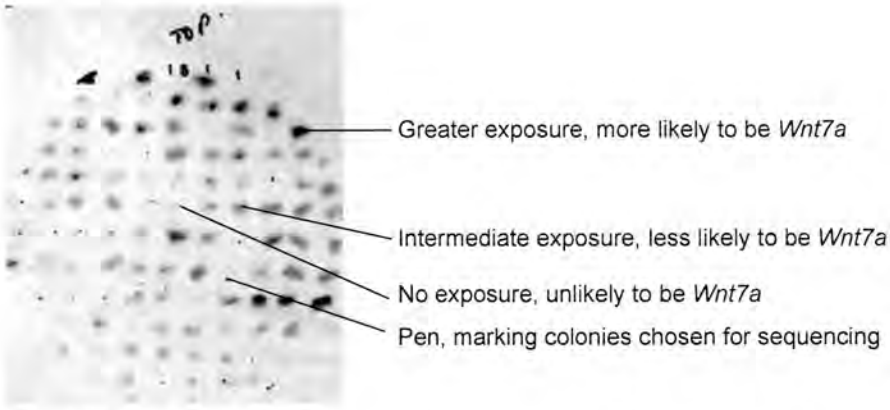

Figure 3.13
Autoradiograph showing photographic film exposed to radiolabelled Wnt7a fragment bound to a colony screen membrane. Darker areas represent regions of higher radioactivity, and therefore should have more Wnt7a bound. Colonies were chosen that did not strongly expose the photographic film, as they were less likely to be Wnt7a-containing colonies.

3.3.3 RT-PCR

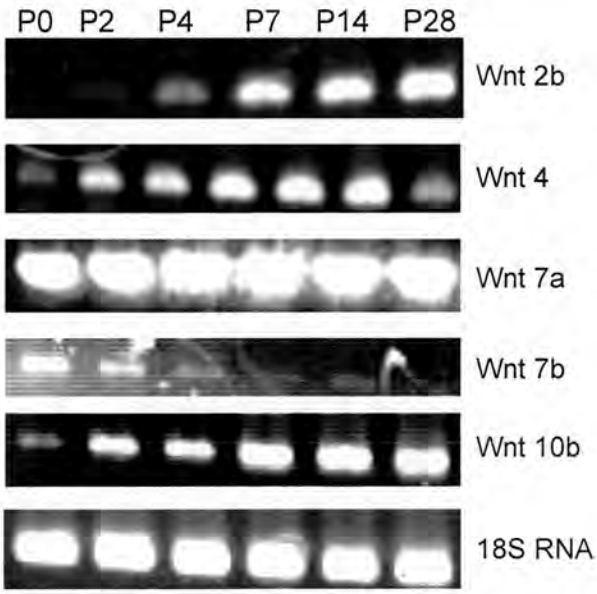

Figure 3.14
Non-quantitative agarose gel PCR, showing PCRs performed on P0, P2, P4, P7, P14 and P28 cDNA. Wnt2b, Wnt4, Wnt7a, Wnt7b and Wnt10b were found to be expressed in barrel cortex by this method. When expression levels are visually assessed by comparing band size and intensity to housekeeping control gene, 18S, Wnt2b and Wnt10b show an apparent general increase in expression over development, Wnt4 follows a similar expression profile to Wnt10b, but exhibits a drop in expression at P28. Wnt7a seems highly expressed throughout development; Wnt7b seems to be expressed in decreasing amounts over development.

Individual primer RT-PCR was used to amplify *Wnt* genes from barrel cortex dissections taken from mice at different ages throughout postnatal development. *Wnts 4, 7a, 7b* and *10b* were found to be expressed at P0 and P2 in presumptive barrel cortex and within barrel cortex at P4, P7, P14 and P28. *Wnt2b* was not detected at P0 in presumptive barrel cortex but exhibited an increase in PCR product at each age over development. *Wnt4* exhibited a similar profile over development, but showed reduced expression in Adult. *Wnt7a* expression was consistently highly expressed across all ages. *Wnt7b* was expressed in decreasing amounts between P0 and P7 and was not detected at any later ages, whereas *Wnt10b* was expressed at lowest amounts at P0, but *Wnt10b* levels increase over development until P14 where expression levels stabilise. *Wnt* genes not discovered by degenerate *Wnt* primer PCR were revealed by this method (*Wnt7b* and *Wnt10b*, Figure 3.14). Although not quantitative, I loaded equal amounts of RNA into the cDNA synthesis so the result gave some indication of potential expression profiles. Many of the genes seem to be developmentally regulated (Figure 3.14). All reaction products were verified as being the gene of interest by cloning and sequencing of each PCR product.

3.3.4 SYBRgreen RT-PCR

Wnt expression profiles

Throughout this section, all graphs containing data that was normalised to Adult have yellow coloured bar charts; all data normalised to P14 has purple-coloured bar charts. Error bars represent the standard error of the mean. Expression profiles have been grouped into three categories:

1. Genes that are expressed in decreasing amounts between P4 and Adult
2. Genes that are expressed in increasing amounts between P4 and Adult
3. Genes that showed no statistically significant differences in expression over the ages observed

Genes that are expressed in decreasing amounts between P4 and Adult

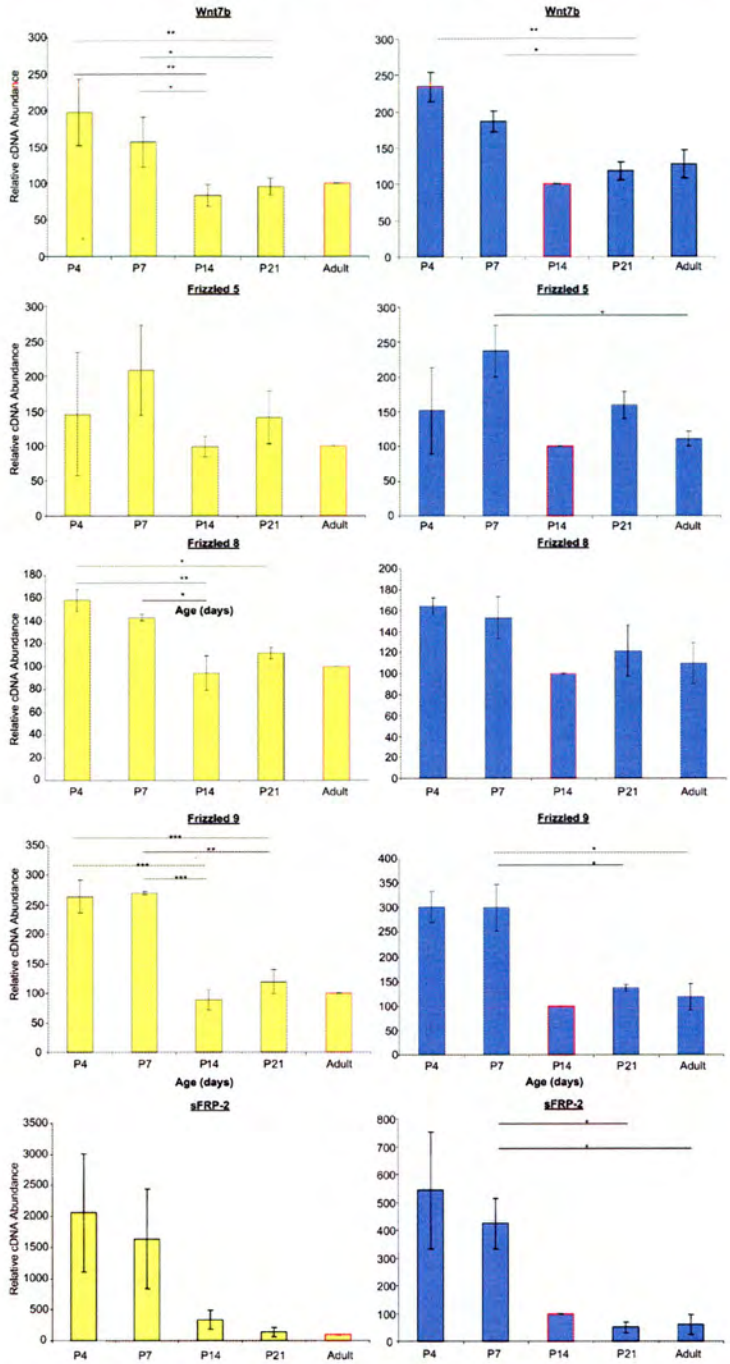

Figure 3.15
Genes that are expressed in decreasing amounts between P4 and Adult. Temporal expression profiles of Wnt7b, Frizzled 5, 8 and 9 and sFRP-2. Yellow bars = data normalised to Adult=100%, blue bars, data normalised to P14=100%. Red line around a bar indicates the age to which the data is normalised. * = $p < 0.05$; ** = $p < 0.01$; *** = $p < 0.001$, as determined by Student-Newman-Keuls post-hoc testing following one-way ANOVA testing. All genes charted above show statistically significant reduction in expression levels over development (discussed in text).

One *Wnt*, one *sFRP* and three *Frizzled* genes were found to be expressed in decreasing amounts between P4 and Adult. *Frizzled 8, Frizzled 9* and *Wnt7b* showed greatest downregulation with all three genes downregulated after the peak of dendritogenesis (P14).

Frizzled 8 exhibits statistically significant decreases in expression levels when normalised to Adult values, between P4 and P21 ($p<0.05$), P4 and P14 ($p<0.01$) and between P7 and P14 ($p<0.05$, Figure 3.15). *Frizzled 9*, when normalised to Adult values exhibits highly statistically significant reductions ($p<0.001$) in expression levels between P4 and P14, P4 and P21, plus P7 and P14, whilst the p-value of the difference between P7 and P21 is less than 0.01 (Figure 3.15). When normalised to P14 values, a statistically significant difference between P7 and Adult ($p<0.05$) is revealed (Figure 3.15). *Wnt7b* exhibits a pattern of decreasing expression over development, with statistically significant reduction in expression between P4 and P14 ($p<0.01$), P14 and P21 ($p<0.05$); P7 and P14 ($p<0.05$), and P7 and P21 ($p<0.05$, Figure 3.15). When normalised to P14 values, *Frizzled 5* exhibits a statistically significant drop in expression between P7 and Adult ($p<0.05$, Figure 3.15). *sFRP-2* exhibits significant down-regulation between P7 and P21 ($p<0.05$) in addition to P7 and Adult, when datasets are normalised to P14 values (Figure 3.15).

3.3.4.1 Genes that are expressed in increasing amounts between P4 and Adult

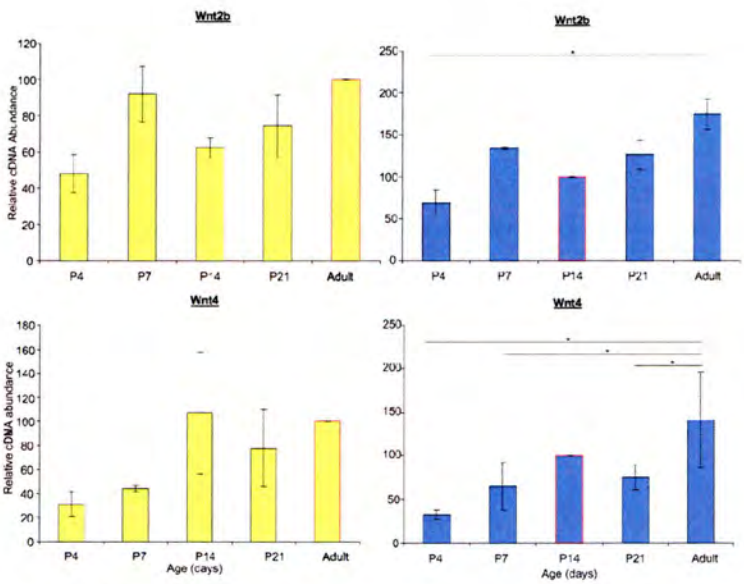

Figure 3.16
Genes that are expressed in increasing amounts between P4 and Adult. Temporal expression profiles of Wnt2b and Wnt4. Yellow bars = data normalised to Adult=100%, blue bars, data normalised to P14=100%. Red line around a bar indicates the age to which the data is normalised. * = $p < 0.05$, as determined by Student-Newman-Keuls post-hoc testing following one-way ANOVA testing.

Wnt2b exhibits statistically significant increases in expression levels when normalised to P14 values, between P4 and Adult ($p<0.05$, Figure 3.16), and *Wnt4* shows significant ($p<0.05$) increases in expression levels between P4 and Adult, P7 and Adult in addition to P21 and Adult, when normalised to P14 levels (Figure 3.16).

3.3.4.2 *Genes that showed no statistically significant differences in expression over the ages observed*

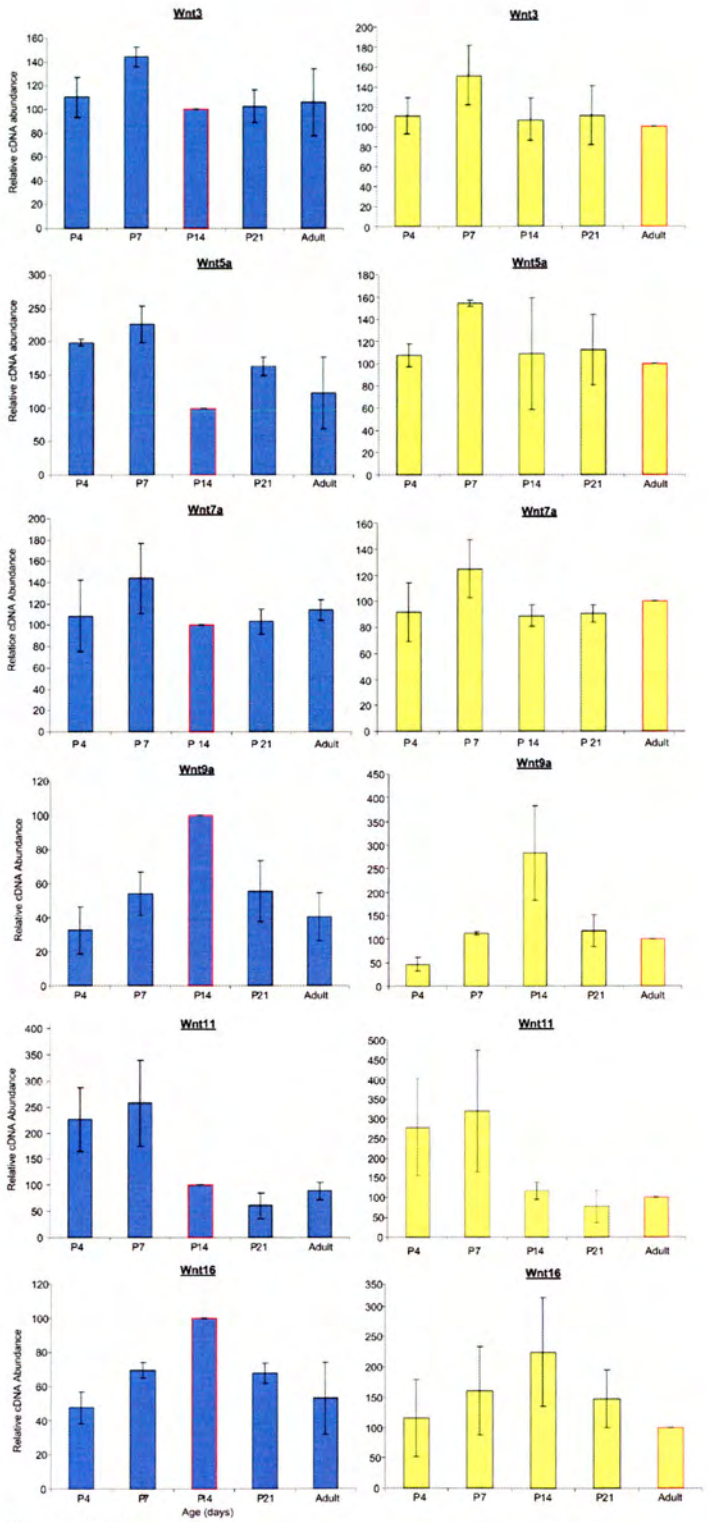

Figure 3.17

Genes that showed no statistically significant differences in expression over the ages observed: Wnts.

No statistically significant differences between age groups were observed for data normalised to either P14 or Adult values. All ages failed one-way ANOVA statistical testing. All that can be deduced from this data is that *Wnt3*, *Wnt5a*, *Wnt7a*, *Wnt9a*, *Wnt11* and *Wnt16* are present in barrel cortices at P4, P7, P14, P21 and Adult.

The vast majority of Wnts, Frizzled and sFRP genes showed no statistically significant differences between any of the age groups. No differences in expression levels between age groups were found for *Wnt5a*, *Wnt7a*, *Wnt9a*, *Wnt11*, *Wnt16* (Figure 3.17), *sFRP-1*, *sFRP-4* (Figure 3.18), *Frizzleds 1*, *2*, *3*, *4*, *6*, *7* and *10* (Figure 3.19) since all of these genes failed One-way ANOVA statistical tests. Although some expression profiles look interesting (e.g. *Wnt16* with an apparent increase in expression from P4-14 then subsequent reduction expression until adulthood) the standard errors within each age group are large (Figure 3.17) so no conclusions can be drawn. In summary, *Wnt5a*, *Wnt7a*, *Wnt9a*, *Wnt11* and *Wnt16* are present at all ages examined.

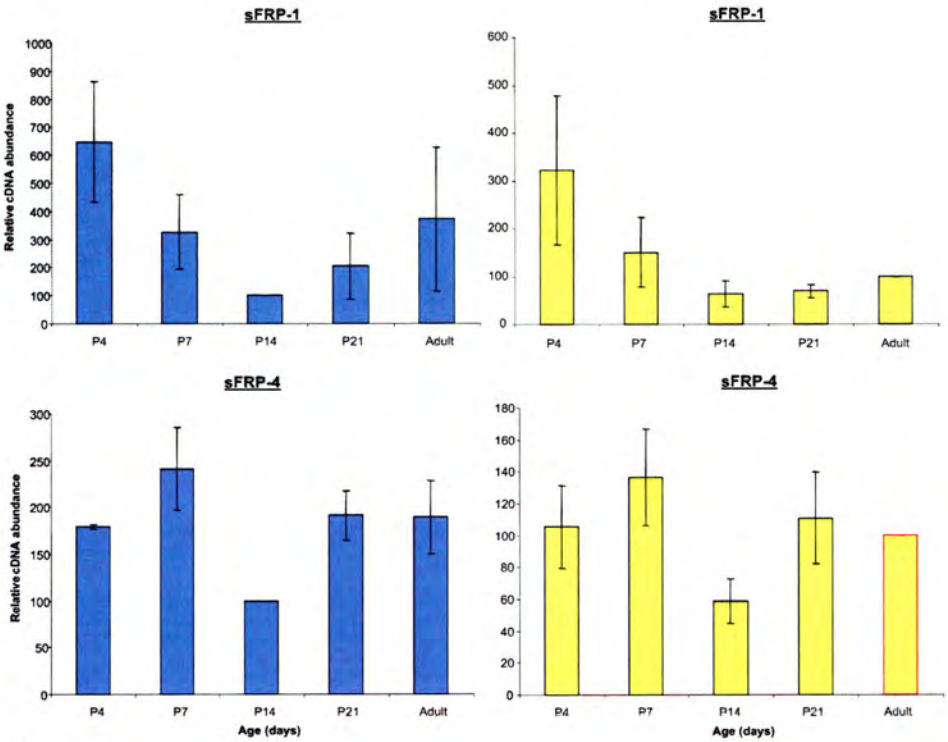

Figure 3.18
Genes that showed no statistically significant differences over the ages observed: sFRPs
No statistically significant differences between age groups were observed for data normalised to either P14 or Adult values. All ages failed one-way ANOVA statistical testing. All that can be deduced from this data is that *sFRP-1* and *sFRP-4* are present in barrel cortices at P4, P7, P14, P21 and Adult.

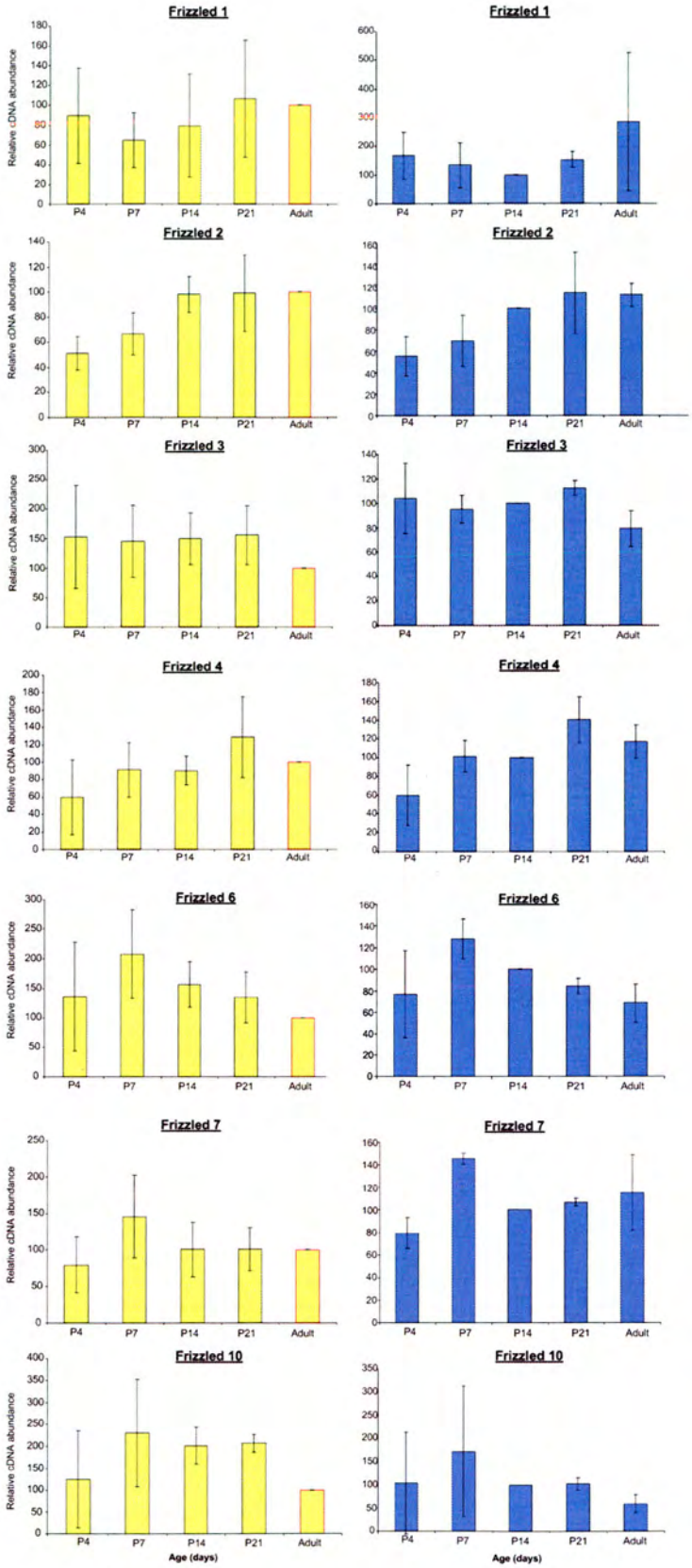

Figure 3.19
Genes that showed no statistically significant differences over the ages observed: Frizzleds
No statistically significant differences between age groups were observed for data normalised to either P14 or Adult values. All ages failed one-way ANOVA statistical testing. The graphs show that *Frizzleds 1, 2, 3, 4, 6, 7* and *10* are present in barrel cortices at P4, P7, P14, P21 and Adult.

Wnt8b was detected by SYBRgreen qRT-PCR

Interestingly, *Wnt8b* expression was detected using SYBRgreen RT-PCR in postnatal cDNAs, but linearity in the dilution series was never achieved. However, the primers did function properly on cDNAs taken from embryonic ages, and the sequencing of the PCR product did confirm that *Wnt8b* was amplified from postnatal cDNAs. This suggests that at postnatal ages *Wnt8b* expression is very close to the threshold of detection of this method.

3.3.5 Screen of differences in Wnt, Frizzled and sFRP expression in barrel cortices of *Plc-β1*, *Mglur5* and *Pkar2β* mutant mice

All of the mutant brains examined expressed the same complement of *Wnts*, *Frizzleds* and *sFRPs* as wild-type brains, but many are expressed in significantly lower amounts.

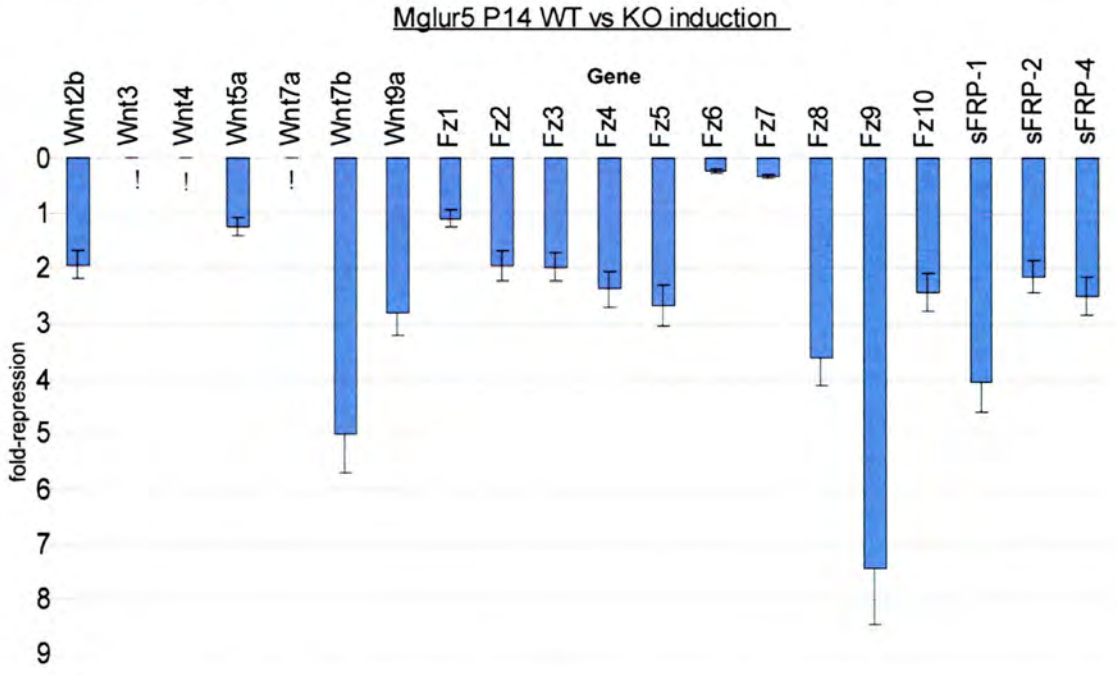

Figure 3.20
Relative gene expression profiles generated using the ΔΔCT method between P14 wild-type and Mglur5 knockout mice. Positive numbers equal wild-type expression is greater than that in knockout mice. Exclamation marks signify that no data was obtained from this particular gene. A value of zero means no change in expression, a positive value means wild-type expression is greater than mutant; a negative value means knockout expression is greater than wild-type. Error bars are standard error of the mean.

Mglur5$^{-/-}$ mice express most *Wnt*, *Frizzled* and *sFRP* genes at about half the expression levels observed in wild-type mice (Figure 3.20), although *Frizzled 6* and *Frizzled 7* expression levels are relatively unchanged between genotypes. Interestingly, *Wnt7b* and

Frizzled 9 expression levels are greatly reduced in Mglur5$^{-/-}$ mice; in wild-type mice, both of these genes are expressed at their lowest amounts at P14 (as displayed earlier in Figure 3.15 on page 127). *Wnt9a, Frizzled 8* and *sFRP-1* are the next set of molecules that are more down-regulated in Mglur5$^{-/-}$ mice than the others (Figure 3.20) and, as described previously, expression of *Frizzled 8* is lowest at P14 (Figure 3.15).

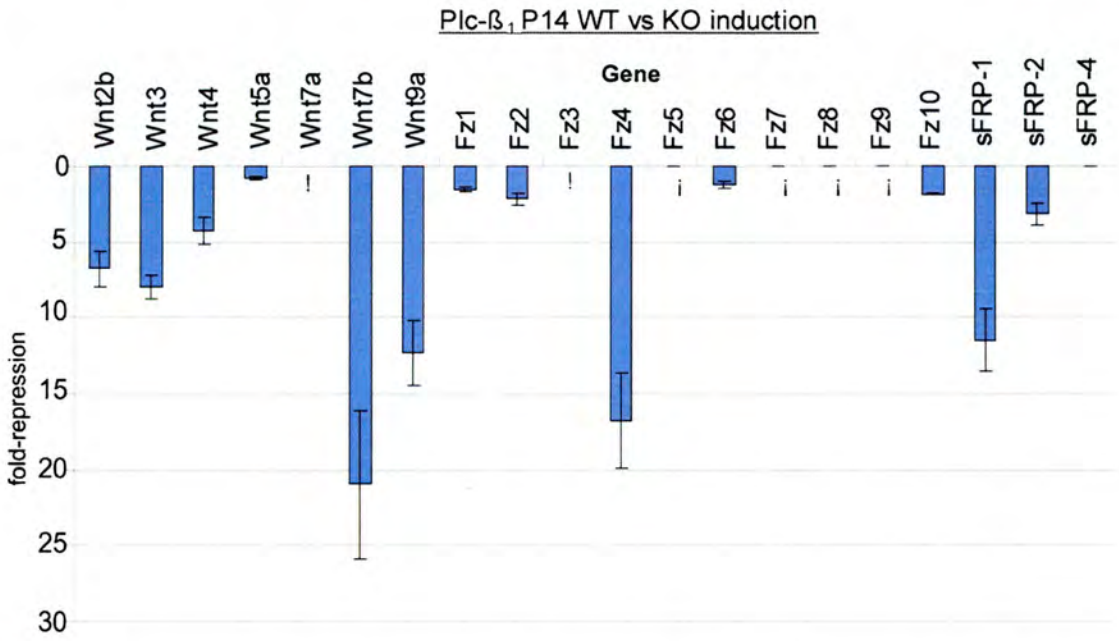

Figure 3.21
Relative gene expression profiles generated using the ΔΔCT method between P14 Wild-type and Plc-β1 knockout mice. Positive numbers equal wild-type expression is greater than that in knockout mice. Exclamation marks represent failed runs. A value of zero means no change in expression, a positive value means wild-type expression is greater than mutant; a negative value means knockout expression is greater than wild-type. Error bars are standard error of the mean.

Wnt7b, sFRP-1 and *Wnt9a* are also greatly down-regulated in *Plc-β_1*$^{-/-}$ mice (Figure 3.21). Unfortunately, the failure of one 18S control sample for *Frizzled 8* and another for *Frizzled 9* meant that no meaningful statistics could be performed at this age, and the runs could not be analysed. Nevertheless, *Frizzleds 8* and *9* are already candidates for further investigation from the results of analysis of the *Mglur5*$^{-/-}$ mice (Figure 3.20). An additional candidate from *Plc-β_1*$^{-/-}$ mice has been revealed: *Frizzled 4*, as it exhibits the second highest down-regulation in this genotype.

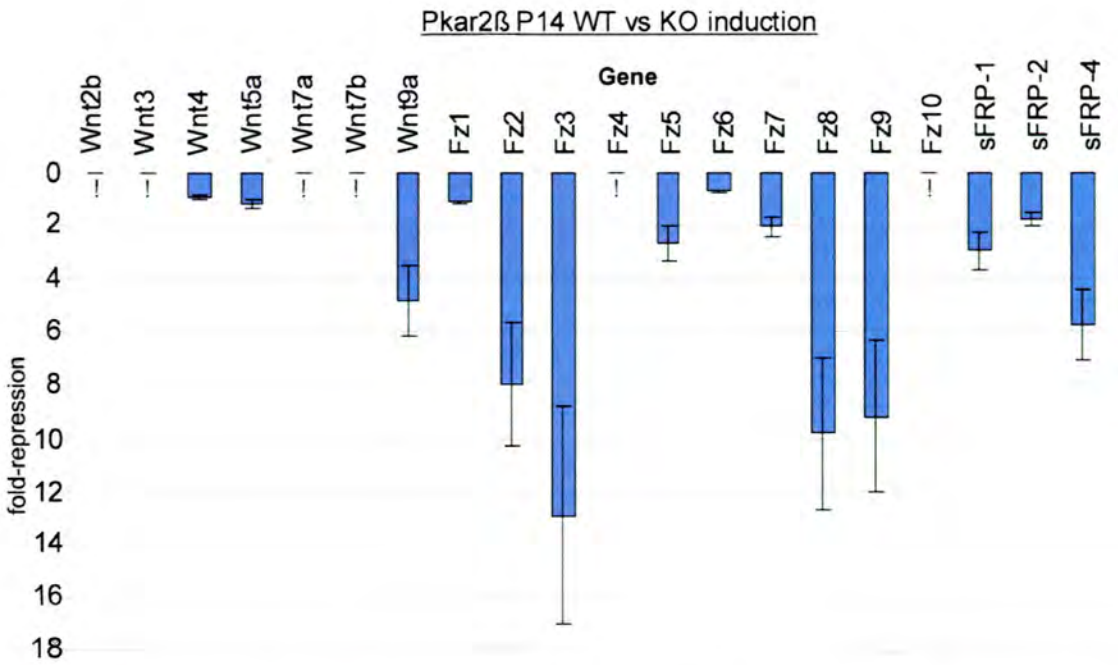

Figure 3.22
Relative gene expression profiles generated using the ΔΔCT method between P14 Wild-type and Pkar2β knockout mice. Positive numbers equal wild-type expression is greater than that in knockout mice. Exclamation marks represent failed runs. A value of zero means no change in expression, a positive value means wild-type expression is greater than mutant; a negative value means knockout expression is greater than wild-type. Error bars are standard error of the mean.

The genes that are down-regulated in the *Pkar2β*$^{-/-}$ mice (Figure 3.22) are broadly different to those down-regulated in the *Mglur5*$^{-/-}$ (Figure 3.20) and *Plc-β*$_1^{-/-}$ (Figure 3.21) mice, with the exception of *Frizzled 8* and *Frizzled 9*. *Wnt9a* is the most down-regulated *Wnt* observed in *Pkar2β*$^{-/-}$ mice, exhibiting fivefold down-regulation. *Frizzled 2* is down-regulated eightfold in *Pkar2β*$^{-/-}$ mice and *Frizzled 3* exhibits the greatest down-regulation in *Pkar2β*$^{-/-}$ mice with a thirteen fold down-regulation (Figure 3.22). The down-regulation in *Mglur5*$^{-/-}$ mice is only threefold (Figure 3.20). *Frizzled 8* and *Frizzled 9* are also down-regulated in this genotype group and are also notably down-regulated in *Mglur5*$^{-/-}$ mice (Figure 3.20). As mentioned earlier in this chapter, *Frizzled 8* and *Frizzled 9* are expressed at greatest amounts at P4 and P7, and expression levels remain at lower levels at all ages observed from P14 through to adulthood (Figure 3.15, page 127). These genes could be playing a role in barrel formation at P4 and P7, but are less likely to play a role in dendritogenesis, which peaks at P14. *sFRP-4* exhibits approximately sixfold down-regulation in *Pkar2β*$^{-/-}$ mice (Figure 3.22).

Candidate genes for further characterisation of any barrel defect from mutant screen qRT-PCR

Thus far, the candidate genes generated from the mutant screens that are most likely to play a role in barrel development are: *Frizzled 9*, *Wnt7b*, *Wnt9a*, *sFRP-1*, *Frizzled 4*, *Frizzled 8*, *Wnt3*, *Frizzled 7*, *Frizzled 10*, *Wnt4* and *sFRP-4*. Notably *Wnt7b* was strongly downregulated in both *Mglur5*$^{-/-}$ and *Plc-β*$_1^{-/-}$ mice, and *Frizzled 9* was strongly downregulated in both *Mglur5*$^{-/-}$ and *Pkar2β*$^{-/-}$ mice.

3.3.6 *In situ* hybridisations

3.3.6.1 MRCT: In situ hybridisations performed on cryosections stored at 4°C in 70% ethanol.

The first *in situ* hybridisation runs were performed on cryostat sections that were post-fixed in 4% paraformaldehyde and stored in 70% ethanol, 30% DEPC-treated water at 4°C until use (see Materials and Methods chapter). However, *in situ* hybridisation runs performed on tissue stored in this manner were unsuccessful, with no observable staining and poor tissue integrity. The P7 *β-actin* probe control experiment was performed to determine RNA integrity in the sections (Figure 3.23). Staining appeared to be restricted to the cytoplasm of cells, and was sparse in thalamus, in contrast with the prediction that β-actin should be expressed highly throughout the developing brain. Strong signal was observed in neocortex (Figure 3.23b), the CA1, CA2 and CA3 regions of the hippocampus (Figure 3.23c). The probe bound cutting artefacts strongly (Figure 3.23a, asterisks). The high level of staining in cortex and hippocampus indicates good RNA integrity in these regions. The lack of staining observed in thalamus may result from either significantly less *β-actin* expression in thalamic cells, or mRNA degradation in these deeper brain structures. Possible reasons for poorer mRNA integrity in the deeper brain structures might include differences in the amount of paraformaldehyde that was perfused into each brain region, or differences in the rate of freezing of each area.

No-probe control experiments were performed to determine what proportion of signal was due to factors after hybridisation, and these sections appeared free of signal, with only Nuclear Fast Red counterstaining visible. A representative section is shown in Figure 3.24, showing strong Nuclear Fast Red staining of the hippocampal formation, and good staining of the outer cortical layers, and the striatum is also visibly stained.

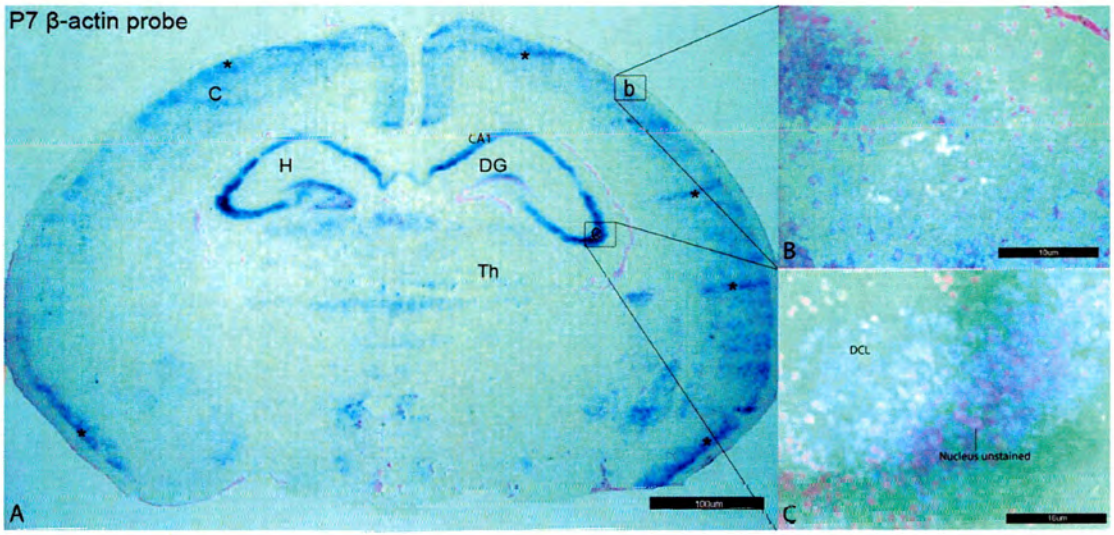

Figure 3.23
β-actin probe on P7 cryostat coronal sections. *In situ* hybridisation on coronal cryostat sections of P7 wild-type brains for β-actin. NBT/BCIP staining appears to be strongest in the cortex (b) and hippocampus (c), and regions of tissue cutting artefact (*), but sparse staining was seen in deeper brain structures such as the thalamus. Staining was cytoplasmic in location (b) and (c). Scale bar = 100μm (a) and 10μm (b and c). Slides were counterstained with Nuclear Fast Red. C, cortex; H, hippocampus; DG, dentate gyrus; CA1, CA1 region of the hippocampus; Th, Thalamus; *, cutting artefacts.

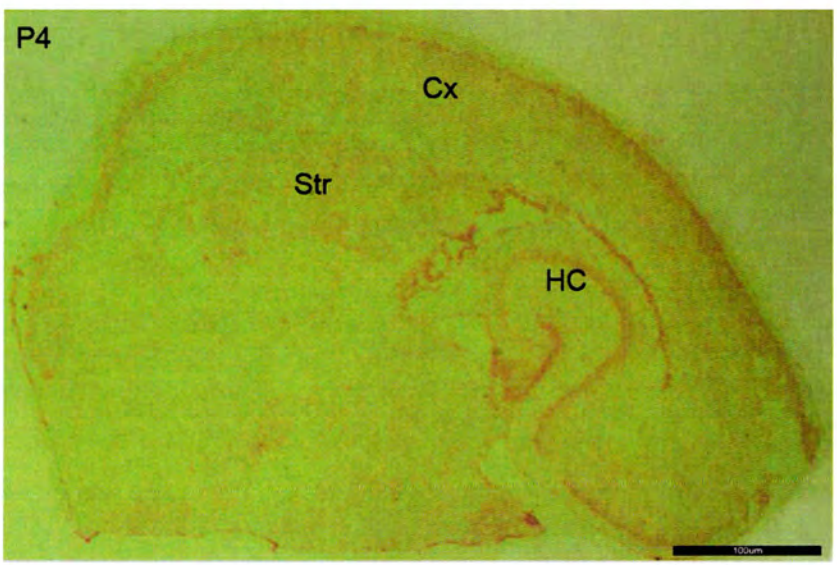

Figure 3.24
No riboprobe control on a P4 cryostat section. Coronal P4 section was counterstained with Nuclear Fast Red. The hippocampus, cortex and striatum are more strongly stained than other grain regions. No NBT/BCIP precipitate is visible, demonstrating that the DIG-labelled antibody is not non-specifically binding tissue. Cx = Cortex, Str = Striatum, HC = Hippocampus. Scale bar = 100μm

3.3.6.2 MRCT: In situ hybridisations performed on freshly cut cryosections

In situ hybridisation runs, performed on freshly cut cryostat sections improved the quality of tissue in subsequent ISH runs at MRCT, although the actual riboprobe staining patterns remained unsatisfactory, with extremely weak staining (Figure 3.25 and Figure 3.26).

Riboprobes for *Wnt* genes gave rise to exceptionally weak staining that was not improved by reducing the hybridisation temperature from 60°C to 50°C or maximising the concentration of riboprobe in the hybridisation mixture. Because of this, counterstaining with Nuclear Fast Red could not be performed as it masked the low signal present and the sections presented were imaged using Differential Interference Contrast (DIC) optics in order to see the differences in cellular densities that permit visualisation of cortical lamination. Representative sections showing staining using maximal antisense probe concentrations for *Wnt7a* in P14 sections are presented in Figure 3.25 and for P4, P7 and Adult sections in Figure 3.26.

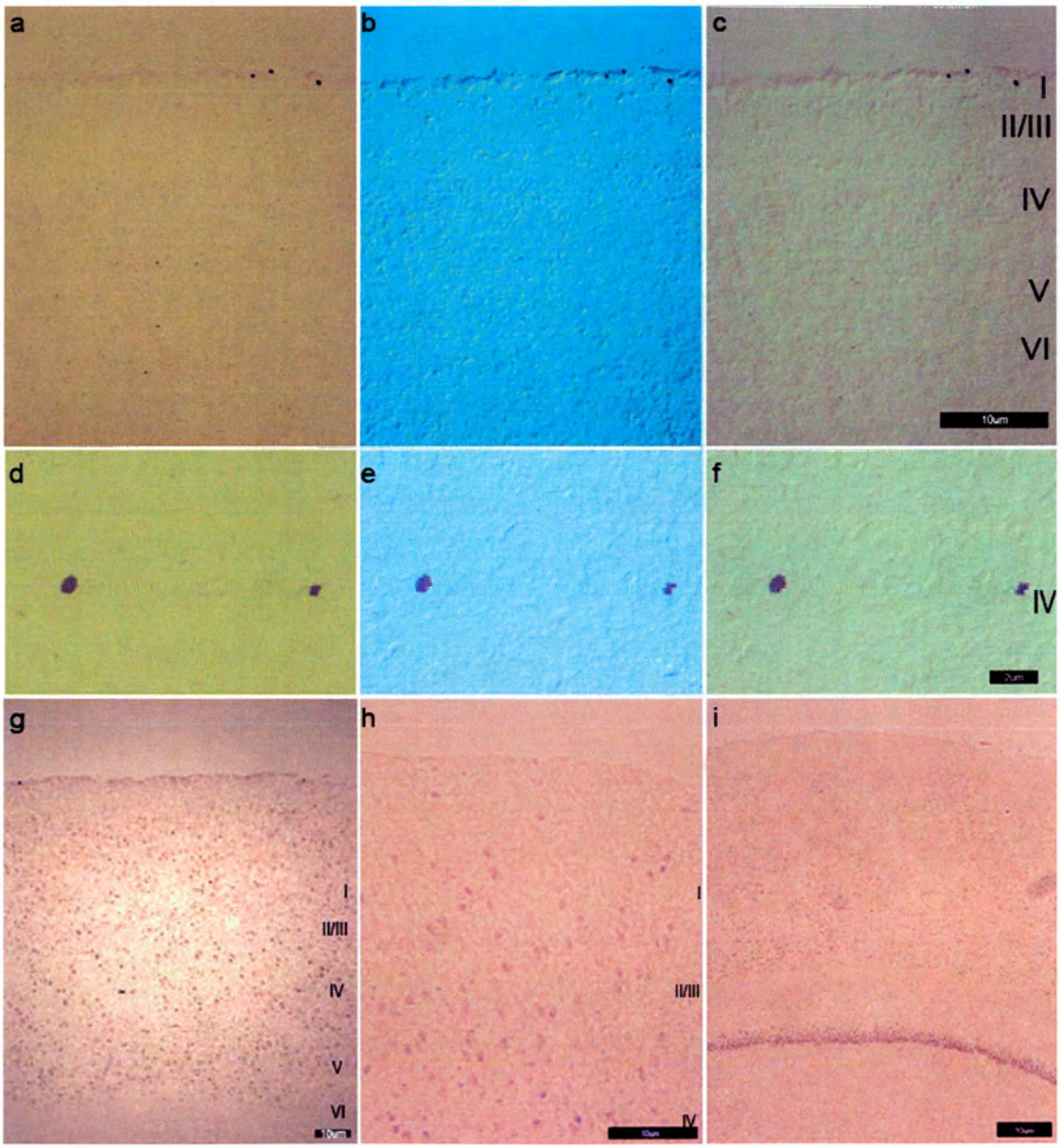

Figure 3.25
P14 Wnt7a in situ hybridization on freshly cut and fixed coronal sections. Panels a-c: *Wnt7a* antisense riboprobe on P14 sections. (a), BF microscopy. Few spots of staining are visible. (b), DIC microscopy,

reveals the cellular morphology and permits visualisation of the cell layers (c), merged image of panels (a) and (b). This demonstrates that the few spots of staining are seen in layers IV, V and VI. (d). BF microscopy of layer IV, revealing two spots of NBT/BCIP precipitate. (e). DIC microscopy of layer IV, showing the cellular structure of this region. (f). Merged images of panels (d) and (e). The two spots of NBT/BCIP precipitate do not appear to be either nuclear or cytoplasmic, and are most likely artefactual speckles of NBT/BCIP precipitate. Panels (g) and (h), BF microscopy, *Wnt7a* sense control riboprobe, counterstained with Nuclear Fast Red. The *Wnt7a* sense probe yielded an apparent specific staining pattern with punctate, cytoplasmic staining throughout all layers of the cortex. (i). *β-actin* positive control riboprobe. Strong cytoplasmic staining was seen throughout the cortex, and in the hippocampus. mRNA integrity was therefore good. BF = Bright Field microscopy, DIC = Differential Interference Contrast microscopy. Scale bars = 1μm (a-c), 2μm (d-f), 10μm (g-i).

Wnt7a antisense probe *in situ* hybridisation runs on P14 cryostat sections (Figure 3.25a, b and c) show extremely sparse *Wnt2b* signal in the cortex. Panels d, e and f of this figure contain magnified images of a region of layer IV where speckles of NBT/BCIP precipitate are present. *Wnt7a* antisense probe (Figure 3.25g and h) show an apparently specific staining pattern, which is cytoplasmic in location and is observable throughout all cortical layers apart from layer I, which is a mostly aneuronal layer. The β-actin positive control riboprobe (Figure 3.25i) did produce a reasonable staining pattern, with signal present in the cytoplasm of every cell, suggesting RNA integrity was adequate for this probe to generate successful staining.

Wnt7a antisense probe also gave rise to a sparse, almost non-existent signal for P4 (Figure 3.26a-c), P7 (Figure 3.26d-f) and Adult sections (Figure 3.26g-i) with occasional dark speckles visible in all layers of the cortex. P4 sections (Figure 3.26a-c) had more staining throughout the cortical layers than later ages, and this result is in agreement with Shimogori et al., (2004) paper, which describes similar *Wnt7a* staining at this age. This could indicate that *Wnt7a* is actually expressed at extremely low levels in developing barrel cortex, which is at odds with the robust detection of *Wnt7a* expression by RT-PCR (Figure 3.14) and qRT-PCR (Figure 3.19). It is more likely, however, that there is a problem with the riboprobe. Notably, Elizabeth Grove and colleagues did not observe *Wnt7a* specific staining in adulthood (Shimogori et al., 2004), yet the Adult *Wnt7a* antisense staining patterns in Figure 3.26g-i look similar to the staining patterns for this probe at all other ages (Figure 3.25a-f and Figure 3.26a-f) suggest that the *Wnt7a in situ* hybridisation runs presented in Figure 3.25 and Figure 3.26 failed. However, the Salinas laboratory *in situ* hybridisation experiments did demonstrate low levels of *Wnt7a* expression throughout the cortex at later postnatal ages (P. Salinas, personal communication), similar to that observed at P4 in Figure 3.26a-c.

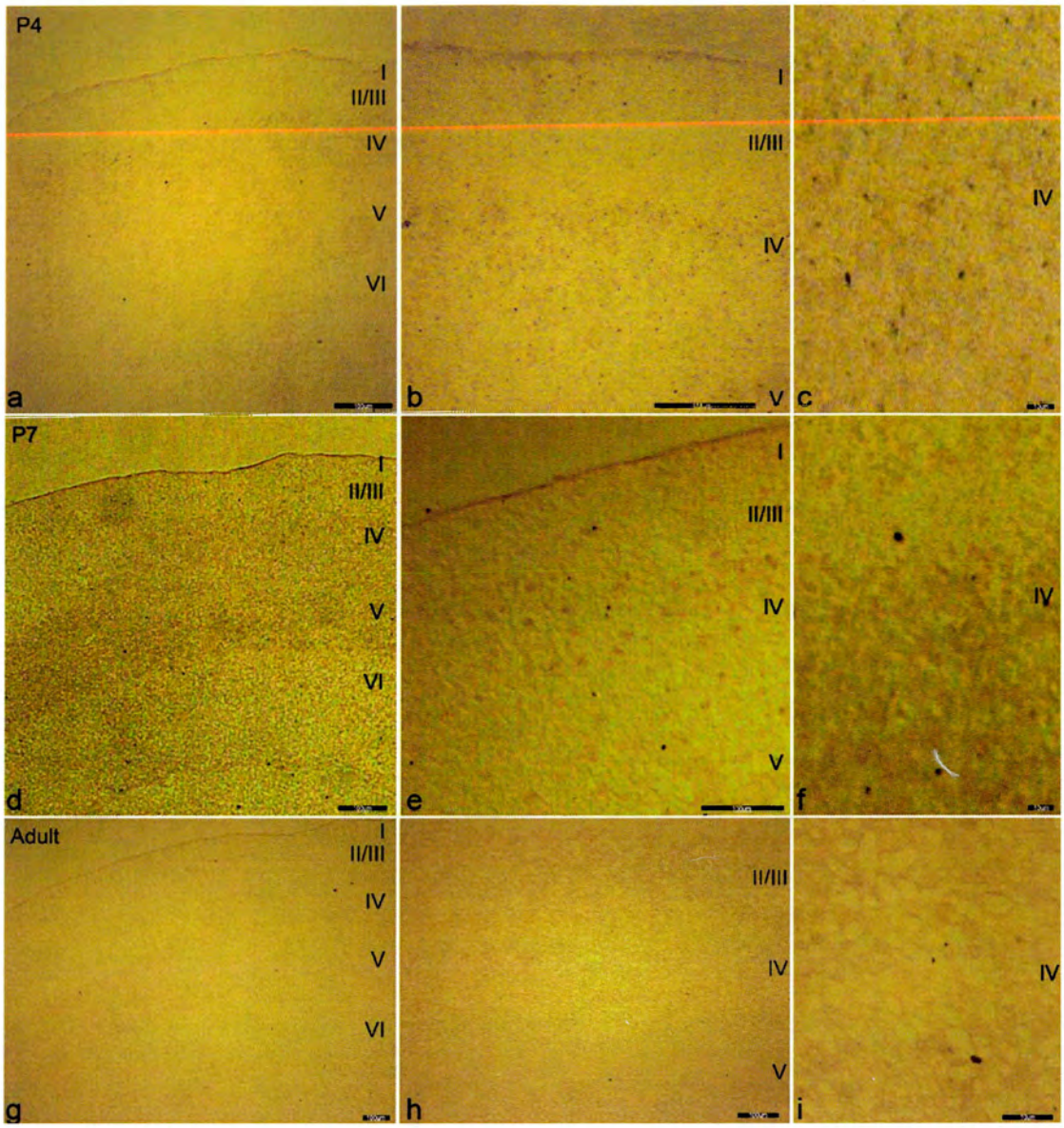

Figure 3.26
Wnt7a in situ hybridisation on coronal sections from P4, P7 and Adult ages. Merged images of DIC and bright field imaged sections are shown to emphasise cellular structure. (a), *Wnt7a* antisense probe on P4 coronal section. Sparse staining is observed in cortex, with less staining seen in layers I and II/III than layer IV. (b), Magnification of panel (a), showing in greater detail that greater staining in layer IV exists than in layers I and II/III. (c), shows a magnification of layer IV and shows that the staining observed is punctate. (d). *Wnt7a* antisense probe on P7 coronal section. Very sparse staining is observed in cortex. (e) shows a magnification of panel (d); there few dots of NBT/BCIP precipitate present in each layer of the cortex, and panel (f) shows a magnification of layer IV of this section; the few speckles of staining that are observed may just be artefacts from the *in situ* hybridisation protocol method. However, all staining was observed on-section and not off-section, suggesting that the staining is not random precipitation of NBT/BCIP. Scale bar = 100μm (a, b, d, e, g, h) and 10μm (c, f, i).

3.3.6.3 *In situ hybridisation performed in Edinburgh University: Wnt2b*

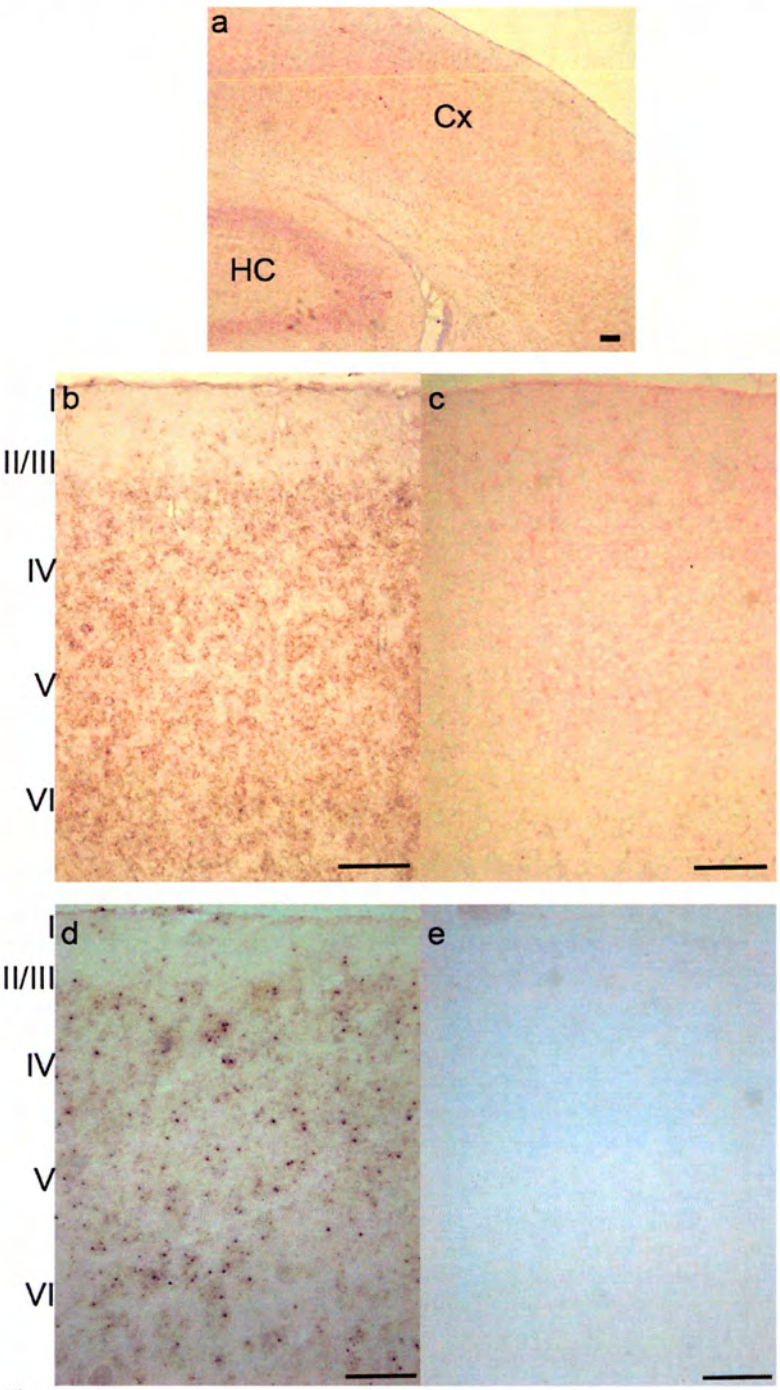

Figure 3.27
Wnt2b in situ hybridisation on P7 wax and cryostat sections. (a) *Wnt2b* antisense signal on a P7 wax-embedded coronal section. The *Wnt2b* signal appears to be located in the cytoplasm and distributed in all cortical layers except layer I, and also in the CA1, CA2 and CA3 regions of the hippocampus. (b), *Wnt2b* antisense signal on a P7 wax-embedded coronal section; staining appears to be cytoplasmic and in all cortical layers, although with much sparser staining in layer I. (c), *Wnt2b* sense control probe on P7 wax-embedded coronal sections. Very sparse staining is observed throughout all cortical layers, including the mostly aneuronal layer I, suggesting that this staining pattern is merely background staining. (d), *Wnt2b* antisense probe on a P4 cryostat coronal section. A more punctate signal is observed than was seen in wax-embedded sections, although the distribution of staining throughout the cortical layers is similar, with strong staining throughout the cortex, but sparser staining was present in layer I. (e). The sense control sections had virtually no background staining. Roman numerals indicate cortical layer; scale bars = 10μm.

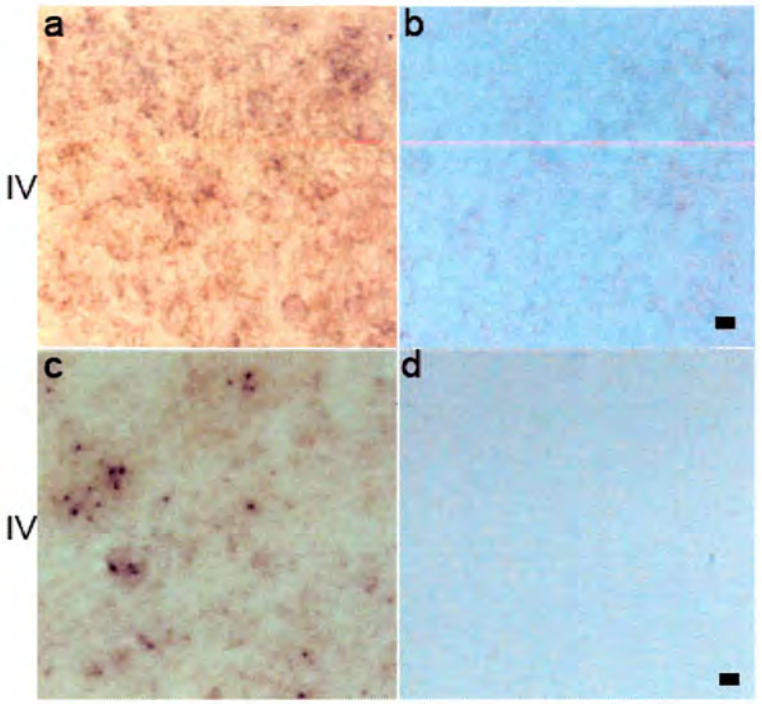

Figure 3.28
Wnt2b ISH on P7 wax and cryostat sections at x40 magnification. (a). Layer IV of P7 wax-embedded section probed with *Wnt2b* antisense riboprobe. Staining appears to be cytoplasmic in nature, with no obvious dendritic staining. (b). Matched no riboprobe control for panel (a). Light background staining of the cytoplasm was observed and staining levels were much lower than in panel (a). (c). *Wnt2b* antisense probe on P7 cryostat coronal sections. These sections exhibit a more punctate *Wnt2b* AS signal, which again, appears mostly cytoplasmic in location, with no evidence of staining in dendrites. (d) The sense control sections have virtually no background staining. The difference between the more diffuse wax-embedded section and the more punctate cryostat section staining could be due to differences in tissue sectioning or preparation during the prehybridisation steps. Roman numerals indicate cortical layer. Scale bar = 1μm

P7 *in situ* hybridisation runs on wax and cryostat sections are presented in Figure 3.27 and Figure 3.28. Although the prehybridisation steps differed according to the type of section used, the posthybridisation steps were identical and performed together (see Materials and Methods chapter). *Wnt2b* antisense probe staining for both wax and cryostat sections were located within the same regions— all cortical layers exhibited strong cytoplasmic staining patterns (except for layer for the mostly aneuronal layer I, Figure 3.27a,b,d and Figure 3.28a,c). Both wax-embedded and cryostat sections exhibited staining that was cytoplasmic in location, in all cortical layers below layer I, with no evidence of dendritic staining. Cryostat sections showed dense punctate staining, whereas a more diffuse staining was observed on the wax sections (Figure 3.27a,b,d and Figure 3.28a,c). *Wnt2b* sense control probes applied to cryostat sections exhibited virtually no staining (Figure 3.27c,e and Figure 3.28b,d), whereas on wax-embedded sections this probe gave rise to very mild cytoplasmic background staining. *Wnt2b* staining appears not to be localised to barrel walls (as is the case with the Shimogori *et al.*, (2004) paper, although they examined different ages) but rather spread throughout the layer in the same manner as layers II/III, V and VI (Figure 3.27).

3.4 Discussion

The objective of the experiments detailed in this chapter was to establish the presence of *Wnt*, *Frizzled* and *sFRP* genes and reveal candidate genes for further investigation using SYBRgreen qRT-PCR and to describe the laminar localisation of *Wnt* gene expression in cortex by ISH. Many *Wnt*, *Frizzled*, and *sFRP* genes were shown to be expressed in barrel cortex, and many of the genes found to be expressed in barrel cortex were downregulated in mutant mice that lack barrels. The *in situ* hybridisations runs were mostly unsuccessful, although a *Wnt2b* expression pattern in P7 cortex was characterised.

3.4.1 Degenerate and individual primer RT-PCR

Wnt gene expression in barrel cortex was demonstrated by degenerate primer RT-PCR, cloning and sequencing. Although the degenerate primers used would not amplify *Wnt8a*, *9a*, *9b*, *11* and *16*, this strategy did demonstrate the expression of *Wnts 3*, *5a*, *7a* and *7b* in presumptive barrel cortex at P0 and these genes, with the addition of *Wnt2b* were found to be expressed in barrel cortex at P7. However, since over 70% of the clones sequenced were *Wnt7a*, the colony screen shown in Figure 3.13 was performed. This yielded *Wnt2b* at P0. Since degenerate primers would not amplify certain *Wnt* genes, and we could not be certain that other Wnt genes were not missed by this technique, RT-PCR using individual primers for each gene was performed. This demonstrated the presence of *Wnts 4* and *10b* in addition to the previously discovered *Wnt* genes.

3.4.2 qRT-PCR: *Wnt* expression profiles

The genes found to be expressed in barrel cortex were: *Wnts 2b, 3, 4, 5a, 7a, 7b, 8b, 9a 10b, 11, 16*, all *Frizzleds* and *sFRP-1*, *-2* and *-4*. Interestingly, all genes that were expressed were present at every age examined; no developmental switch off or on of *Wnt, Frizzled or sFRP* expression was observed.

3.4.2.1 Timing of events during barrel formation

In order to correlate expression levels to the processes occurring during barrel formation, the times and processes occurring during barrel formation are listed below:

1 TCAs invade layer IV and segregate into whisker related patches (Senft and Woolsey, 1991; Rebsam et al., 2002). Occurs between P0-P3.

2 After TCA segregation, layer IV cells bodies begin to aggregate and form cell-dense barrel walls, and evidence for this can be observed by P4 and a full barrel field can be seen by late P6 (Rice and Van der Loos, 1977). Septae are visible by P7 and barrel segregation is most distinct by P10-P14 (Rice and Van der Loos, 1977), although the specific mechanisms underlying these processes are yet to be identified (Barnett et al., 2006b).

3 Dendrites in layer IV cells selectively elaborate into barrel hollows, prune inappropriate branches and this selective dendritic orientation persists into adulthood (Woolsey et al., 1975; Greenough and Chang, 1988). However, it is unclear when dendritic reorientation starts, with some studies indicating that this occurs as late as P10. Nonetheless, dendrites are growing rapidly at P14, and rapid growth and synaptogenesis occurring during the second postnatal week (Greenough and Chang, 1988; Upton et al., 2006; Barnett et al., 2006b).

4 Synaptic plasticity. Anatomical plasticity in response to whisker-follicle ablation occurs in layer IV from P0-P3. NMDAR-dependent synaptic plasticity occurs from P3-P7 (Crair and Malenka, 1995; Lu et al., 2001) and in layer II/III, synaptic plasticity occurs and from birth into adulthood (Fox, 1992; Fox, 1994; Fox, 2002).

3.4.2.2 Genes whose expression decreased between P4 and Adult

Wnt7b, *Frizzled 5*, *Frizzled 8*, *Frizzled 9* and *sFRP-2* show a trend of greater expression at earlier ages (P4 and P7) than at later ages (Figure 3.15). For example, *Frizzled 8* expression levels at P4 and P7 are at least twice that of all later ages. This profile of high expression during the first postnatal week correlates with the early events of barrel formation, namely the cellular segregation that forms the barrel structure. This suggests that the genes that follow this expression profile could play a role in the cellular aggregation events, with later lower expression levels maintaining the barrel structure.

3.4.2.3 Genes that are expressed in increasing amounts between P4 and Adult

Wnt4 and *Wnt2b* were expressed in increasing amounts over the timecourse of barrel development (Figure 3.16). Greater expression of these genes in barrel cortex over development might indicate an increasing role in stabilisation and maintenance of the barrel structure. Other roles these genes might play might include: maintenance of TCA-barrel cortex synapses, dendritic shape change, or later-stage plasticity found in layers II/III (Fox, 1992). Our results show that *Wnt2b* is expressed in adulthood at almost double the level of P4 (Figure 3.16) and *in situ* hybridisations have shown that *Wnt2b* is present throughout the cortex at P7 (Figure 3.27, Figure 3.28). However, *Wnt2b* has been reported elsewhere to be expressed in cortex at P20 by in situ hybridisation, with the highest expression levels in layer IV and most prominent expression present in barrel walls (Shimogori et al., 2004). The Shimogori et al. (2004) paper also demonstrated that *Frizzled 3* (which is also expressed in barrel cortex at all ages examined by qRT-PCR, Figure 3.19) exhibits the same expression pattern and timing as *Wnt2b*. Shimogori and colleagues hypothesised from their data that some thalamocortical interactions are mediated by Wnt2b signalling (Shimogori et al., 2004). Bearing this in mind, the data presented in Figure 3.16 might suggest that even if *Wnt2b* expression is required to mediate thalamocortical interactions, *Wnt2b* expression may be required in greater amounts later in development for other purposes, such as maintenance of barrels, either in cellular structure, dendrite shape, or synaptic plasticity. However, during the time of barrel formation and maturation, there is a massive turnover of dendrites and synapses, as these structures are rapidly projecting and retracting, stabilising only when they find an appropriate binding partner. The rapid turnover of protein and mRNA required for this behaviour can mean that large increases in mRNA are required just to maintain protein levels at a steady state, especially if the protein is expressed in dendrites. If this is the case, *Wnt4* and *Wnt2b* may play more than one role at different stages in barrel development, perhaps directing the earlier cellular aggregation processes or thalamocortical interactions, yet at later ages play a role in regulating dendritic elaboration, synaptic plasticity or barrel structure maintenance.

Genes that showed no statistically significant differences in expression over the ages observed

SYBRgreen qRT-PCR revealed that *Wnt3*, *Wnt5a*, *Wnt7a*, *Wnt9a*, *Wnt11*, *Wnt16*, *Frizzleds 1*, *2*, *3*, *4*, *6*, *7*, *10*, *sFRP-1* and *sFRP-4* are present in barrel cortices at P4, P7, P14, P21 and Adult, but no statistically significant changes were seen between age groups when the

expression profiles of these genes were examined by one-way ANOVA. The fact that many *Wnts*, all *Frizzleds* and all but one *sFRP* gene are expressed in barrel cortex at all ages examined is nevertheless a surprising result. With so many potential pathways and mechanisms that can be activated or inhibited by this repertoire of molecules, this result demonstrates that there is a complex framework of Wnt signalling occurring in barrel cortex throughout barrel development. Since all of these genes are present, it is possible that any of these genes could play a role in one or many of the events required to form barrels (listed above). Notably, Frizzleds 1, 2, 4, and 7 can interact with the PDZ domains of PSD-95 *in vitro*, which if this is the case *in vivo* in barrel formation, would bring together the most prominent scaffolding molecule in the NRC and Frizzled receptors, providing a potential link between the NMDA receptor and the Wnt signalling pathways. Alternatively, these genes may be expressed in cortex, and play multiple roles in barrel formation and maintenance. It is possible that the *Wnts*, *Frizzled* and *sFRP*s expressed do not play a critical role in barrel formation. Finally, mRNA expression does not always directly relate to the levels of protein produced due to variations in regulated mRNA degradation (reviewed in Valencia-Sanchez et al., 2006), the duration of mRNA binding by RNA binding proteins (reviewed in Ule and Darnell, 2006) or the protein turnover rates at synapses. The qRT-PCR studies did not address these issues, although qRT-PCR has confirmed the expression of many *Wnt*, *Frizzled* and *sFRP* genes throughout barrel cortex development. These expression profiles generated candidate genes for further investigation, namely *Wnt2b*, *Wnt4*, *Wnt7b*, *Frizzled 5*, *Frizzled 8*, *Frizzled 9* and *sFRP-2*.

3.4.3 Wnt, Frizzled and sFRP screening of *Mglur5*, *Plc-β1* and *Pkar2β* knockout mice by qRT-PCR

Wnt, *Frizzled* and *sFRP* expression levels were screened in *Mglur5*$^{-/-}$, *Plc-β1*$^{-/-}$ and *Pkar2β*$^{-/-}$ mice and compared to wild-type expression levels. This screen was performed at P14, as we decided to focus on a role for *Wnt*, *Frizzled* and *sFRPs* in dendrite shape. *Mglur5*$^{-/-}$, *Plc-β1*$^{-/-}$ and *Pkar2β*$^{-/-}$ mice were assumed to have a defect in dendritic elaboration. Since no barrels were observed, it was believed that dendrites did not selectively elaborate into the barrel hollow, although this is now known not to be the case in *Plc-β1*$^{-/-}$ mice (Upton et al., 2006). Surprisingly, almost every *Wnt*, *Frizzled* and *sFRP* gene that was present in wild-type P14 barrel cortices was down-regulated in *Pkar2β*$^{-/-}$, *Mglur5*$^{-/-}$ and *Plc-β1*$^{-/-}$ mice; none were upregulated. Notably, the pattern of genes that were greatly down-regulated in mutant mice were similar for both *Mglur5*$^{-/-}$ and *Plc-β1*$^{-/-}$ mice. mGluR5 has been shown to signal through

PLCβ_1 during barrel formation; knockout of *Mglur5* causes a loss of PLCβ_1-mediated phosphoinositide turnover in barrel cortex (Hannan et al., 2001) so this result is not unexpected. The genes that exhibited the largest down-regulation in these mutants, and therefore were the strongest candidate genes for further investigation, were *Wnt7b*, *Frizzled 9* and *sFRP-1*.

Pkar2β$^{-/-}$ mice exhibited a comparatively different profile of genes that were down-regulated compared to *Mglur5*$^{-/-}$ and *Plc-β*$_1^{-/-}$ mice; *Wnt9a*, *Frizzleds 2*, *3*, *8*, *9* and *sFRP-4* were downregulated. Only *Frizzleds 8* and *9* were genes that were notably down-regulated in both *Pkar2β*$^{-/-}$ and *Mglur5*$^{-/-}$ mice. Surprisingly, expression levels of *Wnt2b*, the only *Wnt* gene to have a published expression pattern in barrel cortex (Shimogori et al., 2004), is one of least altered in all three knockouts.

With so many *Wnts*, *Frizzleds* and *sFRPs* down-regulated in these mice, added to the fact that little is known about the nature and specificity of most Wnt-Frizzled binding interactions in mice, it is difficult to interpret these results and build a model of Wnt signalling in barrel cortex. Unfortunately, in the light of the Upton et al., (in preparation) showing *Plc-β*$_1^{-/-}$ mice have normally orientated dendrites, the choice of P14 (the peak of dendritogenesis) as the age to examine these mice now looks a poor choice when examining the *Plc-β*$_1^{-/-}$ mice. It was incorrectly assumed that dendritic orientation was defective in mice that lack barrels (Datwani et al., 2002b) and we had chosen to examine P14 with that process in mind. In retrospect, this study would have been more informative if performed at P3/P4, which is the age where the cellular segregation starts in layer IV that will eventually form barrels; a defect known to be present in all three mutant mice examined. Nevertheless many Wnt, Frizzled and sFRP genes are down-regulated in barrel cortex at P14 in *Plc-β*$_1^{-/-}$, *Mglur5*$^{-/-}$ and *Pkar2β*$^{-/-}$ mice, and the strongest candidate genes generated from this analysis were *Wnts 2b*, *3*, *7b*, *9a*, *Frizzleds 3*, *4*, *8*, *9*, *sFRP-1* and *sFRP-2* (Table 3.2).

Table 3.2
Table of the average down-regulation values of selected *Wnt*, *Frizzled* and *sFRP* genes across *Pkar2β*, *Plc-β*$_1$ and *Mglur5* mutants. * = data from only one mutant.

Gene	Average Down-regulation
Wnt7b	13.0
Frizzled 4	9.2
Frizzled 9	8.2
Wnt3	8.0*
Frizzled 3	7.5
Frizzled 8	6.8
Wnt9a	6.7
SFRP-1	6.3

SFRP-2	5.3
Wnt2b	5.2
Wnt4	4.0
Frizzled 2	3.4
SFRP-4	2.8
Wnt5a	1.2
Frizzled 7	1.2
Frizzled 10	1.1
Frizzled 1	1.1
Frizzled 5	1.1
Frizzled 6	0.7

3.4.4 SYBRgreen RT-PCR as a technique for investigating mRNA expression levels

Since every SYBRgreen RT-PCR run had to pass dilution series linearity tests, the data generated in each run should be an accurate representation of the cDNA species present. However, few datasets passed one-way ANOVA tests and there are many potential reasons for this. First, it could be that no significant difference in mRNA expression levels exists between each age group for most genes examined. However, if this is not the case, additional replicate runs would yield statistically significant expression levels between each age group. Additional runs were not performed because of time and cost restraints. Nevertheless, a definite answer to the question of what *Wnts* are expressed in barrel cortex during barrel development has been generated, and general expression profiles for each gene examined have been made. Further repetitions would require the sacrifice of more mice, and consumption of expensive reagents, yet might not reveal significantly more information. Potential reasons for the variability seen for each sample are discussed below.

3.4.5 SYBRgreen qRT-PCR variability issues

The SYBRgreen qRT-PCR protocol has been successfully used in the Kind laboratory to assay mRNA expression levels for many genes expressed over the course of barrel development (Barnett et al., 2006a). It was possible to recapitulate these expression profiles on the same tissue used for the qRT-PCR studies presented in this chapter (Figure 3.9), yet it was difficult to obtain expression profiles for *Wnt*, *Frizzleds* and *sFRP* genes that did not have significant variation between repetitions of the same experiment, and this section discusses possible reasons for the large variations observed.

3.4.5.1 Variability in extraction and degradation of mRNA

If RNA extraction quality varies between brains, then this is potentially a significant source of experimental variation. Not only would the ratio of 18S to mRNA vary (making the choice of 18S as a housekeeping gene a poor choice), but the cDNA species synthesised in the reverse transcription procedure can be altered; low-expressed genes can be less amplified by this technique. However, great care was taken at every step from dissection to cDNA synthesis to overcome this problem and avoid RNA degradation; barrel cortex dissections were performed as fast as possible, in ice-cold buffer, and the time taken from decapitation to completed dissection was under five minutes. Brains were immediately frozen on dry ice, and once dried, placed in pre-chilled RNase free tubes and placed directly into a -80°C freezer. The tissue was transported from the freezer to the laboratory on dry ice for RNA extraction, and the extracted RNA was kept on dry ice when used on the bench, and only thawed briefly when the RNA was required for cDNA synthesis or running on a gel. Materials, reagents and the laboratory bench were RNase free. RNA quality was assessed by electrophoresis of samples on an RNase-free agarose gel, and samples that exhibited smearing of bands were discarded. Despite careful handling of tissue and mRNA, which minimises RNA degradation, small variations in RNA degradation are inevitable. However, normalisation of the raw qRT-PCR data to a housekeeping gene controls for this. 18S was chosen as the reference housekeeping gene after careful examination of developmental regulation over barrel development; 18S showed no discernable regulation (Figure 3.9).

3.4.5.2 Low levels of gene expression

Since many *Wnt*, *Frizzled* and *sFRP* genes are expressed in low abundance in barrel cortex, these genes are therefore more susceptible to small variations in RNA quality. This has a direct effect on the amount of cDNA synthesised for each gene and therefore the amount amplified between each PCR run. For example, the expression pattern of *SynGAP-c* (a gene expressed in far greater abundance than *Wnts;* Mark Barnett, personal communication) as validation of qRT-PCR was successfully performed and analysis using one-way ANOVA followed by Student-Newman-Keuls post-hoc statistical tests revealed significant differences at all ages (Figure 3.9). However, many *Wnt*, *Frizzled* and *sFRP* genes showed no statistically significant differences between all ages observed (Figure 3.17, Figure 3.18, Figure 3.19).

3.4.5.3 Pipetting errors

Finally, the SYBRgreen PCR protocol required the use of separate wells for housekeeping gene controls. Two sets of cDNA and PCR reaction mastermixes were pipetted into each PCR reaction well and small variations in pipetting these volumes can introduce experimental variation. Small pipetting errors are inevitable, but the key to successful and reproducible qRT-PCR is minimising these errors. Other qRT-PCR systems are capable of minimising the amount of pipetting, such as TaqMan™ (ABgene) probes using dual-channel fluorescence optical PCR machines (such as the ABI Prism 7000). This system can accommodate two fluorophores and perform internal controls using probes that fluoresce at a different wavelength to the probe to the gene of interest, thus allowing both reactions to be performed in the same well. Using SYBRgreen on a single-channel optical PCR engine stresses the importance of the ability of the scientist to reproducibly and accurately pipette 1.0µl cDNA into each well. If this is not performed properly in the dilution series for each gene, then linearity tests will fail. However, there is no test for slight variations in the volume of cDNA pipetted between each run outside of the linearity tests, and can therefore one cannot exclude this as a potential cause of variation between replicate PCR runs.

3.4.6 *In situ* Hybridisations

The *Wnt in situ* hybridisations presented in this chapter were unsuccessful for all genes examined, apart from *Wnt2b* (Figure 3.27 and Figure 3.28). The following section discusses possible reasons why most *in situ* hybridisation runs failed.

Initial *Wnt in situ* hybridisations were performed under the supervision of post-doctorate researchers that run a commercial *in situ* hybridisation service at MRC Technologies (MRCT) at the Western General Hospital, Edinburgh, UK. *In situ* hybridisation experiments performed at MRCT all failed. Initial runs were performed on cryostat sections that were fixed in 4% PFA, and stored in 70% ethanol/ 30% DEPC-treated water until use. This storage technique is standard operating procedure at MRCT. However, most tissue used at MRCT is embryonic tissue, and whilst this method of storage is suitable for embryonic cryostat sections, it did not maintain the tissue integrity of postnatal brain sections and produced poor *Wnt in situ* staining patterns (Figure 3.23 and Figure 3.24). In the case of *Wnt* probes, no detectable signal was produced even after three days of developing in NBT/BCIP

solution that was replaced four times daily. Variation of hybridisation between 50 to 60°C made no difference to the staining patterns observed.

In an attempt to improve signal from *Wnt* gene riboprobes, the protocol was modified so that sections were cut fresh, fixed and used on the same day as the *in situ* hybridisation run. The quality of tissue obtained was greatly improved; however, the strength of *Wnt* riboprobe signal was not (Figure 3.25, Figure 3.26). Variation of hybridisation temperature between 50 to 60°C made no difference to the staining patterns observed. Oddly, for *in situ* hybridisations performed on P14 tissue, the antisense *Wnt7a* probe produced meagre amounts of signal, yet the *Wnt7a* sense control probe produced what looked like a specific staining pattern (Figure 3.25). *β-actin* positive control slides performed at the same time appeared to have worked, suggesting that the problem was with the *Wnt* riboprobes used (Figure 3.25).

I returned to Edinburgh University to perform *in situ* hybridisations using a variety of different protocols. By this time, the Shimogori et al., (2004) paper had been published, showing expression of *Wnt2b* in barrel walls in P20 mice. Because if this paper, I focussed on recapitulating this expression profile, and tried to extend it to other ages throughout barrel development. *Wnt2b in situ* hybridisations at P7 gave rise to a specific staining pattern from the antisense probe, and a clear signal in the sense control probes. *Wnt2b* antisense probe signal was localised to the cytoplasm and distributed evenly in all cortical layers except layer I, and was cytoplasmic in location, although the cryostat sections exhibited a more punctate staining than the wax-embedded sections (Figure 3.27 and Figure 3.28). The *Wnt2b* sense control probe showed a generalised low level of background staining, at a much lower level of staining than the antisense probe generated, suggesting specific staining by the antisense probe. However, the *Wnt2b* expression profile published in by the Grove laboratory (Shimogori et al., 2004) appears to be different to the pattern of staining during this study. They observed *Wnt2b* expression in layers IV and VI, most prominently in barrel walls, although published data is at a later age, P20. Additionally, the riboprobes (Zakin et al., 1998) and genetic background of mice (B6/129) we used were different from the ones used by the Grove laboratory (Grove et al., 1998; Shimogori et al., 2004) which may explain the differences observed between the two groups. After my time in the laboratory, I discovered that the temperature gauge on the hybridisation ovens was faulty, consistently underreporting the temperature of the oven by 15 to 20°C.

3.5 Conclusion

The fact that many *Wnt*, *Frizzled* and *sFRP* genes are expressed in barrel cortex and that most of these genes that are present are down-regulated in mice mutant for molecules that are crucial for barrel formation (*Mglur5*, *Plc-β1* and *Pkar2β*) suggests that Wnts could be playing a role in barrel formation. The sheer number of *Wnts*, *Frizzleds* and *sFRPs* that are expressed, in addition to the promiscuity of Wnt proteins in binding Frizzled receptors, hints that a complex system of Wnt signalling is present in the barrel cortex during barrel formation. The complexity is exacerbated by the observation that one Frizzled receptor can activate more than one signalling pathway, depending on the Wnt bound and the co-receptor(s) it interacts with (discussed in (Cadigan and Liu, 2006). In addition, Wnt signalling pathways can act in an antagonistic manner, whereby non-canonical Wnt signalling can inhibit β-catenin-dependant signalling (Topol et al., 2003; Weidinger and Moon, 2003). Furthermore, sFRPs are present in barrel cortex, which suggests that Wnt binding of Frizzleds is modulated by sFRPs. The sheer potential complexity of interplay between the Wnts, sFRPs and Frizzleds that are expressed throughout the development of the barrel cortex in addition to the many potential mechanisms through which Wnts might act, means that the elucidation of what role any of these molecules actually play in barrel formation and the signalling pathways involved will be a lengthy task. As research into Wnt signalling progresses, we will be better able to understand which Wnt/Frizzled combinations signal through a given Wnt signalling pathway, and how this signalling can be antagonised by other molecules, or Wnts signalling through different pathways. This, allied with conditional knockouts of *Wnts*, *Frizzleds* and *sFRPs* specifically in cortex (and combined knockouts thereof) will best enable investigation of the role of Wnt signalling in barrel cortex development.

4 Characterisation the barrel phenotype of mice mutant for components of the Wnt and NMDAR pathways.

4.1 Introduction

4.1.1 Wnts in the barrel cortex

NMDAR signalling complexes play a key role in the morphological differentiation of primary somatosensory cortex. Several studies have shown that key NMDAR components are also present in Wnt signalling complexes, raising the possibility that Wnt signalling may act in concert with NMDAR in barrel formation. Work in preceding chapters has demonstrated that many *Wnt, Frizzled* and *sFRP* genes are expressed in the developing mouse barrel cortex, and previous studies have shown the presence of NRC components, PSD-95 and SAP-102 in this region (Kornau et al., 1995; Muller et al., 1996; Lau et al., 1996; Kennedy, 1997; Migaud et al., 1998; Porter et al., 2005; Elwood et al., 2005; Barnett et al., 2005a). We hypothesised that *Wnt* gene knockout mice may have defects in barrel development, since:

- Many *Wnts, Frizzleds, sFRPs* and NMDAR components are co-expressed during barrel cortex development (Barnett et al., 2006b), Chapter 3).
- There are components common to both Wnt/Frizzled and NMDAR signalling (Makino et al., 1997; Husi et al., 2000; Hanada et al., 2000).
- Pathways downstream of both Frizzled and NMDAR control similar cellular processes (Huang and Klein, 2004; Bejsovec, 2005; Barnett et al., 2006b).
- Wnt release has been shown to be dependent on activity (Yu and Malenka, 2003; Yu and Malenka, 2004) and NMDAR and Ca^{2+}-dependent pathways (Wayman et al., 2006).
- Wnts can regulate cell migration in mouse embryos (Kimura-Yoshida et al., 2005).
- Wnts have been shown to regulate hippocampal dendrite development (Rosso et al., 2005) and synapse development in the cerebellum (Hall et al., 2000).
- Interactions between neuronal activity and secreted factors has precedence. The actions of neurotrophins on cortical dendrites are blocked by NMDAR antagonists (reviewed in Wong and Ghosh, 2002; Hua and Smith, 2004). Furthermore, BDNF

release is also activity-dependent and controls ocular dominance segregation (Cabelli et al., 1995; Galuske et al., 1996; Cabelli et al., 1997; Hanover et al., 1999; Huang et al., 1999; Maffei, 2002; Imamura et al., 2006).

A logical extension of this work was to obtain any available *Wnt* knockout mice, then examine their barrel phenotype.

Dishevelled proteins are an essential component in almost all Wnt signalling pathways (reviewed in the Introduction chapter and Wharton *et al.* 2003, Seto and Bellen, 2004, Wallingford and Habas, 2005 and Ciani and Salinas, 2005), and interactions between Axin, Dvl1 and GSK3β regulate axonal cytoskeleton (Lucas and Salinas, 1997; Lucas et al., 1998; Krylova et al., 2000; Hall et al., 2000; Krylova et al., 2002; Hall et al., 2002; Ciani et al., 2004). Dvl is associated with pools of stabilised of microtubules in neurons and increases microtubule stability by reducing the phosphorylation of microtubule-associated protein 1B (MAP-1B) by inhibition of GSK3β (Krylova et al., 2000; Ciani et al., 2004). Recently it has been shown that *Wnt7b* expressed in cultured hippocampal neurons increases dendritic arborisation during dendritogenesis (Rosso et al., 2005). Expression of *Dvl1* mimics this effect, and *Dvl1*$^{-/-}$ mice exhibit reduced dendritic arborisation (Rosso et al., 2005). Since Dvl is essential to Wnt signalling, and is involved in dendritic shape change (a process that was thought to be important for barrel formation), we hypothesised that *Dvl* gene mutant mice would have defects in barrel formation, and so the barrel phenotype of brains from *Dvl1* and *Dvl2* mutant mice was investigated. In addition, *Wnt7a*$^{-/-}$*Dvl1*$^{-/-}$ mice exhibit more severe defects in glomerular rosette formation than the *Wnt7a*$^{-/-}$ mutant (Ahmad-Annuar et al., 2006). If the additional deletion of *Dvl1* causes a more severe glomerular rosette phenotype than the loss of *Wnt7a* alone, we hypothesised that *Wnt7a*$^{-/-}$*Dvl1*$^{-/-}$ mice may reveal (or exacerbate) a barrel defect that may be present in *Wnt7a*$^{-/-}$ mice.

4.1.2 NRC Scaffolding molecules link the NMDA receptor to molecules crucial for barrel formation

Two key NMDA receptor scaffolding molecules, SAP-102 and PSD-95, have the potential to interact with Wnt signalling components (Makino et al., 1997; Masuko et al., 1999; Kuwahara et al., 1999; Hanada et al., 2000; Hering and Sheng, 2002). In addition to their scaffolding role in the NRC, PSD-95 and SAP-102 play important roles in many signalling

pathways downstream of the NMDA receptor (Kornau et al., 1995; Niethammer et al., 1996; Masuko et al., 1999; Tezuka et al., 1999; Moyner et al., 1999; Husi et al., 2000; Sans et al., 2000; Rutter et al., 2002; Lim et al., 2002; Porter et al., 2005). PSD-95 and SAP-102 directly bind SynGAP, AKAP150 and GKAP (Kim et al., 1997; Schnell et al., 2002). AKAP150 binds PKARIIβ, and GKAP binds Shank, which binds Homer, which binds mGluR5. It is through these molecules that PSD-95 and SAP-102 can link glutamate signalling through NMDA receptors with SynGAP, PLCβ$_1$, PKARIIβ or mGluR5 (Figure 4.1). SynGAP mutant mice exhibit a complete loss of cellular segregation into barrels and TCAs cluster into rows, but not individual patches (Barnett et al., 2006a). Mice lacking *Pkar2β* have normally segregated TCAs in PMBSF but not in anterior snout regions. *Pkar2β*$^{-/-}$ mice have poorly defined barrel walls and hollows and do not display the reduction in number of cells seen in wild-type animals (Inan et al., 2006; Watson et al., 2006b). *Plc-β1*$^{-/-}$ mice lack cortical barrels, but TCA patterning, distribution and size are normal (Hannan et al., 2001). *MgluR5*$^{-/-}$ mice display segregation of large whisker TCAs into rows but not individual patches within rows, and lack barrels (Hannan et al., 2001)

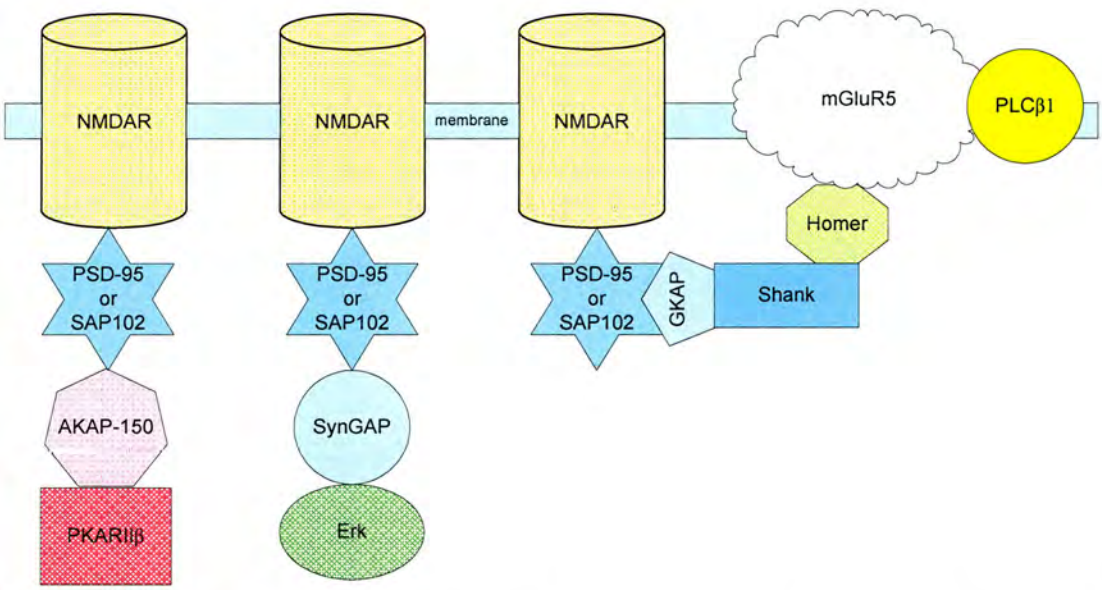

Figure 4.1
PSD-95 and SAP-102 integrate the NMDAR with signalling pathways known to be crucial for barrel formation. PKARIIβ, SynGAP, and mGluR5/ PLCβ$_1$. PSD-95 and SAP-102 bind AKAP150, which then binds PKARIIβ. PSD-95 and SAP-102 bind GKAP, which binds Shank, which binds Homer, binding mGluR5. PSD-95 and SAP-102 also directly bind SynGAP, which mediates its effects through Erk (Barnett et al., 2006a).

Since genetic knockout of other NRC components that are downstream of PSD-95 and/ or SAP-102 have been shown to affect barrel formation (Erzurumlu and Kind, 2001; Barnett et

al., 2006b), it was decided to investigate the barrel phenotypes of *Psd-95*$^{-/-}$ and *Sap-102*$^{-/-}$ mice. This work complements the barrel phenotype examination of the *Wnt* and *Dvl* knockout brains as both MAGUKs can interact with components of the Wnt signalling pathway. The PDZ domains of PSD-95 have been shown to bind Frizzled receptors Fz-1, Fz-2, Fz-4 and Fz-7 (albeit only by yeast two-hybrid and in transfected COS-7 cells, Hering and Sheng, 2002). SAP-102 binds the NMDA receptor strongly with its first two PDZ domains (Kuwahara et al., 1999; Husi et al., 2000) and the PDZ domains of SAP-102 have been shown to downregulate β-catenin levels (Hanada et al., 2000). The SH3 domain of SAP-102 binds Calmodulin in a calcium ion dependent manner, linking SAP-102 to NMDA receptor mediated Ca^{2+} influx dependent plasticity (Masuko et al., 1999; Xia and Storm, 2005). Dishevelled proteins are essential components of almost all known Wnt signalling pathways (Nusse, 2005) and *Dvl1*$^{-/-}$ and *Wnt7a*$^{-/-}$*Dvl1*$^{-/-}$ mice have been shown to have altered morphologies of mossy fibre terminals in cerebellar glomerular rosettes, likely due to alterations in microtubule or actin structure (Ahmad-Annuar et al., 2006).

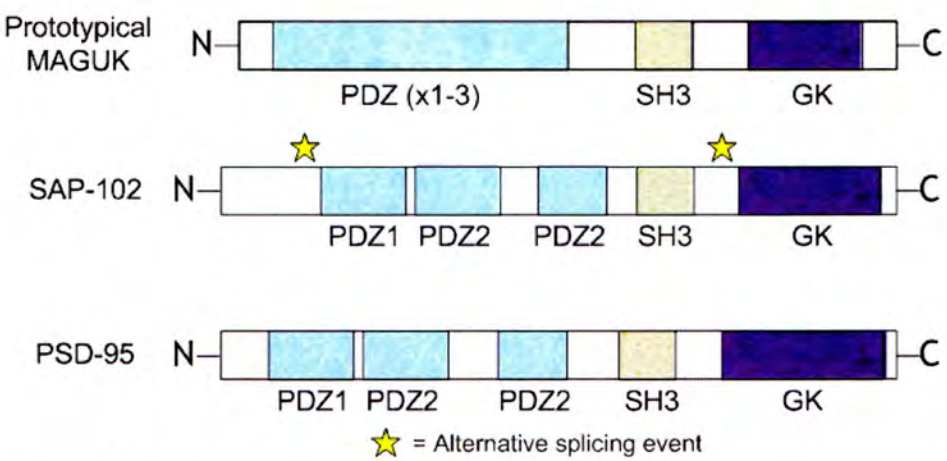

Figure 4.2
Notable MAGUKS in the PSD. Schematic diagram of the structural domains of two membrane associated guanylate kinases (MAGUKs) of the PSD-95 family that are present in the post synaptic density, SAP-102 and PSD-95. Light blue bars are PDZ domains; greyish-pink bars are SH3 domains; purple bars are guanylate kinase (GK) domains; white bars are regions of low sequence homology; stars are alternative splicing events.

4.1.3 Mice

4.1.3.1 Wnt and Dishevelled mutants

It transpires that for all of the published *Wnt* gene knockout mice generated to date, the only ones that survive to an age where barrels can be observed are *Wnt2*, *Wnt2b*, *Wnt7a* and *Wnt8b*.

Wnt2$^{-/-}$ mice exist only as frozen embryos in the laboratory of Brandon Wainwright (University of Queensland, Australia) and are unavailable for screening. Although *Wnt2* transcript was not detected in barrel cortex in the previous chapter, a barrel defect might still exist the loss of *Wnt2* alters earlier structures in the whisker-barrel pathway, e.g. barreloid formation.

Wnt2b transcript expression was detected throughout barrel cortex development by qRT PCR (Chapter 3) and mRNA of this gene has been shown to be present at P20 in barrel walls by in situ hybridisation (Shimogori et al., 2004). Three P7 *Wnt2b*$^{-/-}$ and three *Wnt2b*$^{+/-}$ brains were generously provided by Prof. Terry Yamaguchi of the National Cancer Institute, NIH, Bethesda, MD, USA

Wnt7a transcript was detected by qRT-PCR throughout barrel cortex development (Chapter 3) and has shown to be crucial for the formation of glomerular rosettes, a structure that requires cellular migration and dendritic rearrangement processes; these events are also required for barrel formation. Furthermore, Dishevelled proteins are essential component in many of the Wnt signalling pathways, and have been implicated changes in axonal cytoskeletal shape (Ciani et al., 2004). In collaboration with Dr. Patricia Salinas (University College London, London, UK), we examined three P7 brains of each of the following genotypes: *Wnt7a*$^{-/-}$, *Dvl1*$^{-/-}$, *Dvl2*$^{-/-}$ and *Wnt7a*$^{-/-}$*Dvl1*$^{-/-}$.

Wnt8b transcript was detected during barrel cortex development by qRT-PCR (Chapter 3), although levels were so low that quantification of expression levels was not possible. *Wnt8b*$^{-/-}$ mice were examined in collaboration with Dr. John Mason of Edinburgh University, UK.

4.1.3.2 Psd-95 and Sap-102 mutants

Sap-102$^{-/-}$, *Psd-95*$^{-/-}$ and *Psd-95GK*$^{-/-}$ mice were obtained from the laboratory of Professor Seth Grant of the Sanger Institute, Hinxton, Cambridgeshire, UK and colonies established within Edinburgh University.

The *Psd-95GK* mutant was generated in order to knock-out the Guanylate Kinase (GK) domain of *Psd-95*, but instead generated a completely null mutant producing mice with no detectable levels of *Psd-95* cDNA or PSD-95 protein. This differs from the previously reported *Psd-95* mutant (Migaud et al., 1998) which produces a small amount of truncated protein containing part of the information encoded in exon 1 of unknown function (personal communication, Prof. Seth Grant). As such, the *Psd-95GK* is a novel genotype for barrel phenotype characterisation. Since the original *Psd-95*$^{-/-}$ mice have normal barrels (previous work in our laboratory), it was hypothesised that compensation by other MAGUKs that could rescue any barrel phenotype that would otherwise be generated. By crossing *Psd-95*$^{-/-}$ (not the *Psd-95GK*$^{-/-}$) mice with *Sap-102*$^{-/-}$ mice and characterising the barrel phenotype, one can test if *Sap-102* can compensate for the lack of *Psd-95* during barrel formation. Genetic backgrounds of each colony used in this chapter are discussed in the Materials and Methods chapter.

4.2 Methods of Barrel and TCA Characterisation

The barrel phenotype is usually characterised at P7, because by this age TCAs have already segregated into a barrel-like pattern and a full barrel field can be seen. If a genetic knockout delays or prohibits barrel formation, it will be observed at P7, as underdeveloped or missing barrels would be observed.

There are two main ways to undertake the initial characterisation of a barrel phenotype. Firstly, Nissl staining on cortical flat sections reveals the extent of cellular segregation into the characteristic barrel field. Secondly, performing anti-5-hydroxytryptamine (α-5-HT) or anti-5-HT transporter (α-5-HTT) immunohistochemistry reveals the extent of TCA segregation into individual patches that correspond to a single barrel. 5-HT and 5-HTT staining in barrel cortex is transient and ends by P9. Examination of TCAs after P9 involves carbocyanine dye tracing of the TCAs, and this labelling requires long incubations to permit the dye to transport to the cortex.

Previous experience of the Kind laboratory has shown that a preliminary analysis of a barrel phenotype (i.e. the methods shown above) requires two to three animals per genotype. Further in-depth characterisation of the barrel phenotype, such as quantification of cell

densities in barrel walls and hollows with propidium iodide and confocal microscopy (Barnett et al., 2006a; Watson et al., 2006b) or Golgi staining of dendrites (Datwani et al., 2002b; Upton et al., 2005) requires in excess five to seven animals or up to twenty animals for each genotype respectively. Unfortunately, all of the colonies managed by the Kind laboratory were culled following a Mouse Hepatitis Virus outbreak within the animal facility in which they were kept. Nevertheless, all of the mice harvested prior to the cull are presented in this thesis. In general, the laboratory only asks for two to three mutant P7 brains for screening of a barrel phenotype by Nissl staining and α-5-HT(T) immunohistochemistry. If an obvious defect is found, only then would more brains be requested.

4.2.1 Nissl Stain on cortical flats

Cresyl Violet or Thionin was used to stain Nissl substance (rough endoplasmic reticulum and associated ribosomes) in cortical flat sections (see Materials and Methods chapter and Figure 4.3), revealing the general cellular structure of the tissue. This is an effective method for determining if barrels have formed properly, as the whole barrel field should be able to be seen in one or two 48μm sections, although sub-optimal flattening of the cortex may result in the barrel field being spread over more sections.

4.2.2 Cortical Flat dissection

With restricted numbers of brains available for each genotype, it was decided to obtain flattened cortical sections by using a dissection method that minimised distortion of barrel shape. This would enable optimal visual assessment of any cortical cell segregation into barrel walls that may have occurred. After separating the two hemispheres and removing of the cerebellum and brainstem, this dissection method required removal of all tension points from the cortex, namely the olfactory tubercles, entorhinal cortex, striatum and hippocampus. The result is an unstressed cortex that can be flattened directly onto a freezing microtome stage. As minimal tissue distortion occurs with this method, a superior barrel field is seen, compared to other cortical flattening methods involving sandwiching the cortex between two slides. However, the trade-off for obtaining minimally distorted barrels is the loss of anatomical landmarks when removing tension points. This makes the precise position of the barrel field in the anterior-posterior and medial-lateral planes impossible, and subtle shifts in the barrel field would be missed.

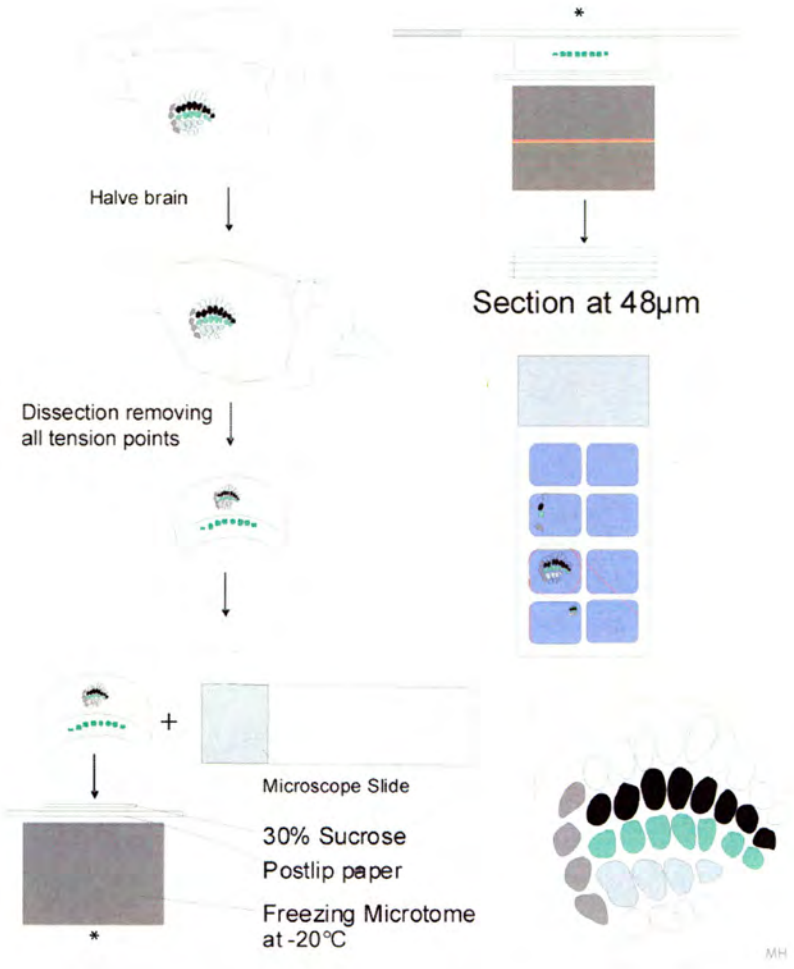

Figure 4.3
Dissection and flattening of the cortex. One hemisphere had the olfactory bulbs and the cerebellum removed, followed by removal of the hippocampus and striatum. The remaining cortex was flattened with a glass microscope slide onto a piece of Postlip paper covered with 30% sucrose, placed on a freezing platform on the freezing microtome. Sections were cut and placed in cold PBS in individual wells of a 24-well plate, prior to staining and mounting.

4.2.3 Anti-5-hydroxytryptamine transporter immunohistochemistry on coronal sections

Prior to P10, 5-HT and 5-HTT are found in TCA terminals but are not found postsynaptically in cortical cells, therefore staining for these molecules reveals only TCA patterning. Defects in TCA patterning confers defects in barrel formation (Abdel-Majid et al., 1998; Erzurumlu and Kind, 2001; Hannan et al., 2001; Inan et al., 2005; Watson et al., 2005; Barnett et al., 2005b; Barnett et al., 2006a), although mice can have normal TCA

patterning, yet lack cortical barrels, as is the case with *Plc-$\beta_1^{-/-}$* , *Pkar2$\beta_1^{-/-}$* and *SynGAP$^{-/-}$* mice (Hannan et al., 2001; Barnett et al., 2006a; Watson et al., 2006b).

4.2.4 Visual ranking analysis of the barrel phenotypes of mutant mice

A qualitative analysis of cortical cells in PMBSF was conducted in P7 animals. This age was chosen as barrels delayed barrel formation would result in an unformed or immature barrel field. A qualitative index has already been established to determine the existence and extent of any defect in barrel formation (Katsnelson, 2002). Barrels were ranked blind of identity, with slides chosen at random, with scores ranging from 0 to 4 in 0.5 increments according to the following criteria (Figure 4.4):

0 = Complete absence of cellular differentiation into barrels

1 = Hint of uneven cell distribution, but few, if any identifiable barrels

2 = Discernable barrel field, but no clear septae and weak distinction between barrel walls and barrel hollows; barrels generally seen only in PMBSF, though sometimes a few are seen in the anterior snout region

3 = Barrels visible throughout S1, including in the anterior snout region, although less distinct than normal, and septae are often difficult to define.

4 = Full barrel field visible with clearly defined barrel walls and septae.

Slide images were coded for analysis by Kimmi Luo and each slide was ranked blind to identity by Dr. Peter Kind and me, then the order of the slides was then randomised by Miss Luo, and each slide was ranked again. The code was then broken for analysis and the scores of individual observers were averaged and grouped by age and genotype. The assessment of barrels was performed for every section, and an average of the barrel ranks was generated for each brain. One way ANOVA followed by Student-Newman-Keuls post hoc tests (where appropriate) statistical analysis were performed (Figure 4.18).

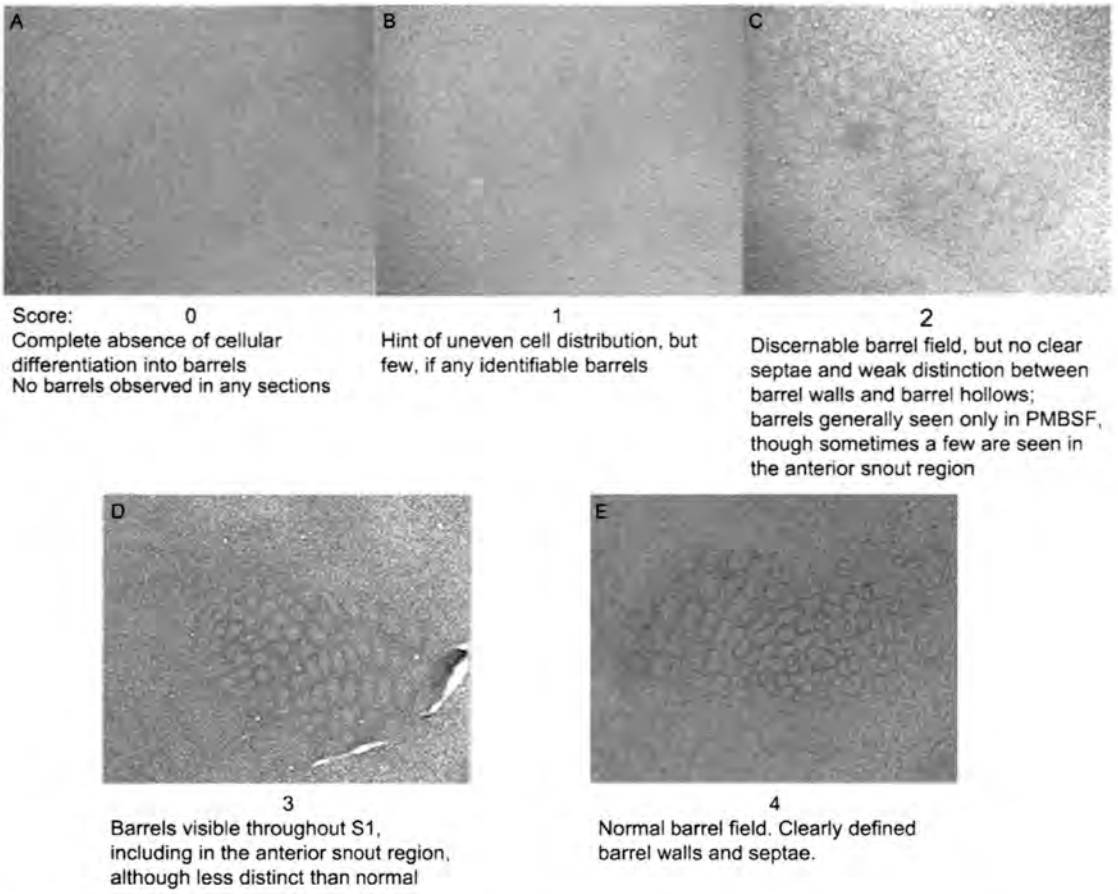

Figure 4.4
Representative images of sections that scored 0, 1, 2, 3 and 4 in the visual barrel ranking analysis. 0, a complete absence of cellular differentiation into barrels; 1, a hint of uneven cell distribution, but few, if any identifiable barrels; 2, a discernable barrel field, but no clear septae and weak distinction between barrel walls and barrel hollows; barrels generally seen only in PMBSF, though sometimes a few are seen in the anterior snout region; 3, barrels visible throughout S1, including in the anterior snout region, although less distinct than normal; 4, a normal barrel field with clear barrel walls and septae.

4.3 Results

4.3.1 Description of the barrel phenotypes of mutant mice

4.3.2 *Wnt 2b*$^{-/-}$ barrel phenotype

Nissl staining of adjacent cortical flat sections revealed the presence of a full barrelfield in both *Wnt2b*$^{+/-}$ and *Wnt2b*$^{-/-}$ mice (Figure 4.5a-c), with cell soma having clustered to form clearly visible cell-dense barrel walls (arrowheads, Figure 4.5c), cell-sparse barrel hollows and clearly defined barrel septae present (arrows, Figure 4.5c). α-5-HT immunohistochemistry revealed clearly defined patches of TCAs terminating in layer IV,

and lighter α-5-HT staining was observed in layer VI, where some TCAs also terminate (Figure 4.5c, d).

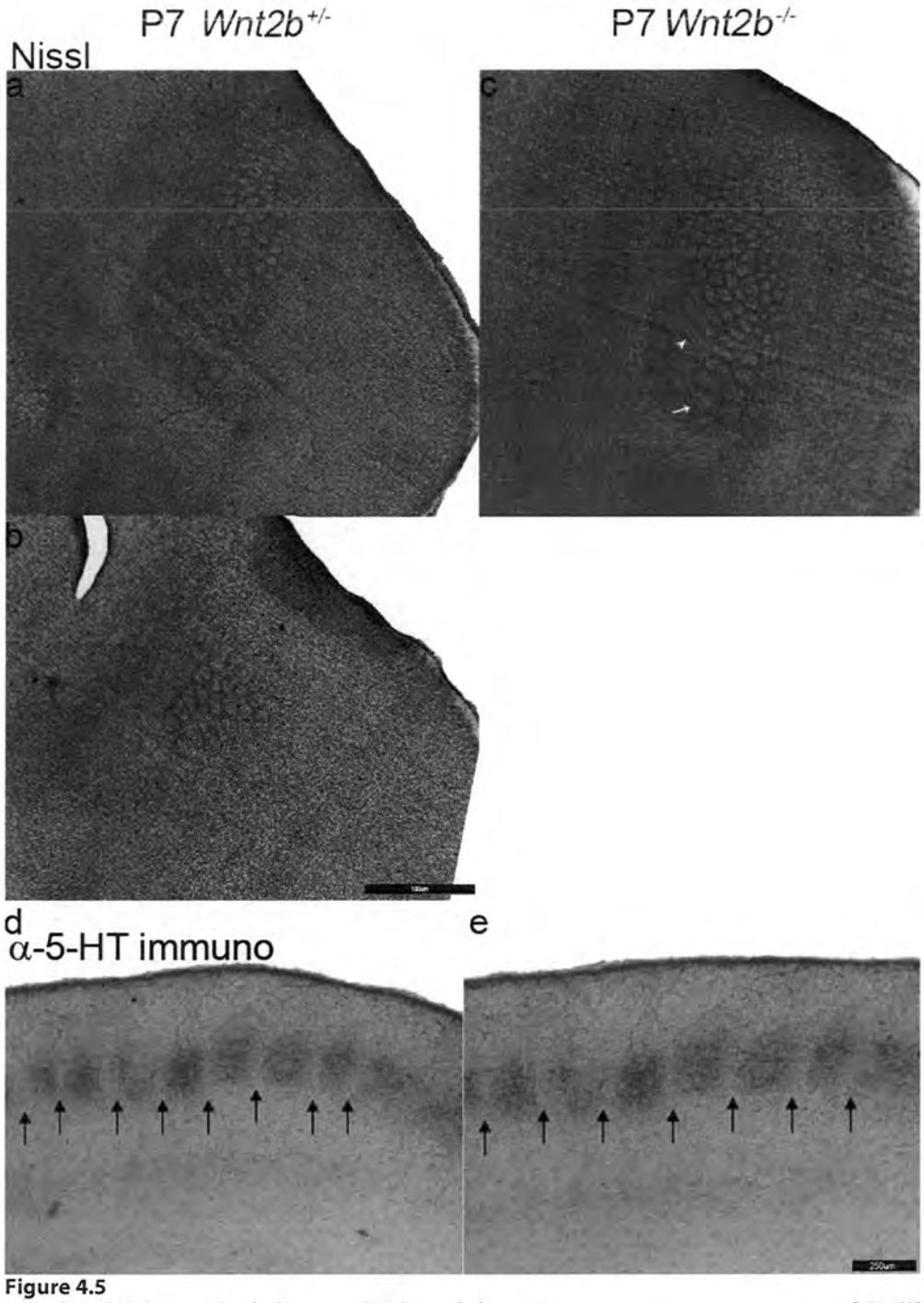

Figure 4.5
Barrel and TCA terminal characterisation of the primary somatosensory cortex of P7 Wnt2b$^{-/-}$ and Wnt2b$^{+/-}$ mice
Nissl staining of adjacent 48μm cortical flat sections (a, b) and α-5-HT immunohistochemistry on 48μm coronal sections (c, d) of P7 *Wnt2b*$^{-/-}$ and *Wnt2b*$^{+/-}$ mice. For both heterozygous and homozygous mutants, it appears that a normal barrel field is present. Cell soma are clearly clustered to form a dark cell-dense barrel walls (arrowhead), surrounding a cell-sparse barrel hollow, giving rise to exceptionally well defined barrel walls and septae (arrow) which are most prominently visible in panel (c), a *Wnt2b*$^{-/-}$ mouse. TCA patches, as revealed by α-5-HT immunochemistry shows normal segregation and termination in layer IV. Arrows mark barrel septae (d,e). *n*=3 per genotype. Scale bar = 100μm (a-c) and 250μm (d-e).

4.3.3 *Wnt7a*$^{-/-}$ barrel phenotype

Wnt7a$^{-/-}$ mice had a full barrelfield, as revealed by staining of Nissl substance of 48μm cortical flat sections (Figure 4.6a). The barrels showed no obvious deviation from normal cell density, as cell soma had clustered to form clearly visible cell-dense barrel walls (arrowheads, Figure 4.6a) and clear barrel hollows and septae (arrows in Figure 4.6a) were observed (Figure 4.6a). Clear patches of TCAs terminating in layer IV are visible by α-5-HT immunohistochemistry, and lighter staining was also observed in layer VI, a region where some TCAs also terminate (Figure 4.6).

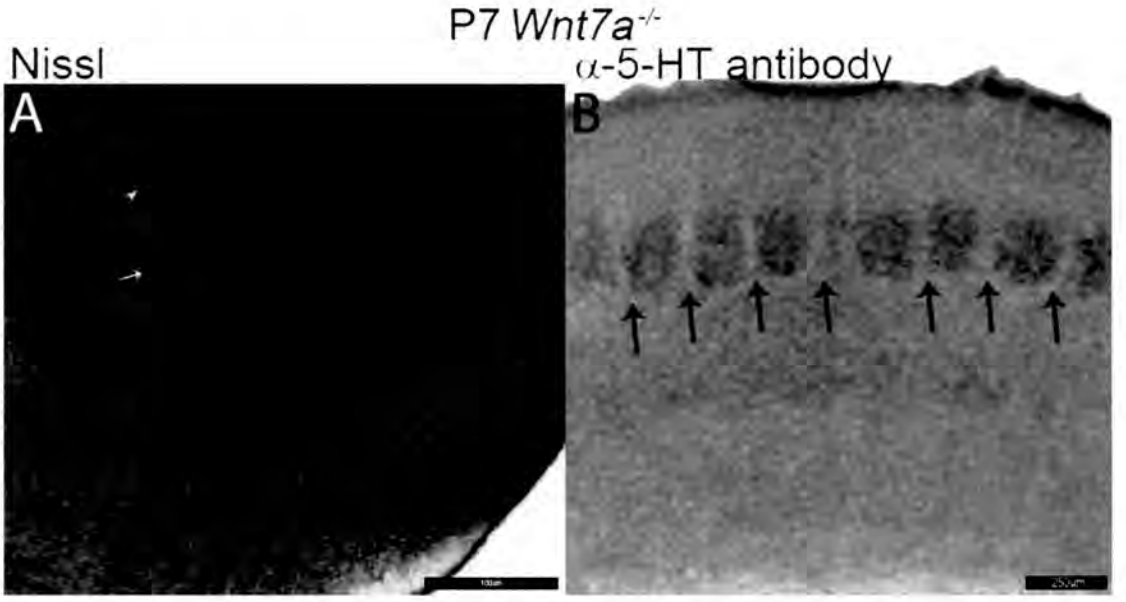

Figure 4.6
Barrel and TCA terminal characterisation of the primary somatosensory cortex of P7 *Wnt7a*$^{-/-}$ mice. (a) A normal barrel field is present in *Wnt7a*$^{-/-}$ mice. Cell soma are clearly clustered to form dark blue cell-dense barrel walls (arrowhead), surrounding a cell-sparse barrel hollow, giving rise to well defined barrel walls and septae (arrow). (b) TCA patches, as revealed by α-5-HT immunochemistry show normal segregation and termination in layer IV. Arrows mark barrel septae (b). *n*=3. Scale bar = 100μm (a) and 250μm (b).

4.3.4 Wnt8b$^{-/-}$ barrel phenotype

Wnt8b$^{-/-}$ mice (Figure 4.7a,b,c) and *Wnt8b*$^{+/+}$ mice (Figure 4.7d,e,f) had full barrelfields; cell soma had segregated to form exceptionally well defined barrel walls and hollows, and clearly visible septae were observed in both genotypes by Nissl staining in 48μm cortical flat sections (Figure 4.7a-f). Clear patches of segregated TCAs terminating in layer IV were visible by α-5-HT immunohistochemistry, and lighter staining of the small number of TCAs that terminate in layer VI were observed (Figure 4.7g,h) in both *Wnt8b*$^{-/-}$ and *Wnt8b*$^{+/+}$ mice.

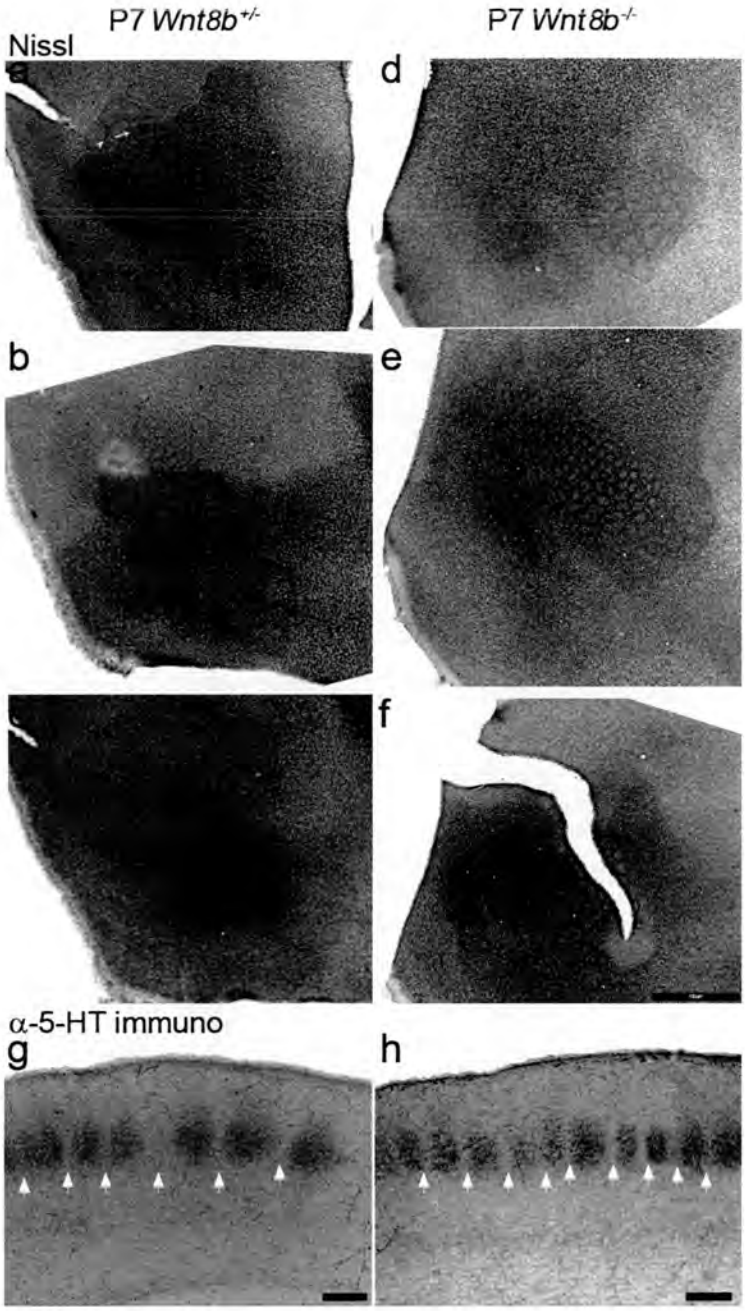

Figure 4.7
Barrel and TCA terminal characterisation of the primary somatosensory cortex of P7 *Wnt8b*$^{-/-}$ and *Wnt8b*$^{+/-}$ mice.
Nissl staining of adjacent 48μm cortical flat sections (a-f) and α-5-HT immunohistochemistry on 48μm coronal sections (g, h) of P7 *Wnt8b*$^{-/-}$ (a, b, c, g) and *Wnt8b*$^{+/-}$ (d, e, f, h) mice. For both heterozygous and homozygous mutants, it appears that a normal barrel field is present. Cell soma are clearly clustered to form dark cell-dense barrel wall (arrowhead), surrounding a cell-sparse barrel hollow, giving rise to exceptionally well defined barrel walls and septae (arrow) which are most prominently visible in panel (a). A full barrelfield is present. TCA patches, as revealed by α-5-HT immunochemistry shows normal segregation and termination in layer IV for both genotypes (g,h). Arrows mark barrel septae (d,e). *n*=3 per genotype. Scale bar = 100μm (a-c, d-f) and 250μm (g-h).

4.3.5 *Dvl1*$^{-/-}$ barrel phenotype

Dvl1$^{-/-}$ mice had a full barrelfield, and cell soma had clustered to form exceptionally well defined barrel walls (arrows, Figure 4.8b), hollows and inter-barrel septae (Figure 4.8b) as revealed by Nissl staining of adjacent cortical flat sections (Figure 4.8a-c). Clear patches of TCAs terminating in layer IV were revealed by α-5-HT immunohistochemistry, and some lighter α-5-HT staining was observed in layer VI, a region where some TCAs also terminate (Figure 4.8b).

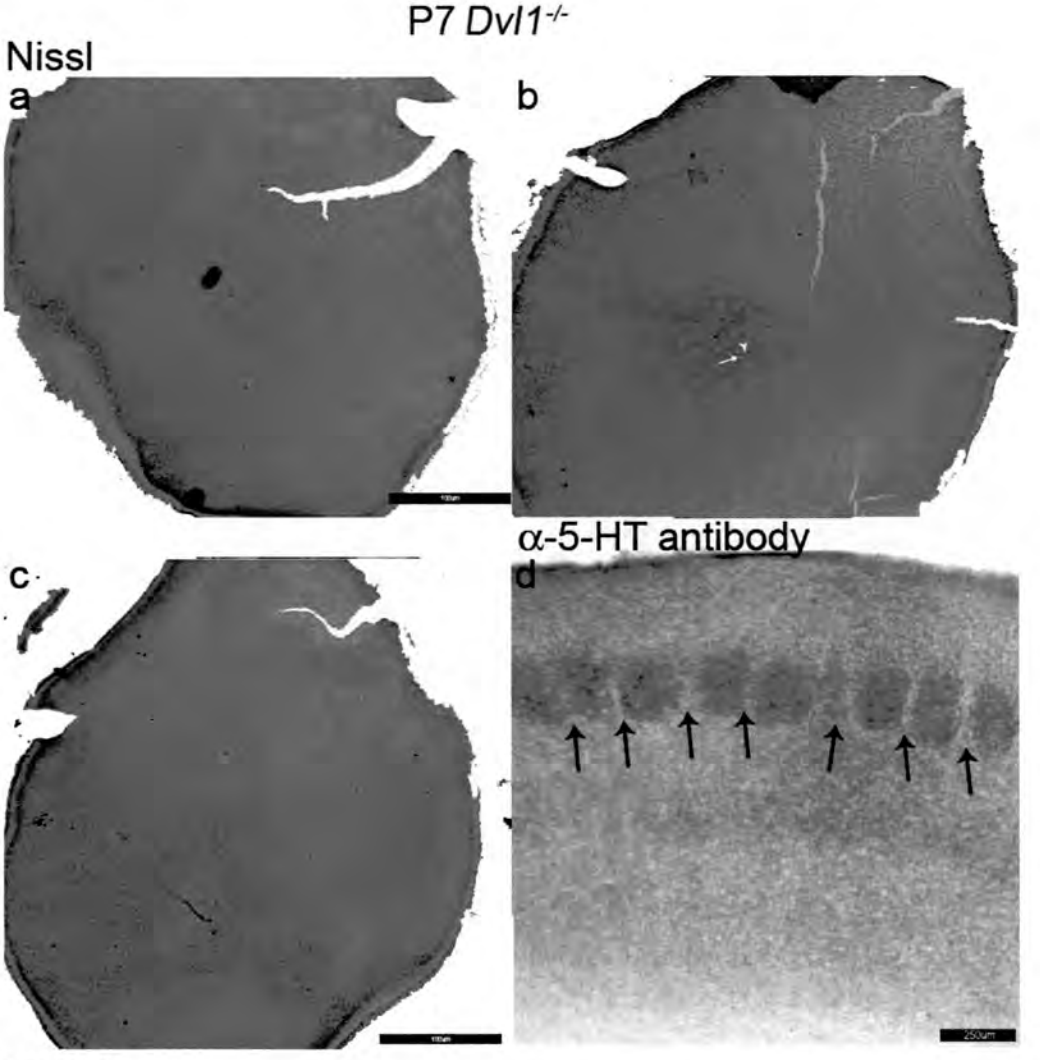

Figure 4.8
Barrel and TCA terminal characterisation of the primary somatosensory cortex of P7 *Dvl1*$^{-/-}$ mice
Nissl staining adjacent of cortical flat sections (a-c) and α-5-HT immunohistochemistry on coronal sections (d) of P7 *Dvl1*$^{-/-}$ mice. Panels (a-c), cell soma are clearly clustered to form dark cell-dense barrel walls (arrowhead), surrounding a cell-sparse barrel hollow, giving rise to exceptionally well defined barrel walls and septae (arrow) which are most prominently visible in panel (b. A full barrelfield is present. Panel (d) TCAs terminate normally and segregate in layer IV. *n*=3. Arrows mark barrel septae (d). Scale bar = 100μm (a-c) and 250μm (d).

4.3.6 *Dvl2*$^{-/-}$ barrel phenotype

Nissl staining of adjacent cortical flat sections (Figure 4.9a-c) revealed that *Dvl2*$^{-/-}$ mice have full barrelfields, and that cell soma cluster to form exceptionally well defined barrel walls (arrows, Figure 4.9b), barrel hollows and inter-barrel septae (Figure 4.9b). Clear patches of TCAs terminating in layer IV were revealed by α-5-HT immunohistochemistry, and some lighter α-5-HT staining was observed in layer VI, a region where some TCAs also terminate (Figure 4.9b).

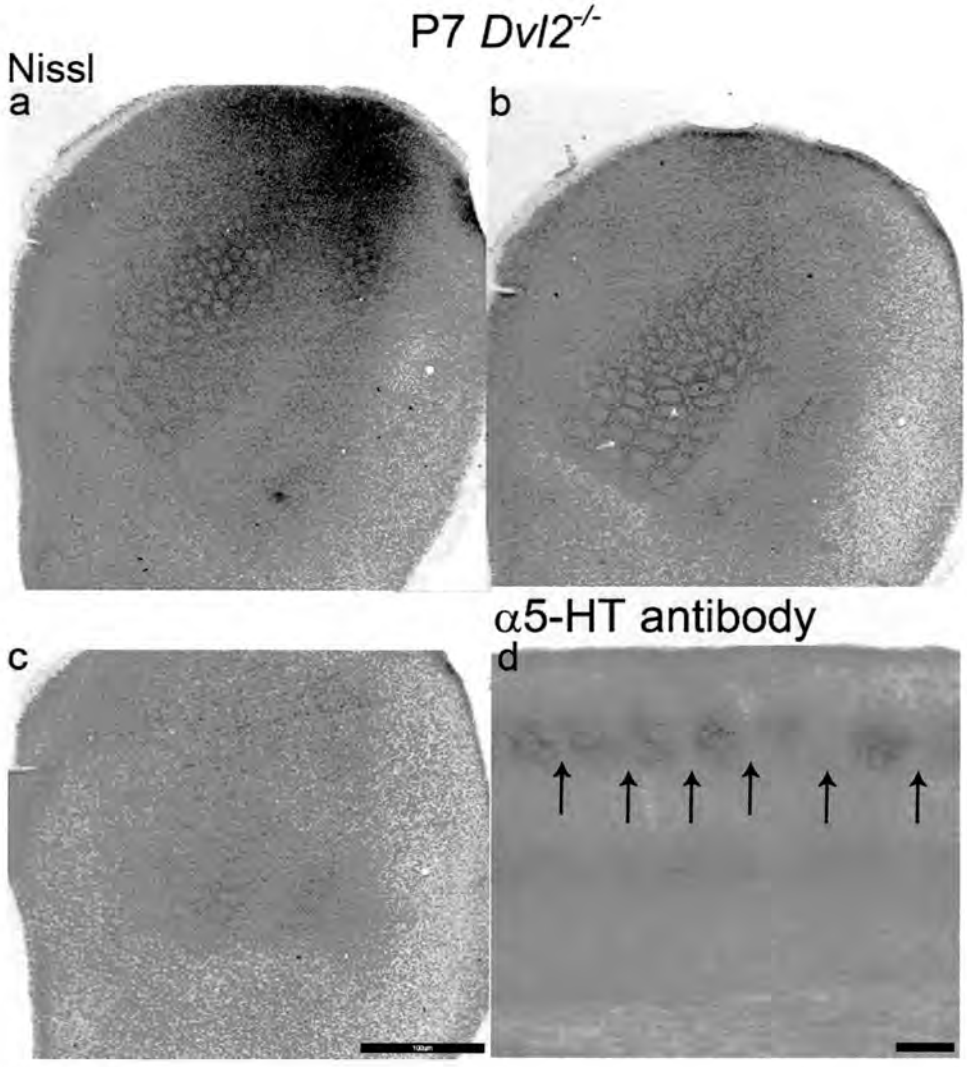

Figure 4.9
Barrel and TCA terminal characterisation of the primary somatosensory cortex of P7 *Dvl2*$^{-/-}$ mice
Nissl staining adjacent of cortical flat sections (a-c) and α-5-HT immunohistochemistry on coronal sections (d) of P7 *Dvl2*$^{-/-}$ mice. Panels (a-c), cell soma are clearly clustered to form dark cell-dense barrel walls (arrowhead), surrounding a cell-sparse barrel hollow, giving rise to exceptionally well defined barrel walls and septae (arrow) which are most prominently visible in panel (b. A full barrelfield is present. Panel (d) TCAs terminate normally and segregate in layer IV. *n*=3. Arrows mark barrel septae (d). Scale bar = 100μm (a-c) and 250μm (d).

4.3.7 *Wnt7a*$^{-/-}$*Dvl1*$^{-/-}$ barrel phenotype

Wnt7a$^{-/-}$*Dvl1*$^{-/-}$ mice exhibit more severe defects in glomerular rosette formation than the *Wnt7a*$^{-/-}$ mutant (Ahmad-Annuar et al., 2006). Since the additional knockout of *Dvl1* in *Wnt7a*$^{-/-}$*Dvl1*$^{-/-}$ mice yields a more severe glomerular rosette defect phenotype than the loss of *Wnt7a* alone, then it is conceivable that the loss of *Dvl1* in addition to knockout of *Wnt7a* may reveal a barrel defect that was not present in *Wnt7a*$^{-/-}$ (Figure 4.6) or *Dvl1*$^{-/-}$ mice (Figure 4.8). To determine if *Wnt7a* expression in tandem with *Dvl1* expression is necessary for barrel formation, Nissl substance was stained in 48μm cortical flat sections, and α-5-HT immunohistochemistry was performed. *Wnt7a*$^{-/-}$*Dvl1*$^{-/-}$ mice have a full barrelfield (Figure 4.10a-c), and cell soma cluster to form clearly visible cell-dense barrel walls (arrowheads, Figure 4.10c), barrel hollows and well-defined septae (arrows, Figure 4.10c) were observed. α-5-HT immunohistochemistry revealed clearly defined patches of TCAs terminating in layer IV (Figure 4.10d).

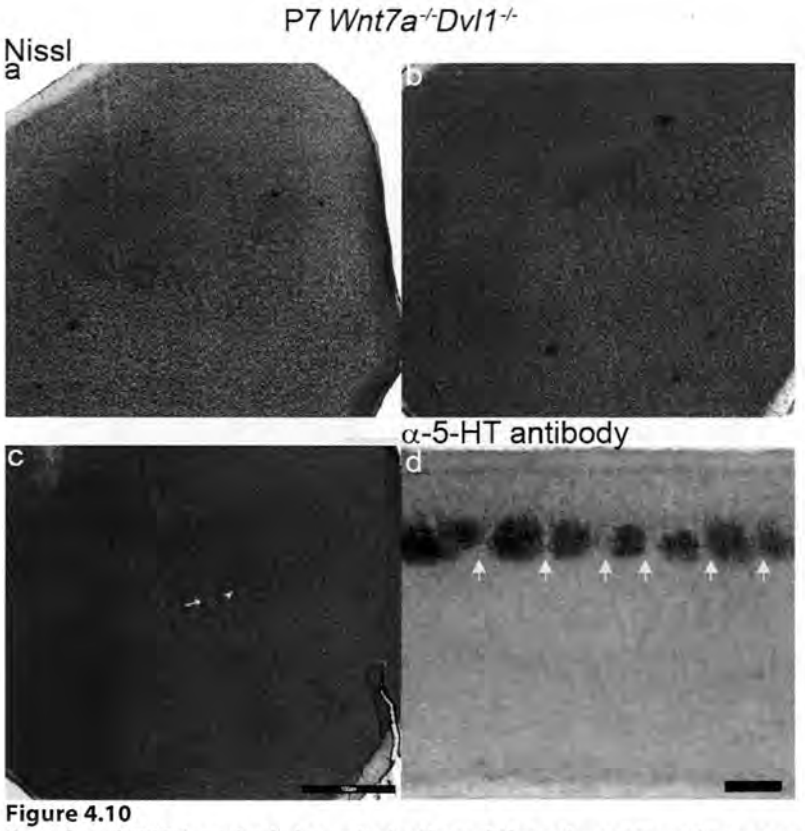

Figure 4.10
Barrel and TCA terminal characterisation of the primary somatosensory cortex of P7 *Wnt7a*$^{-/-}$ *Dvl1*$^{-/-}$ mice
Nissl staining of cortical flat (a-c) and α-5-HT immunohistochemistry on coronal sections (d) of P7 *Wnt7a*$^{-/-}$ *Dvl1*$^{-/-}$ mice. The whole barrel field is represented, and segregation and septae of barrel walls and septae are clearly defined, as cell soma are clearly clustered to form a dark blue cell-dense barrel wall (arrowhead), surrounding a cell-sparse barrel hollow. TCAs terminate and segregate normally in layer IV (d). Arrows mark barrel septae (d). *n*=3. Scale bar = 100μm (a-c) and 250μm (d).

4.3.8 Visual ranking analysis of *Wnt* and *Dvl* mutant barrel phenotypes

All mice presented above had barrels that were visible throughout primary somatosensory cortex, with definite barrel walls and identifiable septae. There was no statistically significant difference in barrel ranking scores seen between any of the genotypes examined (Figure 4.11) indicating that normal cortical segregation to form barrels has occurred in these genotypes.

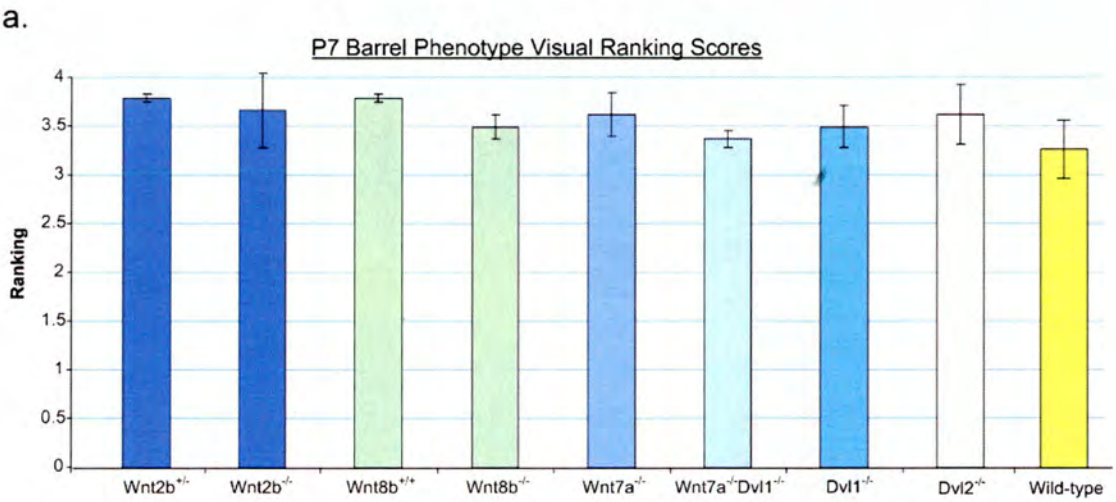

Figure 4.11
Visual ranking scores of the barrel phenotypes of various *Psd-95* and *Sap-102* compound mutant mice. A. Ranking scores for wild-type and mice mutant for at least one allele of *Wnt2b*, *Wnt8b*, *Wnt7a*, *Dvl1* or *Dvl2*. No significant difference was observed between each genotype and paired control (*Wnt2b*$^{-/-}$ *vs.* *Wnt2b*$^{+/-}$ or *Wnt8b*$^{+/+}$ *vs.* *Wnt8b*$^{-/-}$) or between each genotype and wild-type (section a).

4.3.9 *Sap-102*$^{-/-}$ barrel phenotype

SAP-102 is the prominent scaffold protein within the NRC during the period of barrel formation, is a prominent protein that links the NMDAR, either directly or indirectly, to proteins known to be crucial to barrel formation (Figure 4.1) and SAP-102 also binds the Wnt signalling component, APC (Yanai et al., 2000). Genetic abrogation of *Sap-102* could potentially cause a defect in barrel formation. To determine if *Sap-102* is necessary for barrel formation, α-5-HT immunohistochemistry was performed on coronal sections to determine the segregation of TCAs into a barrel-like pattern and if correct termination in layer IV occurs, and Nissl-stained 48μm cortical flat sections were examined to determine if the

cellular movement required to form barrels had occurred. *Sap-102*$^{-/-}$ mice have a full barrelfield (Figure 4.12a,b), and cell soma have segregated to form well-defined barrel walls (arrowhead, Figure 4.12a), hollows and inter-barrel septae (arrows, Figure 4.12a). TCAs terminate in layer IV, and segregated patches of TCAs were revealed by α-5-HT immunohistochemistry (Figure 4.12c,d).

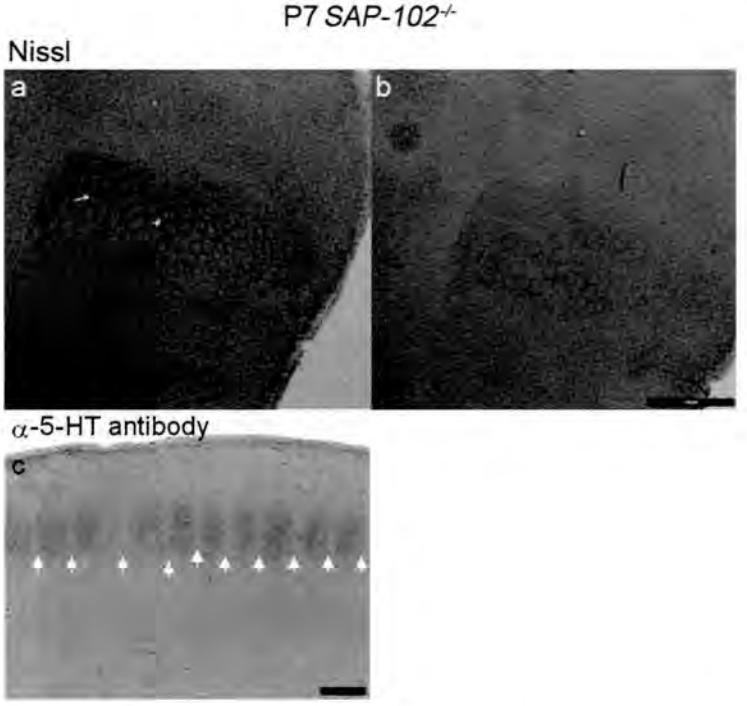

Figure 4.12
Nissl staining of adjacent cortical flat sections (a, b) and α-5-HT immunohistochemistry on coronal section (c) of P7 SAP-102$^{-/-}$ mice. Panels (a-b), cell soma are clearly clustered to form dark cell-dense barrel walls (arrowhead), surrounding a cell-sparse barrel hollow, giving rise to exceptionally well defined barrel walls and septae (arrow) which are most prominently visible in panel (a). A full barrelfield is present. Panel (c) TCAs terminate normally and segregate in layer IV. *n*=3. Arrows mark barrel septae (d). Scale bar = 100μm (a-b) and 250μm (c).

4.3.10 *Psd-95GK*$^{-/-}$ barrel phenotype

PSD-95 is the prominent scaffold protein within the NRC in adult mice, and is also present in increasing amounts during barrel formation (Barnett et al., 2006a). PSD-95 can function to link the NMDAR, either directly or indirectly, to proteins known to be crucial to barrel formation (Figure 4.1) and can also bind the Wnt receptor Frizzled (Hering and Sheng, 2002). Genetic knockout of *Psd-95* could potentially cause a defect in barrel formation.

A full barrelfield was observed in Nissl-stained coronal sections from *Psd-95GK*$^{-/-}$ mice (Figure 4.13a-b). Cell soma segregate to form clearly visible, cell-dense barrel walls

(arrowheads, Figure 4.13c), cell-sparse barrel hollows and well-defined barrel septae (arrows, Figure 4.13c). α-5-HT immunohistochemistry revealed clearly defined patches of TCAs terminating in layer IV, and lighter α-5-HT staining was observed in layer VI, where some TCAs also terminate (Figure 4.13c, d).

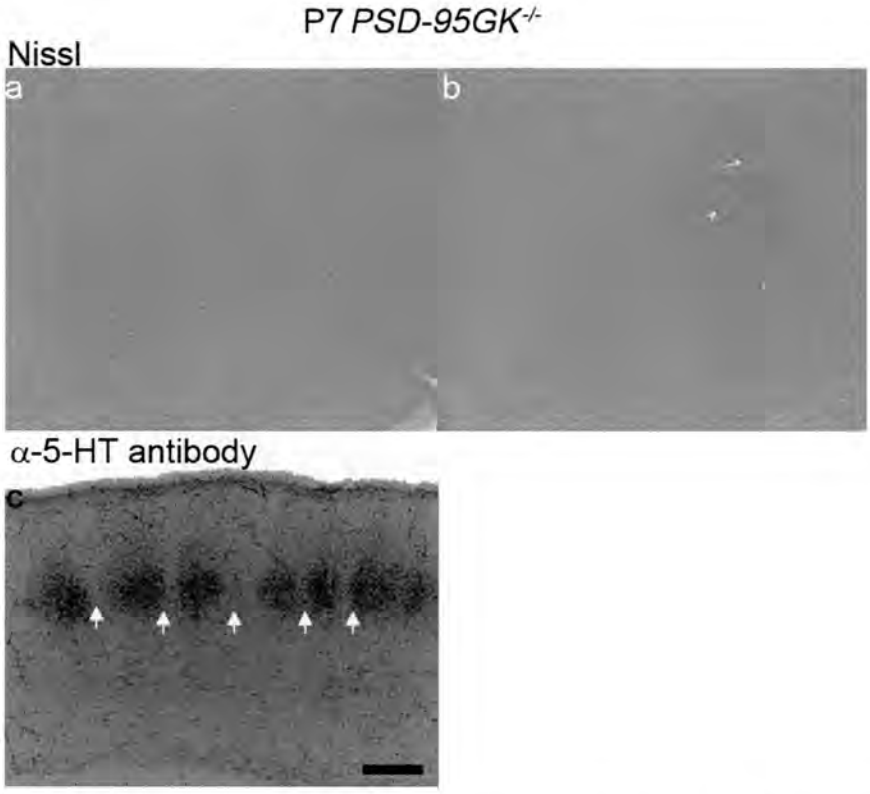

Figure 4.13
Nissl staining of cortical flat (a, b) and α-5-HT immunohistochemistry on coronal section (c) of P7 *Psd-95GK*$^{-/-}$ mice. Panels (a-b), cell soma are clearly clustered to form dark cell-dense barrel walls (arrowhead), surrounding a cell-sparse barrel hollow, giving rise to exceptionally well defined barrel walls and septae (arrow) which are most prominently visible in panel (a). A full barrelfield is present. Panel (c) TCAs terminate normally and segregate in layer IV. *n*=3. Arrows mark barrel septae (d). Scale bar = 100μm (a-b) and 250μm (c).

4.3.11 Barrel phenotypes of Sap-102$^{+/-}$Psd-95$^{-/-}$ *and* Sap-102$^{-/-}$Psd-95$^{+/-}$

Since both *Psd-95* and *Sap-102* knockout mice have normal barrels, an interpretation of this result is that compensation for the loss of one MAGUK occurs by upregulation of another MAGUK. Crossbreeding various combinations of *Psd-95* and *Sap-102* knockout and heterozygote mice generates a range of compound knockouts and heterozygotes. By examining the offspring of these mice, we can test whether compensatory upregulation of *Psd-95* or *Sap-102* is rescuing the defect in barrel formation.

Calretinin immunohistochemistry is used as a marker of layer IV cortical cells and is useful for helping to judge cortical lamination. Using this technique, cortical lamination appeared normal and layer IV was found to be present in the correct location in both *Sap-102*$^{+/-}$*Psd-95*$^{+/-}$ and *Sap-102*$^{-/-}$*Psd-95*$^{+/-}$ mice (Figure 4.14a,b), suggesting that the cortex forms normally.

Figure 4.14c and Figure 4.14d show α-5-HTT immunohistochemistry on P9 cortical flat sections, revealing TCA terminal patterning. Normal TCA segregation is observed in both *Sap-102*$^{+/-}$*Psd-95*$^{+/-}$ and *Sap-102*$^{-/-}$*Psd-95*$^{+/-}$ mice, indicating that there is no obvious anatomical presynaptic defect in TCA segregation for either genotype.

On examination of Nissl stained cortical flat sections, all mice other than the *Psd-95*$^{+/-}$*Sap-102*$^{-/-}$ mice show normal barrel segregation; cortical cell soma segregate forming well defined barrel walls, hollows and inter-barrel septae (Figure 4.15). *Psd-95*$^{+/-}$*Sap-102*$^{-/-}$ mice (Figure 4.15c, d, g, i, Figure 4.16, Figure 4.17) show defective barrel segregation, since their barrel walls and septae are less well defined compared to wild-type and the other genotypes presented.

mGluR5 immunohistochemistry was performed (Figure 4.14 a and b), since mGluR5 is thought to be expressed only in postsynaptic cortical dendrites (Reid et al., 1995). This technique revealed that in coronal sections from *Sap-102*$^{+/-}$*Psd-95*$^{+/-}$ mice, mGluR5 staining is located in layer IV in a barrel like pattern (Figure 4.14a). This was not the case in *Sap-102*$^{-/-}$*Psd-95*$^{+/-}$ mice, which exhibited no such segregation. This suggests that dendrites are not orienting properly in *Sap-102*$^{-/-}$*Psd-95*$^{+/-}$ mice.

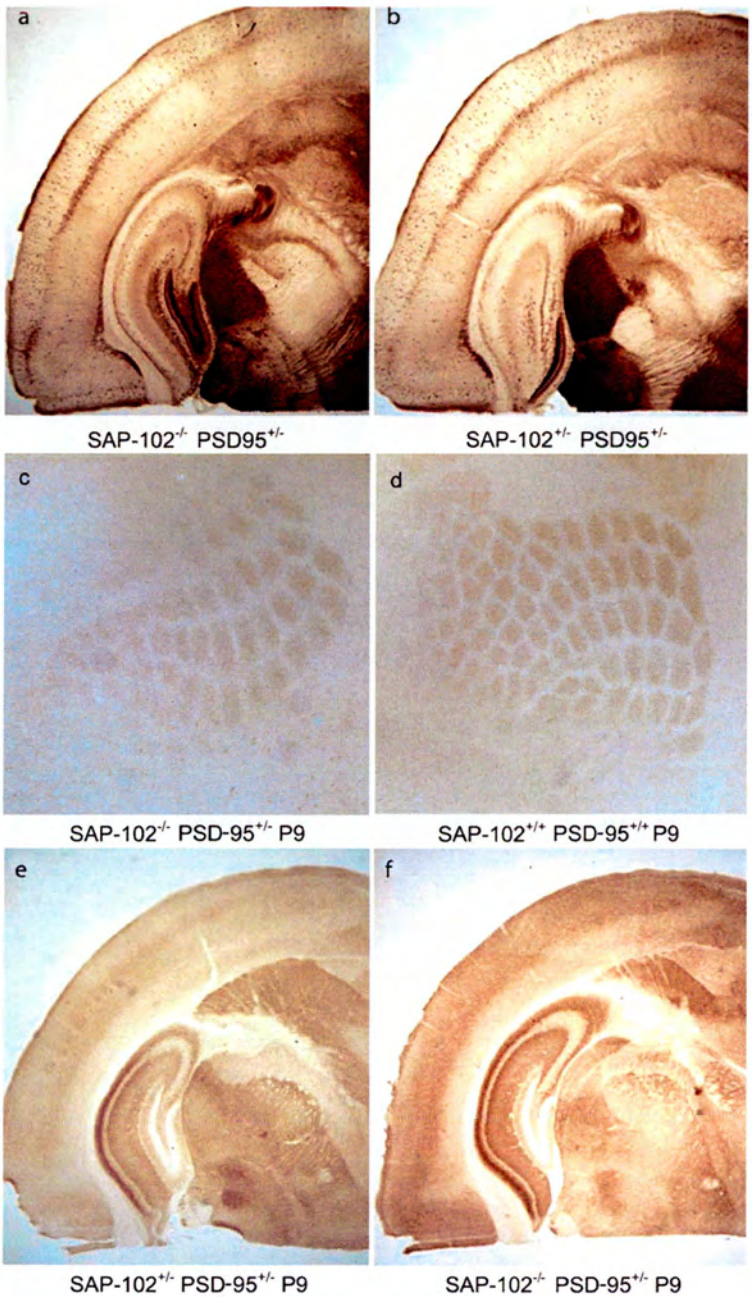

Figure 4.14
mGlurR5 and calretinin immunohistochemistry. Panels (a) & (b) show mGluR5 immunohistochemistry, a marker of dendrites in cortical barrels. P9 *Sap-102$^{+/-}$Psd-95$^{+/-}$* brains show normal barrels in layer IV cortex whilst P9 *Sap-102$^{-/-}$ Psd-95$^{+/-}$* brains do not. Panels (c) & (d) show 5-HTT immunohistochemistry on P9 cortical flat sections, revealing TCA terminal patterning. Normal TCA segregation is observed in both *Sap-102$^{+/-}$Psd-95$^{+/-}$* (c) and *Sap-102$^{-/-}$Psd-95$^{+/-}$* (d) mice. Panels (e) & (f) show immunohistochemistry for calretinin, a marker of layer IV cortical cells. Layer formation and the presence of layer IV looks normal in both *Sap-102$^{+/-}$Psd-95$^{+/-}$* (e) and *Sap-102$^{-/-}$Psd-95$^{+/-}$* (f) mice.

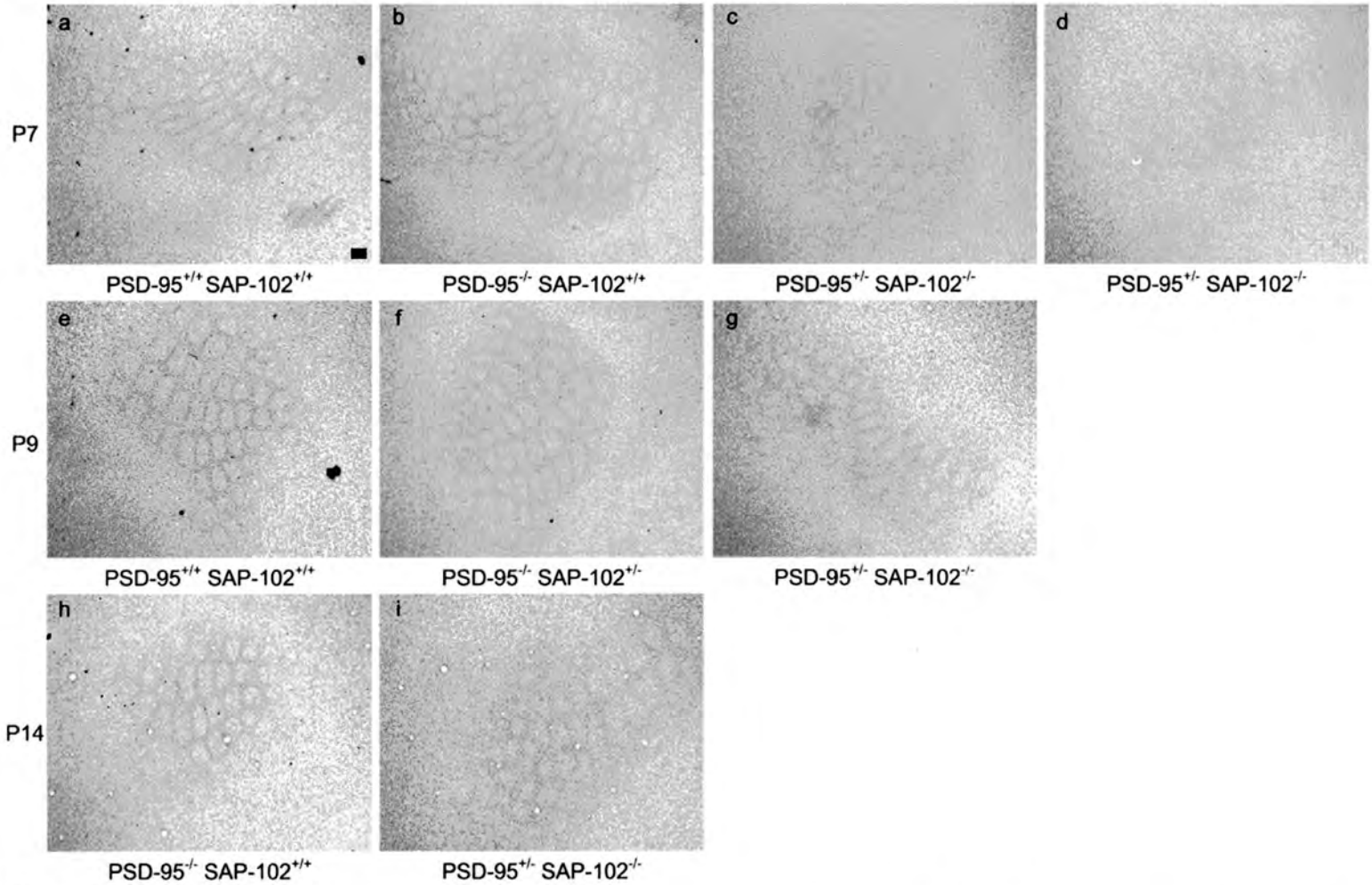

Figure 4.15
Nissl stain on cortical flat sections. P7, a-d, P9, e-g, P14, h-i. Wild-type, (a, e) single knockout (b, h) and *Psd-95*$^{-/-}$*Sap-102*$^{+/-}$ (f) mice show normal barrel segregation, with cell soma clearly clustering to form clear barrel walls and septae, whereas *Psd-95*$^{+/-}$*Sap-102*$^{-/-}$ (c, d, g, i) show defective barrel segregation, with poor definition of barrel walls, septae and segregation ranging from fair at P14 (i) to very poor at P7 (d). Serial sections from the brains shown in panels (c), (d), (g) and (i) are presented in greater detail in Figure 4.16 and Figure 4.17. Scale bar = 20μm.

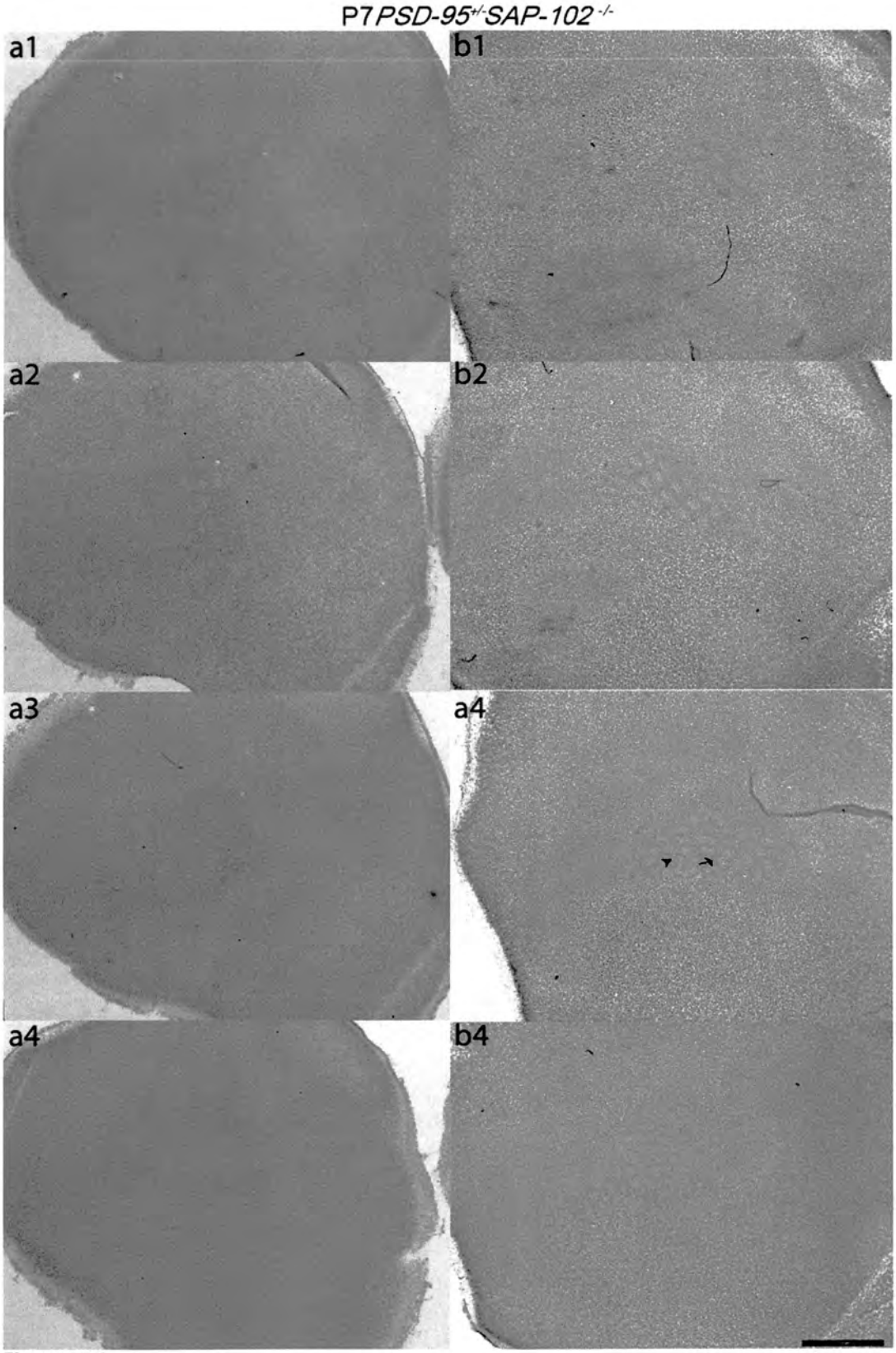

Figure 4.16
Serial sections of P7 *Psd-95*$^{+/-}$ *Sap-102*$^{-/-}$ Nissl-stained flattened cortices sectioned at 48μm thickness. Letters denote individual animals, numbers denote section number. Scale bar = 100μm. Sections (a1 and a2) exhibit poorly defined large barrels and very poorly visible inter-barrel septae, and most small barrels are missing (b1-4). (b1-3) exhibit slightly better defined large barrels than (b1-4) and additional smaller barrels are visible (b3-4), but all barrels are blurry and septae definition is poor.

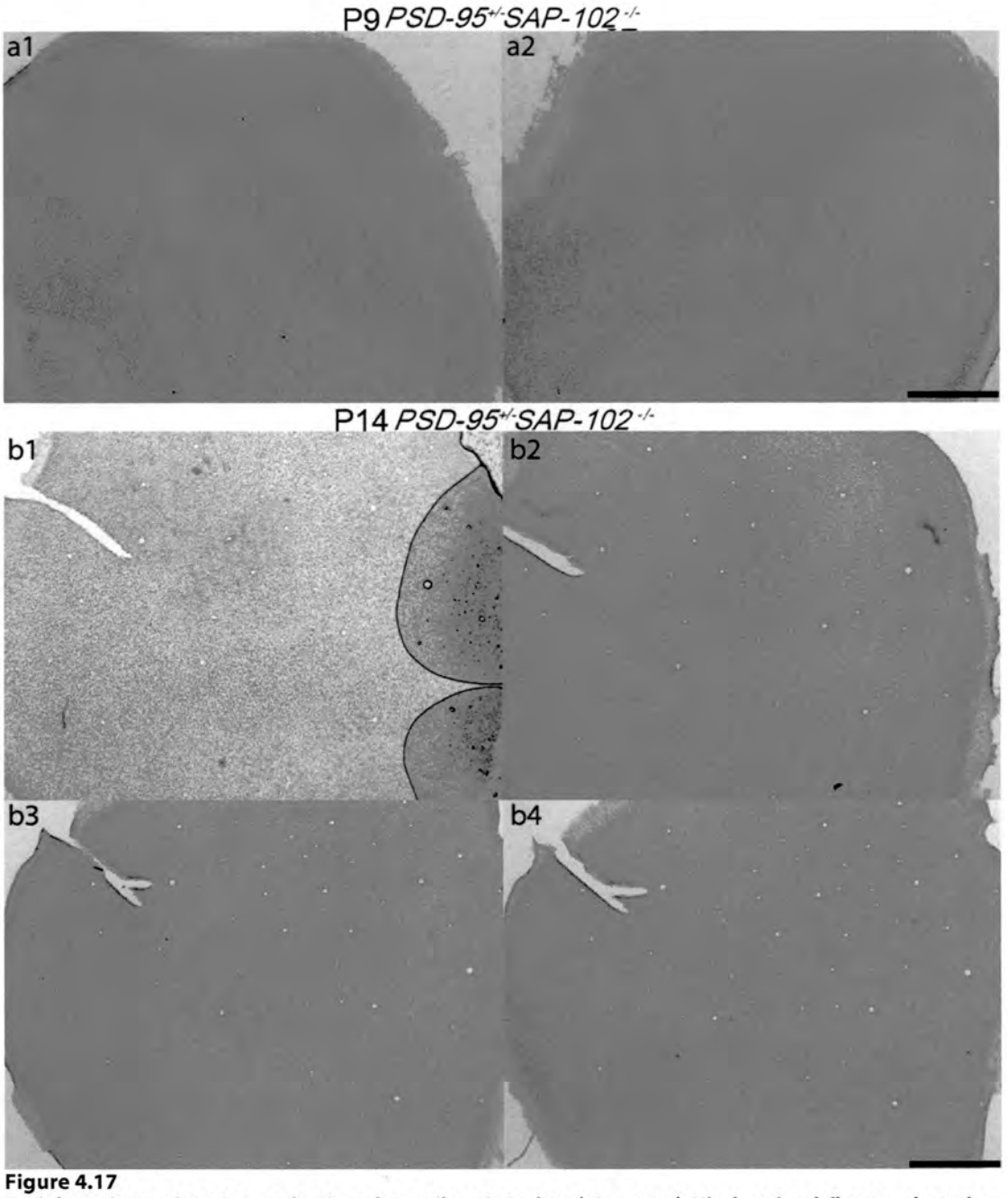

Figure 4.17
Serial sections of P9 (a1 and a2) and P14 (b1-4) *Psd-95*$^{+/-}$*Sap-102*$^{-/-}$ Nissl-stained flattened cortices sectioned at 48μm thickness. Letters correspond to individual animals, numbers denote section number. P9 sections have most of the large barrels and some of the small barrels, but barrel definition appears poor, and septae definition is extremely poor, with cell soma having segregated to a lesser extent than normal. P14 sections have most of the barrel field present, spread over sections (b1) to (b3), and the definition of both barrels and septae look better than at P9, but the large barrels in (b2) look blurred, although the septae and barrels in (b3) look fair. Scale bar = 100μm

4.3.12 *Psd-95* and *Sap-102* compound mutants

Visual assessment and ranking of barrel phenotypes (Figure 4.18) revealed that there was no significant difference in averaged ranked scores between each genotype and wild-type,

except for P7 *Psd-95*$^{+/-}$*Sap102*$^{-/-}$ mice, where average scores were significantly lower than wild-type P7 mice (mean difference=-1.688, q=12.794, p <0.001), and P14 *Psd-95*$^{+/-}$*Sap102*$^{-/-}$ mice, where average scores were significantly lower than wild-type P14 mice (mean difference=-0.8750, q=6.142, p<0.01). These mice have poorly defined barrel walls and septae compared to wild-type mice (Figure 4.15, Figure 4.16, Figure 4.17). No statistically significant differences between any of the remaining genotypes when compared to wild-type mice of corresponding ages, indicating that normal cortical segregation to form barrels has occurred in these genotypes.

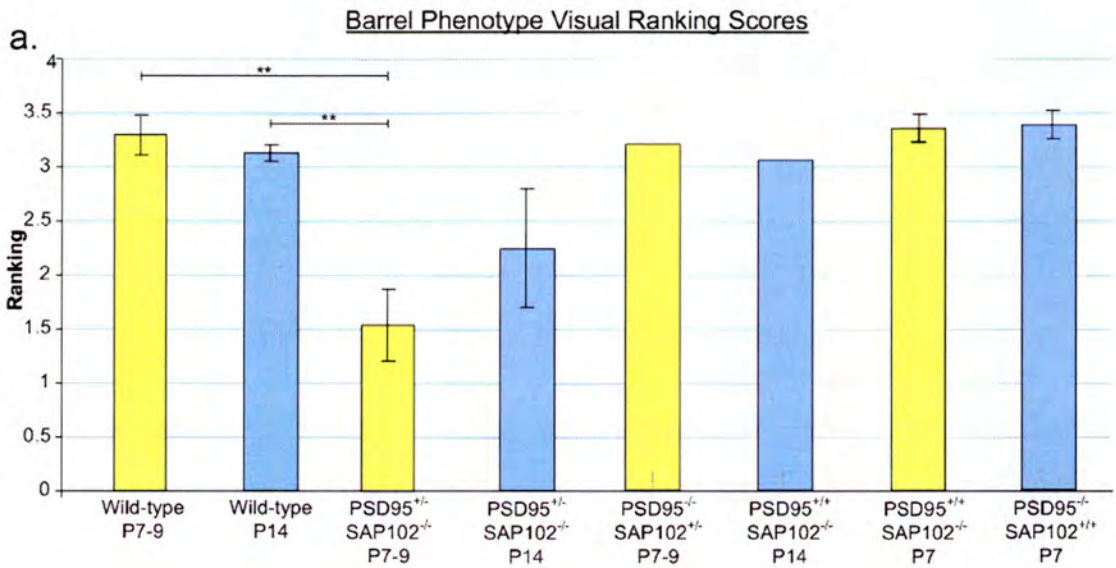

Figure 4.18
Visual ranking scores of the barrel phenotypes of various mutant mice. A. Ranking scores for wild-type and mice lacking at least one allele of *Psd-95* or *Sap-102*, at ages P7-9 and P14. P7 *Psd-95*$^{+/-}$*Sap102*$^{-/-}$ mice have a significantly lower average visual barrel ranking than P7 wild-type mice. $n \geq 3$, except for bars marked with "!", which have an n of 2, as tested by a one-way ANOVA with Student-Newman-Kuels post hoc tests. !, n=1, otherwise *** = p <0.001 ** = p <0.01.

4.4 Discussion

4.4.1 Wnt and Dishevelled mutants

The specific aim of this chapter was to determine the barrel phenotype of all available *Wnt* and *Dvl* knockout mice. We managed to obtain P7 brains from all *Wnt* knockout mice that live to this age, and were able to examine the barrel phenotype of P7 *Dvl1*$^{-/-}$ and *Wnt7a*$^{-/-}$ *Dvl1*$^{-/-}$ mice in addition to *Wnt2b*$^{-/-}$, *Wnt7a*$^{-/-}$ and *Wnt8b*$^{-/-}$ mice.

It was unfortunate that no defects in barrel formation were observed in any of the *Wnt*, *Dvl* and *Wnt7a*$^{-/-}$*Dvl1*$^{-/-}$ mutants. If a defect had been observed, this would have provided strong evidence that *Wnts* are involved in barrel formation. Since many *Wnt* genes and all *Frizzleds* are expressed during barrel formation (Chapter 3) and many different Wnts can stimulate the same Frizzled receptor (Takada et al., 2005) then there are numerous alternative Wnts that can signal through the same (or an alternative) Frizzled receptor to compensate for the loss of one *Wnt* gene. The *Dishevelled* knockouts might have been expected to have a barrel defect since virtually all Frizzled signalling is mediated through Dishevelled (Boutros and Mlodzik, 1999; Miller, 2002; Takada et al., 2005). Since Dvl is thought to be involved in almost all Wnt signalling pathways, and Wnt signalling is crucial for some of the most essential embryonic development events (reviewed in the Introduction section), the fact that *Dvl1*$^{-/-}$ mice survive to adulthood is surprising. *Dvl1*$^{-/-}$ mice exhibit only relatively minor neurological and neuroanatomical phenotypes, such as abnormalities in sensorimotor gating, social interaction disorders (Lijam et al., 1997) and reduced dendritic arborisation in the hippocampus (Rosso et al., 2005). This suggests that extensive compensation by other *Dvl* genes is occurring, especially during embryonic development. Three Dishevelled genes are present in the mouse genome (Beier et al., 1992; Tsang et al., 1996; Greco et al., 1996) and genetic knockout of any individual *Dishevelled* could potentially be compensated for by increased expression of either or both of the other two *Dvl* genes. The double knockout of *Wnt7a*$^{-/-}$*Dvl1*$^{-/-}$ might have revealed a barrel phenotype. If Wnt7a signalling through Dvl1 was involved in barrel formation, the loss of *Wnt7a* could be compensated by expression other Wnts that signal through Dvl1, the additional loss of *Dvl1* would end this compensatory signalling. However, *Wnt7a*$^{-/-}$*Dvl1*$^{-/-}$ mice have normal barrels. It seems that although many *Wnts*, *Frizzleds* and *sFRPs* are expressed in barrel cortex during barrel formation and maturation (Chapter 3), their knockout is either entirely compensated for by other Wnts (and in the case of *Wnt7a*$^{-/-}$*Dvl1*$^{-/-}$ mice, other *Dishevelleds*) or completely unrelated to barrel formation.

After the experiments described in this chapter were concluded, a study using a modified Golgi-Cox impregnation performed on cortical flat sections was completed (Upton et al., 2006). This method (Izzo et al., 1987; Upton et al., 2006) stains barrel hollows in addition to normal Golgi staining. It was discovered that layer IV cell dendrites orient normally towards the plexus of TCA terminals in the *Plc-β*$_1^{-/-}$ mice, despite dramatically reduced cellular segregation. This study demonstrated that the previous belief that dendritic orientation contributes to the cellular segregation that underlies formation of the barrel structure

(Datwani et al., 2002b) is not the case, and therefore examination of Nissl stained cortical flats is therefore uninformative regarding dendritic shape.

As it is now known that the two processes of cellular segregation into barrels, and dendritic reorientation of cortical cell dendrites towards segregated TCA patch plexus are genetically separable, it is possible that the dendrites in the *Wnt*, *Dvl* and *Wnt7a*$^{-/-}$*Dvl1*$^{-/-}$ mutant mice examined above may have defects in selective dendritic orientation, despite still having normally segregated TCAs and barrels in layer IV of the cortex, and as such dendritic analysis as performed in the Upton et al., (in preparation) paper would be the next step in characterising barrels in these mutants.

Finally, the cortical flat dissection used in the experiments presented above involved the removal of all cortical tension points, enabling sections to be flattened with minimum distortion of the barrel structure. However, all anatomical landmarks were also lost in this dissection, which meant that identifying the location of the barrel field in the anterior-posterior and medial-lateral planes were impossible. FGF8 appears to specify cortical areas and early guidance of TCAs, as ectopic electroporation of FGF8 at E11.5 into the anterior cortical primordium causes a duplication of the barrel field. Since *Wnts* are expressed alongside FGF family molecules in developing embryonic cortex (Shimamura and Rubenstein, 1997; Grove et al., 1998; Bachler and Neubuser, 2001) and have to potential to regulate FGF signalling (Wilson et al., 2001), it is entirely possible that they might have an effect on cortical area specification, TCA guidance and the ultimate location of barrels. A cortical flat dissection that includes landmarks would therefore be required to assess this aspect of barrel development.

4.4.2 *Sap-102* and *Psd-95* mutants

Psd-95GK$^{-/-}$ and *Sap-102*$^{-/-}$ mice have normal barrels, TCA patterning and cortical lamination. *Psd-95*$^{+/-}$*Sap-102*$^{-/-}$ and *Psd-95*$^{-/-}$*Sap-102*$^{+/-}$ mice have normal TCA patterning and cortical lamination. *Psd-95*$^{-/-}$*Sap-102*$^{+/-}$ mice have normal barrels and a normal mGluR5 expression in layer IV cortex which matches the periodicity of barrels. *Psd-95*$^{+/-}$*Sap-102*$^{-/-}$ exhibit poorly defined barrel walls and septae, and mGluR5 expression in cortex appears to be homogenously expressed in layer IV cortex, suggesting a deficit in dendrite orientation.

SAP-102 is the predominant NRC scaffold protein present in the barrel cortex during barrel formation, whilst PSD-95 expression relatively very low during this period compared to adult levels. Since the NMDAR and many NRC components are crucial for barrel formation (Abdel-Majid et al., 1998; Iwasato et al., 2000; Hannan et al., 2001; Watson et al., 2005), SAP-102 binds a different subset of NRC components to PSD-95 (Appendix A and B), SAP-102 couples preferentially to NR2B NMDAR subunits (Muller et al., 1996), and SAP-102 is the primary MAGUK present at NMDAR synapses at early postnatal ages when NR2B-containing NMDARs are most prevalent (Shi et al., 1997; Sans et al., 2000; Yoshii et al., 2003; van Zundert et al., 2004) and also at the time of barrel formation (Barnett et al., 2006a), it has been hypothesised that temporal expression of MAGUKs effects changes in trafficking and synaptic localization of NR2A-rich and NR2B-rich NMDAR (van Zundert et al., 2004). *Sap-102*$^{-/-}$ mice had a strong possibility of an altered barrel phenotype, as the lack of SAP-102 could disrupt the amount of NR2B-containing synapses in barrels, altering NMDAR channel kinetics, and altering the signal transduction machinery that would normally be present to respond to NMDAR-dependent Ca^{2+} influx..

Since PSD-95 is also present during barrel formation, albeit in lower amounts than adult, it was possible that the loss of this gene would lead to an altered barrel phenotype. However, *Psd-95*$^{-/-}$ and *Sap-102*$^{-/-}$ mice have normal barrels (Figure 4.12 and Figure 4.13). Since both MAGUKs have the same number and types of functional domains (Figure 4.2) the most likely explanation is that compensatory upregulation of *Sap-102* occurs in *Psd-95*$^{-/-}$ mice and upregulation of *Psd-95* in *Sap-102*$^{-/-}$ mice. Alternatively, the presence of normal barrels may indicate that *Psd-95* and *Sap-102* are not necessary for barrel formation.

Sap-102$^{+/-}$*Psd-95*$^{-/-}$ mice have normal barrels (Figure 4.15), yet *Sap-102*$^{-/-}$*Psd-95*$^{+/-}$ exhibit defects in cortical cell segregation, with less well defined barrel walls and septae, although TCA segregation and cortical lamination are normal (Figure 4.14, Figure 4.15, Figure 4.16, Figure 4.17). Possible reasons for the normal barrel phenotype observed in the single knockouts of *Psd-95* or *Sap-102* are that although PSD-95 and SAP-102 have preferences for particular NR2 subunits and certain NRC components, they can still bind many of the NRC components that the other would normally do (Appendix A, Appendix B). Additionally, the number and composition of synaptic NMDARs can be modulated by several factors, including interaction with MAGUKs (reviewed in Wenthold et al., 2003). Finally, the loss of *Psd-95* or *Sap-102* could cause a compensatory upregulation of the appropriate NR2- subunit that preferentially binds the remaining MAGUK, which can function sufficiently for normal barrel formation.

Since *Sap-102*$^{+/-}$*Psd-95*$^{-/-}$ mice have normal barrels, yet *Sap-102*$^{-/-}$*Psd-95*$^{+/-}$ mutants do not, this suggests that SAP-102 is more important for barrel formation than *Psd-95*. In other words, one functioning allele of *Psd-95* is not sufficient to compensate for the total loss of *Sap-102*, but one working allele of *Sap-102* is sufficient to compensate for the loss of *Psd-95*. This result reaffirms the role of glutamate signalling through NMDAR and the NRC in normal barrel formation.

4.5 Further Work

4.5.1 Further characterisation of *Sap-102* and *Psd-95* mutants

The dendrite phenotypes in these mutants have yet to be investigated. Since the *Sap-102*$^{-/-}$ *Psd-95*$^{+/-}$ mice exhibit a deficit in cortical cell segregation into barrel walls, these mice would be good candidates to have an altered dendritic phenotype. However, *Plc-β*$_1$$^{-/-}$ mice lack barrels, yet have segregated TCAs. Recent studies have shown that cortical cell dendritic orientation towards the TCA plexus still occurs in these mice (Upton et al., 2006). Since *Sap-102*$^{-/-}$*Psd-95*$^{+/-}$ mice have segregated TCAs, they might also exhibit "normal" dendritic orientation towards the TCA terminals.

The Mouse Hepatitis Virus (MHV) outbreak in our animal facility massively hindered the examination of the compound mutants of *Psd-95* and *Sap-102*; the colonies were just beginning to produce these mutants of *Sap-102* and *Psd-95*, when MHV was detected and all colonies had to be culled. All mice harvested before the MHV outbreak of the genotypes *Sap-102*$^{-/-}$*Psd-95*$^{+/-}$ and *Sap-102*$^{+/-}$*Psd-95*$^{-/-}$ are presented in this chapter. The *Sap-102* and *Psd-95* mutant colonies are still undergoing rederivation and once re-established, further characterisation of these mutants, such as counting the ratio of cells in the barrel wall to barrel hollow, performing barrel cortex dissections that retain brain landmarks and the Golgi method employed in the Upton *et al.* (in preparation) paper mentioned above are logical next steps for further investigation of the barrel defects observed in *Sap-102*$^{-/-}$*Psd-95*$^{+/-}$ mice.

4.5.2 *Wnt* and *Dvl* mutants

Examination of cortical cell dendrites in the *Wnt* and *Dvl* knockouts may yet still reveal a phenotype of abnormal dendritic structure in barrels since Wnts and their signalling molecules can effect cytoskeletal shape change. Upton *et al.* (in preparation) demonstrated that cortical cell migration and selective dendrite elaboration towards the TCA plexus are independent processes, so it is entirely possible that *Wnt* and *Dvl* knockouts can have an altered dendrite phenotype, yet still have properly segregated TCAs and normal cortical cell segregation into barrels, and the most appropriate method to further investigate dendrite shape is to perform the rapid Golgi staining method employed in Upton et al., (in preparation) on cortical flat sections from these mutant mice. Since many of the *Wnt* genes that are expressed in barrel cortex, when genetically knocked out in mice do not survive to an age where barrels can be examined, conditional mutants that restrict the knockout of Wnt genes to the cortex (such as the cortex-specific *NR1* mutant described in the Iwasato *et al.* (2000) paper) are required to investigate the roles of these genes in barrel formation. Based on the results of Chapter 3, the top candidate *Wnt* genes for further investigation in this manner include *Wnts 7b*, *3*, and *9a*. One caveat of the *CxNr1*$^{-/-}$ is apparent—the promoter used to drive *Cre-recombinase* expression, does not delete *NR1* expression in all cell types in the cortex. The *Emx1* promoter was used to drive *Cre-recombinase* expression in order to delete the floxed NR1 alleles of *CxNr1*$^{-/-}$ mice. *Emx1* is expressed exclusively in the dorsal telencephalon from embryonic stages to adulthood (Ottersen and Storm-Mathisen, 1984). *Emx1-Cre* expression causes deletion of *NR1* in cells of cerebral cortex, hippocampus and the olfactory bulbs, but spares GABA-containing interneurons that are present in the cortex (Iwasato et al., 2000) as these neurons are derived from the ganglionic eminence of the ventral telencephalon where *Emx1* gene is not expressed (Parnavelas, 2000). Furthermore, if certain embryonic-lethal *Wnt* genes are essential for the embryonic formation of the cortex, floxed *Wnts* deleted by *Emx1-Cre* may not form cerebral cortices, and therefore barrels would not be formed.

4.6 Conclusion

The main hypothesis for this thesis was that *Wnts*, *Frizzleds* and *sFRPs* are required to form barrels, and the two specific aims for this chapter were to determine the barrel phenotype of all available *Wnt* and *Dvl* knockout mice and to determine whether the major NRC scaffolding molecules SAP-102 and PSD-95 are required for barrel formation. The work performed in this chapter has only partially disproven the main hypothesis. By addressing

the first specific aim for this chapter, we have discovered that *Wnt2b*$^{-/-}$, *Wnt7a*$^{-/-}$, *Wnt8b*$^{-/-}$, *Dvl1*$^{-/-}$ and *Wnt7a*$^{-/-}$*Dvl1*$^{-/-}$ mice have normal barrels; these genes are not required for barrel formation. It remains to be seen if other *Wnt* genes are involved in barrel formation, and this work will require the generation of conditional *Wnt* mutants (discussed above). The second specific aim was addressed by characterising the barrel phenotypes of *Sap-102*$^{-/-}$, *Psd-95GK*$^{-/-}$, *Sap-102*$^{-/-}$*Psd-95*$^{+/-}$ and *Sap-102*$^{+/-}$*Psd-95*$^{-/-}$ mice. This work revealed that the loss of *Sap-102* or *Psd-95* does not affect barrel formation, but the additional deletion of one copy of *Sap-102* in a *Psd-95*$^{-/-}$ mouse causes defects in the segregation of cortical cells into barrel structures in response to properly segregated TCA input, whereas *Sap-102*$^{+/-}$*Psd-95*$^{-/-}$ have normal barrels. Thus SAP-102 is required for barrel formation when *Psd-95* is knocked out.

5 Development of the barrelgene.info database

5.1 Introduction

This chapter describes the design, development and data entry strategies employed in creating a database that intends to help barrel cortex researchers find pertinent information in the literature and genome databases. Since much of the terminology of this chapter is computing-related, a glossary of the terms used is present at the end of this chapter.

5.1.1 The abundance of information in the post-genome era

Researchers in today's laboratories are fortunate enough to have abundance of information available to them. For one working within the mouse barrel cortex neurodevelopment community, information starting with databases of the mouse genome map and sequence are available, through mRNA transcripts and splice variants, to protein sequence, structure, modification and interactions. The knowledge from such data is now starting be applied to humans, where many of the genes studied in cortical plasticity have become relevant to the pathologies of learning impairment in children, dementias, schizophrenias and brain injury.

Databases exist for genes knocked out or modified in mice, gene expression profiles, most notably the Jackson Laboratories' (Jax) Mouse Genome Informatics (MGI). (http://www.informatics.jax.org). On top of that is the existing literature— there are currently at least 20,000 refereed journals across all fields of scholarship, publishing more than two million refereed articles each year (http://www.nature.com/nature/debates/e-access/Articles/harnad.html). Out of all the biology journals that could potentially publish a relevant paper, six-hundred and twenty-six such journals currently exist (http://directory.google.com/Top/Science/Biology/Publications/Journals/). A massive amount of information is present in the literature, and there are tools to query this, of which the most popular are PubMed (www.pubmed.gov), Web of Knowledge (http://wok.mimas.ac.uk), the services within BIDS (http://www.bids.ac.uk) and Google Scholar (http://scholar.google.com). Apart from the latter search engine, the information within these services is restricted to the information in the abstract and keywords, and extracting relevant information can sometimes need carefully structured queries of the databases. Google Scholar also searches the content of available papers (including those in Adobe Acrobat Portable Document Format (PDF) format) and certainly has a far more familiar and easy-to-use query interface, but it does produce a disarmingly large number of false-positive hits for each query

submitted. This is often in contrast with the narrow speciality of a researcher's field. If the question is asked "has anyone performed an *in situ* hybridisation in mouse of NMDA receptor subunit NR1, at P7, in layer IV somatosensory cortex", for example, it may take a considerable amount of time mining the databases to determine whether anyone has performed and published this experiment.

5.1.2 Data mining using current web-based academic text search engines

5.1.2.1 Jackson Laboratories MGI

If a researcher wished to investigate the literature for *NR1* expression patterns, an excellent place to start would be Jax MGI. By first searching for *NR1* (called *Grin1* in MGI) then reading the Expression profile section of that gene, it would be possible to narrow down the query to Theiler Stage 28 (postnatal week 6-8) and structure: cerebral cortex. However, the only technique in the database is RT-PCR, and message was detected by this method.

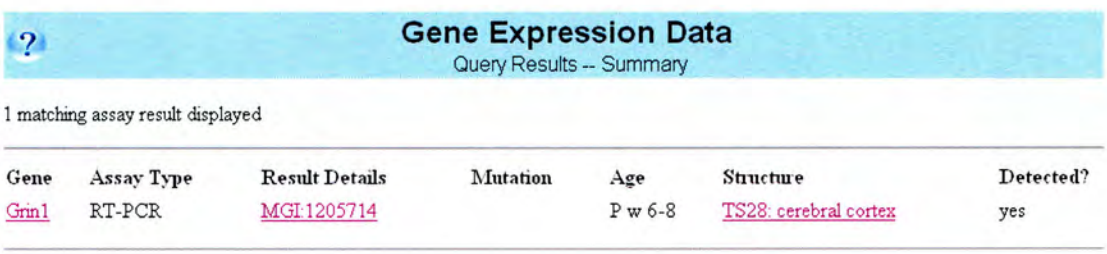

Gene Expression Data

Query Results -- Summary

1 matching assay result displayed

Gene	Assay Type	Result Details	Mutation	Age	Structure	Detected?
Grin1	RT-PCR	MGI:1205714		P w 6-8	TS28: cerebral cortex	yes

Figure 5.1
Result of querying Jax MGI for Gene Expression Data for the NR1 subunit of the NMDA receptor. The only entry in the database for NR1 gene expression in cerebral cortex is RT-PCRs performed between postnatal weeks 6 to 8.

Although the database does offer the chance to view the image of gel and the primers used, it is unlikely that *in situ* hybridisation has never been performed for NR1, nor that RT-PCRs have not been performed at other ages, and information is likely to be missing from this database. Thus far, the only gene or protein entered in Jax MGI that is present in cerebral cortex, layer IV is *Apc2*, Figure 5.2.

Anatomical Dictionary Browser

Term Detail

Structure **cerebral cortex layer;layer IV** (View within the full anatomical hierarchy.)

TS 28
- organ system
  - nervous system
    - central nervous system
      - brain
        - forebrain
          - telencephalon
            - cerebral cortex
              - cerebral cortex layer
                - layer I
                - layer II
                - layer III
                - layer IV (1 gene expression results - show all or refine search)
                - layer V
                - layer VI

Gene Expression Data

Query Results -- Summary

1 matching assay result displayed

Gene	Assay Type	Result Details	Mutation	Age	Structure	Detected?
Apc2	RNA in situ	MGI:3043016		P adult	TS28: cerebral cortex layer; layer IV	yes

Figure 5.2
Querying Jax MGI by anatomical structure. The only postnatal gene expression profile entered in Jax MGI for layer IV cerebral cortex is an *in situ* hybridisation for *Apc2*.

Nevertheless, the database has been well designed and there is the capacity to add such information at a later date.

5.1.2.2 NCBI PubMed

A major method to find information within the academic literature is to search abstracts and keywords held in PubMed, hosted by the National Center for Biotechnology Information (NCBI). A well structured PubMed query might be:

```
(grin1 OR nr1) AND (layer IV cortex OR barrel OR somatosensory) AND mouse
```

This yields the following results (Figure 5.3):

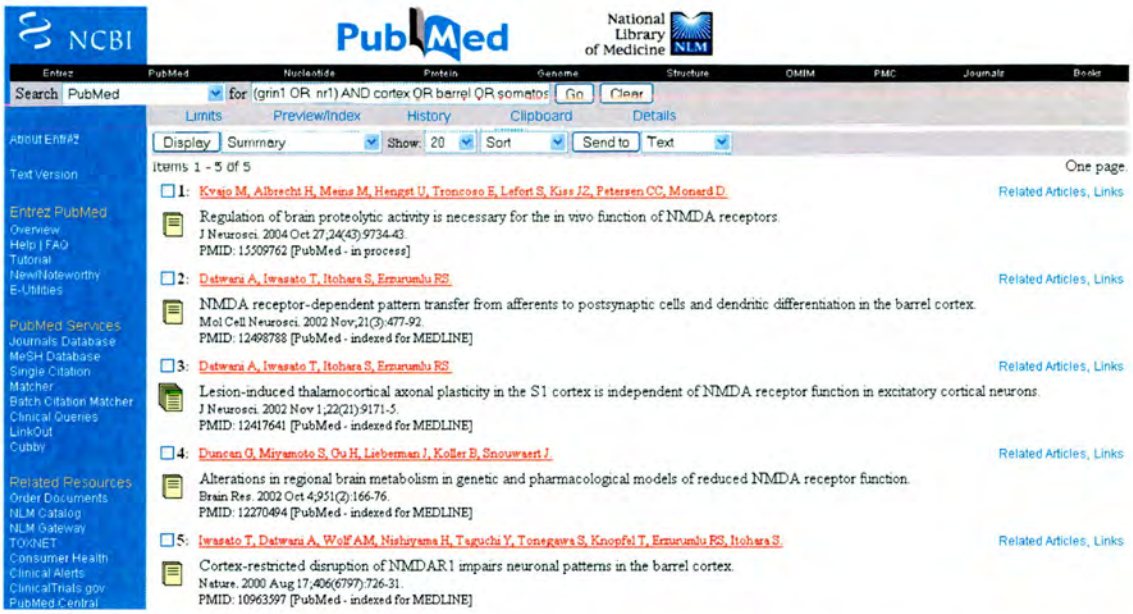

Figure 5.3
PubMed search results for a nested query of NR1 in mouse somatosensory cortex, using synonyms of each term to maximise query results, but still restricted to this brain region.

However, perhaps there are papers in the literature that show the data in layer IV in a figure that is not mentioned in the keywords or abstract. Relaxing the search terms by reducing the number keywords used to restrict the search to the following:

```
(grin1 OR nr1) AND mouse
```

will produce an extra thirty-five papers (Figure 5.4). This is time consuming to obtain and read the papers, but done in the spirit of "three weeks of labwork can save an hour in the library", if the experiment in question had been published, the researcher will be spared the time organising and preparing animals, reagents and performing the experiment.

Figure 5.4
PubMed search results for a nested query of NR1 in all of mouse cortex. The extra papers now included in results will show expression patterns in cortex. These may include regions of somatosensory cortex, but these extra papers did not have "somatosensory cortex" included in the abstract and keywords. Since these papers might have the information required, they are worthy of examination, and the broader search term is required.

5.1.2.3 Google Scholar

If PubMed did not present results that contain papers with the NR1 expression pattern, the researcher might then try Google Scholar (Figure 5.5), although searching through the full text of 229 hits resulting from this query would be very time-consuming.

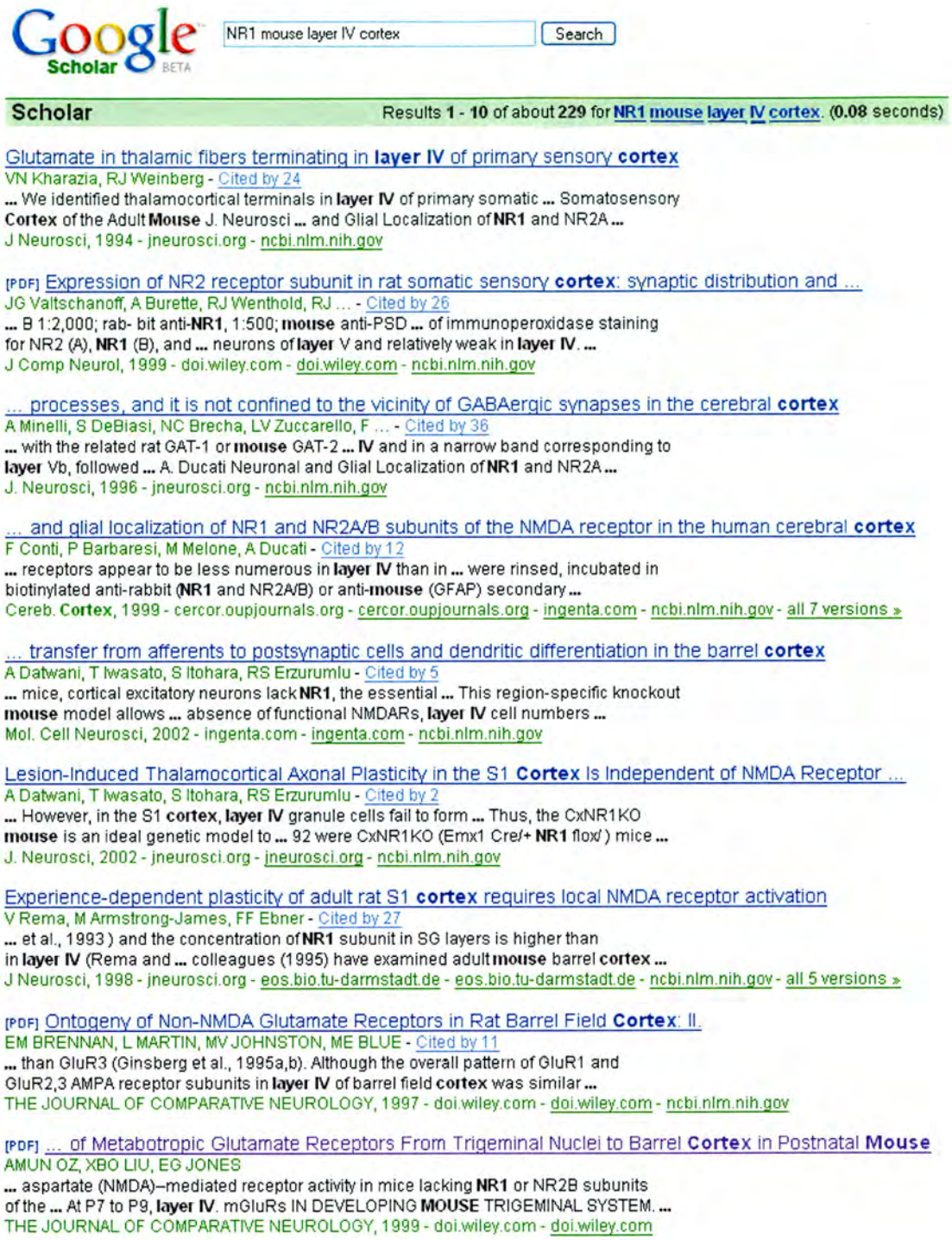

Figure 5.5
Google Scholar search for NR1 in mouse layer IV cortex. Google Scholar searches the entirety of the text in every paper available to it. Consequently more results are generated, although a large proportion are irrelevant, because if the search terms appear in one of the references, a hit is still generated.

5.1.3 Data Mining: an example

If we assume the researcher decides to perform a NR1 *in situ* hybridisation at P7 and could not find a suitable probe in the literature. A good place to start is Jax MGI's database Molecular Reagents listings (Figure 5.6).

Molecular Probes and Clones

Query Results -- Summary

45 matching items displayed

Nucleotide Probe/Clone AccID	Name	Clone Collection	Seq Type	Seq Link?	Markers	Chr
MGI:23514	Grin1 probe1		Not Specified	no	Grin1	2 (12.0 cM)
MGI:620984	IMAGE clone 1139712	IMAGE	cDNA	yes	Grin1(PUTATIVE)	2 (12.0 cM)

Figure 5.6
Jackson Labs MGI query results for NR1 (Grin1) molecular reagents, yielding two results for *in situ* hybridisation probes. As denoted by the Yes entry under Seq Link, MGI:235214 has been verified and submitted to external nucleotide sequence databases.

MGI:235214 is the only promising result, and following the link yields this (Figure 5.7):

Molecular Probes and Clones

Query Results -- Details

Nucleotide Probe/Clone: Grin1 probe1
Sequence type: Not Specified
Species of origin: Not Specified
Strain: Not Specified
Sex: Not Specified
Age: Not Specified
Tissue: Not Specified
Cell line: Not Specified
Vector type: Plasmid
Insert site: BamHI
Insert size: 3.4kb
MGI Accession ID: MGI:23514

Markers *(chromosome)*:

- Grin1 (Chr 2)

References:

J:22833 Pilz A, Genomics 1995 Jan 1;25(1):139-49

Endonuclease	Marker	Allele	Fragments	Strains
TaqI	Grin1	a	6.0,5.2,2.8kb	AN
		s	6.0,4.0,3.0kb	M. spretus

J:38089 Pilz A, Mouse Genome 1996;94(4):877-9

Endonuclease	Marker	Allele	Fragments	Strains
TaqI	Grin1	b	6.0, 5.2, 2.8kb	C57BL/6J
		s	6.0, 4.0, 3.0kb	M. spretus

Figure 5.7
Molecular reagents for NR1 (Grin1): Jax MGI has information listing the cDNA sequence used to generate probe and references to the original papers, insert size, and insert site.

If the researcher wishes to create a new probe from scratch. Jax MGI offers transcript and protein sequence information; the RefSeq link takes the researcher to the sequence (Figure 5.8).

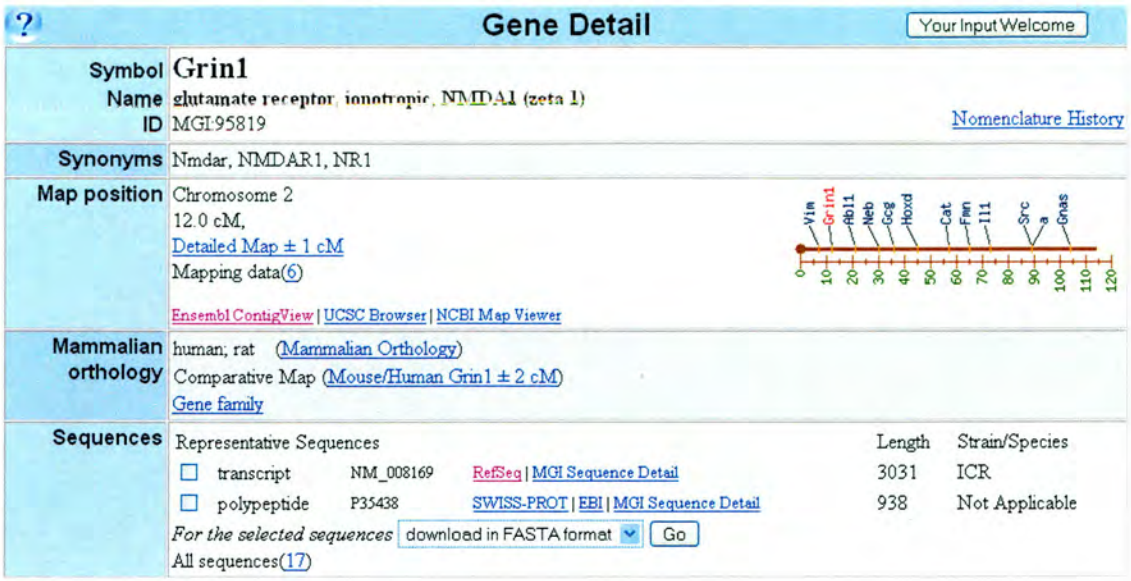

Figure 5.8
Jax MGI Gene Detail view showing links to external gene and protein sequence databases.

Immediately below "Sequences" in the Gene Detail page for *Grin1* is "Phenotypes" (Figure 5.9).

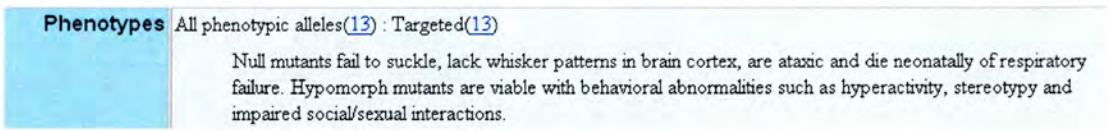

Figure 5.9
Jax MGI Gene Detail Phenotypes section, containing links to pages containing information on all published knockout mice and a short description of the phenotypes of these genetic knockouts.

The information contained within the "phenotypic alleles" section ("targeted" refers to the fact that the mouse knockout was made by recombinant techniques and not a spontaneously occurring mutation) describes how each knockout mouse was made. One mutant mouse is present that is known to have a barrel phenotype, the cortex-specific NR1 NMDAR subunit knockout mouse. Figure 5.10 shows *Grin1*^{tm2Stl} is the floxed NR1 mutant made by Susumu Tonegawa, and was bred with the (cortex-specific) *Emx1-cre* mice (*Emx1*$^{tm1(Cre)Rik}$) mouse and characterised in Iwasato *et al.*, 2000. The database does include information on a barrel phenotype:

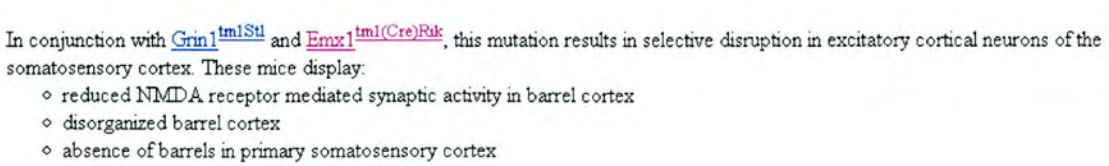

Figure 5.10
Jax MGI Gene Detail Phenotypes for *Emx1*$^{tm1(Cre)Rik-/-}$ mice, and description of barrel phenotype.

However, there is no information on what methods were used to characterise the barrel phenotype, and the reference (J64064) is buried amongst all the others pertaining to the Grin1^{tm2Stl} knockout (Figure 5.11):

References:

J:37456, McHugh TJ, Blum KI, Tsien JZ, Tonegawa S, Wilson MA, Impaired hippocampal representation of space in CA1-specific NMDAR1 knockout mice [see comments], Cell 1996 Dec 27;87(7):1339-49

J:37457, Tsien JZ, Huerta PT, Tonegawa S, The essential role of hippocampal CA1 NMDA receptor-dependent synaptic plasticity in spatial memory [see comments], Cell 1996 Dec 27;87(7):1327-38

J:41316, Tonegawa S, Tsien JZ, McHugh TJ, Huerta P, Blum KI, Wilson MA, Hippocampal CA1-region-restricted knockout of NMDAR1 gene disrupts synaptic plasticity, place fields, and spatial learning., Cold Spring Harb Symp Quant Biol 1996;61():225-38

J:60730, Rampon C, Tang YP, Goodhouse J, Shimizu E, Kyin M, Tsien JZ, Enrichment induces structural changes and recovery from nonspatial memory deficits in CA1 NMDAR1-knockout mice [see comments], Nat Neurosci 2000 Mar;3(3):238-44

J:60770, Huerta PT, Sun LD, Wilson MA, Tonegawa S, Formation of temporal memory requires NMDA receptors within CA1 pyramidal neurons., Neuron 2000 Feb;25(2):473-80

J:64064, Iwasato T, Datwani A, Wolf AM, Nishiyama H, Taguchi Y, Tonegawa S, Knopfel T, Erzurumlu RS, Itohara S, Cortex-restricted disruption of NMDAR1 impairs neuronal patterns in the barrel cortex., Nature 2000 Aug 17;406(6797):726-31

J:68059, Rondi-Reig L, Libbey M, Eichenbaum H, Tonegawa S, CA1-specific N-methyl-D-aspartate receptor knockout mice are deficient in solving a nonspatial transverse patterning task., Proc Natl Acad Sci U S A 2001 Mar 13;98(6):3543-8

J:77659, Shimizu E, Tang YP, Rampon C, Tsien JZ, NMDA receptor-dependent synaptic reinforcement as a crucial process for memory consolidation., Science 2000 Nov 10;290(5494):1170-4

J:77718, Nakazawa K, Quirk MC, Chitwood RA, Watanabe M, Yeckel MF, Sun LD, Kato A, Carr CA, Johnston D, Wilson MA, Tonegawa S, Requirement for hippocampal CA3 NMDA receptors in associative memory recall., Science 2002 Jul 12;297(5579):211-8

J:80900, Datwani A, Iwasato T, Itohara S, Erzurumlu RS, NMDA Receptor-Dependent Pattern Transfer from Afferents to Postsynaptic Cells and Dendritic Differentiation in the Barrel Cortex., Mol Cell Neurosci 2002 Nov;21(3):477-92

J:83403, Fukaya M, Kato A, Lovett C, Tonegawa S, Watanabe M, Retention of NMDA receptor NR2 subunits in the lumen of endoplasmic reticulum in targeted NR1 knockout mice., Proc Natl Acad Sci U S A 2003 Apr 15;100(8):4855-60

J:84354, South SM, Kohno T, Kaspar BK, Hegarty D, Vissel B, Drake CT, Ohata M, Jenab S, Sailer AW, Malkmus S, Masuyama T, Horner P, Bogulavsky J, Gage FH, Yaksh TL, Woolf CJ, Heinemann SF, Inturrisi CE, A conditional deletion of the NR1 subunit of the NMDA receptor in adult spinal cord dorsal horn reduces NMDA currents and injury-induced pain., J Neurosci 2003 Jun 15;23(12):5031-40

J:88689, Cui Z, Wang H, Tan Y, Zaia KA, Zhang S, Tsien JZ, Inducible and reversible NR1 knockout reveals crucial role of the NMDA receptor in preserving remote memories in the brain., Neuron 2004 Mar 4;41(5):781-93

Figure 5.11
Jax MGI Gene Detail Phenotypes reference lists for NR1 (Grin1) knockout mice. References are listed in ascending chronological order.

Of course, these tools are designed with the entire biology community in mind and are vastly ambitious projects to undertake, and it is equally evident just how important and useful these tools are, especially if the knowledge obtained from the genome are to be realised. For example, the current build of Ensembl's *Mus Musculus* database (http://www.ensembl.org/Mus_musculus/), the European Bioinformatics Institute (EBI)'s mouse genome sequence server, predicts 28,055 genes. Full annotation and exploration of the literature of that number of genes (many of them only existing as a sequence produced by the mouse genome consortium) is a heroic task that will take decades to complete.

Nevertheless, a database designed for a relatively smaller group of researchers, containing genes of potential interest to the barrel community and those interested in that subset of markers, could contain the sequence, gene expression and knockout characterisation

information needed to be truly useful to the barrel community. We believe there is a need for this tool.

5.1.4 Information to be incorporated into database

In order to create a useful database, the tasks a researcher in the barrel cortex field would want to perform in the lab were considered, and how the database would facilitate this, in terms of experimental design and implementation. For molecular biology, a researcher would need easily accessible sequence information and links to the databases that would allow them to explore it in more detail. For each gene, the researcher might want links to the Ensembl *Mus Musculus* database, allowing browsing of intron/exon boundaries of the gene of interest in designing intron-spanning primers for RT-PCR; a link to Online Mendelian Inheritance in Man (OMIM) database for an explanation of gene function, interaction and the history of its discovery; and a query of the Jax MGI suite for up-to-date sequence information on the gene, if a knockout mouse exists, and if any published molecular reagents exist.

In terms of knockouts, it is often highly useful in interpreting the literature to have reference to what type of barrel defect a transgenic mouse has, the techniques used to ascertain this, the background strain of the mouse, and links to papers in which these observations were published. It is important to know these details, as barrel phenotypes can vary by background strain of mouse. Barrel phenotypes need to be ascertained by methods that can determine TCA segregation (serotonin, 5-HTT immunohistochemistry or fluorescent carbocyanine dye labelling using, for example (1,1'-dioctadecyl-3,3,3',3'-tetramethylindocarbocyanine perchlorate (DiI)) and the arrangement of layer IV cortical cells (by staining for cell makers using Cresyl Violet staining for Nissl substance or Cytochrome Oxidase). Previously it was assumed that the two process of forming barrels, segregation of TCAs and cortical cells was one process, and therefore only one of the aforementioned techniques were routinely used to ascertain the barrel phenotype. Since it was shown that the two processes in barrel formation are genetically distinct (Iwasato et al., 2000; Hannan et al., 2001) it is important to know the techniques used for mutant barrel phenotype characterisation as papers that omit one technique cannot demonstrate the true phenotype.

Jax MGI is capable of displaying that information in the database, but in most cases the information is not present and, in some cases it is wrong— one example, according to MGI is that NR2B knockout mice have no barrels in S1 Cortex: `http://www.informatics.jax.org/javawi2/servlet/WIFetch?page=alleleDet`

ail&key=3024. Since these mice exhibit perinatal lethality, and barrels form at P4, whether or not NR2B is necessary for barrel formation cannot be assessed.

Since the expression profiles of Jax MGI are not complete or discrete enough for the barrel community, a database of expression profiles, over age, categorised by technique, with links to the relevant papers would also be a powerful tool for understanding the literature and planning experiments.

5.1.5 Databases linked to from within Barrelgene.info

OMIM: Online Mendelian Inheritance in Man— Information most genes, providing useful synopses of gene discovery, function and its role in disease.

Jax MGI: Jackson Laboratories Mouse Genome Informatics Suite— Continually updated links to genomic DNA sequences and mRNA splicing information contained in Ensembl, cDNA and RNA sequence information contained in NCBI Genbank and Unigene and protein sequence information contained in EMBLs Swissprot.

PPID: Protein-Protein Interaction Database— A database created by Prof. Seth Grant and Dr. Holger Husi, containing protein-protein interaction for members of the NRC.

5.2 Planning Barrelgene.info

5.2.1 Databases

Databases are just a collection of information stored a computer in a systematic way, such that a computer program can consult it (query) to answer questions. The software used to manage and query a database is known as a database management system (DBMS). A glossary of these terms can be found at the end of the chapter.

The data is organized into files called tables. These tables provide a systematic way of accessing, managing, and updating data. There are two forms of database, flat file and relational. Flat file databases are easy to create and use; they consist of a single table of data, for example, like a list of genotyping results, listed by animal numbers that have been typed

into a spreadsheet like Microsoft Excel. However, flat file databases are inflexible, cannot handle large amounts of information, and are prone to problems in data entry and querying. In essence, they are not scaleable. For example, BGI was initially designed in this way (Figure 5.11), and soon became an inflexible behemoth of a database. The basic unit of the data in the database was the gene; the flat file format meant that everything associated with the gene had to be on the same row as the gene name. If anything had to be changed, it had to be done manually; a time consuming process. To overcome this problem, the database was redesigned from scratch as a relational database (Figure 5.12).

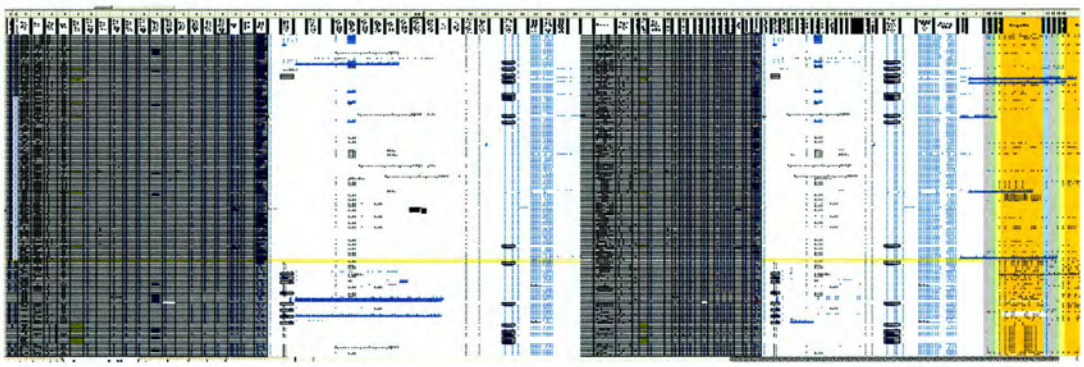

Figure 5.12
The original version of BGI, as designed as a flat-file database. Large, complex, repetitive, inflexible and unwieldy.

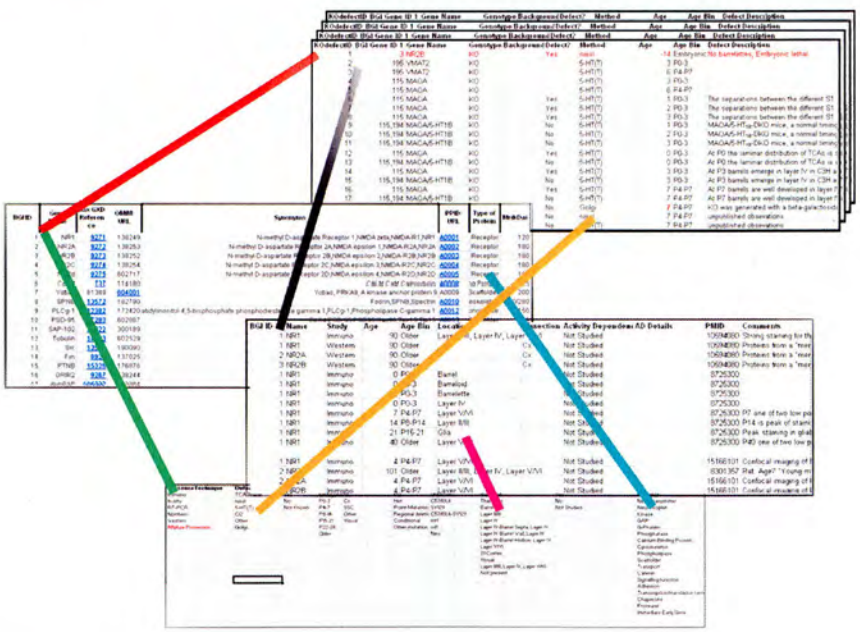

Figure 5.13
A relational database. Data is indexed by different keys. These keys can form links to the keys of any other data in the database.

Relational databases contain multiple tables of data that relate to each other through special key fields—a number or text string that allows the DBMS to keep track of which data relates

to what. Relational databases are far more flexible (though harder to design and maintain) than flat file databases.

Rather than having all of the information associated with one gene in one row of data in a spreadsheet, if each group of information has its own table, and the information in that table is identified with a unique key, then only these identifying keys need to be associated with the genes (Figure 5.14). If any of that information needs to be updated; only the table that requires alteration has to be changed. Furthermore, relational databases can extract more out of the data that it contains. In a flat-file database, querying for a gene would produce lots of data, of which can be sorted and restricted to show the information required. However, if the database was to be further developed, and a query such as "show me all of the genes associated with this paper" were required, a flat file database could not perform this. A relational database could, as it can follow the links back from the paper to the gene and give a result. Furthermore, the flexibility that a relational database allows means that adding extra features involves adding an extra table, and referencing it correctly (Begg and Connolly, 2005).

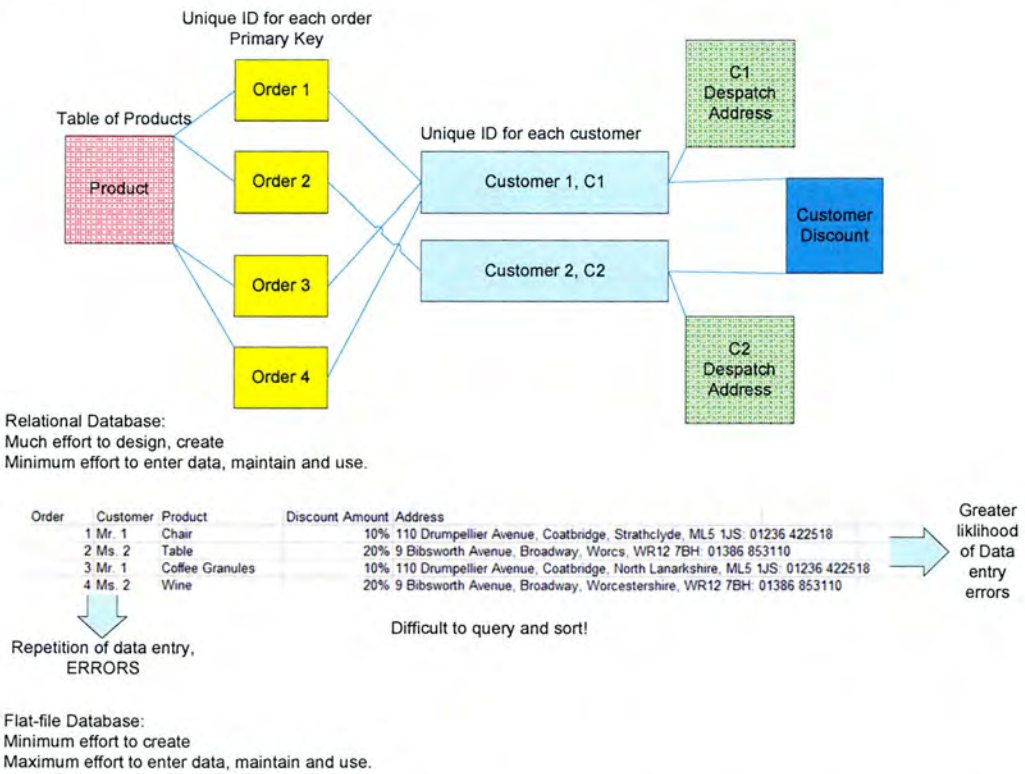

Figure 5.14
Simplified example of the differences between relational and flat-file databases, based on a company handling orders for products, and a fuller explanation of the above relational database is present in the Glossary section (below). In essence, by having multiple tables of information, and storing the links between information as new tables, no data is duplicated, and data storage and retrieval is most efficient. Flat file spreadsheets rapidly contain repeated data, are inefficient at storage and errors in data entry will corrupt any searches made.

5.2.2 Running the Website

5.2.2.1 Hosting

Since barrelgene.info is to be a free-to-use, publicly available web-accessible database, website hosting was needed. BGI could be hosted with a commercially run company, at the cost of £20 to £50 per month depending on the amount of network traffic, or it could be hosted on a computer—our webserver—running within the University, which would have no such bandwidth costs, only the cost of the machine. The most popular software to run webservers and databases, Apache, MySQL and PHP are actually free-to-use as part of an Open-Source community project (http://www.apple.com/opensource/). Open source software is free to use, modify and distribute, and a community of programmers spend their free time continually developing, fixing and improving this software, all unpaid. Although commercial alternatives exist and come with professional support, the database can effectively be hosted at no cost after the initial expenditure on a computer.

5.2.2.2 Webserver

The BGI webserver is a Apple iMac G3, running Mac OS X 10.3.9, generously donated by Prof. Jonathan Bard. Mac OS X is in essence an attractive graphical front end built on top of the foundations of a FreeBSD UNIX distribution called Darwin (http://www.apple.com/macosx/features/unix/). Darwin is stable; the webserver has not crashed in the nine months since it went live, and Darwin has few of the documented security vulnerabilities of a Microsoft Windows operating system based webserver.

Figure 5.15
The BGI webserver. An Apple iMac G3 233Mhz, running Max OSX 10.3.9, Apache Webserver v1.33, PHP 5.0 and MySQL 5.0.

5.2.2.3 Apache HTTP Server

Apache is a HyperText Transport Protocol (HTTP) Server (Fielding and Kaiser, 1997); it is built into Darwin, and allows a website to be presented to the world. It handles requests for the HyperText Markup Language (HTML) code of webpages and returns (serves) the appropriate page if present, using HTTP. Other modules can be added into Apache, such as PHP (see below) to extend its functionality beyond serving webpages and images, dynamically generating web content, see Figure 5.16.

5.2.2.4 PHP

PHP is a popular open-source programming language and is particularly useful for server-side applications and dynamic web content (http://www.php.net). The name is a recursive acronym for "PHP: Hypertext Preprocessor". PHP, like Apache is open source software, and can be incorporated into the Apache server service to allow tasks involved in running the database to be performed on the server, whilst all a user of the database needs is a web browser and an internet connection to perform a search.

The problem with HTML code is that it is entirely static—the content does not change unless manually altered. It would be almost impossible to create a usable database from HTML code alone. In developing this database, PHP performs two main tasks: performing data retrieval/ manipulation, and providing the link between the web page and the database tables.

For a simple example of a server-side script, when Apache reads a HTML page and comes across some PHP, as denoted by `<?php insert code here ?>` or `<? Insert code here ?>` it performs the function that the code tells it to, and presents to Apache the result of the operation, normally text retrieved from the database, which Apache sees as plain HTML and serves this to the person browsing the website.

Assume that there is a bit of text in the database that is the web address for BGI. Previously, the web address was `http://clarke.bms.ed.ac.uk/~barrelgene`, but is now `http://barrelgene.info`.

With HTML, you would need to change the code in any hyperlinks to BGI manually:

```
Here is the link to <a href="http://www.example.com/nr2a-mRNA.html"
target="_blank">NR2A mouse mRNA sequence</a>
```

to

```
Here is the link to <a href="http://www.adifferentexample.com/mRNA-NR2A.html"
target="_blank"> NR2A mouse mRNA sequence</a>
```

It would be tedious to modify many links. However, if the web address of BGI was just an entry in a database, all that would need modified would be that entry. Using PHP define the entry as a variable called BGI, what would be required is:

```
Here is the link to <a href="<?=$BGI?>" target="_blank">BarrelGeneInfo</a>
```

It is possible to change the variable depending on user input—in our case, the variable could be defined as whatever the result of a database query was. While a tutorial on the programming of the database is beyond the scope of this thesis, this example illustrates how it is possible to serve dynamic data to users over the web (Figure 5.16).

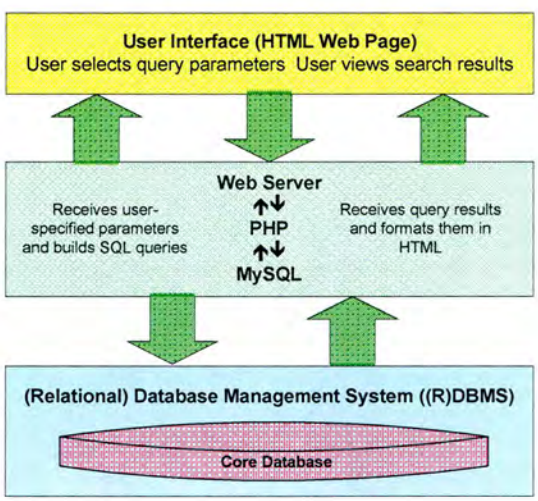

Figure 5.16
Diagram showing how the website, webserver, DBMS and database tables all interrelate and interact in the process of serving data from the core database to the user.

5.2.2.5 SQL and MySQL

Structured Query Language (SQL) is the standard computer language used to create, modify and retrieve data from relational database management systems (RDBMS). The RDBMS used for BGI is MySQL (www.mysql.com), a free-to-use system that accepts SQL commands to create, modify, delete and retrieve databases and the data therein.

SQL allows the specification of queries in a high-level, declarative manner. For example, to select rows from a database, the user need only specify (declare) the criteria that they want to search by; the details of performing the search operation efficiently is left up to the database system, and is invisible to the user. This structure allows the user/programmer to be less

familiar with the technical details of the data and how they are stored, and relatively more familiar with the information contained in the data.

Example of an SQL Query:

```
SELECT columns FROM table_name
WHERE some_condition_is_true
ORDER BY some_column
LIMIT offset, rows;
```

In our context:

```
SELECT gene_name FROM list_of_genes
WHERE protein_type = Scaffolder
ORDER BY gene_name;
```

would list all of the genes in the table `list_of_genes` that had the attribute `Scaffolder`.

This is simply a basic illustration of how the database can function. MySQL is more sophisticated and capable of far more than shown above, and again further elaboration would be beyond the scope of this thesis.

5.3 Database design

5.3.1 Fundamentals of good database design.

Databases need to be efficient and easy to maintain. This is helped greatly at the design stage where careful consideration of structuring the data tables and the relationships between data in those tables, a process termed normalisation, can save time-consuming trouble later.

The main dogma of database design is to store the least amount of data possible, yet still serve all of the information the user requires. This is best managed by eliminating duplication of data. If there is a lot of repetitive data, and one instance of that data undergoes a change (for example, a name change), then that change has to be made for all occurrences of that data. However, if a table was to be created containing all of the possible values, and a key was used to refer to that value, all that would be needed to effect the required change would be to alter the one value in the master table. The reference in all of the other tables would remain unaltered.

In order to design the database, and then perform normalisation, a database schema needs to be made. An Entity-Relationship (E-R) schema was produced allowing a graphical method of seeing how the data in the tables should interact. Methods of normalising the schema are well documented elsewhere (Begg and Connolly, 2005), but in essence, it involves looking at the data tables, and seeing if they can be made more efficient by being broken down into smaller tables and referenced by a key, just as in the example above.

Once the content and structure of BGI have been defined, the tables now need to be filled with data. The major source of errors in databases is humans mistyping information. A strategy to reduce the amount of errors by a combination of automated processes, choosing from restricted lists instead of typing, and requiring a minimum of data entry was chosen.

One of the features of BGI was a centralised resource of nucleotide and protein sequences. These are volatile—highly likely to change, be revised, deleted, and yet data entered into a database is static. It only updates when someone types in new, altered data. BGI approaches this task differently to most databases by automatically retrieving data from external sources, rather than enter all of the data manually and then have to check and update the contents regularly.

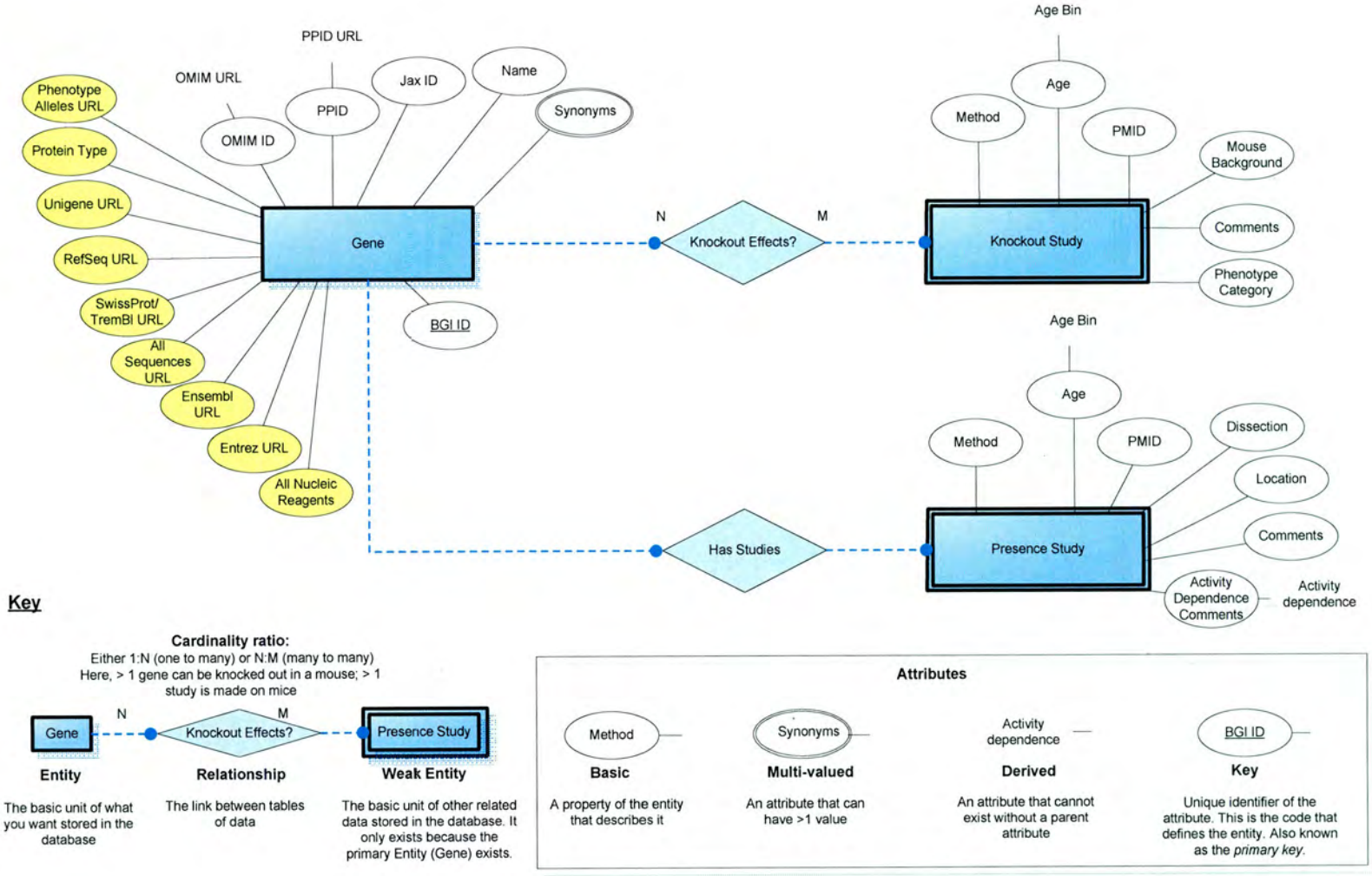

Figure 5.17
Entity-Relationship Schema of barrelgene.info showing how the queries made in the database define how the data in tables relate to each other. Refer to the Key for details of its content.

5.3.2 Database schema

In designing a relational database it is imperative that it is structured carefully from the start. Once the database is generated there is rigid structure to it and there is very limited flexibility in modifying any aspect of this. To ensure that what is produced meets the need of the users, and to allow flexibility for future requirements, it all has to be planned from the start. The most efficient way of performing this is to design a Conceptual Model with the user, outlining requirements and how the data relates to each other. A commonly used way of presenting the Conceptual Model is the Entity-Relationship (E-R) model, whereby a relatively user-friendly E-R diagram or "schema" is generated. The E-R schema for BGI is shown in Figure 5.17.

In our database the main Entities are Gene, Knockout Study and Presence Study. Much like in the primary dogma of biology, everything stems from the Primary Entity, Gene. Gene has many attributes; information associated with Gene such as a unique identifying number (BGI ID, an acronym of Barrel Gene Info Identity), sequence information, links to other databases, and its names. To help understand the concept of the database, imagine a list of all the genes along the Y-axis of a graph. All of the attributes are columns along the X-axis. In this database, there are three of these tables. The way the information in those tables link to each other is the "relationship" between the two datasets. To further complicate matters, consider the Knockout Study table (although it also applies to the Presence Study table). On top of this two dimensional table one has to imagine a third, Z-axis, for each age entered into the database, and yet another axis for each method used to study the knockout. How the database software deals with this is to generate many two-dimensional tables and link the data together appropriately.

One might query why Synonyms is not a derived attribute of Name. Firstly, the data in Name is the name the barrel community uses (as determined by the Kind lab and not necessarily the name that the wider informatics community calls the gene, e.g. *NR1* compared to *Grin1*) and is most likely to be queried by the user. Secondly, Synonyms are still attributes of the gene; they still exist independently of the Name attribute.

Once the E-R schema was designed, it was then possible to start data collection. Each Entity was given its own tab in a Microsoft Excel spreadsheet, and the columns in that sheet are the attributes specified in the E-R schema. The BGI ID is the Key Attribute; it is a unique identifier that the database will use to link it to its related data in the other tables for the other Entities.

5.4 Data Entry

5.4.1 Obtaining sequence information

The sequence information we wished to include in barrelgene.info is already available online. The Jackson Labs Mouse Genome Informatics (MGI) project provides links to the up-to-date genomic, transcript and polypeptide sequence information for any gene in its database. Should a sequence be withdrawn or updated from the available sequencing projects, Jax MGI is rapidly updated. Instead of copying and pasting, or worse, retyping sequence information already available on MGI, a PHP script was used to extract the relevant sequence information from the MGI page available for each gene in the database.

The script works by removing spaces and Javascript code from the HTML of any MGI webpage presented to it, which helps to make the code presented to the next part of the script consistent and easier to parse (Figure 5.20). It then searches for text that conforms to a certain type that always follows a given, constant phrase and syntax, extracting that text, and the URL associated with it. This data is then saved in a table associated with the gene currently being queried (so that this process need not be run again) and this is then presented via another PHP script that generates the sequence information page for that particular gene.

For example, the link on MGI's website to Ensembl's page for any gene is always after Ensembl and is always of the format `EMSMUSG+[DIGITS]`. The text, and URL for the link to this information is contained within:

```
<TD WIDTH="20%">Ensembl</TD>

<TD><HREF='http://www.ensembl.org/Mus_musculus/geneview?gene=ENSMUSG0
0000002771'>ENSMUSG00000002771</A></TD>
```

Utilisation of regular expression (regex, see Glossary) pattern matching allows the identification of the text of interest and the stripping of the extraneous code.
Running the script importjax.php (see attached CD) yields:

```
ENSMUSG00000002771
http://www.ensembl.org/Mus_musculus/geneview?gene=ENSMUSG00000002771
```

which is then stored in a table within the database. This process of pattern matching then data stripping was repeated for each sequence link of interest on MGI. Whilst optimising the script so that it runs correctly for each gene is extremely time consuming, the overall process is far speedier and less error prone than manual data entry.

The Uniform Resource Locator, (URL, web address) for the information on any gene in MGI is of the format (address stub + unique ID); in the case of NMDA receptor unit NR2D:

```
http://www.informatics.jax.org/javawi2/servlet/WIFetch?page=markerDetail&key=9275
```

Only the last four digits, the gene ID, actually change. A four-digit MGI gene ID was entered for each gene in the database (called JaxID). Whenever a gene is chosen by a user for the first time, a PHP script adds JaxID to the address stub, loads the HTML code the page generated, and strips out and stores the useful information.

Data in table:

```
9275
```

Resulting page (Figure 5.18):

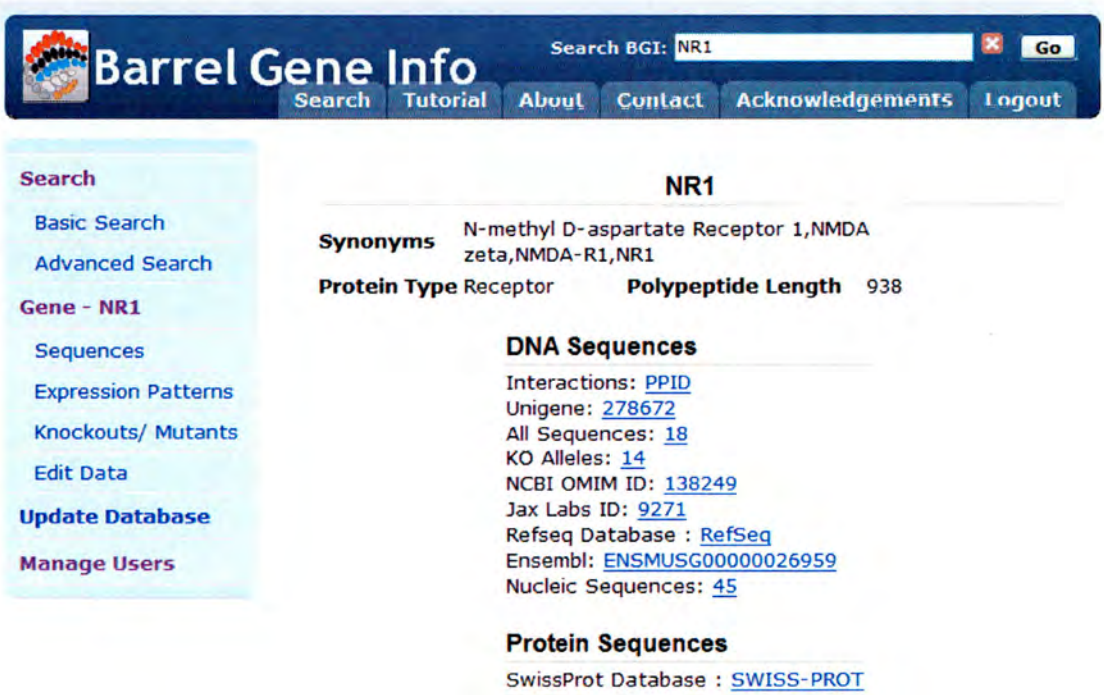

Figure 5.18
The power of PHP: Four digits are enough data to generate an entire page of up-to-date sequence database links for one gene.

5.4.2 Obtaining OMIM data and PubMed paper references.

The same (address stub + unique ID) format and information stripping principles apply to generating links to Online Mendelian Inheritance in Man (OMIM) articles and obtaining the references from paper abstract entries in Entrez PubMed. Thus, in the same manner, all that needs to be entered into the database is the unique ID, and added to the relevant stub URL, the

BGI webserver can produce background and sequence information for any gene in the database, and references for any paper referenced, so long as the reference is contained in PubMed.

For example, PubMed ID entered into spreadsheet for the paper reference `10721990` results in the reference:

```
Hall AC, Lucas FR, Salinas PC.
Axonal remodelling and synaptic differentiation in the cerebellum is
regulated by WNT-7a signaling.
Cell. 2000 Mar 3;100(5):525-35.
```

5.4.3 Restricted Lists in Microsoft Excel to reduce input error

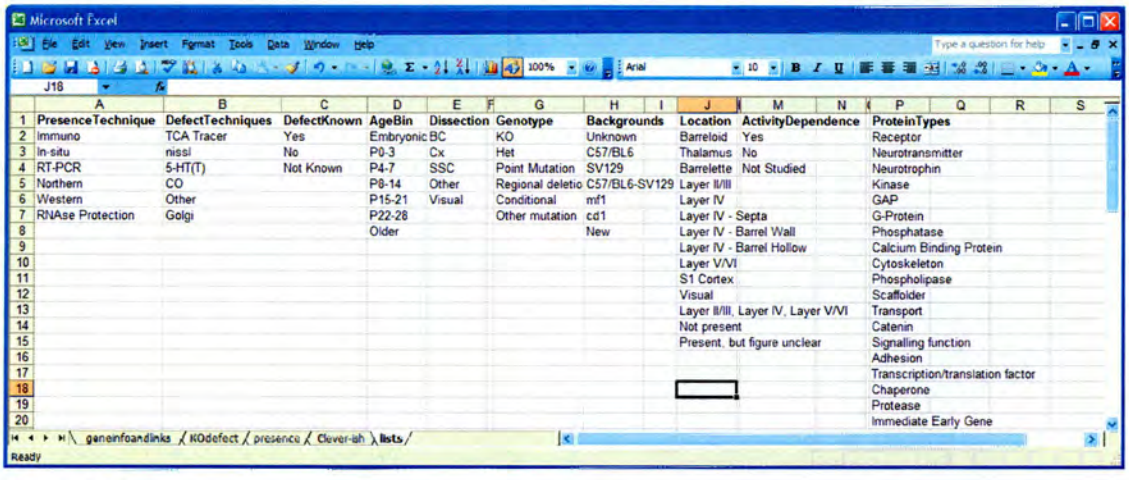

PresenceTechnique	DefectTechniques	DefectKnown	AgeBin	Dissection	Genotype	Backgrounds	Location	ActivityDependence	ProteinTypes
Immuno	TCA Tracer	Yes	Embryonic	BC	KO	Unknown	Barreloid	Yes	Receptor
In-situ	nissl	No	P0-3	Cx	Het	C57/BL6	Thalamus	No	Neurotransmitter
RT-PCR	5-HT(T)	Not Known	P4-7	SSC	Point Mutation	SV129	Barrelette	Not Studied	Neurotrophin
Northern	CO		P8-14	Other	Regional deletio	C57/BL6-SV129	Layer II/III		Kinase
Western	Other		P15-21	Visual	Conditional	mf1	Layer IV		GAP
RNAse Protection	Golgi		P22-28		Other mutation	cd1	Layer IV - Septa		G-Protein
			Older			New	Layer IV - Barrel Wall		Phosphatase
							Layer IV - Barrel Hollow		Calcium Binding Protein
							Layer V/VI		Cytoskeleton
							S1 Cortex		Phospholipase
							Visual		Scaffolder
							Layer II/III, Layer IV, Layer V/VI		Transport
							Not present		Catenin
							Present, but figure unclear		Signalling function
									Adhesion
									Transcription/translation factor
									Chaperone
									Protease
									Immediate Early Gene

Figure 5.19
Lists that restrict what users can enter into cells in Microsoft Excel spreadsheets. When entering data, all that the user can input into the Excel spreadsheet is values restricted to those contained in the appropriate table in this part of the Excel document.

One problem in databases is that they are unforgiving of typographical errors. One example is this: a paper showing an *in situ* hybridisation of a gene, called for example, NR2A. If in the location column someone types "Layer IV" (with a space between Layer and IV), and for another gene, e.g. NR2B types "LayerIV" (with no space), and for NR2C, types "Layer 4" (using Arabic, as opposed to Roman numerals), the database would treat all three versions as different, and a query for all genes expressed in "Layer IV" would miss NR2B and NR2C. However, if the location was restricted to a pre-defined list, then this would be avoided. Furthermore, if others are allowed to enter data into the database, it avoids text like "a bit of layer II and some of layer III" being entered. MySQL absolutely requires predefinition of what will go into each table, from the type of data (numbers, letters, strings, a mixture of letters and numbers, verbose text, and so on). Entry of verbose text in a field that should not contain that will break the database—all subsequent entries will be ignored after this error and to any user and the data might as well not exist. This underlines the importance of proper

training for anyone that might perform data entry for BGI, and the same restriction on user input was used wherever possible, see Figure 5.19. In addition, restricted lists avoids problems with different spellings in U.S. and U.K. English.

Age bins are automatically generated within Microsoft Excel using nested `=IF...THEN` statements, however MySQL ignores this and generates age bins from the numbers entered into BGI. The reason for this is that some papers in the literature do not specify the age of mice other than "Adult", so to denote this, an age of 101 days is entered into Excel, and when age 101 is retrieved from MySQL, part of a PHP script converts that age to "Adult", and displays it appropriately. The age bins in Excel function only as visual reassurance that the data is being entered correctly.

Figure 5.20
Raw HTML without formatting or images. This is how the webpage is presented to PHP, whereupon it searches for certain patterns of text, in this context sequence information links, and strips them out into a new table.

The source of the information is acknowledged within barrelgene.info; this information is in the public domain, a link to the original source page is provided, and as the information, once obtained, is stored locally on the BGI web server, the financial cost of internet traffic load on MGI is reduced, and users of BGI are presented with the relevant information sooner, in a central resource.

5.4.4 Automated Insertion of Data into the Database

The information in the database is entered into Microsoft Excel. The information is exported in comma separated format (CSV), and uploaded to the webserver. In order to convert a list of text and numbers into a format that MySQL can handle, a PHP script, `install.php` issues SQL insert commands for each part of data, inserting it into the correct table, as defined previously when the database was created. Unfortunately, this is practically a rigid structure, so adding another column in Excel between the columns that contain data will break the database. Data will end up in the wrong tables, unless the import PHP script is altered to take account of the changes in the resulting PHP, or the extra column is removed. This underscores the importance of careful planning and initial design of the database, and also proper training in data entry before allowing individual users to manipulate critical components of the database. Regular backups of the database must also be made, so that roll-backs to an earlier, problem-free version are relatively easy to do.

5.5 Web page design

BGI needed to be not only easy to use, but also powerful enough to search the data by useful criteria, such as by age, location, or if the molecule has an effect on barrel formation if knocked out or mutated.

In order to design a simple, attractive and easy to query database, design cues were taken from popular websites and applications (Figure 5.21). The most popular search website, Google (http://www.google.com), is simple-to-use, yet extremely effective in use at presenting relevant search results to the user. BGI's simple search was designed to mimic this. However, in terms of limiting the results down to a category (e.g. all expression profiles at P0-P3, of scaffolding molecules) there were two ways of performing this: searching within search results, or a more advanced query with pull-down menus restricting what is being searched. The latter method was chosen, as it is similar to the methods deployed in PubMed and certain BIDS website searching interfaces, and as such, is familiar to people in the scientific field. Furthermore, it avoids users having to perform two queries.

Figure 5.21
User interface cues taken from Google, PubMed, iTunes and Mozilla Thunderbird.
Simple search was inspired by Google, the Advanced Search was inspired by PubMed, and the clear box used in the search field is commonly used to clear searched, as seen in iTunes and Thunderbird.

In order to produce a website that is viewable on any device that can browse the web, that looks attractive on a personal computer, yet is still functional on a mobile phone, and is compatible with devices that permit disabled users to use the web, a basic text website was generated, and Cascading Style Sheets (CSS) were utilised to superimpose an attractive design. CSS works by instructing the browser to substitute HTML tags, or anything defined within the HTML as to be modified, with an alternative text, graphic, or indeed, code such as Javascript or PHP, that is specified within the CSS code. Mobile phones and text-to-speech interfaces can ignore the images and pretty graphics specified by CSS, yet still be able to use BGI (Figure 5.22).

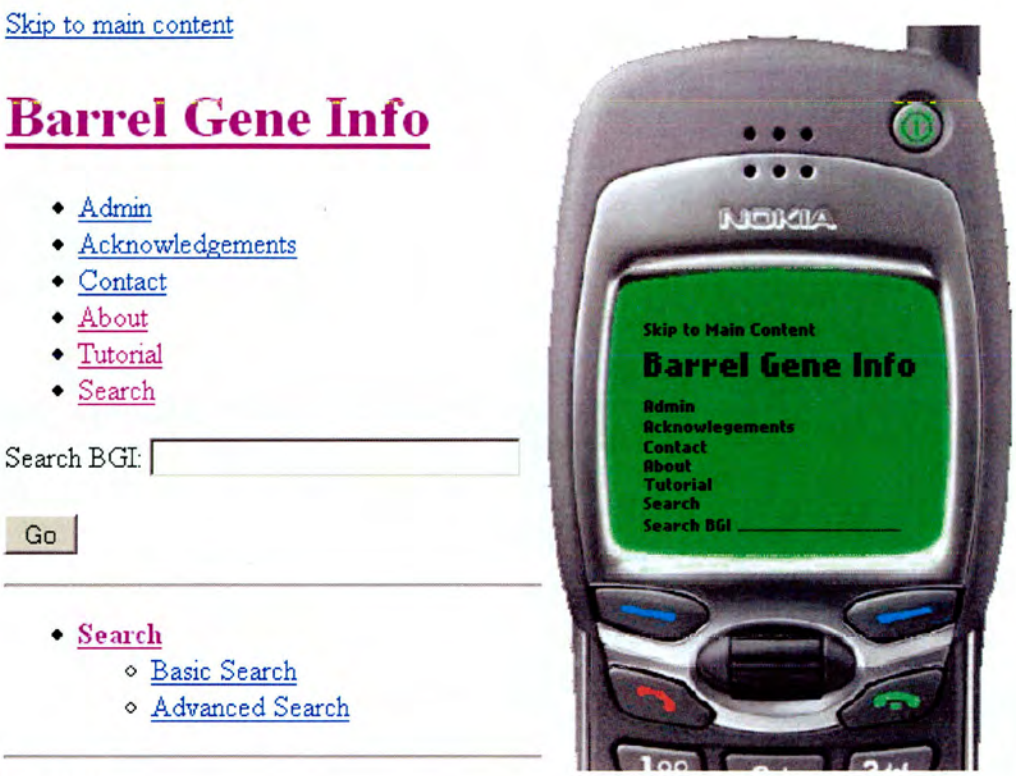

Figure 5.22
Left: BGI running without Cascading Style Sheets. This is the interface that text-to-speech interfaces for the visually impaired will use, and also how lower specification mobile phones will view the website (right).

One nicety that is currently popular is a clear text button that appears to the right of the text box whenever text is entered (Figure 5.23), as present in applications such as Mozilla Thunderbird or Firefox, or Apple's iTunes program (Figure 5.21). Another is the miniature search bar at the top of every page (Figure 5.23). Users can initiate a new simple search from any part of the website.

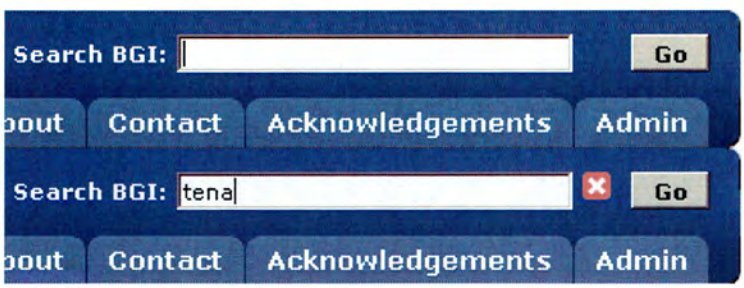

Figure 5.23
Search clear button in text entry fields. As text is entered, a red button appears to clear the text.

5.6 Tutorial

5.6.1 Basic Search

In Basic search, typing in a gene name searches against the text held within the gene name and gene synonyms categories. As all of the synonyms contain more than one word, searching

for " " (one press of the spacebar) would list every gene in the database. Searching for "NR" would yield first the NMDA NR-subunits, as they are called "NR1, NR2" etc., in the gene name category, as that take precedence over names containing NR in the gene synonyms category.

Figure 5.24
Basic Search interface. Text entered in this box is searched against all gene names and gene synonyms, and results listed by their BGI ID number.

5.6.1.1 Advanced Search

In Advanced Search (Figure 5.25) typing in a gene name limits the results in the same manner as Basic search, but the pull down lists further restrict the results to those that match the item selected from the pull down list. Leaving the Name blank, but searching for all Protein Type: Receptors would result in all of the receptors present in BGI to be presented. Inserting NMDA into the name box and querying again would then yield only receptors with NMDA in the title; this would include NR1, NR2 etc, as in their gene synonyms category, their full title would contain the phrase NMDA, in this case "N-Methyl-D-Aspartate (NMDA) Receptor subunit 1" would generate the hit.

5.6.1.2 Search Results

Clicking on the name or the green and white arrow button (Figure 5.25) takes the user to the sequence information page. The menu column to the left allows the user to navigate between this page, Knockouts/ Mutant information, Expression patterns, Basic Search or Advanced Search.

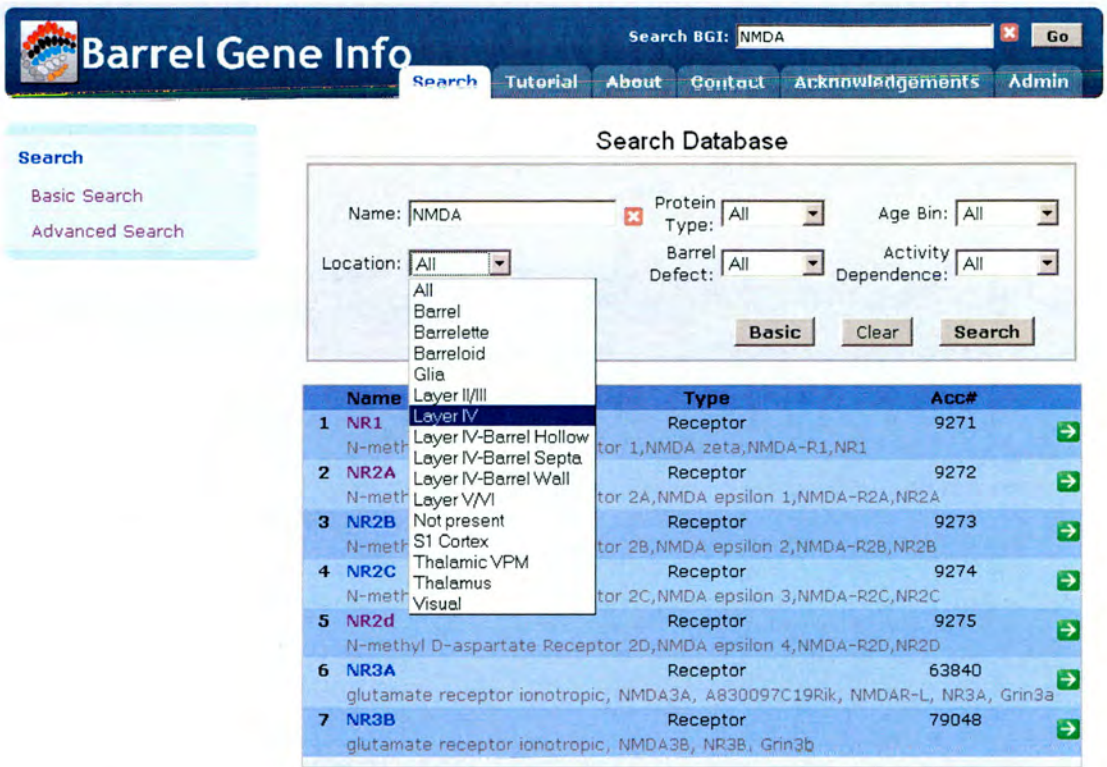

Figure 5.25
Advanced Search Interface showing pull down list-boxes to restrict search parameters.
Users are able to refine searches by Location, Age Bin, Protein Type, Barrel Defect and Activity Dependence of the gene. Clicking on the gene name, synonyms or the green arrow takes the user to the information for that gene.

Choosing either expression patterns or Mutant information generates two tables; one of technique used to study by age, and another of signal location by age (Figure 5.26). The numbers within the table represent the number of unique papers in that category. Clicking on that number displays the Title, authors and reference of that paper, and clicking on that or the green and white arrow icon will bring up the PubMed abstract of that paper. If the article is available online to the user's institution, then PubMed will display a link taking the user to that site.

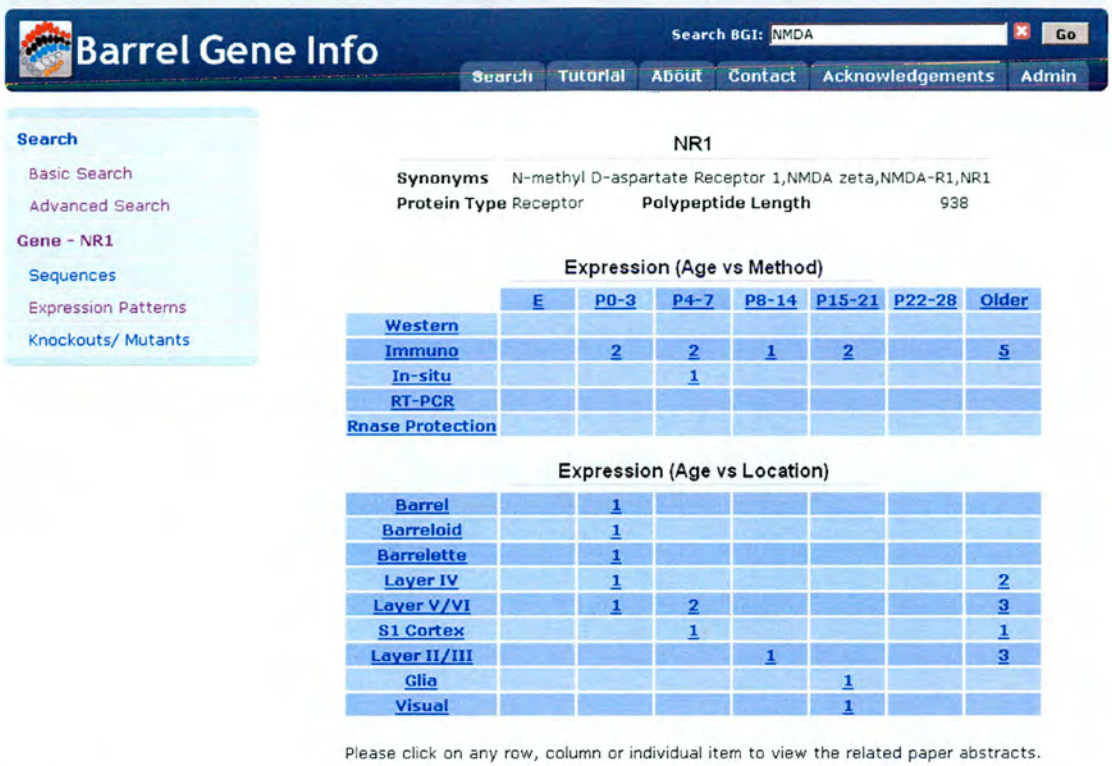

Figure 5.26
Results: Expression Patterns. The database lists the number of papers associated with each age bin by Method in the top table, and location, in the lower table.

5.7 Administration

One can administrate the database (Figure 5.27 and Figure 5.28). The current version of the database is stored on the server, and a backup (of both data and site) is mirrored on two other machines and saved to media. In order to update the database, a username and password is needed to access the administration area of the website. Once the Admin tab has been clicked on the top right hand side of the webpage, and the Administrator has logged in, then the user is presented with links to the three CSV files in the database; `mutants.csv`, `expression.csv` and `geneinfo.csv`. One can download these, alter and add to them, save them with the same filename, and upload them again, using the admin tools on that page.

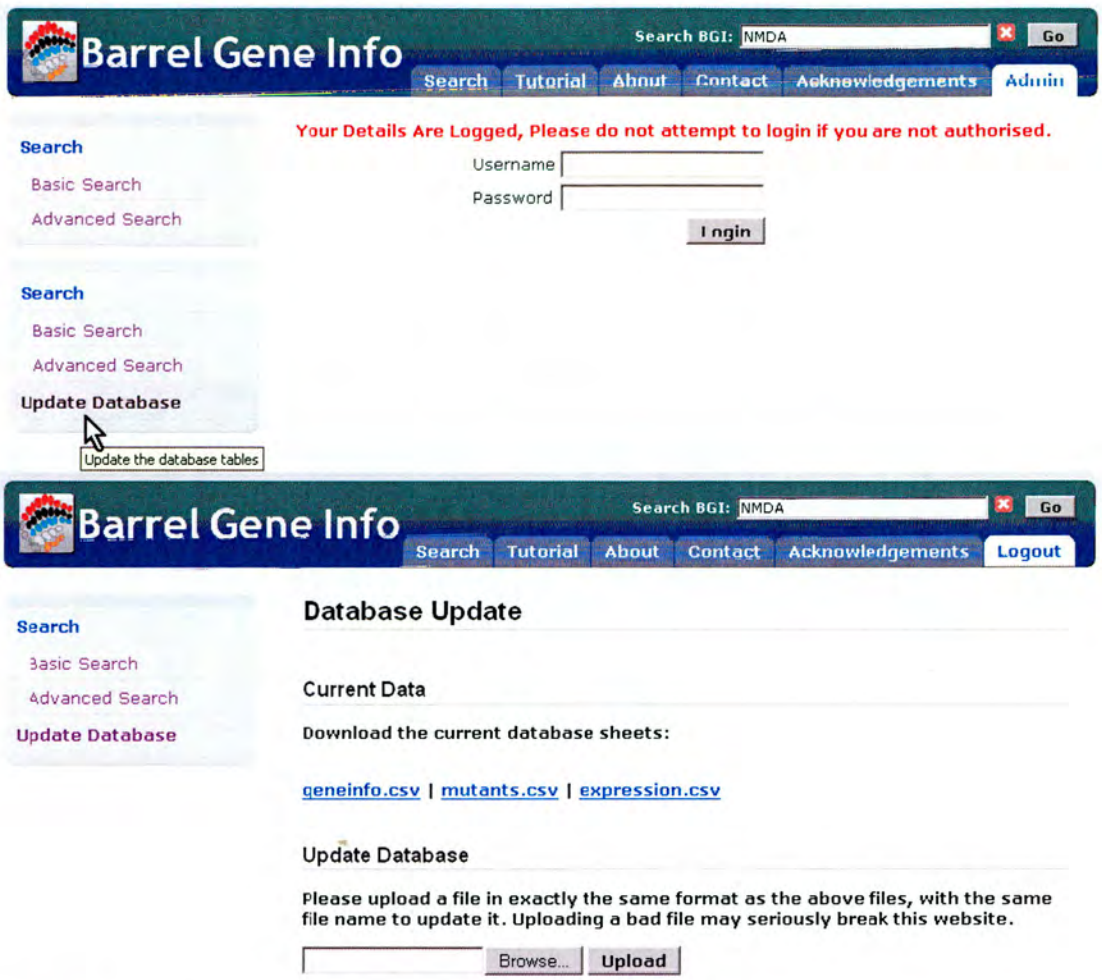

Figure 5.27
Administrator login enables the uploading and downloading of the database tables, allowing the database to be updated, and the server version to be viewed from any location with a web browser.

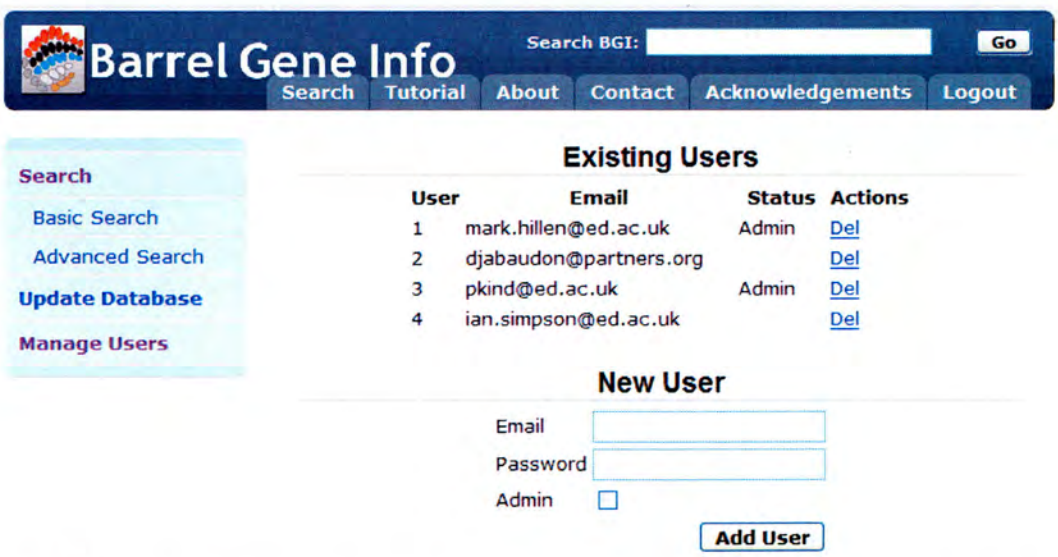

Figure 5.28
Administration login required to update data and manage users. This enables tracking of who uses the database, and forms the basis of a system to charge non-academic users in the future, if required.

5.8 Future directions

5.8.1 Collaboration

The time required to enter papers into BGI, whilst minimised by design, is still immense. Other laboratories are interested in participating in what has been received as a generally useful resource for the barrel cortex community. The more data contained in the database, and the more up-to-date it is, then the more use it can be to researchers. This database has been presented at the Society for Neuroscience 2005 meeting and has generated a large amount of support from the barrel community; from aid in data entry to support for grant applications to further this project.

5.8.2 Expansion

Although nominally restricted to NRC components, BGI has incorporated some other genes of interest that are not members of this complex. Furthermore, BGI was designed so that adding other regions of the brain, in our case most likely the first candidate would be visual cortex, is a matter of adding more regions to a list.

Increasing the number of genes it contains would increase the usefulness of this resource, however, but the cost of expansion would be increased staffing commitment for data mining and entry.

5.8.3 Improvement

Currently, if data entry has to be performed by more than one person, it has to be coordinated carefully, and I, as administrator, check for errors, duplication and problems, before committing any changes to the data that goes on the webserver.

Microsoft Excel 2003 has excellent collaborative functions to allow people from around the world to work on the same file, at the same time, and make changes, track them and publish them. However, this does require all collaborators to invest in the latest commercial software, to be trained in its correct usage, and to work together closely. This is not always easily done. Either the administrator keeps track of all changes, or a suitable web-based collaborative tool needs to be made, something along the lines of Mediawiki (http://www.mediawiki.org/wiki/MediaWiki) whereby any user with an account can edit the database, but all changes are tracked and easily undone.

5.8.4 Data mining

Data mining, also known as knowledge-discovery in databases (KDD), is the practice of automatically searching large stores of data for patterns. To do this, data mining uses computational techniques from statistics and pattern recognition.
Data mining has been defined as "the nontrivial extraction of implicit, previously unknown, and potentially useful information from data" (Frawley et al., 1992) and "the science of extracting useful information from large data sets or databases" (Hand et al., 2001). Although it is usually used in relation to analysis of data, data mining, like artificial intelligence, is an umbrella term and is used with varied meaning in a wide range of contexts.

Within the field of neuronal plasticity, a properly developed set of pattern recognition algorithms, could automatically mine the literature and generate a database such as BGI without human input. Furthermore, this technology has the potential to mine the literature, dissect signalling pathways, and form new ones, or draw links between them that are currently unknown. Humans cannot possibly know the entire literature, but a powerful computer could have access to most of it. The European Bioinformatics Institute (EBI) in Hinxton, Cambridge is at an advanced stage of development of such technology (http://www.ebi.ac.uk/Rebholz-srv/whatizit/help.jsp). The *caveat* here is that the literature available to a computer is only that that is available online. As with many students today, if the paper is not available online, or the abstract on PubMed does not mention something in the paper that may be of interest, it does not exist to them. Without journals returning to older articles, digitising them and republishing them as e-journal articles, knowledge from the past, pre-1996 Adobe Acrobat era will effectively be invisible. However, many journals are now beginning to do this, the most prominent being the journal of the Proceedings of the National Academy of Sciences (PNAS) and Nature magazine. Whilst PNAS are in the process of making all of their archives freely available, Nature are not, and are charging institutions that have already bought the paper copies of the articles for the electronic versions. It seems that any academic institution wishing to pursue KDD that includes older articles will require to purchase licences for such content.

5.9 Conclusion

Barrelgene.info has the potential to create a great impact in not only the field of barrel cortex development and NRC research, but also the wider fields of synaptic plasticity. It is simple to use, provides information for those who are interested in the molecular biology behind barrel formation, links to information elsewhere for information regarding any gene present in the database, and is easily expandable to incorporate more molecules and brain areas. Furthermore, it provides an important avenue to publish the barrel phenotypes of mutant mice—even if there is no phenotype, this is important to know to avoid duplication of work.

5.10 Glossary

Webserver

A computer responsible for serving web pages, mostly HTML documents, via the HTTP protocol to clients, which are web browsers such as Internet Explorer, Safari, Netscape and Firefox.

HTML

In computing, HyperText Markup Language (HTML) is a markup language—text, with extra information about the text, such as formatting, designed for the creation of web pages and other information viewable in a browser. HTML is used to structure information— denoting certain text as headings, paragraphs, lists and so on— and can be used to define the semantics of a document.

PHP

PHP is a popular open-source programming language and is particularly useful for server-side applications and dynamic web content (http://www.php.net). The name is a recursive acronym for "PHP: Hypertext Preprocessor". PHP is the server-side programming language that relays requests from users on their web browsers, via the webserver, to the database, then returns the data and presents it as HTML so that the user can see the data in their web browser.

Database

A database is a collection of data elements (facts) stored in a computer in a systematic way, such that a computer program can consult it to answer questions. The answers to those questions become information that can be used to make decisions that may not be made with the data elements alone. The computer program used to manage and query a database is known as a database management system (DBMS). The properties of database systems are studied in information science.

SQL

Structured Query Language. The most popular computer language for create, modify and retrieve data from relational database management systems. MySQL is the program on the server that queries the data using this language.

RDBMS

A relational database management system (RDBMS) is a database management system (DBMS) that is based on the relational model as introduced by Edgar F. Codd.

DBMS

A database management system (DBMS) is a computer program (or more typically, a suite of them) designed to manage a database, a large set of structured data, and run operations on the data requested by numerous users.

Relational Database

A relational database is in essence a data structure organized so that it is perceived by its users as a collection of tables, and the data in the tables is organised and accessed according to how each table relates to other tables.

To understand the concepts and advantages of a relational database, imagine the needs of two small companies that take customer orders for their products. Company A uses a flat file database with a single table named orders to record orders they receive, while Company B uses a relational database with two tables: orders and customers.

When a customer places an order with Company A, a new record (or row) in the table orders is created. Because Company A has only one table of data, all the information pertaining to that order must be put into a single record. This means that the customer's general information, such as name and address, is stored in the same record as the order information, such as product description, quantity, and price. If customers place more than one order, their general information will need to be re-entered and thus duplicated for each order they place.

Whenever there is duplicate data, as in the case above, many inconsistencies may arise when users try to query the database. Additionally, a customer's change of address would require the database manager to find all records in orders that the customer placed, and change the address data for each one.

Company B is much better off with its relational database. Each of its customers has one and only one record of general information stored in the table customers. Each customer's record is identified by a unique customer code that will serve as the relational key. When a customer orders from Company B, the record in orders need contain only a reference to the customer's code, because all of the customer's general information is already stored in customers.

This approach to entering data solves the problems of duplicate data and making changes to customer information. The database administrator need change only one record in customers if someone changes addresses.

Syntax

In linguistics, syntax is the study of the rules, or "patterned relations", that govern the way the words in a sentence come together. In computing science, the set of allowed reserved words and their parameters and the correct word order in the expression is called the syntax of the language.

String

In computer programming and some branches of mathematics, strings are sequences of various simple objects. These are selected from a predetermined set each entry of which is usually allocated a code. Most commonly these simple objects will be printable characters and the control codes that are used with them. The data types in which these are stored are also called strings and it is fairly common to use these types to store arbitrary variable length lumps of binary data. Generally a string can be placed directly in the code usually by surrounding it with some form of quote marks (usually ' or " as these are typeable on a standard computer keyboard). Sometimes the term binary string is used to refer to an arbitrary sequence of bits.

Regular expression

A regular expression (abbreviated as regexp, regex, or regxp, with plural forms regexps, regexes, or regexen) is a string that describes or matches a set of strings, according to certain syntax rules. Regular expressions are used by many text editors and utilities to search and manipulate bodies of text based on certain patterns. Many programming languages support regular expressions for string manipulation.

Set

A set is just a well-defined collection of objects considered as a whole. The objects of a set are called elements or members. The elements of a set can be anything: numbers, people, letters of the alphabet, other sets, and so on. Sets are conventionally denoted with capital letters, A, B, C, etc. Two sets A and B are said to be equal, written A = B, if they have the same members.

A set may be described in words, for example:

A is the set whose members are the first four positive whole numbers.

B is the set whose members are the colours of the French flag.

By convention, a set can also be defined by explicitly listing its elements between brackets, for example:

C = {vodka, tomato juice, Tabasco sauce}

D = {mirror, signal, manoeuvre}

High Level Programming language

High Level Programming languages (HPLs) are the easiest to use of all available methods of programming a computer. They are closest to the English language in terms of structure and grammar. In contrast, low level programming languages, such as coding in Assembler, basically involves coding directly in the processor's own language of hexadecimal numbers and generates the fastest-running software. HPLs need another layer or layers of software to convert the language into assembler to run, at a performance overhead.

6 General Discussion

A principal aim of this thesis was to identify candidate genes of the Wnt signalling pathway that may regulate postnatal development of the primary somatosensory cortex of rodents. To accomplish this aim, I first identified the *Wnt*, *Frizzled* and *sFRP* genes expressed in S1 cortex during barrel formation. I then determined which of these genes showed altered expression patterns in a range of mutant mice that show defects in barrel development (Chapter 3). These studies identified four candidate molecules, namely *Wnt7b* and *Frizzleds 3*, *4* and *9* for potentially playing a crucial role in barrel formation. The mRNA for these genes are significantly down-regulated after barrel formation and both demonstrated a large, significant down-regulation in mutant mice lacking barrels (*Pkar2b*$^{-/-}$, *Plc-β1*$^{-/-}$ and/or *Mglur5*$^{-/-}$). In Chapter 4, I examined the barrel phenotype of all available *Wnt* mutant mice as well as mice lacking key components of the Wnt signalling pathway namely *Wnt2b*$^{-/-}$, *Wnt8b*$^{-/-}$, *Wnt7a*$^{-/-}$, *Wnt7a*$^{-/-}$*Dvl1*$^{-/-}$, *Dvl1*$^{-/-}$, *Dvl2*$^{-/-}$, *Sap-102*$^{-/-}$, *Psd-95gk*$^{-/-}$, *Psd-95*$^{+/-}$*Sap-102*$^{-/-}$ and *Psd-95*$^{-/-}$*Sap-102*$^{+/-}$. All mice examined had normal TCA segregation and termination in layer IV, and all but *Psd-95*$^{+/-}$*Sap-102*$^{-/-}$ mice had normal barrels. P7 *Psd-95*$^{+/-}$*Sap-102*$^{-/-}$ exhibit a defect in cortical cell segregation, with poorly defined barrel walls and septae. Finally, a Web-accessible database was made that contains expression profiles and patterns of genes and proteins that are members of the NRC. The database also incorporated links to useful information associated with any chosen gene— the availability of mutant mice, mRNA, genomic DNA and protein sequences and published molecular reagents such as PCR primer sequences and *in situ* hybridisation probes. Barrelgene.info can serve as a central portal for sequence information, mutant mouse availability and expression patterns for researchers in the barrel community.

6.1 Investigation of the original hypotheses and aims

6.1.1 Main Hypothesis: Wnts, Frizzleds and sFRPs are required to form barrels.

Specific Aim 1: To determine the Wnts, Frizzleds and sFRP genes present in developing barrel cortex and the expression profiles of these genes at crucial ages for barrel formation

To address Specific Aim 1, expression levels of *Wnt*, *Frizzled* and *sFRP* genes in barrel cortex were examined by SYBRgreen qRT-PCR at the following ages: P4, P7, P14, P21 and

Adult. To ensure the amplified PCR product represented the genes of interest, all PCR products were cloned and sequenced. Expression of *Wnts 2b*, *3*, *4*, *5a*, *7a*, *7b*, *9a*, *11* and *16* was observed at all ages observed (Table 5.1). Since the technique reliably detected new *Wnts*, the study was expanded to also screen for *Frizzled* and *sFRP* expression. All ten *Frizzleds* and *sFRPs 1*, *3* and *4* were expressed at all ages observed. From previous experience, three repetitions of SYBRgreen RT-PCR is sufficient to reveal statistically significant differences between each age groups, generating expression profiles over the development of barrel cortex of these genes. The only genes that showed any significant differences between age groups were *Wnt7b*, *Frizzleds 5*, *8* and *9* and *sFRP-2*, which were expressed in decreased amounts between P4 and Adult ages; *Wnt2b* and *Wnt4* were expressed in increased amounts between P4 and Adult ages (These data are summarised in Table 5.1).

Table 5.1
Summary of the *Wnt*, *Frizzled* and *sFRP* genes discovered by degenerate primer RT-PCR, individual primer RT-PCR and SYBRgreen RT-PCR. Genes that were expressed in decreasing amounts between P4 and Adult are presented in green text, whereas genes that were expressed in increasing amounts between P4 and Adult presented in blue text. ✓ = detected × = not detected.

Gene/ Method	Degenerate Primer RT-PCR	Individual Primer RT-PCR	SYBRgreen RT-PCR
Wnt1	×	×	×
Wnt2	×	×	×
Wnt2b	✓	✓	✓
Wnt3	✓	×	✓
Wnt3a	×	×	×
Wnt4	✓	✓	✓
Wnt5a	✓	×	✓
Wnt5b	×	×	×
Wnt6	×	×	×
Wnt7a	✓	✓	✓
Wnt7b	×	✓	✓
Wnt8a	×	×	×
Wnt8b	×	×	✓
Wnt8a	×	×	×
Wnt9a	×	×	✓
Wnt9b	×	×	×
Wnt10a	×	×	×
Wnt10b	×	×	×
Wnt11	×	×	✓
Wnt16	×	×	✓
Frizzled 1	-	-	✓
Frizzled 2	-	-	✓
Frizzled 3	-	-	✓
Frizzled 4	-	-	✓
Frizzled 5	-	-	✓
Frizzled 6	-	-	✓
Frizzled 7	-	-	✓
Frizzled 8	-	-	✓

Frizzled 9	-	-	✓
Frizzled 10	-	-	✓
sFRP-1	-	-	✓
sFRP-2	-	-	✓
sFRP-3	-	-	×
sFRP-4	-	-	✓

Since the cortex contains many different cell types and inputs from many different regions of the brain, it is perhaps not surprising to find so many *Wnt, Frizzled and sFRP* genes expressed in barrel cortex. It is possible that different *Wnts* are expressed by different cell types during barrel formation, and that different *Wnts* are required the many different cellular processes that are occurring in the developing barrel cortex. In support of my findings, the laboratory of Elizabeth Grove published *in situ* hybridisation expression patterns for many *Wnt*, *Frizzled* and *sFRP* genes (Shimogori et al., 2004). Shimogori and colleagues restricted the *Wnt* genes examined to those *Wnts* previously shown to be expressed in the cerebral cortex primordium by *in situ* hybridisation, namely *Wnts 2b*, *3a*, *5a*, *7a*, *7b* and *8b* (Lee et al., 2000a) but also examined the expression of all *Frizzled* and *sFRP* genes in the 2004 paper The qRT-PCR work presented in Chapter 3 adds *Wnts 3*, *4*, *9a*, *11*, *16*, *Frizzleds 1*, *2*, *4*, *5*, and *sFRP-4* to the list reported by Shimogori and Grove, 2004 (Table 5.1). Since our study did not restrict the number of *Wnts* examined and utilised an extremely sensitive qRT-PCR method amplify genes of interest (rather than probing by radioactively labelled riboprobe) it was likely that we would detect the expression of more genes than Shimogori et al., (2004) found by *in situ* hybridisation.

6.1.2 Expression Profiles

The finding that *Wnt7b* and *Frizzled* 9 mRNAs are expressed in greater amounts at younger rather than older ages suggests these genes likely play a role in the earlier cellular segregation events required to form a barrel. In general, genes that are expressed in highest amounts at P14 are likely to play a role in dendritogenesis, the peak of which is at P14. Genes expressed in greater amounts in adulthood than at earlier ages (*Wnt2b*, *Wnt4*) may play roles in later cellular events such as maintenance of the barrel structure and/or processes of synaptic plasticity that persist into adulthood (reviewed in Fox, 2002). Those genes (*Wnt5a*, *Wnt7a*, *Wnt9a*, *Wnt11*, *Wnt16*, *Frizzleds 1*, *2*, *3*, *4*, *6*, *7*, *10*, *sFRP-1* and *sFRP-4*) that showed no significant difference between age groups may be playing different roles in barrel development at different ages or cellular event comment to all ages such as synaptic plasticity, spine shape plasticity and/or housekeeping functions (Fox, 1992; Fox, 1994; Lendvai et al., 2000; Trachtenberg et al., 2002; Holtmaat et al., 2006; De Paola et al., 2006).

However, the fact that increased gene expression levels at a certain age happen to correlate with developmental events does not necessarily imply a causal link between the two processes. However, in the absence of functional data generated from mutant mice or through pharmacological intervention, assaying of mRNA (and protein) levels is the only method available to screen for genes that might be involved in any of the processes involved in barrel formation. The data provided in Chapter 3 identified good candidate genes (*Wnts 2b, 4, 7b, Frizzleds 5, 8, 9* and *sFRP-2*) to focus future research into what role these Wnts and Wnt signalling components play in barrel formation.

6.1.3 *In situ* hybridisations

In situ hybridisations for many of the *Wnt* genes discovered by SYBRgreen RT-PCR were performed in order to determine the localisation of mRNA expression of these genes. These experiments were ultimately unsuccessful, as inadequate staining of Wnt genes was observed for all probes used, except *Wnt2b*, which gave specific punctate staining patterns throughout all cortical layers at P7. Although these expression patterns differ to those published by the laboratory of Elizabeth Grove (Shimogori et al., 2004), her group examined different ages, using a different probe, on mice with a different genetic background. One possible reason for the lack of probe staining observed for most *Wnt* riboprobes was that DIG-labelled probes were used in all *in situ* hybridisation runs. DIG-labelled riboprobes were chosen as they avoid many of the problems associated with radioactively labelled riboprobes, such as limited radioisotope shelf life and the extensive time required for autoradiography. Furthermore, the scatter inherent in radioactive decay limits the spatial resolution of the technique, which is not an issue with DIG-labelled probes. However, long periods of autoradiography permit detection of extremely low amounts of mRNA expression (Brady and Finlan, 1990), and perhaps this method should have been used in conjunction with DIG-labelled riboprobe *in situ* hybridisations.

6.1.4 Conclusions from specific Aim 1

Despite the failure of almost all of the *in situ* hybridisations, the experiments performed to investigate Aim 1 have demonstrated that *Wnts*, *Frizzleds* and *sFRPs* are expressed in postnatal barrel cortex, and that some of these genes undergo developmental regulation. These experiments add to our knowledge of *Wnt*, *Frizzled* and *sFRP* expression in barrel cortex; the only other report of Wnt or Frizzled gene expression in this region is by *in situ* hybridisation,

and only *Wnt2b* and *Frizzled 3* expression were observed to be specifically expressed in barrel cortex (Shimogori et al., 2004). The work in Chapter 3 currently represents the largest scale analysis of a family of proteins in the developing mouse somatosensory cortex, spanning thirty-three genes over five ages. However, cDNA microarray analysis of gene expression levels during the critical period in visual cortex has been performed on tissue taken at two ages from rat visual cortex (Ossipow et al., 2004), at three ages in cat visual cortex (Prasad et al., 2002), two ages in old-world monkey (*Cercopithicus aethiops*) at three different age groups (Lachance and Chaudhuri, 2004) and four ages in mouse visual cortex (Majdan and Shatz, 2006) although no *Wnts*, *Frizzleds or sFRPs* were included in these microarray experiments.

Since the experiments performed to investigate Aim 1 revealed the expression of many *Wnt*, *Frizzled* and *sFRP* genes in barrel cortex, a second approach was taken to identify candidate genes. I reasoned that if Wnt signalling was playing a role in barrel formation, then mice with defects in barrel development may also show mis-regulation of key Wnt signalling components. Therefore I examined the expression levels of *Wnt*, *Frizzled* and *sFRP* genes in mutant mice (*Plc-β1*$^{-/-}$, *Pkar2β*$^{-/-}$ and *Mglur5*$^{-/-}$ mice) that lack barrels. A discussion of the candidate genes identified in the work performed to address both Aim 1 and Aim 2 is included in the discussion of Aim 2.

6.2 Specific Aim 2: To determine if Wnt, Frizzled and sFRP expression is dysregulated in barrel cortices of mice with barrel defects, namely: Pkar2b$^{-/-}$, Plc-β1$^{-/-}$ and Mglur5$^{-/-}$ mice.

In Chapter 2, I identified ten *Wnt*, ten Frizzled and three sFRP genes expressed in the developing postnatal cortex. To gain further insight into the particular *Wnt*, *Frizzled* and sFRP genes that regulate barrel cortex development and to refine the list candidate *Wnt*, *Frizzled* and *sFRP* genes for regulating barrel development, I examined whether the expression patterns of these signalling molecules is dysregulated in mice with defects in barrel formation, namely *Pkar2b*$^{-/-}$, *Plc-β1*$^{-/-}$ and *Mglur5*$^{-/-}$ mutants. In all three genotypes, all *Wnt*, *Frizzled* and *sFRP* genes that are expressed in barrel cortex exhibited downregulation in the mutant mice (Table 5.2), although the interpretation of this result is difficult due to the lack of knowledge of the nature of many of the interactions between Wnts, sFRPs and Frizzleds. Interestingly, the genes that showed the greatest downregulation in these mutants were *Wnt7b*, *Frizzled 4*,

Frizzled 9 and *Frizzled 3*, two of which (*Wnt7b* and *Frizzled 9*) I showed were down-regulated after barrel formation.

Table 5.2
Table of the average down-regulation values of selected *Wnt*, *Frizzled* and *sFRP* genes across *Pkar2β*, *Plc-β1* and *Mglur5* mutants. The data presented in this table summarises the average downregulation of Wnt, Frizzled and sFRP genes in barrel cortices of *Pkar2β*$^{-/-}$, *Plc-β*$_1^{-/-}$ and *Mglur5*$^{-/-}$ mice compared to wild type mice as identified by $\square\square C_T$ qRT-PCR studies * = Data from only one mutant.

Gene	Average Down-regulation
Wnt7b	13.0
Frizzled 4	9.2
Frizzled 9	8.2
Wnt3	8.0*
Frizzled 3	7.5
Frizzled 8	6.8
Wnt9a	6.7
SFRP-1	6.3
SFRP-2	5.3
Wnt2b	5.2
Wnt4	4.0
Frizzled 2	3.4
SFRP-4	2.8
Wnt5a	1.2
Frizzled 7	1.2
Frizzled 10	1.1
Frizzled 1	1.1
Frizzled 5	1.1
Frizzled 6	0.7

6.2.1 Candidate genes generated from qRT-PCR experiments

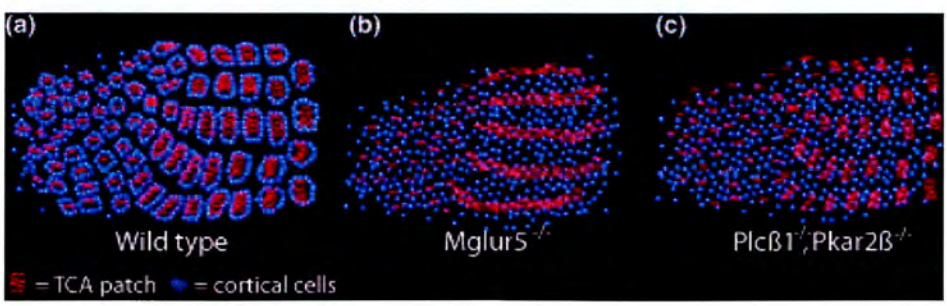

Figure 5.29
Barrel phenotypes of wild type, *Mglur5*$^{-/-}$, *Plc-β1*$^{-/-}$ and *Pkar2β*$^{-/-}$ mice. (a) Wild type mice have TCA terminals that segregate into individual whisker related patches (red labelled cells) and layer IV cortical cells segregate to form cell-dense barrel walls (blue cells) and cell sparse barrel hollows. (b) *Mglur5*$^{-/-}$ mice have

TCAs that segregate into rows, but not into individual whisker-related patches. Cortical cells in these mutants do not segregate to form barrel walls. (c) *Plc-βl*$^{-/-}$ and *Pkar2β*$^{-/-}$ mice have TCAs that segregate into whisker-related patches, although cortical cells do not segregate into barrels. Based on Erzurumlu and Kind (2001).

6.2.2 Barrel phenotypes of *MgluR5*$^{-/-}$, *Plc-β1*$^{-/-}$ and *Pkar2b*$^{-/-}$ mice.

As mentioned above, the mutants examined in the screen of the differences in expression levels of *Wnt*, *sFRP* and *Frizzled* genes in between wild type and mutant mice were *Mglur5*$^{-/-}$, *Pkar2b*$^{-/-}$ and *Plc-β1*$^{-/-}$ mice. I present a recap of the mechanisms and processes that are altered in these mutant mice.

6.2.2.1 *MgluR5*$^{-/-}$ and *Plc-β1*$^{-/-}$ mutants

Mglur5$^{-/-}$ mice display segregation of large whisker TCAs into rows but not individual patches within rows (Figure 5.29b), and lack barrels (Hannan et al., 2001). This total loss of barrels, despite partial segregation of TCAs into whisker rows in PMBSF, signifies that mGluR5 signalling is crucial for the normal transfer of patterns from TCAs to their postsynaptic partners during barrel development, since no megabarrel is formed (Van der Loos and Woolsey, 1973a). mGluR5 appears to signal through PLCβ_1 in barrel formation. *Plc-β1*$^{-/-}$ mice also lack barrels; cortical cell segregation does not occur, but TCAs do segregate into a barrel-like pattern (Hannan et al., 2001, Figure 5.29). In addition, Phosphoinositide (PI) hydrolysis is drastically reduced in *Plc-β1*$^{-/-}$ mice following type I mGluR stimulation (Hannan et al., 2001). Notably, TCA segregation in *Mglur5*$^{-/-}$ mice is different to that observed in *Plc-β1*$^{-/-}$ mice (Figure 5.29). Since mGluR5 immunoreactivity in adult mice appears to be entirely postsynaptic (Romano et al., 1996), and barreloids are normal in both *Mglur5*$^{-/-}$ and *Plc-β1*$^{-/-}$ mice (Hannan et al, 2001) this suggests that the site of action of both mGluR5 and PLCβ_1 is cortical. If the barrel phenotype observed in *Mglur5*$^{-/-}$ mice is indeed solely cortical, it could be that a retrograde signal is for proper TCA patterning (Erzurumlu and Kind, 2001). Studies using Rapid Golgi staining show that dendrites of *Plc-β1*$^{-/-}$ layer IV neurons orient toward TCA patches as normal (Upton et al., in preparation). This suggests that either dendritic reorientation does not require PLCβ_1 or selective dendritic reorientation within TCA patches is insufficient (although possibly necessary) to form barrels.

6.2.2.2 *Pkar2b*$^{-/-}$ mice

Our laboratory has recently shown that barrel morphology is affected in *Pkar2b*$^{-/-}$ mice (Watson et al., 2006b). These mice have a 40% reduction in PKA activity in cortex, have poorly defined barrels and the septa and barrel hollows do not display the reduction in number of cells seen in wild-type animals (Inan et al., 2006; Watson et al., 2006b). The ratio of cells in the barrel wall to barrel hollow is reduced from the wild-type ratio of 1.8:1 down to 1.3:1 (Watson et al., 2006b). However, *Pkar2b*$^{-/-}$ mice show good segregation of TCAs in PMBSF (Figure 5.29).

6.2.3 Regulation of Wnts in *MgluR5*$^{-/-}$, *Plc-β1*$^{-/-}$ and *Pkar2b*$^{-/-}$ mice.

Since mGluR5 signals through PLCβ_1 in order to form barrels, it might be expected that a similar profile of dysregulated *Wnt*, *Frizzled*, and *sFRP* genes would be observed in both *Mglur5*$^{-/-}$ and *Plc-β1*$^{-/-}$ mice. However, the differences in TCA segregation in *Mglur5*$^{-/-}$ compared to *Plc-β1*$^{-/-}$ mice (Figure 5.29b,c) indicate that mGluR5 does not signalling exclusively through *Plc-β1*$^{-/-}$ and as discussed above, mGluR5 may produce a retrograde signalling molecule that patterns TCAs into individual patches. Notably Wnt7a has been identified as retrograde signalling factors that cause axonal remodelling in the cerebellum (Hall et al., 2000; Salinas, 2005). PKARIIβ signals via a different set of molecules than mGluR5/PLCβ_1, and as such the *Wnt, Frizzled* and *sFRP genes* that might be dysregulated might be different across genotypes.

6.2.4 Candidate Genes

The best candidate genes identified for further investigation were *Wnt7b* and *Frizzleds 3, 4* and *9*

Wnt7b was one of the most downregulated genes in both the *Mglur5*$^{-/-}$ and *Plc-β1*$^{-/-}$ mutants at P14. *Wnt7b* is expressed in decreasing amounts over barrel cortex development, with expression highest over the first postnatal week (Chapter 3). *Wnt7b* has been shown to be expressed throughout the neocortex at low levels by *in situ* hybridisation (Shimogori et al., 2004). The work performed in Chapter 3 has demonstrated that *Wnt7b* is expressed in significantly higher amounts during the first postnatal week than at alter ages.

Wnt7b has been shown to play a role in hippocampal dendritic branching by signalling through Dvl, Rac and JNK (Rosso et al., 2005), raising the possibility that Wnt7b may be

regulating similar processes in developing barrel cortex, perhaps in the early stages of cortical cell dendrite growth and orientation. However, recent evidence from our laboratory shows that *Plc-β1*$^{-/-}$ mutants exhibit normal dendrite complexity and orientation (Upton et al., in preparation). This, in conjunction with *Wnt7b* expression being significantly higher at P4 and P7 than at later ages, despite the fact that dendritogenesis continues until P28, suggests that Wnt7b may be more likely to play a role in the cellular clustering that occurs between P4 and P7. Nevertheless, Wnt7b is still a strong candidate for further investigation into a role in barrel formation because of the large downregulation seen in *Mglur5*$^{-/-}$ and *Plc-β1*$^{-/-}$ mice. Unfortunately, *Wnt7b*$^{-/-}$ mutants die embryonically (Parr et al., 2001), therefore, conditional mutants with genetic deletion restricted to the cortex would be required to examine barrels in *Wnt7b* mutants.

Frizzled 9 was significantly downregulated in both *Mglur5*$^{-/-}$ and *Pkar2b*$^{-/-}$ mice, and was expressed in significantly greater amounts at P4 and P7 than later ages (Chapter 3). Frizzled 9 plays a role in hippocampus development; *Frizzled 9*$^{-/-}$ mice live to adulthood, but have abnormal dentate gyrus morphology (Zhao et al., 2005). In adult *Frizzled 9*$^{-/-}$ mice, a 20% decrease in the number of dentate granule cells is observed, although there is no change in the number of pyramidal cells. A dramatic increase in the mossy cell number and a substantial increase in neuronal density are seen in the hilus. Furthermore, visually mediated and spatial memory is impaired (Zhao et al., 2005). It is possible that since *Frizzled 9* is also expressed in barrel cortex, it mediates similar processes, such as the differential cell densities to generate the barrel walls and hollows. All three *Frizzled 9*$^{-/-}$ mouse mutant strains generated so far live into adulthood (Zhao et al., 2005; Jackson Laboratories Mouse Genome Informatics direct submission, 2005; Ranheim et al., 2005), so examination of the barrel phenotype of these mice may yet reveal a defect in barrel formation, most likely a defect in cortical cell segregation .

Frizzled 4 was also greatly downregulated in P14 *Mglur5*$^{-/-}$ and *Plc-β1*$^{-/-}$ mutants. *Frizzled 4* is expressed in barrel cortex, and showed no difference in expression between all ages observed (Chapter 3), and Shimogori et al., (2004) reported "no striking expression pattern in cortex". About half of all *Frizzled 4*$^{-/-}$ mice born die within the first five months of live, and all exhibit progressive cerebellar degeneration associated with severe ataxia. This is manifested as extensive granule cell death, and occurs during the peak of cerebellar synaptogenesis during P10 to P20. This suggests that granule cell death could arise from a defect in some aspect of synaptogenesis (Wang et al., 2001). Although no barrel phenotype in *Frizzled 4*$^{-/-}$ mice has been published it is possible that Frizzled 4 plays a role in barrel synaptogenesis or selective

cell death/survival. A logical extension of the work presented in this thesis would be to examine the barrel phenotype of *Frizzled 4*$^{-/-}$ mice.

Frizzled 3 was strongly downregulated in *Pkar2b*$^{-/-}$ mice only (Chapter 3). *Frizzled 3* is required for normal thalamocortical and corticothalamic axon formation and guidance (Wang et al., 2002), possibly through interaction with the Wnt/PCP pathway. When the protocadherin *Celsr3*, a Wnt/PCP pathway component, is genetically knocked out in mice, an almost identical phenotype is observed to the *Frizzled 3*$^{-/-}$ mouse (Tissir et al., 2005) suggesting a role for Wnt/PCP signalling in thalamocortical circuit generation. Mice mutant for either of these genes die perinatally, lack the anterior commissure and the internal capsule and have neocorticies that are entirely disconnected from other structures (Wang et al., 2002; Tissir et al., 2002; Tissir et al., 2005; Tissir and Goffinet, 2006). Another example of the role of Frizzled 3 in axon guidance is that *Frizzled 3*$^{-/-}$ mice also display anterior-posterior guidance defects after midline crossing in dorsal spinal cord commissural neurons (Lyuksyutova et al., 2003).

Frizzled 3 is expressed throughout barrel development (Chapter 3) and has shown to be expressed selectively in barrel walls (Shimogori et al., 2004). Since *Pkar2b*$^{-/-}$ mice have a much reduced cell density ration in this region compared to wild type, perhaps glutamate signalling through NMDARs and PKA directs *Frizzled 3* expression and subsequent barrel wall formation. However, examination of the barrel phenotype of *Frizzled 3*$^{-/-}$ mice is not possible, since these mice die within thirty minutes of birth of respiratory failure, and barrels begin to be visible at late P3 (although barrelettes and barreloids could be assessed in P0 *Frizzled 3*$^{-/-}$ mice). Therefore generation of a cortex-specific conditional *Frizzled 3*$^{-/-}$ mutant would be required to examine the barrel phenotype in this mouse. It is possible that in even the cortex-specific deletion *Frizzled 3*$^{-/-}$ mice that TCAs and corticothalamic axons may still not form and therefore the defect is entirely thalamocortical. Alternatively introduction of small interfering RNA (siRNA) injected into barrel cortex at crucial stages of barrel development to knock-down *Frizzled 3* expression may reveal further insight into the role of Frizzled 3 in barrel formation, by letting the mouse survive long enough to form barrels.

6.2.5 Potential roles in barrel formation of remaining candidate *Wnt, Frizzled* and *sFRP* genes discovered in barrel cortex

Interestingly, *Wnt2b* was shown to be expressed in barrel cortex throughout barrel development by qRT-PCR (Chapter 3) and in barrel walls by *in situ* hybridisation (Shimogori et al., 2004), yet *Wnt2b*$^{-/-}$ mutants have normal barrels (Chapter 4). It is likely that if Wnt2b plays a role in barrel formation, the loss of *Wnt2b* expression in *Wnt2b*$^{-/-}$ mutants could be compensated for by altered regulation of expression of other *Wnts* and Wnt-related genes. One way of assessing this would be to repeat the screening of Wnt, Frizzled and sFRP expression in *Wnt2b*$^{-/-}$ mice to determine which of these genes are dysregulated.

6.2.5.1 TCA Guidance

Wnt3, signalling in conjunction with Ryk can act as an axon guidance molecule in medial-lateral retinotectal topographic mapping (Schmitt et al., 2006). Furthermore Wnt3 expressed by motoneurons can act as a target-derived retrograde signal that regulates the terminal arborisation of proprioceptive NT-3 responsive sensory neurons *in vitro* (Krylova et al., 2002). Within the CNS, Wnt4 signalling through Frizzed 3 in the spinal cord regulates the axon guidance of commissural axons (Lyuksyutova et al., 2003). It is possible that the Wnt3 and/ or Wnt4 present in barrel cortex playing role in TCA guidance to S1 cortex prior to barrel formation, or the arborisation and elaboration of TCA terminals in the during barrel formation and maturation. *Wnt3*$^{-/-}$ mice die *in utero* at E10.5 (Liu et al., 1999a), and to examine barrels at P4 or later, a conditional mutant with deletion of Wnt3 in the cortex is required. Fortunately, the laboratory of Andrew McMahon have created a floxed *Wnt3* mutant (Barrow et al., 2003) which could be cross-bred with the *Emx-Cre* mice that was utilised in *CxNr1*$^{-/-}$ mice to delete *NR1* specifically in cortex. *Wnt4*$^{-/-}$ mice die within 24 hours of birth (Stark et al., 1994) and the only reported defect in the CNS in these mutants is abnormal pituitary gland which is devoid of all cell types except corticotropes (Heikkila et al., 2002). Again, cortex-specific Wnt4 mutants would be required to examine the role of Wnt4 in barrel cortex development. If either Wnt3 or Wnt4 play a role in TCA guidance, one might expect that cortex-specific deletions of *Wnt3*$^{-/-}$ or *Wnt4*$^{-/-}$ mice might have defects in TCA pathfinding and/ or layer termination.

6.2.5.2 TCA remodelling

TCAs that originate from VpM thalamus invade the cortex, terminate in layer IV and refine and remodel their organisation from a large bundle of axons into five principal rows, with each row consisting of individual whisker related patches. There is strong evidence for Wnts

performing an axonal remodelling function the role of Wnt7a in cerebellar synapse formation. In the developing cerebellum, multi-synaptic glomerular rosettes (GR) are formed as mossy fibre growth cones establish synaptic interactions with postsynaptic granule cell neurons (GCs). Hall et al. (2000) demonstrated that Wnt7a is expressed by GCs as they are contacted by mossy fibres, and that Wnt7a induces axonal remodelling, a crucial process for GR formation. In cultures of mossy fibres, Wnt7a induces synapsin I clustering in a GSK-3β-dependent manner. *Wnt7a*$^{-/-}$ mice exhibit a delay in accumulation of synapsin I staining. This indicates that Wnt7a influences the development of presynaptic mossy fibres in vivo. Wnt7a was also found to enhance growth cone complexity and to regulate microtubule dynamics in culture, and these effects were antagonized by a soluble Wnt inhibitor, secreted Frizzled-related protein (sFRP-1). *Wnt7a*$^{-/-}$ mice display a delayed maturation of glomerular rosettes, but this effect is transient. If Wnt7a is playing a role in barrel formation, it would be most likely to play a role in the elaboration of TCA terminals in barrel related patches in layer IV that occurs during the first postnatal week (Rebsam et al., 2002). However, the work performed in Chapter 4 in addressing Aim 3 (below) has revealed that P7 *Wnt7a*$^{-/-}$ mice have normal barrels, demonstrating that Wnt7a is not required for barrel formation, and any role it might play in forming barrels is adequately compensated for by altered regulation of other molecules, most likely upregulation of other *Wnt* genes.

6.2.5.3 The remaining genes

Many of the remaining *Wnts*, *Frizzleds* and *sFRPs* that are expressed in barrel cortex have not yet been shown to play any role within the CNS, and many knockout mice remain to be generated. Of the ten mouse *Frizzled* genes, *Frizzleds 1*, *6*, *8* and *10* have no observable mutant phenotype, and mutant mice for *Frizzleds 2* and *7* have not yet been generated (Mouse Genome Informatics, 2006). Of the *sFRP*s discovered in neocortex, *sFRPs -1* and *-2* have been genetically knocked out. *sFRP-1*$^{-/-}$ mice exhibit a general reduction in brain weight, and *sFRP-2*$^{-/-}$ mice die at around E16 with major defects throughout the whole of the embryo. However, for some, parts of the signalling pathways employed by these molecules are beginning to become known and it is from this knowledge that we can begin to speculate on links between these molecules and the processes that underlie barrel formation.

For example, there is very little in the literature regarding the role of Wnt5a in mammalian brain development, other than *Wnt5a* is expressed in the hem of the embryonic cerebral cortex of mice (Grove et al., 1998) and can signal through Frizzleds 4, 6 and 7 to activate β-catenin

(Umbhauer et al., 2000). Of *Wnt9a*, *Wnt11*, both have been shown to be expressed in postnatal whole brain extracts by RT-PCR (Freeman et al., 1998; Katoh, 2002) and as yet, no postnatal expression patterns are published for *Wnt16* to date outside of this thesis.

Frizzled 1 can behave as an antagonist of Wnt/β-catenin signalling by signalling through the G-protein, $G_{\alpha q}$ (Roman-Roman et al., 2004) although *Frizzled 1*$^{-/-}$ mice have no observable mutant phenotype (Mouse Genome Informatics, 2006). Both Frizzled 4 and Frizzled 6 can stimulate PKC activation (Sheldahl et al., 1999) and also activate β-catenin (Umbhauer et al., 2000), depending on the cellular context in which these Frizzleds reside. Shimogori et al., (2004) showed *in situ* hybridisation experiments that showed *Frizzled 7* expression in cortex at P7 only, which is at odds with our observation by qRT-PCR that *Frizzled 7* is expressed at P4, P7, P14, P21 and adult ages. No *Frizzled 7*$^{-/-}$ mouse has yet been generated. Frizzled 8 and 10 are expressed ubiquitously, but in low amounts throughout the cerebral cortex (Shimogori et al., 2004). Interestingly, Frizzled 8 can be activated by members of the Mouse cristin/R-spondin family and signal through the Wnt/β-catenin pathway. This causes the activation of TCF/LEF-dependent gene expression, even in the absence of any Wnts (Nam et al., 2006), and screening for the presence of cristin/R-spondin family genes by qRT-PCR is a possible avenue for further work. However, *Frizzled 8*$^{-/-}$ mice have no apparent defects (Mouse Genome Informatics, 2006). Frizzled 10 interacts with Wnt7b in epithelial and vascular smooth muscle cells to activate Wnt/β-catenin pathway signalling (Wang et al., 2005). However, *Frizzled 10*$^{-/-}$ mice have no identifiable knockout phenotype (Mouse Genome Informatics, 2006) and no expression patterns.

6.2.6 Methodological considerations for qRT-PCR studies in Aims 1 and 2.

6.2.6.1 Limitations of experimental approach

qRT-PCR

All interpretation of the qRT-PCR results assumes that mRNA expression levels directly correlate to the amount of protein produced. However, this is not always the case. For example, the developmental mRNA expression profiles of *Pkar2b* and *Syngap* do not relate to protein levels present during barrel formation. *Pkar2b* mRNA expression is high at P4 and P7, and then drops sharply to a low, constant level for the rest of barrel development, yet protein

levels remain constant throughout (Watson et al., 2006b). *Syngap* mRNA expression peaks at P14 and drops off afterwards, yet protein levels in barrel cortex increase throughout barrel development (Barnett et al., 2006a). This is because during the time of barrel formation and maturation, there is a massive turnover of dendrites and synapses, as these structures are rapidly projecting and retracting, stabilising only when they find an appropriate binding partner. The rapid turnover of protein and mRNA required for this behaviour can mean that large increases in mRNA are required just to maintain protein levels at a steady state, especially if the protein is expressed in dendrites. If this is the case, a gene expressed in similar amounts through barrel development (such as *Wnt2b* and *Wnt4*) might only result in low protein levels from the translated mRNA message, but at later ages accumulation of protein results in much higher protein levels. Additionally, the same gene can play different roles at different stages in barrel development. For example, *Wnt2b* expression might direct the early cellular aggregation processes or thalamocortical interactions, yet at later ages plays a role in regulating dendritic elaboration, synaptic plasticity or barrel structure maintenance. Nevertheless, no better method than screening of mRNA and protein levels has yet been identified for the initial screening processes of identifying candidate genes involved in barrel formation.

Barrel cortex dissection

It should also be noted that the barrel cortex dissection samples all six layers of the cortex. Most of the events required to form a barrel occur in layer IV, so visualisation of the laminar gene expression pattern by *in situ* hybridisation is necessary to determine if a gene is involved in barrel formation. It is possible that if a gene is expressed in equal amounts in layers I, II/III and VI at earlier ages, yet in layers IV at later ages, RT-PCR would generate an expression profile that showed high expression levels during the early cellular segregation events in barrel formation, yet lower expression at later ages. This expression profile would suggest that this gene was involved in the early cellular segregation events in layer IV, even though this gene is not expressed in this layer until later ages. This reiterates the requirement for *in situ* hybridisations for better interpretation of qRT-PCR data from the cortex.

Dissection of cortical layer IV alone is technically challenging and yields unfeasibly small amounts of tissue for routine mRNA or protein extraction. Furthermore since mRNAs can be located in dendrites and layer IV contains dendrites that originate from layers II, III and V, even if a gene is shown to be expressed in layer IV, this does not necessarily mean that a TCA or layer IV cell expressed it. Since almost all of the cellular processes (such as synaptogenesis

and dendritogenesis) that occur in layer IV during barrel formation also occur in the other cortical layers (apart from the cortical cell segregation events) then the difference in gene expression patterns between layer IV "contaminated" by dendrites from other layers, and a dissection sampling all six layers should not be great. Any selective regulation of genes required to effect these changes in layer IV should be reflected in an alteration in expression levels detected by this method. Since the cortex develops in a hierarchical manner, it is to be expected that during the first postnatal week, the first synapses to form would be TCA-cortical cell synapses, and then cortico-cortical cell synapses form later. Indeed, at P3 whilst TCAs are segregating, functional TCA synapses have been detected by electrophysiological methods (Lu et al., 2003). At later stages of development, TCA-cortical cell synapses comprise between 10-23% of the synapses present in S1 cortex, the majority of the remaining synapses being cortico-cortical (Benshalom and White, 1986). As such, barrel cortex dissections at earlier ages should have a greater representation of TCA-cortical cell synapses than at later ages. Again, the events occurring in layer IV are similar to the events occurring in other layers, so the gene expression levels in whole barrel cortex should still give a broadly informative picture of gene expression occurring in barrels. In essence, the barrel cortex dissection is practically the only way of assessing what genes are being expressed during barrel formation. This technique, when allied with *in situ* hybridisations to determine the location of expression is currently the best way of ascertaining gene expression levels in barrels during barrel development.

Aspects of Wnt signalling not addressed by the qRT-PCR studies

Antagonism of Wnt signalling by factors such as sFRPs might not directly modulate the levels of *Wnts* expressed (i.e. those levels detected by the qRT-PCR studies), but sFRPs do directly modulate the ability of certain Wnts to signal, although many of the specific interactions between Wnts and sFRPs are unknown. Furthermore, the complement of Wnt co-receptors had not been assessed in this study, and so the levels of Wnt activation of Frizzled receptors may vary depending on the co-receptors present and this variable would need to be investigated in any future work.

The complement of Wnts and Frizzleds present in barrel cortex has the capability to activate the Wnt/β-catenin, Wnt/PCP, Wnt/Ca^{2+} pathways. The known interactions of Wnts, sFRPs and Wnt signalling components are reviewed by Kohn and Moon, 2005; Kuhl, 2004; Willert and Nusse, 1998; Mikels and Nusse, 2006; Nusse, 2005, and are mapped online at http://www.networksandpathways.org/pathway?name=Wnt&description=Wnt. However,

there are large gaps in our knowledge about many Wnt/ Frizzled interactions and the signalling pathways these combinations activate. The work performed in this thesis has not managed to address what molecular interactions might occur in this system, rather, it has instead hinted at the complex nature of interactions of the Wnts, sFRPs and Frizzleds present in barrel cortex during its formation and maturation. It has also identified interesting candidates for further investigation by demonstrating that certain *Wnt*, *Frizzled* and *sFRP* genes that are significantly regulated over barrel development.

The technical considerations of performing qRT-PCR and the use of control genes are discussed in detail in Chapter 3.

This work to date represents the only screening of members of a gene family in somatosensory cortices of mice that are mutant for genes crucial to barrel formation. The only other example of a barrel mutant *versus* wild-type screen published was Western blots performed on wild-type and *Syngap*$^{-/-}$ P5 whole brain homogenates, with NR1, NR2B, SAP-102, PSD-95, GluR1, GRIP and GRASP proteins being probed (Kim et al., 2003a).

6.3 Specific Aim 3: To determine the barrel phenotype of all available Wnt and Dvl knockout mice.

The aim of the first part of Chapter 4 was to examine the barrel phenotype of all available *Wnt* and *Dvl* knockout mice, since the presence of a defect would be suggestive of a link between Wnt signalling and barrel formation. The methods used to characterise the barrel phenotype were α-5-HT immunochemistry to label TCAs on P7 sections, and staining of Nissl substance, revealing the extent of cortical cell segregation that should form the characteristic barrel field. The visual assessment of barrel ranking is believed to be an accurate way of determining the quality of barrel formation, since the human eye is extremely capable of assessing small variations in cell density and contrast (Katsnelson, 2002). Furthermore, all mutants that have an altered barrel phenotype have been initial identified by visual assessment screening (Personal communication, Dr. Peter Kind). Previous experience in the Kind laboratory indicated that Propidium iodide- or Topro-labelled cell counting of cell density variations in barrel walls and hollows requires sections from approximately seven animals per genotype. However, in all cases where this quantification was used the defect was first noticed in Thionin-labelled sections from two to three brains. A major advantage of a blind, visual assessment is smaller sample numbers are needed; however, subtle differences between

phenotypes may be missed. Therefore it is excellent method for identifying mutants with defects in barrel formation, but once identified, a more quantitative method is warranted prior to publication. *Wnt2b*$^{-/-}$, *Wnt7a*$^{-/-}$, *Wnt8b*$^{-/-}$, *Dvl1*$^{-/-}$, *Dvl2*$^{-/-}$ and *Wnt7a*$^{-/-}$*Dvl1*$^{-/-}$ mice all had normal TCA and cortical cell segregation, thus these genes are not required for the cell segregation needed to form a barrel. The presence of barrels in the mutants, however, does not negate a role for these genes in barrel development, as compensatory regulation of some of the many other *Wnts*, *Frizzleds* or *sFRPs* present in barrel cortex may occur. In addition, the genetic background of mutant mice can determine whether altered phenotypes are expressed. *Mglur5*$^{-/-}$ mice lack barrels and have TCAs that segregate only into rows and not individual whisker-related patches when on a BL6/129 background. When on a CD-1/129 mixed background, the segregation of cortical barrels and thalamic axons appears normal (Hannan et al., 2001). At the time that the experiments were performed, it was thought that selective dendritic elaboration into the barrel hollow was an integral requirement to form barrels (Datwani et al., 2002b). As such, it was assumed that any defects in dendritic shape would be reflected in a deficit in cellular segregation. However, recent data from our laboratory shows that in *Plc-β1*$^{-/-}$ mice, which have segregated TCAs but lack cortical barrels, layer IV cortical cells exhibit normal dendrite elaboration and orientation into the TCA plexus, demonstrating that the dendritic reorganisation and cellular segregation processes can be genetically dissociated (Upton et al., in preparation). As such, examination of TCA and cortical cell segregation in these mutants is uninformative about the dendritic phenotype in these mutant mice, and utilisation of the rapid Golgi staining technique or other techniques that label dendrites in their entirety are necessary to investigate the role of Wnts in orientation of cortical cell dendrites in barrels. Such analysis was beyond the scope of this thesis as it requires at least fifteen brains for each genotype.

6.4 Specific Aim 4: To determine whether the major scaffolding molecules SAP-102 and PSD-95 are required for barrel formation

The aim of part of Chapter 4 was to examine the barrel phenotype of *Psd-95GK*$^{-/-}$, *Psd-95*$^{-/-}$, *Sap-102*$^{-/-}$, *Psd-95*$^{-/-}$*Sap-102*$^{+/-}$ and *Psd-95*$^{+/-}$*Sap-102*$^{-/-}$ mice. *Psd-95GK*$^{-/-}$, *Psd-95*$^{-/-}$, *Sap-102*$^{-/-}$ and *Psd-95*$^{-/-}$*Sap-102*$^{+/-}$ mice have normal TCA segregation and cortical cells in these mice had segregated into a normal barrel field. Notably, *Psd-95*$^{+/-}$*Sap-102*$^{-/-}$ mice exhibit a poorly defined barrel field, with indistinct barrel walls and poorly defined barrel septae at P7 and P9. Additionally, these mice had normal TCA segregation, suggesting that the defect lies in the

ability of cortical cells to respond to TCA input, most likely via glutamate signalling through the NMDAR (Barnett et al., 2006b). The result indicated that expression of one allele of *Sap-102* can compensate for the total lack of *Psd-95*, but expression of one allele of *Psd-95* cannot compensate for the total loss of *Sap-102*. One experiment to directly address whether compensatory upregulation is actually occurring is to perform qRT-PCR experiments (or northern blots) in tandem with Western Blots probing for SAP-102 and PSD-95 levels over barrel cortex development in these mice.

However, at P14 there was no significant difference between the average visual ranking scores of *Psd-95*$^{+/-}$*Sap-102*$^{-/-}$ mice and wild-type mice. The mean score for P14 *Psd-95*$^{+/-}$*Sap-102*$^{-/-}$ (2.25) mice was 27% lower than for a P14 Wild-type mice (3.1). The scores for P14 Psd-*95*$^{+/-}$*Sap-102*$^{-/-}$ mice ranged from 0.5 to 3.5, n=3. One mouse appeared to have much higher barrel ranking scores than the other two, which may be due to a genotyping error. An alternative explanation for a barrel segregation defect being observed at P7/P9 but not P14, is a transient delay or slowing of the rate at which cortical cells respond to the presence of normally segregated TCAs. The only examples in the literature of a transient delay in barrel formation are congenitally hypothyroid mice, which exhibit a three-day delay in barrel formation (Calikoglu et al., 1996) but this defect is more to do with a general effect on brain growth rather than a specific delay in barrel formation. Systemic administration of a variety of 5-HT-depleting agents has been shown cause a delay in barrel pattern maturation (Blue et al., 1991; Osterheld-Haas et al., 1994; Rebsam et al., 2005) although nothing in the literature describes a delay in barrel formation involving NMDAR or indeed glutamate signalling in general; Datwani et al., (2002) report *CxNr1*$^{-/-}$ mice that lack barrels as late as P21. In any event, this work has demonstrated the requirement of *Sap-102* for barrel formation and shown the ability for one functioning copy of *Sap-102* to compensate for the total lack of *Psd-95*. The work in Chapter 4 also demonstrated that two functioning copies of *Psd-95* can compensate for the total loss of *Sap-102*, and that one copy of *Psd-95* cannot compensate for the total loss of *Sap-102* in barrel formation.

6.5 Specific Aim 5: To make a web-accessible database cataloguing the gene and protein expression profiles of NRC components in barrel cortex.

The barrelgene.info project required a four pronged approach to its development.

- Building the webserver, and installing the associated database management systems, querying and programming languages.
- Writing the code required to import and export data from the database, and the web pages that allow the users to query the database and see the results of their queries.
- Design of usable query interface. The database required an easy to use query interface, yet be powerful enough to exploit all of the data contained in the database, for example querying by gene name, location and age in an advanced search, as opposed to gene name in a simple search.
- Creating a user management system. This, in conjunction with analysis of web access logs, allows the administrator to track who uses the database and determine whether the users are from academia or industry and gives the potential to charge accordingly.
- Creating a data entry system, involving maximum automation and minimal data entry by humans to minimise data input errors. This was achieved by limiting as much data entry as possible to restricted lists, maximum use of automatic categorising functions in Microsoft Excel, and scripts running on the server that automatically update the sequence information from other sources.

The resulting database includes all NRC components as identified by Husi *et al.* (2000) and can serve expression patterns present in the literature of western blots, immunohistochemistry, *in situ* hybridisation, RT-PCR and RNase protection assays and sort the results by age or location. The database can also serve data on the barrel phenotype of mutant mice, the methods employed in the literature to assess the defects in barrel formation, the genetic background of the mice examined and the age at which these observations are made.

Barrelgene.info can provide genomic DNA, mRNA and protein sequence information for any gene selected, links to information regarding the protein interaction partners of the gene selected, and a description of the discovery and function of the gene at NCBI's Online Mendelian Inheritance in Man site. Importantly, barrelgene.info updates the sequence information automatically, so it is always current. Finally, the database links to the PubMed page for each publication in the database, allowing access to the article abstract and also the full text of each paper where available.

Barrelgene.info was presented to the Barrels 2005 meeting as an oral talk and also as a poster at the Neurosciences 2005 conference and feedback was invited from delegates. All found it to be easy to use and regarded it as a useful tool.

6.6 Further comments

This thesis aimed to explore the role of Wnt signalling in barrel formation. Barrel formation requires glutamate signalling through the NMDAR; Wnt/Frizzled and glutamate/NMDAR signalling pathways both have signalling components that can interact with each other, such as the interaction of SAP-102 with APC, or PSD-95 with certain Frizzleds (Masuko et al., 1999; Yanai et al., 2000; Hering and Sheng, 2002). Furthermore, certain Wnt signalling components, such as GSK-3β and β-catenin have been amongst the multitude of proteins identified immunoprecipitation of NMDAR subunits and subsequent MALDI-TOF mass spectrometry (H. Husi, personal communication). Since glutamate signalling through the NMDAR and many NRC components is essential for barrel formation, the potential link to Wnt signalling lead to the examination of *Wnt* expression in barrel cortex and the barrel cortex of *Wnt* and *Dvl* mutants in this thesis. However, the work presented here does not address whether there was an interaction between the two signalling pathways. If a barrel phenotype was observed in any of the *Wnt*, *Dvl* or *Wnt7a*$^{-/-}$*Dvl1*$^{-/-}$ mutant mice, then this would have provided strong evidence that Wnts were required for barrel formation. Overall, there is no evidence that Wnts are involved in the cellular processes required to form barrels, despite their presence in barrel cortex throughout postnatal development. However, the barrel phenotype of many Wnts could not be tested as most Wnt mutant mice either have not been generated or die embryonically as they are crucial for early embryonic patterning events. Although cortical slice tissue culture can be used to study dendritogenesis and synaptogenesis *in vitro*, the barrel structure does not persist when cultured. Therefore any genetic or pharmacological intervention to barrel formation has to be performed *in vivo*; in essence, by pharmacological or genetic intervention of live mice. Therefore temporal and spatial conditional deletion of *Wnt* genes that were hitherto unavailable to examine is required to further investigate the roles of these other Wnts in barrel cortex development. Conditional *Wnt* mutants would permit investigation of the function of these genes in cortex, yet leave the rest of the mouse intact to grow normally.

6.7 Hypothetical Exercise: *Wnt7a*$^{-/-}$ mice exhibit a mild barrel phenotype, yet *Wnt7a*$^{-/-}$*Dvl1*$^{-/-}$ mice exhibit a total loss of barrel cortex.

6.7.1 Description of the barrel phenotypes of *Wnt7a*$^{-/-}$, *Dvl1*$^{-/-}$ and *Wnt7a*$^{-/-}$*Dvl1*$^{-/-}$ mice

In Chapter 4, I showed that both wild-type and *Dvl1*$^{-/-}$ mice have normal barrels and TCA patches segregated into a barrel-related pattern. However, for the purpose of this exercise, *Wnt7a*$^{-/-}$ mice have a mild barrel phenotype, which I define as sub-normal segregation of cortical cells into barrel structures and normal TCA segregation (similar to the P7 *Psd-95*$^{+/-}$ *Sap-102*$^{-/-}$ mutants in Chapter 4; Figure 5.30b) and *Dvl1*$^{-/-}$ mice have normal barrels and normal TCA segregation. I will discuss two potential outcomes for the *Wnt7a*$^{-/-}$*Dvl1*$^{-/-}$ mice. In Outcome 1 *Wnt7a*$^{-/-}$*Dvl1*$^{-/-}$ mice exhibit no cortical cell segregation but normal TCA patch segregation (Figure 5.30c). In Outcome 2, *Wnt7a*$^{-/-}$*Dvl1*$^{-/-}$ mice exhibit no cortical cell segregation and no TCA patch segregation (Figure 5.30d).

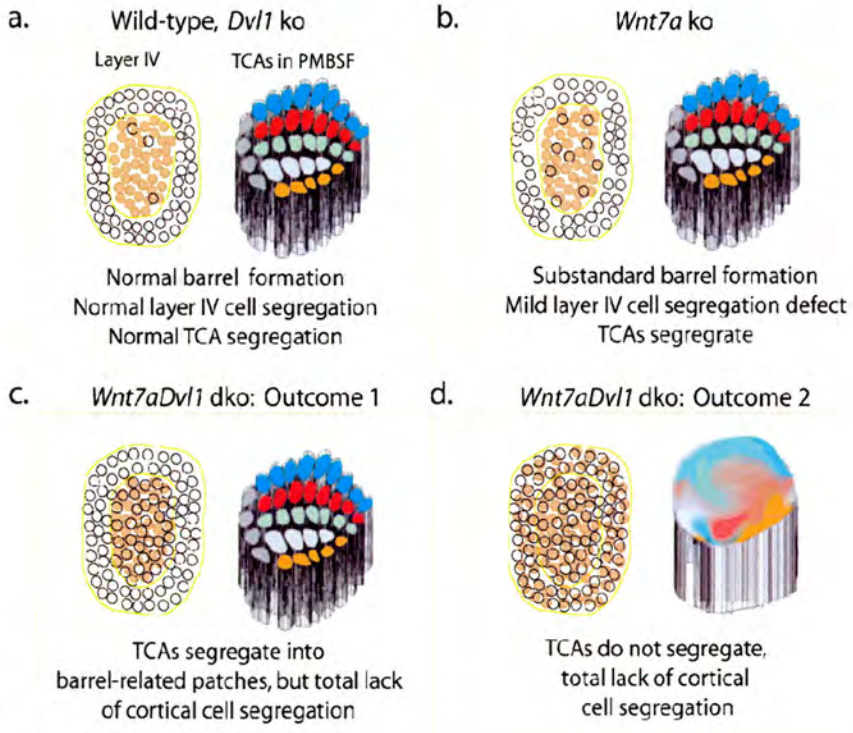

Figure 5.30
Barrel and TCA phenotypes of (a) wild-type and ***Dvl1***$^{-/-}$ mice showing normal TCA and cortical cell segregation, (b) ***Wnt7a***$^{-/-}$ showing a mild defect in cortical cell segregation, but normal TCA segregation, (c) ***Wnt7a***$^{-/-}$***Dvl1***$^{-/-}$ mice showing TCAs segregate into barrel-related patches but no cortical cell segregation occurs (Outcome 1) and (d) ***Wnt7a***$^{-/-}$***Dvl1***$^{-/-}$ mice showing TCAs do not segregate into barrel-related patches and no cortical cell segregation occurs. Open black circles represent cortical cells, tan-filled circles represent TCA terminals, and yellow lines represent the region where the barrel wall should be present.

6.7.2 Location of defects in Wnt signalling

For the purpose of this exercise it is essential to define the location of action of Wnt7a and Dvl1. Wnts may be secreted by the TCAs or cortical cells and may act in a paracrine or autocrine manner. Similarly Wnt release and/or mode of action may be dependent on glutamate activation (see Figure 5.31). Finally, Dvl1 could be acting in the postsynaptic neuron or the presynaptic terminal. Where appropriate, each of these possibilities is discussed.

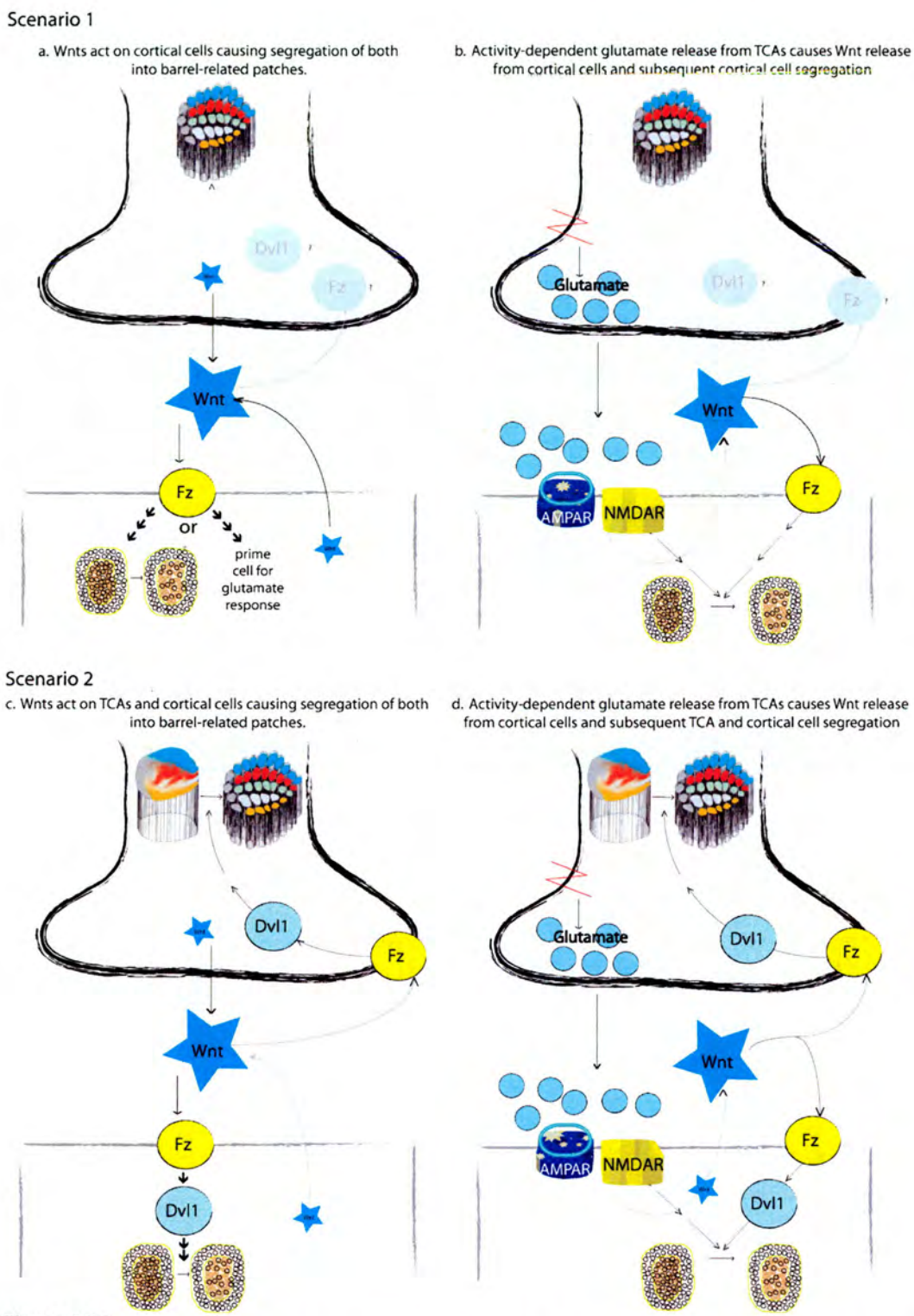

Figure 5.31
Possible locations of Wnt signalling at the TCA-cortical cell synapse. Scenario 1. (a) Wnts, produced by either TCAs or cortical cells act on cortical cells to induce segregation to form barrel walls and barrel hollows. (b) Glutamate release from TCAs causes a depolarisation of the cortical cells, causing release of Wnts (possibly in an NMDAR-dependent manner), which act on cortical cells, causing segregation into barrel walls and barrel hollows **Scenario 2.** (c) Wnts, produced by either TCAs or cortical cells act on cortical cells to induce segregation to form barrel walls and barrel hollows, and on TCAs to cause segregation into individual whisker-related patches. (d) Glutamate release from TCAs causes a depolarisation of the cortical cells that releases Wnts, which can then act as a paracrine/retrograde patterning molecule on TCAs (causing segregation) and in an autocrine manner on cortical cells (causing segregation into barrel walls and barrel hollows).

6.7.2.1 *Wnt7a*$^{-/-}$ mutants have a mild defect in barrel segregation.

The most parsimonious explanation for the phenotype described above is that Wnt7a binds to Frizzleds on layer IV cortical cells to regulate cell adhesion and/or cell migration. The source of Wnt7a could be TCAs or cortical cells (Figure 5.31a). The dependence of barrel formation on glutamate receptor activation raises the possibility that glutamate receptors regulate Wnt release from the postsynaptic cell and the Wnts have an autocrine function in regulating cell segregation (Figure 5.31b). This interpretation would be in good agreement with the findings of Rob Malenka and colleagues that Wnt release is dependent on neuronal activity (Yu and Malenka, 2003). Recently, it has been shown that Wnt release can occur in hippocampal slices via an NMDAR- and Ca^{2+}-dependent pathway (Wayman et al., 2006), adding support to this hypothesis. Alternatively, Wnt7a released from TCAs may play a permissive paracrine role, priming cortical cells and allowing them to respond to glutamate released from TCAs (Figure 5.31a).

The normal segregation of TCAs in *Wnt7a*$^{-/-}$ mice suggests that Wnt7a signalling is not required for this process. However, it is also possible that other Wnts compensate for the loss of Wnt7a to mediate TCA segregation. The large number of *Wnts* present in the developing somatosensory cortex (see Chapter 3) and the high promiscuity of signalling between Wnts and Frizzleds (Cadigan and Liu, 2006) could form the basis of this compensation. This possibility could be addressed by generating compound mutants of Wnt signalling pathway components or by acutely blocking Wnt signalling pharmacologically. An example for the requirement for deletion of two *Wnt* genes to reveal a phenotype is that of the regulation of thymocyte development in embryonic mouse. Deletion of either *Wnt1* or *Wnt4* reduces the number of thymocytes produced, but does not affect the pattern of maturation. Deletion of both *Wnt1* and *Wnt4* reveals a greater reduction of thymocytes and severely disrupts the pattern of thymocyte maturation (Mulroy et al., 2002).

Similarly, it is possible that Wnt7a is the only Wnt involved in the normal development of barrels and the partial defect in cortical cell segregation in *Wnt7a*$^{-/-}$ results from compensation by other Wnts or Wnt signalling components. However, this compensation is not sufficient for normal segregation to occur.

6.7.2.2 A Role for Dvl in barrel formation.

The finding that *Dvl1*$^{-/-}$ mutants have normal barrels would, at first glance, indicate that Dvl1 was playing little or no role in barrel formation. However, as with analysis of all mutants, these data would not rule out a role for Dvl1 in barrel development since compensation either by other Dvls or by other Wnt signalling components could mediate normal barrel formation. Such a compensatory mechanism appears to be taking place in this hypothetical scenario since *Wnt7a*$^{-/-}$*Dvl1*$^{-/-}$ mice show a much more severe phenotype than either single mutant alone. Assuming that this difference is not due to differences in the genetic background of the *Wnt7a*$^{-/-}$, *Dvl1*$^{-/-}$ and *Wnt7a*$^{-/-}$*Dvl1*$^{-/-}$ mice (see Materials and Methods chapter), these findings indicate that Dvl1 does play a role in barrel development and normal TCA patterning (depending on whether TCAs segregate); however, loss of *Dvl1* alone can be compensated for, most likely by Wnt/Fz signalling through other Dvls.

As noted above, I will discuss two possible outcomes for the phenotype of the *Wnt7a*$^{-/-}$*Dvl1*$^{-/-}$ mice. In Outcome 1, these mice show a complete lack of barrel formation, but TCAs segregate normally. In Outcome 2, these mice show a complete lack of barrel formation and TCA do not segregate into whisker related patches.

6.7.2.3 Outcome 1: Wnt7a$^{-/-}$Dvl1$^{-/-}$ mice lack barrels but have normal TCA segregation

Since TCAs segregate normally in *Wnt7a*$^{-/-}$ and *Wnt7a*$^{-/-}$*Dvl1*$^{-/-}$ mice, the location of the defect in barrel formation is likely postsynaptic. Wnt7a may be produced from either the presynaptic terminal or the postsynaptic cell to act on the cortical cells (Figure 5.31a,b). Since *Dvl1*$^{-/-}$ mice have normal barrels, yet *Wnt7a*$^{-/-}$*Dvl1*$^{-/-}$ mice do not, this suggests that in the presence of Wnt7a, the loss of Dvl1 can be completely compensated possibly by Wnt7a signalling through Dvl2 or Dvl3 (Dvl2/3). In the absence of Wnt7a and Dvl1, other Wnts or Wnt signalling components that partially compensating for the loss of Wnt7a, can now only signal through Dvl2/3 and this is insufficient for any cortical cell segregation to occur. A full model is presented in Figure 5.33.

6.7.2.4 Outcome 2: Wnt7a$^{-/-}$Dvl1$^{-/-}$ mice lack both barrels and TCA segregation.

While the very disturbed phenotype in the double mutant indicates a role for both Wnt7a and Dvl1 in barrel development, the complete lack of TCA segregation (and hence barrel formation) gives little additional insight into the locus of action for Wnt7a and Dvl1. Wnt7a

could be produced by the TCAs, and act in an autocrine manner on the TCA terminals to mediate segregation into whisker related patches. Alternatively, the Wnt signal responsible for TCA-patterning could be produced by the cortical cells (perhaps induced by glutamate signalling from TCAs on cortical cells) and act as a retrograde messenger for TCA terminals to mediate TCA segregation (Figure 5.31c,d). In *Dvl1*$^{-/-}$ mice, compensation from other Dvls is sufficient to permit normal TCA segregation, but in *Wnt7a*$^{-/-}$*Dvl1*$^{-/-}$ mice the Wnts that are expressed to compensate for the lack of Wnt7a, signalling through Dvl2/3 is not sufficient for TCA segregation to occur. A full model is presented in Figure 5.34.

6.7.2.4.1 Threshold levels of Wnt activation

In order to explain on how different Wnt/Frizzled combinations signal through different Dishevelleds to generate the phenotypes observed in each mutant mouse in this exercise, I would like to introduce a hypothetical signalling molecule downstream of the Dishevelleds that induces the changes required for barrel formation and/or TCA segregation. For the sake of brevity in discussion, I shall refer to the hypothetical signalling molecule as DISM—Dishevelled-related intracellular signalling molecule. Each mutant has a different capability of raising DISM levels, and various threshold levels of DISM are required for the cortical cell and/ or TCA segregation events to occur (Figure 5.32).

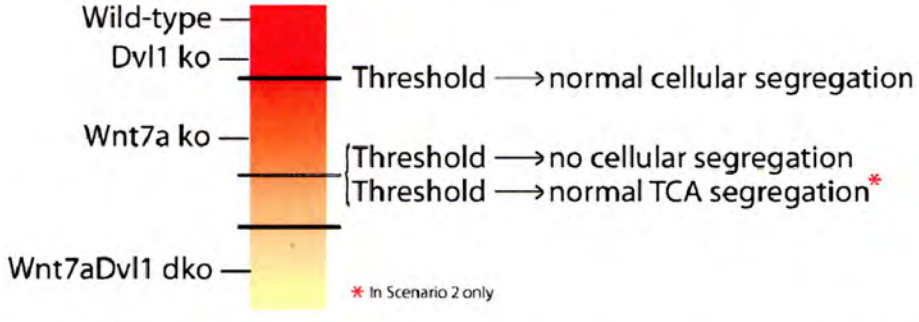

Figure 5.32
Levels of activation of DISM by each genotype in this exercise. Wild-type and *Dvl1*$^{-/-}$ mice raise levels of DISM above threshold levels required for normal barrel formation. In *Dvl1*$^{-/-}$ mice, sufficient compensation for the loss of *Dvl1* by other Dvls occurs and normal barrels are formed. In *Wnt7a*$^{-/-}$ mice, compensatory signalling from other Wnts is sufficient to raise DISM levels above a threshold for some segregation to occur, but not to levels where normal segregation can take place. In *Wnt7a*$^{-/-}$*Dvl1*$^{-/-}$ mutants, DISM levels are below the level required for any cortical cell and/ or TCA segregation to occur (see the description in text of the mechanisms that could underlie the *Wnt7a*$^{-/-}$*Dvl1*$^{-/-}$ phenotype for further information).

Thus, the compensatory upregulation of other Dvls in *Dvl1*$^{-/-}$ mice raises DISM levels above the threshold required for normal cellular segregation (and also TCA patterning in Outcome 2). The compensation in *Wnt7a*$^{-/-}$ mice is only partial; DISM levels are raised to a point where some cellular segregation occurs, but not enough for normal barrels to be observed (but still

above the threshold required for normal TCA segregation to occur in Outcome 2). In *Wnt7a*$^{-/-}$ *Dvl1*$^{-/-}$ mice, compensation by other Wnts and other Dvls is not sufficient for DISM levels to reach the threshold required for any cellular segregation (or also TCA segregation in Outcome 2), see Figure 5.32. The molecules (or combination of molecules) that might mediate the role of DISM are discussed below in Section 6.7.3.

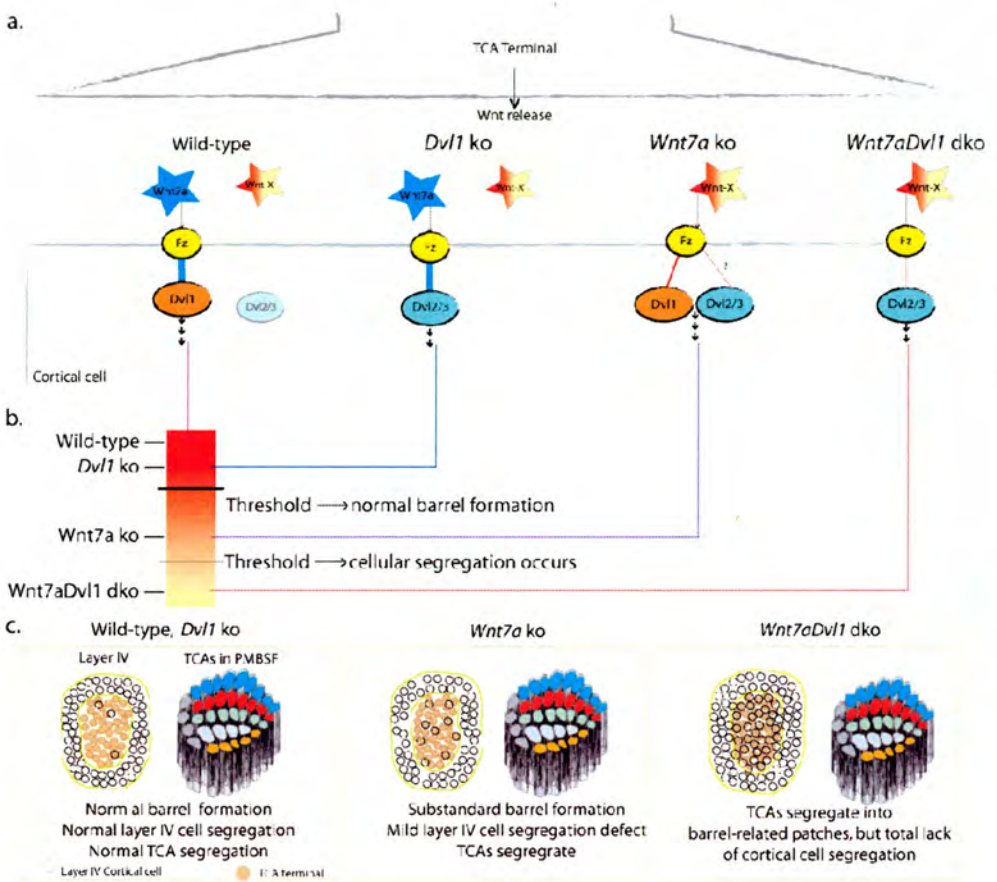

Figure 5.33
Outcome 1: Wnt signalling through Dishevelleds is required for cortical cell segregation. In wild type mice, Wnt7a signals through Frizzled(s) through Dvl1 (a), raising downstream effector molecules (DISM) to a level above what is required (b) for normal cortical cell segregation (c). Other Wnts (Wnt-X) and Dvls are present in this system. When *Dvl1* is lost, sufficient compensatory signalling through Dvl2/3 occurs (a) to raise the levels of signalling effector molecules above a threshold level (b) required for normal cortical cell segregation (c). When Wnt7a is knocked out, Wnt-X signal through Dvl1 (and possibly Dvl2/3); DISM levels are below the level for normal cellular segregation (b), although not low enough to abolish all cellular segregation (c). When both *Wnt7a* and *Dvl1* are knocked out, only weak stimulation of Dvl2/3 occurs from Wnt-X (a). Levels of effector molecules are too low to pass the threshold (b) for even partial cellular segregation (c).

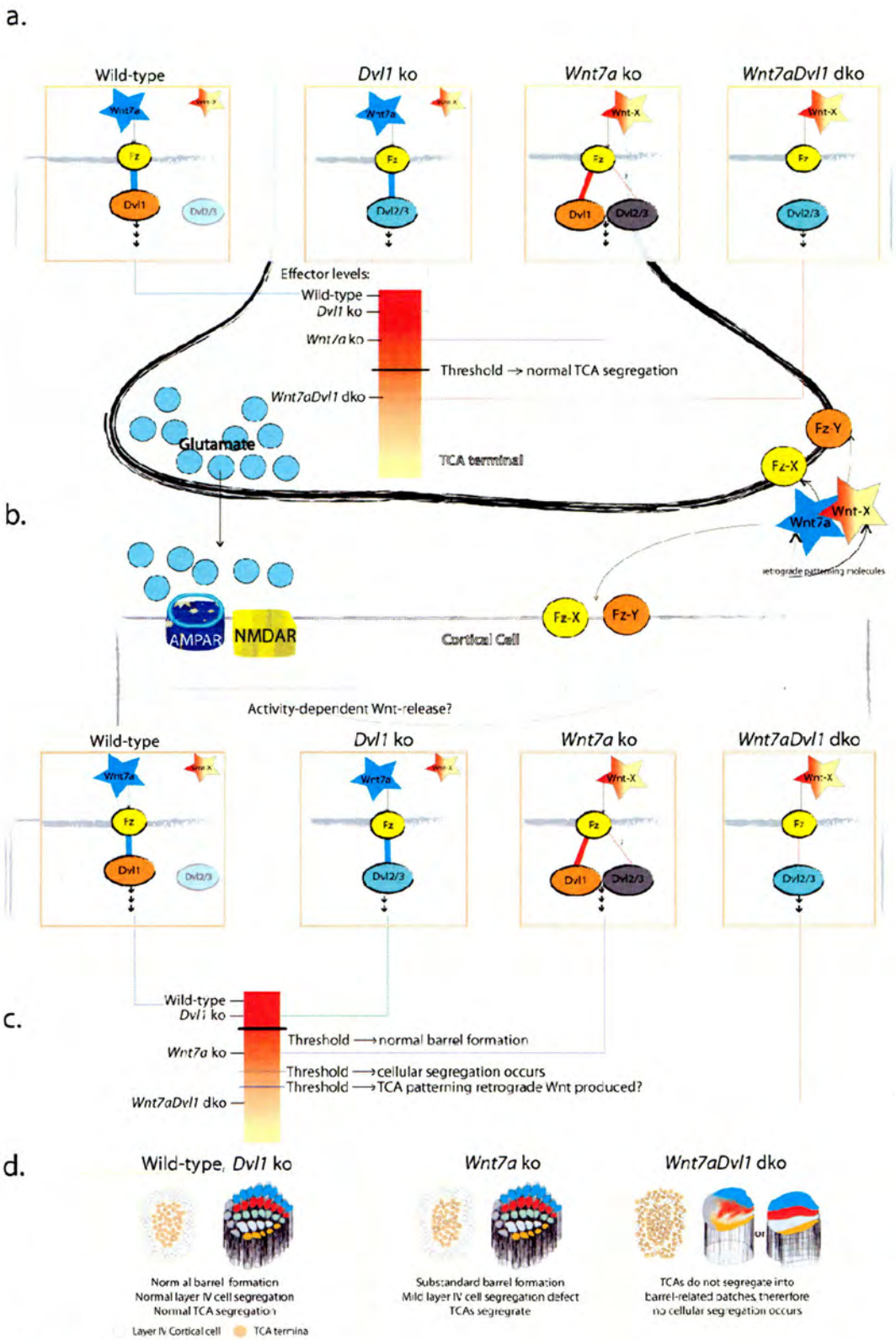

Figure 5.34

Outcome 2: Wnt signalling through Dishevelleds is required for cortical cell and TCA segregation. (a) Presynaptic events. Wnt7a signals through Dvl1 and the levels of DISM are raised sufficiently to permit TCA segregation. *Dvl1*$^{-/-}$ mutants still have normal TCA segregation, as compensatory upregulation of Dvl2/3 compensates sufficiently for the lack of Dvl1. *Wnt7a*$^{-/-}$ mutants have normal TCAs, as other Wnts (Wnt-X) can compensate for the loss of Wnt7a, and raising DISM levels above a threshold required for TCA segregation. *Wnt7a*$^{-/-}$*Dvl1*$^{-/-}$ mice do not raise DISM levels beyond the threshold required for TCA segregation. Insufficient compensation by Wnt-X and Dvl2/3 has occurred. (b) Glutamate/Activity dependent Wnt release from postsynaptic cells may provide Wnt signal for TCAs in a paracrine manner, or cortical cells in an autocrine manner. (c) In wild type mice, Wnt7a signals through Frizzled(s) through Dvl1, raising DISM levels above what is required for normal cortical cell segregation. When *Dvl1* is lost, sufficient compensatory signalling

through Dvl2/3 occurs to raise the levels of signalling effector molecules above a threshold level required for normal cortical cell segregation. When Wnt7a is knocked out, Wnt-X signal through Dvl1 (and possibly Dvl2/3); DISM levels are below the level for normal cellular segregation, although not low enough to abolish all cellular segregation. When both *Wnt7a* and *Dvl1* are knocked out, only weak stimulation of Dvl2/3 occurs from Wnt-X. Levels of effector molecules are too low to pass the threshold for production of a retrograde signal for TCA patterning. These are all possible mechanisms for generating the phenotypes observed in (d), with Wild-type and *Dvl1*$^{-/-}$ mice having normal barrels and TCA patterning, *Wnt7a*$^{-/-}$ mice having normal TCAs, but poorly segregated cortical cells, and *Wnt7a*$^{-/-}$*Dvl1*$^{-/-}$ mice lacking both TCA and cortical cell segregation.

6.7.3 Possible effector molecules

Many *Wnts* and all *Frizzleds* are expressed in barrel cortex during its development (Chapter 3, Shimogori et al., 2004) so it is likely that all Wnt signalling pathways are involved in barrel formation (Figure 5.35). The Wnt/β-catenin pathway can result in TCF/LEF-mediated transcription (Figure 5.35d). In BAT-gal mice, where β-galactosidase is provided as an artificial substrate for the TCF/LEF factors activated by Wnt/β-catenin pathway signalling, strong staining is observed throughout the neocortex (Maretto et al., 2003). One the target genes of β-catenin-mediated TCF/LEF transcription is *NT-3*, a neurotrophin involved in cell survival in many brain structures (Mount et al., 1994; Giehl et al., 2001; Barnabe-Heider and Miller, 2003). Since *Wnt2b* and *Frizzled 3* have been shown to be expressed in barrel walls (Shimogori et al., 2004) then Wnt signalling in the barrel walls may cause selective cell survival within that region, whilst cell death occurs in the region of TCA terminals leading to the generation of the barrel hollow. Another possibility is that β-catenin, generated by Wnt-mediated inhibition of GSK-3β, might bind cadherins, leading to selective cell adhesion around the barrel wall (Figure 5.35b). Notably, β-catenin can bind Cadherin-8 (Kido et al., 1998) and glutamate release by TCAs abolishes *Cdh-8* expression in presumptive barrel hollow.

One potential reason for poorly defined barrels in *Wnt7a*$^{-/-}$ mice could be that Wnt7a is required to signal via the Wnt/Ca^{2+} pathway, through PLC (perhaps even synergistically with mGluR5 through PLCβ_1, Figure 5.35a) to increase production of IP_3 and DAG from PIP_2. This tonic PLCβ_1 activation by Wnt7a may produce optimally segregated barrel walls and septae, via the same pathways that mGlur5/PLCβ_1 signalling employs. Loss of Wnt7a would therefore lead to sub-normal cortical cell segregation. Furthermore, IP_3 acts to release Ca^{2+} from calcium ion stores and this Ca^{2+} can activate calmodulin. Ca^{2+}-calmodulin can activate PKC and PKA. While the signalling pathways that are required to form barrels downstream of the substrates of PKA, PLCβ_1, Adenylate Cyclase I and SynGAP are unknown, it is known that in the hippocampus PKC can interact with two PCP signalling molecules, Rac and Rho. PKC can act through Rac- and Rho- dependent mechanisms to modulate dendritic morphology (Pilpel and Segal, 2004). This alteration in dendritic cytoskeleton may provide

the "pushing" required by the neuropil (Figure 5.35c) which is one of the potential mechanisms hypothesised to form barrels (Barnett et al., 2006b). Although the Upton et al. paper demonstrates that in *Plc-β1*$^{-/-}$ mice, dendrites in cortical cells still orient towards the TCA patch plexus despite the lack of cortical barrels, this does not preclude Wnt/Ca^{2+} or Wnt/PCP pathway signalling from causing neurites to protrude from cortical cell somata during the early stages of barrel formation at around P4. Alternatively, elevated intracellular Ca^{2+} levels can lead to cell death (Schanne et al., 1979; Trump and Berezesky, 1995; Kroemer and Reed, 2000; Orrenius et al., 2003), so perhaps Wnt7a signalling through the Wnt/Ca^{2+} pathway in cortical cells that are located in the regions of TCA patches leads to a large calcium-induced calcium response, generating an intracellular Ca^{2+} levels great enough to start programmed cell death, generating barrel hollows.

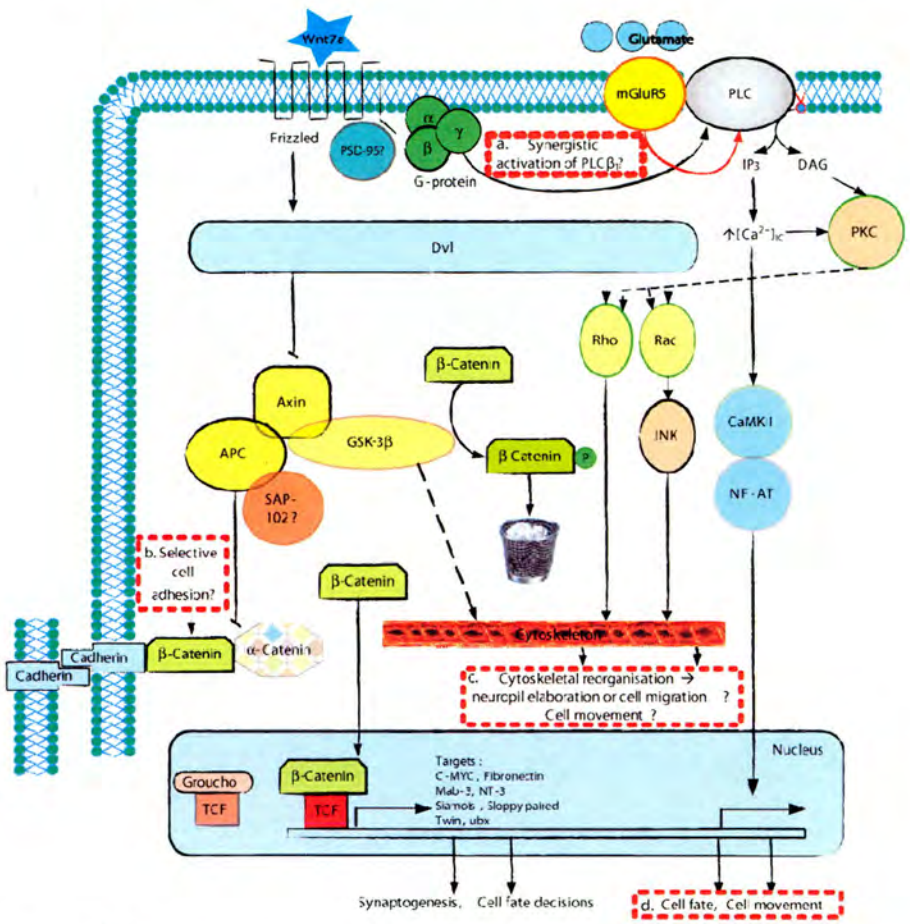

Figure 5.35
Wnt signalling pathways. (a) The Wnt/Ca2+ pathway (Blue). Activation of the Wnt/Ca2+ pathway results in intracellular Ca^{2+} release and activation of CaMKII and PKC in a β-catenin-independent manner, with a potential requirement for G proteins in this pathway. This pathway could play a synergistic role in PLCβ1-mediated cellular segregation that forms barrels. (b, c, d) Canonical/β-catenin pathway (Yellow). Wnt activation of Frizzled causes signalling through Dishevelled, resulting in inhibition of GSK-3β mediated phosphorylation (and subsequent degradation of β-catenin). β-catenin accumulates, translocates to the nucleus, binds TCF and the complex causes transcription of target genes, which can alter cell fate and cell movement (d). GSK3β inhibition can alter the phosphorylation state of microtubule associated proteins and change in cytoskeletal organisation; this could affect neuropil elaboration and cell migration (c). β-catenin can also interact with cadherins and catenins, and cause cell adhesion and dendritic arborisation (b). The PCP pathway (red). Wnt activation of Frizzled causes signalling through Dishevelled, which then signals to

Rac and/ or Rho; Rac activation can signal through JNK, and activation of either Rac or Rho can result in cytoskeletal shape change (c) and also transcription in the nucleus (d).

6.7.4 Further work

The next steps in investigating the barrel phenotype in *Wnt7a*$^{-/-}$ and *Wnt7a*$^{-/-}$*Dvl1*$^{-/-}$ mice would be to investigate the dendritic orientation in each of these mutants, using a histological method that completely labels dendrites of cortical cells and also TCA patches, such as the rapid Golgi method utilised in the Upton et al. paper. Examination of the earlier somatosensory relay stations in the trigeminal neuraxis should be performed to determine where any TCA patterning defects actually originate. If the defect in *Wnt7a*$^{-/-}$*Dvl1*$^{-/-}$ mice is found to be present in VpM thalamus, the proposed model (Figure 5.34) needs only to be modified to shift the presynaptic site of Wnt action from TCA terminals to the thalamus, although no paracrine Wnt signalling could occur from the cortical cells, rather Wnt signal has to be produced in the thalamus.

Further in-depth characterisation of the barrel phenotype, such as quantification of cell densities in barrel walls and hollows with propidium iodide and confocal microscopy (Barnett et al., 2006a; Watson et al., 2006b) would need to be performed prior to publication of this phenotype. Additional methods of investigation include the cross breeding of *Wnt7a*$^{-/-}$ mice with other *Wnt* and *Dvl* knockout mice (*Dvl2*$^{-/-}$ mice exist, Hamblet et al., 2002, but *Dvl3*$^{-/-}$ mice have not yet been generated) and assessing the barrel phenotype of these mice to assess which Wnts might be compensating for the loss of *Wnt7a*. Cross breeding other *Wnt* mutants with each *Dvl* mutant and characterisation of the barrel phenotypes for all of these mice might reveal additional Wnts that are involved in barrel formation that are unmasked by the loss of a *Dvl* gene. Conditional knockouts of *Wnt* genes, restricted to the cortex, would permit investigation and characterisation of *Wnt* genes that are ordinarily embryonic and perinatally lethal when systemically knocked out. Again, each mutant could be cross-bred with other *Wnt* and *Dvl* mutants to assess the contribution of each gene to the barrel phenotype. Examination of *Frizzled* mutants may also reveal which receptor any given Wnt might signal through, although since a single Wnt may signal through more than one Frizzled, the redundancy in this system might mask the role of any Frizzled.

One advantage of cortex specific knockouts would be to address whether Wnt genes, expressed in cortical cells act as retrograde signalling molecules to pattern TCAs. There is evidence for the presence of a retrograde messenger in barrel formation. *CxNr1*$^{-/-}$ mice have the NMDAR NR1 subunit knocked out only cortical cells. Barrels do not form, and TCAs do

segregate into patches, although these patches are smaller and less well defined, despite the genetic defect in these mice being restricted to the postsynaptic partner of the TCAs (Iwasato et al., 2000; Datwani et al., 2002a). Furthermore, mGluR5 has been shown to signal through PLCβ_1 to form barrels, although the TCA phenotype for each mutant differs (Hannan et al., 2001). *Mglur5*$^{-/-}$ mutants have TCAs that cluster into rows but not into individual barrels, whereas *Plc-β1*$^{-/-}$ mice have TCAs that segregate into individual whisker-related patches. Neither *Mglur5*$^{-/-}$ nor *Plc-β1*$^{-/-}$ mice have barrels (Hannan et al., 2001) and it as been hypothesised that a retrograde signalling factor that directs the segregation of the rows of TCAs into individual barrels is produced by *Plc-β1*$^{-/-}$ mice but not by *Mglur5*$^{-/-}$ mice. Recent work in our laboratory has demonstrated that mGluR5 is expressed exclusively postsynaptically in barrel cortex (Personal communication, P. Kind) strongly suggesting the presence of an as-yet unidentified retrograde TCA patterning signal, which could be Wnt7a. Wnt7a has been identified as retrograde signalling factors that cause axonal remodelling in the cerebellum (Hall et al., 2000; Salinas, 2005).

7 Appendix A: Global interaction map of the NMDA receptor complex

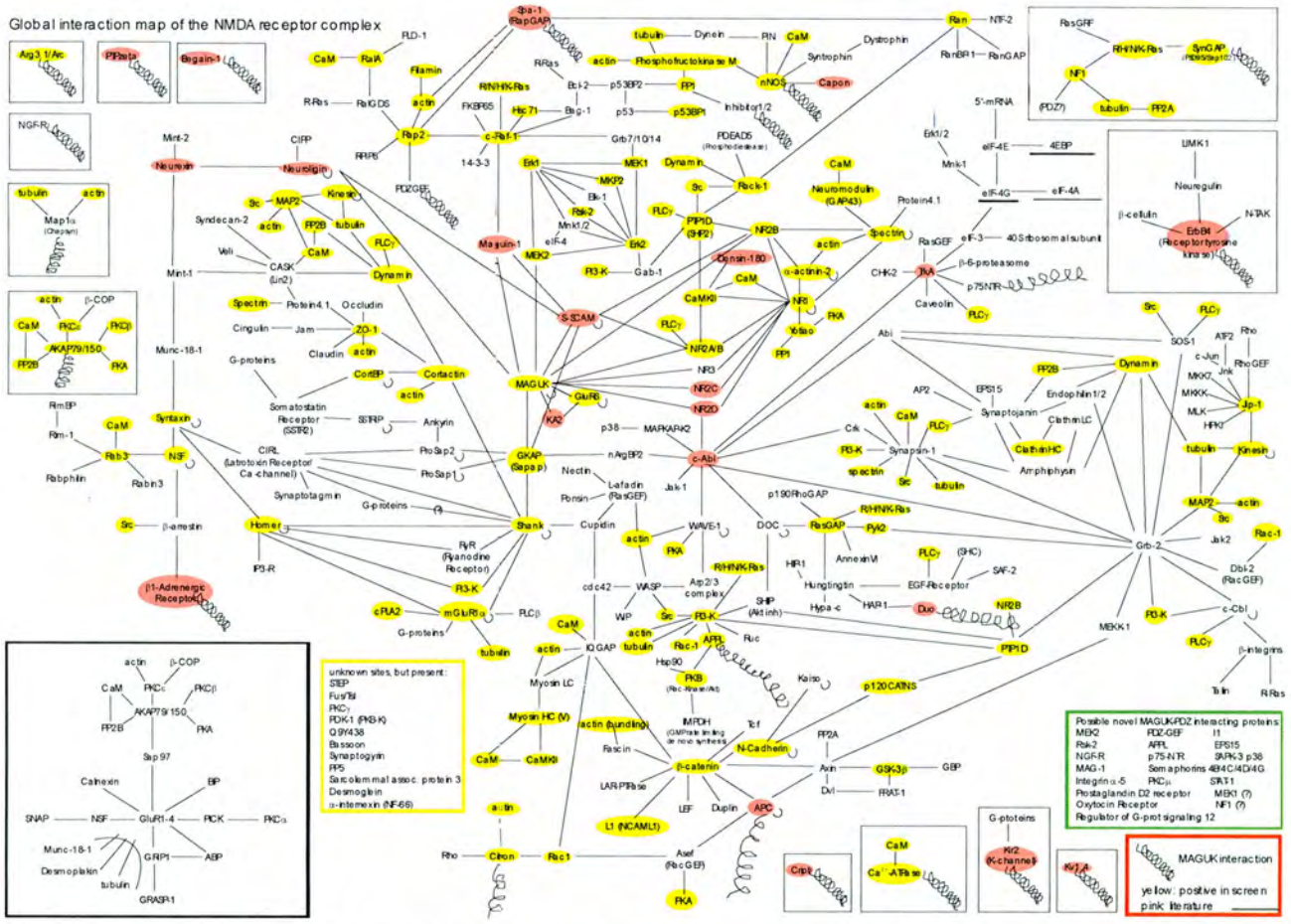

Figure 7.1 Global interaction map of the NMDA receptor complex.
Drawn by Dr. H. Husi. of Team 32, Sanger Centre, Hinxton, Cambridgeshire, UK..
Spiral connectors represent an interaction of a MAGUK with the linked protein, proteins with a pink background represent interactions reported in the literature, whereas proteins with a yellow background represent protein interactions that have been discovered in the NRC screening experiments detailed in Husi et al., (2000)

8 Appendix B: Assembly NRC components at PSD-containing synapses

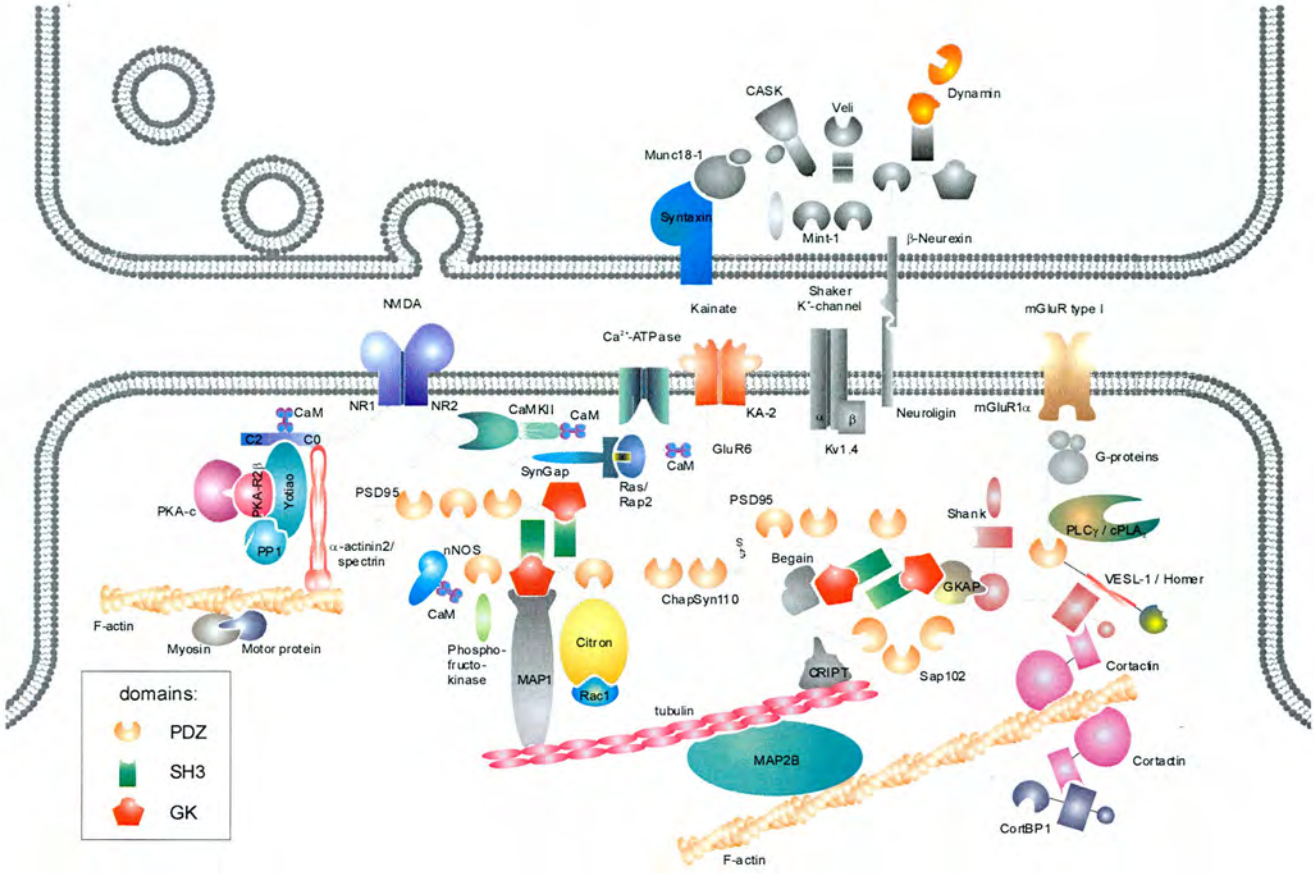

Figure B.1
Putative assembly of proteins found in the NMDA receptor (NMDAR) complex. Molecules found in the analysis of the NMDAR complex are depicted and interactions based on published profiles. Proteins which are shown in grey were not found in our screens, although this does not mean they are present within the network. Some proteins which are composed of known domains are shown in a modular fashion, e.g. PSD-95 with three PDZ-domains, a SH3 domain and a guanylate kinase (GK) domain (see also key). Abbreviations: CaM, calmodulin; CaMKII, calcium calmodulin kinase II; MAP, microtubule associated protein; mGluR, metabotropic glutamate receptor; .nNOS, neuronal nitric oxide synthase; NR1, NMDA receptor subunit 1; PLA, phospholipase A; PLC phospholipase C; PKA, protein kinase A; PP1, protein phosphatase 1; PSD-95, post synaptic density 95. Adapted from Husi and Grant, 2001.

9 Appendix C Interaction partners of PSD-95 in the literature

Name Of Interactor	Experiment Type	Type	Reference
Frizzled 1	In Vivo, Yeast 2 Hybrid	Direct	(Hering and Sheng, 2002)
Frizzled 2	In Vivo, Yeast 2 Hybrid	Direct	(Hering and Sheng, 2002)
Frizzled 4	In Vivo, Yeast 2 Hybrid	Direct	(Hering and Sheng, 2002)
Frizzled 7	In Vivo, Yeast 2 Hybrid	Direct	(Hering and Sheng, 2002)
APC	In Vivo, In Vitro, Yeast 2 Hybrid	Complex	(Kiyono et al., 1997), (Yanai et al., 2000)
SynGAP	In Vivo, In Vitro, Yeast 2 Hybrid	Direct	(Kim et al., 1998)
NR1	In Vivo, In Vitro	Direct	(Rutter et al., 2002) (Allison et al., 1998) (Hughes et al., 2001) (Papadakis et al., 2004), (Ying et al., 2004) (Wyszynski et al., 1997)
NR2A	In Vivo, In Vitro, Yeast 2 Hybrid	Direct	(Lim et al., 2002), (Kornau et al., 1995)
NR2B	In Vivo, In Vitro, Yeast 2 Hybrid	Complex	(Kiyono et al., 1997), (Yanai et al., 2000)
NR2B	In Vivo, In Vitro, Yeast 2 Hybrid	Direct	(Kornau et al., 1995), (Niethammer et al., 1998)
NR2B	In Vivo, In Vitro, Yeast 2 Hybrid	Direct	(Kornau et al., 1995), (Niethammer et al., 1998), (Lim et al., 2002)
NR2C	In Vivo, In Vitro, Yeast 2 Hybrid	Direct	(Lim et al., 2002), (Kornau et al., 1995)
NR2D	In Vivo, In Vitro, Yeast 2 Hybrid	Direct	(Kornau et al., 1995)
NR3A	In Vivo, In Vitro, Yeast 2 Hybrid	Direct	(Kornau et al., 1995)
NR3B	In Vivo, In Vitro, Yeast 2 Hybrid	Direct	(Kornau et al., 1995)
SAP-102	In Vitro, In Vivo, Yeast 2 Hybrid	Direct	(Masuko et al., 1999)
PSD-95	In Vivo	Direct	(Hsueh et al., 1997)
PSD-95	In Vivo, In Vitro, Yeast 2 Hybrid	Direct	(Hu et al., 2000)
kainate 2	In Vivo, In Vitro	Direct	(Hirbec et al., 2003)
kainate 1	In Vitro, In Vivo	Direct	(Hirbec et al., 2003)
kainate 1	In Vitro, In Vivo	Direct	(Hirbec et al., 2003)
5-HT receptor 2C	In Vivo	Direct	(Becamel et al., 2002)
GRIK5	In Vivo, In Vitro	Direct	Mehta et al., 2001
5-HT-2A receptor	In Vitro, In Vivo	Direct	(Xia et al., 2003)
5-HT-2A receptor	In Vivo	Direct	(Xia et al., 2003)
Low density lipoprotein receptor-related protein 1	In Vitro, Yeast 2 Hybrid	Direct	Gotthardt et al., 2000
PKCα	In Vivo	Direct	(Lim et al., 2002)
SAPAP4	In Vitro, Yeast 2 Hybrid	Direct	(Takeuchi et al., 1997)
Discs large associated protein 2	In Vitro	Direct	(Satoh et al., 1997)
K^+ voltage gated channel subfamily A member 2	In Vitro, Yeast 2 Hybrid	Direct	(Eldstrom et al., 2002)
Ca^{2+} channel, voltage	In Vivo, Yeast 2 Hybrid	Direct	(Choi et al., 2002)

dependent, γ subunit 2			
MAP3K10	In Vitro	Direct	Savinainen et al., 2001
Citron	In Vivo, Yeast 2 Hybrid	Direct	Zhang et al., 1999
A kinase anchor protein 5	In Vivo, In Vitro	Direct	(Colledge et al., 2000)
Actinin alpha 2	In Vitro	Direct	(Eldstrom et al., 2002)
Adrenergic receptor, Beta 1	In Vivo, In Vitro, Yeast 2 Hybrid	Direct	(Hu et al., 2000)
Amiloride sensitive cation channel 3	In Vivo, Yeast 2 Hybrid	Direct	Hruska-Hageman et al., 2004
BEGAIN1	In Vitro, In Vivo, Yeast 2 Hybrid	Direct	(Deguchi et al., 1998)
BEGAIN2	In Vitro, In Vivo, Yeast 2 Hybrid	Direct	(Deguchi et al., 1998)
Brain enriched guanylate kinase associated protein	In Vitro, In Vivo, Yeast 2 Hybrid	Direct	(Deguchi et al., 1998)
Brain specific angiogenesis inhibitor 1	In Vivo	Direct	(Lim et al., 2002)
CASK	In Vivo, Yeast 2 Hybrid	Direct	(Chetkovich et al., 2002)
CASK	In Vivo, Yeast 2 Hybrid	Direct	(Chetkovich et al., 2002)
CD46	In Vivo, Yeast 2 Hybrid	Direct	Ludford-Menting et al., 2002
Channel associated protein of synapse 110	In Vivo	Direct	(Hsueh et al., 1997)
Connector enhancer of kinase suppressor of Ras 2	In Vitro, In Vivo, Yeast 2 Hybrid	Direct	Yao et al., 1999
c-Yes	In Vivo	Direct	(Tezuka et al., 1999)
DAP1	In Vitro, In Vivo, Yeast 2 Hybrid	Direct	(Kim et al., 1997)
DAP1	In Vivo, In Vitro	Direct	(Kim et al., 1997), (Satoh et al., 1997)
DAP1	In Vitro, Yeast 2 Hybrid	Direct	(Takeuchi et al., 1997)
Death associated protein	In Vivo	Direct	(Satoh et al., 1997)
Discs large associated protein 2	In Vitro, Yeast 2 Hybrid	Direct	(Takeuchi et al., 1997)
Dynein light chain 1	In Vitro	Direct	Navarro-Lerida et al., 2004
Dynein light chain 2	Yeast 2 Hybrid	Complex	(Naisbitt et al., 2000)
Dynein light chain 2	In Vivo, In Vitro	Direct	(Naisbitt et al., 2000)
E6 targeted protein 1	In Vitro, In Vivo, Yeast 2 Hybrid	Direct	Pak et al., 2001
ERBB2	In Vivo, Yeast 2 Hybrid	Direct	(Huang et al., 2000)
ErbB4	In Vivo, In Vitro, Yeast 2 Hybrid	Direct	(Garcia et al., 2000)
Erbin	In Vivo	Direct	(Huang et al., 2000)
Focal adhesion kinase 2	In Vivo, In Vitro	Direct	(Seabold et al., 2003)
Fyn	In Vivo	Direct	Hou et al., 2002
Glial inwardly rectifying potassium channel Kir4.1	In Vitro, In Vivo, Yeast 2 Hybrid	Direct	Horio et al., 1997
Guanylate cyclase 1 soluble alpha 2	In Vivo, In Vitro	Direct	(Russwurm et al., 2001)
Hrs	In Vivo, Yeast 2 Hybrid	Direct	(Chetkovich et al., 2002)
Interleukin 13 receptor, alpha 1	In Vivo, In Vitro, Yeast 2 Hybrid	Direct	(Kornau et al., 1995)

Inward rectifier potassium channel 4	In Vivo, Yeast 2 Hybrid	Direct	(Nehring et al., 2000)
KCNA5	In Vivo, In Vitro, Yeast 2 Hybrid	Direct	(Eldstrom et al., 2002)
KCND2	In Vitro, Yeast 2 Hybrid	Direct	(Eldstrom et al., 2002)
Kinesin family member 1B	In Vivo, In Vitro, Yeast 2 Hybrid	Direct	Mok et al., 2002
K^+v1.3	In Vitro, Yeast 2 Hybrid	Direct	(Eldstrom et al., 2002)
Lano	In Vivo, In Vitro, Yeast 2 Hybrid	Direct	Saito et al., 2001
Low density lipoprotein related protein 2	In Vivo, In Vitro, Yeast 2 Hybrid	Direct	(Larsson et al., 2003)
Lyn	In Vivo	Direct	(Tezuka et al., 1999)
Microtubule associated protein 1A	In Vivo, In Vitro, Yeast 2 Hybrid	Direct	(Brenman et al., 1996b)
MINT1/CASK/Veli3	In Vivo	Complex	(Becamel et al., 2002)
NADPH dependent diflavin oxidoreductase 1	In Vivo, In Vitro, Yeast 2 Hybrid	Direct	(Kornau et al., 1995)
Neuroligin 1	In Vitro, Yeast 2 Hybrid	Direct	(Irie et al., 1997)
Neuroligin 2	In Vitro, Yeast 2 Hybrid	Direct	(Irie et al., 1997)
Neuroligin 3	In Vitro, Yeast 2 Hybrid	Direct	(Irie et al., 1997)
Neuroligin 3	In Vitro, Yeast 2 Hybrid	Direct	(Irie et al., 1997)
Neuroligin 4	In Vivo	Direct	Bolliger et al., 2001
Nitric oxide synthase 1	In Vivo, Yeast 2 Hybrid	Direct	Brenman et al., 1996a
Plasma membrane Ca^{2+} ATPase type 4	In Vitro	Direct	(DeMarco and Strehler, 2001)
Plasma membrane Ca^{2+} ATPase, type 2	In Vitro	Direct	(DeMarco and Strehler, 2001)
Postsynaptic protein CRIPT	In Vivo, In Vitro, Yeast 2 Hybrid	Direct	(Niethammer et al., 1998)
K^+ channel, inwardly rectifying, J2	In Vivo, Yeast 2 Hybrid	Direct	(Nehring et al., 2000)
K^+ channel, inwardly rectifying, J2	In Vivo	Direct	(Nehring et al., 2000)
K^+ channel, voltage gated, shaker 4	In Vivo, In Vitro, Yeast 2 Hybrid	Direct	(Eldstrom et al., 2002), Kim and Sheng, 1996
K^+ voltage gated channel, shaker 1	In Vitro, Yeast 2 Hybrid	Direct	(Eldstrom et al., 2002), Kim and Sheng, 1996
Protein tyrosine phosphatase, receptor-type, γ	In Vivo, In Vitro, Yeast 2 Hybrid	Direct	Kawachi et al., 1999
RICS	In Vivo	Direct	Okabe et al., 2003
SAPAP3	In Vitro, Yeast 2 Hybrid	Direct	(Takeuchi et al., 1997)
Semaphorin 4C	In Vivo, In Vitro, Yeast 2 Hybrid	Direct	(Inagaki et al., 2001)
Semaphorin 4C	In Vivo, In Vitro, Yeast 2 Hybrid	Direct	(Inagaki et al., 2001)
SEMAW	In Vivo, Yeast 2 Hybrid	Direct	Schultze et al., 2001
SH3 and multiple ankyrin repeat domains 1	In Vivo, In Vitro	Direct	(Naisbitt et al., 1999)

SH3 and multiple ankyrin repeat domains 2	In Vitro, Yeast 2 Hybrid	Direct	Boeckers et al., 1999
Tamalin	In Vitro, In Vivo, Yeast 2 Hybrid	Direct	Kitano et al., 2003
TANC	In Vitro	Direct	Suzuki et al., 2005
Veli 1	In Vitro	Direct	(Jo et al., 1999)
Veli 2	In Vivo	Direct	(Jo et al., 1999)

10 Appendix D: Interaction partners of SAP-102 in the literature

Name Of Interactor	Experiment Type	Type	Reference
NR1 (via SynGAP)	In Vivo	Complex	Kim et al., 1998
NR2A,	In Vivo, In Vitro	Direct	(Choi et al., 2002; Cai et al., 2002)
NR2B	In Vivo, In Vitro	Direct	Lim et al., 2002
NR2C	In Vivo, In Vitro	Direct	Lim et al., 2002
PSD-95	In Vivo, In Vitro	Direct	Masuko et al., 1999
Calmodulin	In Vivo, In Vitro	Direct	Masuko et al., 1999
SynGAP	In Vivo, In Vitro	Direct	Kim et al., 1998
PSD-95	In Vivo, In Vitro	Direct	(Karnak et al., 2002)
Discs large associated protein 4	Yeast 2 Hybrid	Direct	Takeuchi et al., 1997
Synaptic Ras GTPase activating protein 1	Yeast 2 Hybrid	Direct	Kim et al., 1998
Kainate 2			Cai et al., 2002; Lim et al., 2002
Low density lipoprotein related protein 2	In Vitro, Yeast 2 Hybrid	Direct	(Larsson et al., 2003)
ErbB4	In Vitro, Yeast 2 Hybrid	Direct	(Garcia et al., 2000; Huang et al., 2002)
CRIPT	In Vivo, In Vitro, Yeast 2 Hybrid	Direct	Lim et al., 2002
Guanylate cyclase 1, soluble alpha 2	In Vitro		(Russwurm et al., 2001)
Veli 1	In Vitro		(Butz et al., 1998)
Plasma membrane Ca2+ ATPase Type 4	In Vivo, In Vitro, Yeast 2 Hybrid	Direct	(DeMarco and Strehler, 2001)
SEC8 like 1	In Vivo	Complex	Sans et al., 2003
Focal adhesion kinase 2	In Vivo, In Vitro	Direct	Seabold et al., 2003
Cypin	In Vivo, In Vitro	Direct	Kuwahara et al., 1999
SEC8 like 1	In Vivo, In Vitro, Yeast 2 Hybrid	Direct	(Sans et al., 2003)
Neuroligin 3	Yeast 2 Hybrid	Direct	(Irie et al., 1997)
Semaphorin 4C	In Vitro, Yeast 2 Hybrid	Direct	(Inagaki et al., 2001)

11 Appendix E: Mechanisms of axon growth.

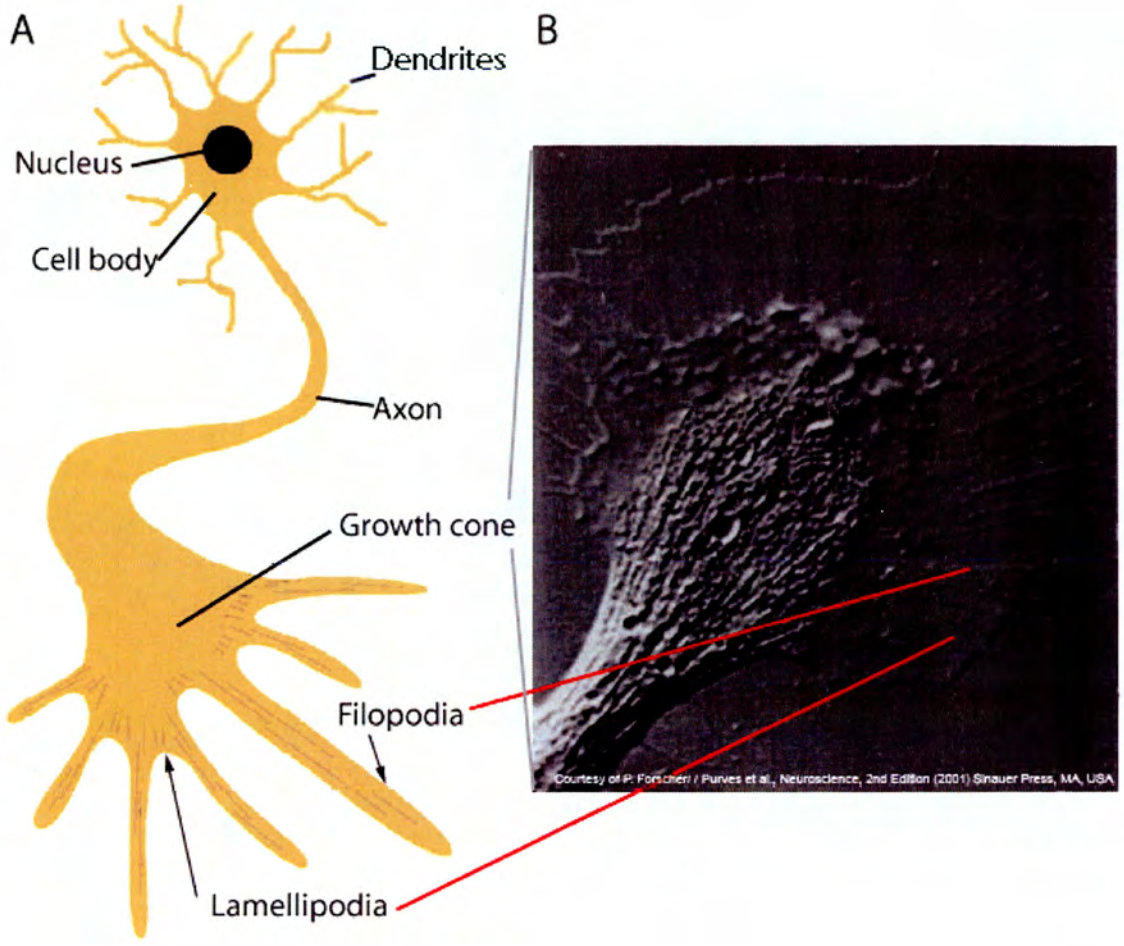

Figure E.1
Diagram of the axon and its growth cone
A typical neuron consists of four morphologically distinct regions; the cell body, axon, dendrites and presynaptic terminals. The cell body normally produces the axon and dendrites. Axons are the main apparatus for conducting action potentials between neurons and grow by extending away from the cell body and move through their environment via the growth cone (inset), a specialised region at the tip of the axon. Dendrites are highly dynamic microstructures and are the site of most neurotransmission in the central nervous system. Filopodia are actin-based finger-like projections from the growth cone that are highly dynamic in their structure, and are hypothesised to sample the surrounding neuronal environment for directional and growth cues. Actin based Lamellipodia also extend with the Filopodia during axon growth and maintains the structure of the growth cone. Inset electomicrograph taken from Purves et al., 2001.

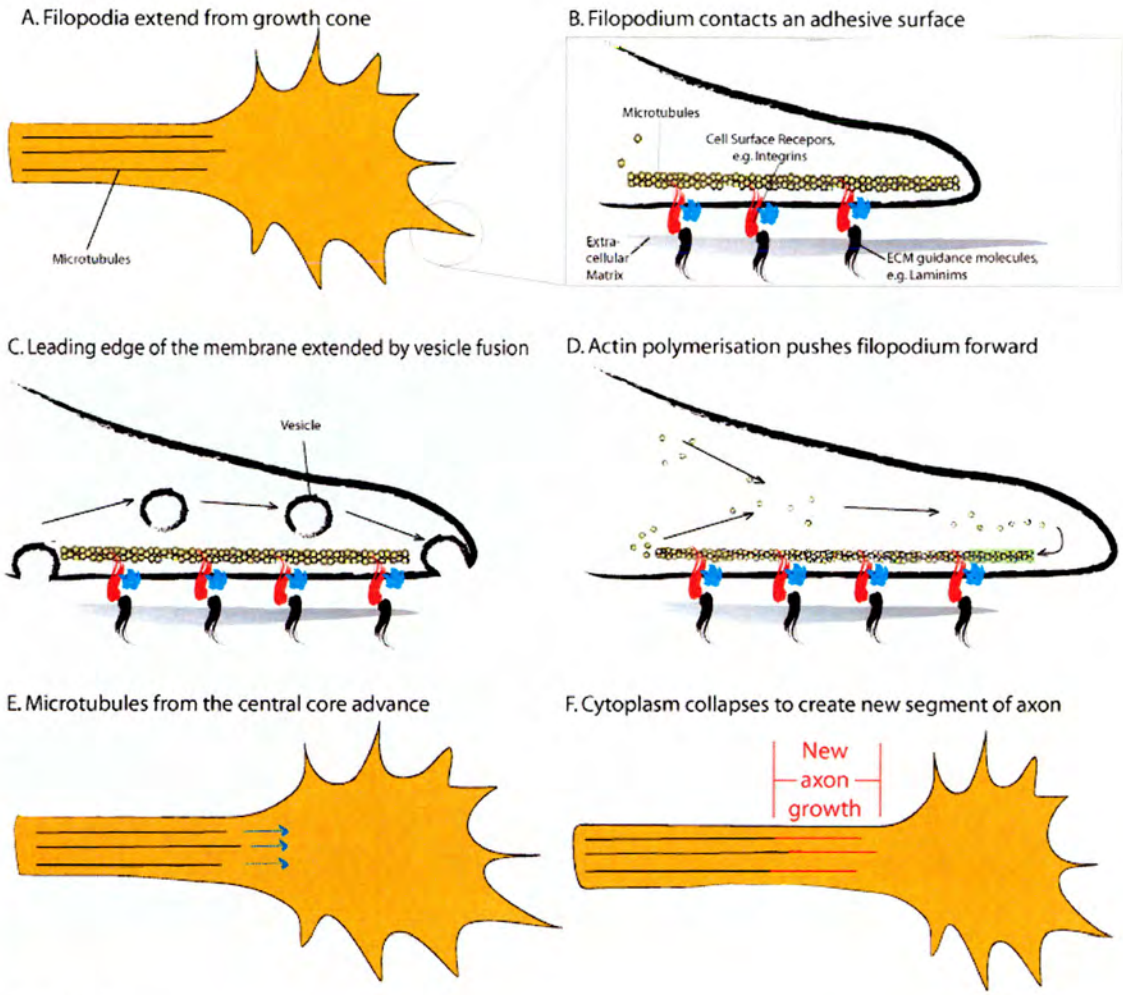

Figure E.2
Mechanism of axonal growth
A. The axon shaft structure length is determined by the state of microtubules present. When filopodia come into contact with a growth-promoting molecule (B, such as the laminin-family of proteins) the filopodia anchors to that molecule. C. The leading edge of the membrane is extended by membrane fusion and (D.) plus-end directed actin polymerisation causes forward growth of the microtubules. E. The microtubules from the central core of the axon shaft advance, and the rear end of the expanded growth cone collapses, forming a new section of axon, and returning an elongated axon to the state observed in (A.) Adapted and redrawn from (Kandel et al., 2000).

Abdel-Majid,R.M., Leong,W.L., Schalkwyk,L.C., Smallman,D.S., Wong,S.T., Storm,D.R., Fine,A., Dobson,M.J., Guernsey,D.L., and Neumann,P.E. (1998). Loss of adenylyl cyclase I activity disrupts patterning of mouse somatosensory cortex. Nat. Genet. *19*, 289-291.

Abe,K., Chisaka,O., van,R.F., and Takeichi,M. (2004). Stability of dendritic spines and synaptic contacts is controlled by alpha N-catenin. Nat. Neurosci. *7*, 357-363.

Adler,P.N. and Lee,H. (2001). Frizzled signaling and cell-cell interactions in planar polarity. Curr. Opin. Cell Biol. *13*, 635-640.

Aerts,J.L., Gonzales,M.I., and Topalian,S.L. (2004). Selection of appropriate control genes to assess expression of tumor antigens using real-time RT-PCR. Biotechniques *36*, 84-1.

Agmon,A., Yang,L.T., Jones,E.G., and O'Dowd,D.K. (1995). Topological precision in the thalamic projection to neonatal mouse barrel cortex. J. Neurosci. *15*, 549-561.

Ahmad-Annuar,A., Ciani,L., Simeonidis,I., Herreros,J., Fredj,N.B., Rosso,S.B., Hall,A., Brickley,S., and Salinas,P.C. (2006). Signaling across the synapse: a role for Wnt and Dishevelled in presynaptic assembly and neurotransmitter release. J. Cell Biol. *174*, 127-139.

Allendoerfer,K.L. and Shatz,C.J. (1994). The subplate, a transient neocortical structure: its role in the development of connections between thalamus and cortex. Annu. Rev Neurosci. *17*, 185-218.

Allison,D.W., Gelfand,V.I., Spector,I., and Craig,A.M. (1998). Role of actin in anchoring postsynaptic receptors in cultured hippocampal neurons: differential attachment of NMDA versus AMPA receptors. J. Neurosci. *18*, 2423-2436.

Andrews,G.J. and Phillips,D.R. (2000). Moral dilemmas and the management of private residential homes: the impact of care in the community reforms in the UK. Ageing & Society *20*, 599-622.

Apel,E.D., Roberds,S.L., Campbell,K.P., and Merlie,J.P. (1995). Rapsyn may function as a link between the acetylcholine receptor and the agrin-binding dystrophin-associated glycoprotein complex. Neuron. *15*, 115-126.

Arnold,S.E., Talbot,K., and Hahn,C.G. (2005). Neurodevelopment, neuroplasticity, and new genes for schizophrenia. Prog. Brain Res. *147:319-45.*, 319-345.

Artola,A. and Singer,W. (1987). Long-term potentiation and NMDA receptors in rat visual cortex. Nature *330*, 649-652.

Baas,P.W. (1999). Microtubules and neuronal polarity: lessons from mitosis. Neuron *22*, 23-31.

Bachler,M. and Neubuser,A. (2001). Expression of members of the Fgf family and their receptors during midfacial development. Mech. Dev. *100*, 313-316.

Bafico,A., Liu,G., Yaniv,A., Gazit,A., and Aaronson,S.A. (2001). Novel mechanism of Wnt signalling inhibition mediated by Dickkopf-1 interaction with LRP6/Arrow. Nat. Cell Biol. *3*, 683-686.

Bamji,S.X. (2005). Cadherins: actin with the cytoskeleton to form synapses. Neuron *47*, 175-178.

Bamji,S.X., Shimazu,K., Kimes,N., Huelsken,J., Birchmeier,W., Lu,B., and Reichardt,L.F. (2003). Role of beta-catenin in synaptic vesicle localization and presynaptic assembly. Neuron *40*, 719-731.

Barnabe-Heider,F. and Miller,F.D. (2003). Endogenously produced neurotrophins regulate survival and differentiation of cortical progenitors via distinct signaling pathways. J. Neurosci. *23*, 5149-5160.

Barnett,M.W., Watson,R.F., Vitalis,T., Porter,K., Komiyama,N.H., Stoney,P.N., Gillingwater,T.H., Grant,S.G., and Kind,P.C. (2006a). Syngap regulates pattern formation in the trigeminal system of mice. J. Neurosci. *26*, 1355-1365.

Barnett, M. W., Watson, R. F., Vitalis, T., Porter, K., Komiyama, N. H., Stoney, P. N., Gillingwater, T. H., Grant, S. G., and Kind, P. C. Syngap regulates pattern formation in the trigeminal system of mice. J.Neurosci. 2005a.
Ref Type: In Press

Barnett,M.W., Watson,R.W., and Kind,P.C. (2005b). Pathways to Barrel Formation. In Development & Plasticity in Sensory Thalamus and Cortex, R.S.Erzumulu and W.Guido, eds. (New Orleans: pp. 124-134.

Barnett,M.W., Watson,R.W., and Kind,P.C. (2006b). Pathways to Barrel Formation. In Development & Plasticity in Sensory Thalamus and Cortex, R.S.Erzumulu and W.Guido, eds. (New Orleans: pp. 124-134.

Barrow,J.R., Thomas,K.R., Boussadia-Zahui,O., Moore,R., Kemler,R., Capecchi,M.R., and McMahon,A.P. (2003). Ectodermal Wnt3/beta-catenin signaling is required for the establishment and maintenance of the apical ectodermal ridge. Genes Dev. *17*, 394-409.

Bates,C.A., Erzurumlu,R.S., and Killackey,H.P. (1982). Central correlates of peripheral pattern alterations in the trigeminal system of the rat. III. Neurons of the principal sensory nucleus. Brain Res. *281*, 108-113.

Bayer,S.A. and Altman,J. (1991). Neocortical Development. (New York: Raven).

Bear,M.F. (1996). A synaptic basis for memory storage in the cerebral cortex. Proc. Natl. Acad. Sci. U. S. A *93*, 13453-13459.

Bear,M.F., Kleinschmidt,A., and Singer,W. (1988). Experience-dependent modifications of kitten striate cortex are not prevented by thalamic lesions that include the intralaminar nuclei. Exp. Brain Res. *70*, 627-631.

Bear,M.F. and Malenka,R.C. (1994). Synaptic plasticity: LTP and LTD. Curr. Opin. Neurobiol. *4*, 389-399.

Beasley,C., Cotter,D., Khan,N., Pollard,C., Sheppard,P., Varndell,I., Lovestone,S., Anderton,B., and Everall,I. (2001). Glycogen synthase kinase-3beta immunoreactivity is reduced in the prefrontal cortex in schizophrenia. Neurosci Lett *302*, 117-120.

Beaver,C.J., Ji,Q., Fischer,Q.S., and Daw,N.W. (2001). Cyclic AMP-dependent protein kinase mediates ocular dominance shifts in cat visual cortex. Nat. Neurosci. *4*, 159-163.

Becamel,C., Alonso,G., Galeotti,N., Demey,E., Jouin,P., Ullmer,C., Dumuis,A., Bockaert,J., and Marin,P. (2002). Synaptic multiprotein complexes associated with 5-HT(2C) receptors: a proteomic approach. EMBO J. *21*, 2332-2342.

Begg,C. and Connolly,T. (2005). Database Systems: A Practical Approach to Design, Implementation and Management. Pearson Education Ltd.).

Beier,D.R., Dushkin,H., and Sussman,D.J. (1992). Mapping genes in the mouse using single-strand conformation polymorphism analysis of recombinant inbred strains and interspecific crosses. Proc. Natl. Acad. Sci. U. S. A *89*, 9102-9106.

Bejsovec,A. (2005). Wnt pathway activation: new relations and locations. Cell *120*, 11-14.

Belford,G.R. and Killackey,H.P. (1979b). The development of vibrissae representation in subcortical trigeminal centers of the neonatal rat. J. Comp Neurol. *188*, 63-74.

Belford,G.R. and Killackey,H.P. (1979a). Vibrissae representation in subcortical trigeminal centers of the neonatal rat. J. Comp Neurol. *183*, 305-321.

Belford,G.R. and Killackey,H.P. (1980). The sensitive period in the development of the trigeminal system of the neonatal rat. J. Comp Neurol. *193*, 335-350.

Bennett-Clarke,C.A., Chiaia,N.L., and Rhoades,R.W. (1997). Contributions of raphe-cortical and thalamocortical axons to the transient somatotopic pattern of serotonin immunoreactivity in rat cortex. Somatosens. Mot. Res. *14*, 27-33.

Benshalom,G. and White,E.L. (1986). Quantification of thalamocortical synapses with spiny stellate neurons in layer IV of mouse somatosensory cortex. J. Comp Neurol. *253*, 303-314.

Benson,D.L. and Tanaka,H. (1998). N-cadherin redistribution during synaptogenesis in hippocampal neurons. J. Neurosci. *18*, 6892-6904.

Berkeley,J.L. and Levey,A.I. (2003). Cell-specific extracellular signal-regulated kinase activation by multiple G protein-coupled receptor families in hippocampus. Mol. Pharmacol. *63*, 128-135.

Bhanot,P., Brink,M., Samos,C.H., Hsieh,J.C., Wang,Y., Macke,J.P., Andrew,D., Nathans,J., and Nusse,R. (1996). A new member of the frizzled family from Drosophila functions as a Wingless receptor. Nature *382*, 225-230.

Bishop,K.M., Garel,S., Nakagawa,Y., Rubenstein,J.L., and O'Leary,D.D. (2003). Emx1 and Emx2 cooperate to regulate cortical size, lamination, neuronal differentiation, development of cortical efferents, and thalamocortical pathfinding. J. Comp Neurol. *457*, 345-360.

Bishop,K.M., Goudreau,G., and O'Leary,D.D. (2000). Regulation of area identity in the mammalian neocortex by Emx2 and Pax6. Science *288*, 344-349.

Bishop,K.M., Rubenstein,J.L., and O'Leary,D.D. (2002). Distinct actions of Emx1, Emx2, and Pax6 in regulating the specification of areas in the developing neocortex. J. Neurosci. *22*, 7627-7638.

Bliss,T.V. and Collingridge,G.L. (1993). A synaptic model of memory: long-term potentiation in the hippocampus. Nature *361*, 31-39.

Bliss,T.V. and Lomo,T. (1973). Long-lasting potentiation of synaptic transmission in the dentate area of the anaesthetized rabbit following stimulation of the perforant path. J. Physiol *232*, 331-356.

Blue,M.E., Erzurumlu,R.S., and Jhaveri,S. (1991). A comparison of pattern formation by thalamocortical and serotonergic afferents in the rat barrel field cortex. Cereb. Cortex *1*, 380-389.

Boeckers,T.M., Winter,C., Smalla,K.H., Kreutz,M.R., Bockmann,J., Seidenbecher,C., Garner,C.C., and Gundelfinger,E.D. (1999). Proline-rich synapse-associated proteins ProSAP1 and ProSAP2 interact with synaptic proteins of the SAPAP/GKAP family. Biochem. Biophys. Res. Commun. *264*, 247-252.

Boggon,T.J., Murray,J., Chappuis-Flament,S., Wong,E., Gumbiner,B.M., and Shapiro,L. (2002). C-cadherin ectodomain structure and implications for cell adhesion mechanisms. Science *296*, 1308-1313.

Bolliger,M.F., Frei,K., Winterhalter,K.H., and Gloor,S.M. (2001). Identification of a novel neuroligin in humans which binds to PSD-95 and has a widespread expression. Biochem. J. *356*, 581-588.

Bortolotto,Z.A., Fitzjohn,S.M., and Collingridge,G.L. (1999). Roles of metabotropic glutamate receptors in LTP and LTD in the hippocampus. Curr. Opin. Neurobiol. *9*, 299-304.

Boutros,M. and Mlodzik,M. (1999). Dishevelled: at the crossroads of divergent intracellular signaling pathways. Mech. Dev. *83*, 27-37.

Brady,M.A.W. and Finlan,M.F. (1990). Radioactive labels: autoradiography and choice of emulsions for in situ hybridization. In In Situ Hybridization: Principle and Practice, J.M.Polack and J.O.McGee, eds. (Oxford: Oxford University Press).

Braun,M.M., Etheridge,A., Bernard,A., Robertson,C.P., and Roelink,H. (2003). Wnt signaling is required at distinct stages of development for the induction of the posterior forebrain. Development *130*, 5579-5587.

Brenman,J.E., Chao,D.S., Gee,S.H., McGee,A.W., Craven,S.E., Santillano,D.R., Wu,Z., Huang,F., Xia,H., Peters,M.F., Froehner,S.C., and Bredt,D.S. (1996a). Interaction of nitric oxide synthase with the postsynaptic density protein PSD-95 and alpha1-syntrophin mediated by PDZ domains. Cell *84*, 757-767.

Brenman,J.E., Christopherson,K.S., Craven,S.E., McGee,A.W., and Bredt,D.S. (1996b). Cloning and characterization of postsynaptic density 93, a nitric oxide synthase interacting protein. J. Neurosci. *16*, 7407-7415.

Brookmeyer,R., Gray,S., and Kawas,C. (1998). Projections of Alzheimer's disease in the United States and the public health impact of delaying disease onset. Am. J. Public Health *88*, 1337-1342.

Bustin,S.A. (2000). Absolute quantification of mRNA using real-time reverse transcription polymerase chain reaction assays. J. Mol. Endocrinol. *25*, 169-193.

Butz,S., Okamoto,M., and Sudhof,T.C. (1998). A tripartite protein complex with the potential to couple synaptic vesicle exocytosis to cell adhesion in brain. Cell *94*, 773-782.

Cabelli,R.J., Hohn,A., and Shatz,C.J. (1995). Inhibition of ocular dominance column formation by infusion of NT-4/5 or BDNF. Science. *267*, 1662-1666.

Cabelli,R.J., Shelton,D.L., Segal,R.A., and Shatz,C.J. (1997). Blockade of endogenous ligands of trkB inhibits formation of ocular dominance columns. Neuron. *19*, 63-76.

Cadigan,K.M. and Liu,Y.I. (2006). Wnt signaling: complexity at the surface. J. Cell Sci. *119*, 395-402.

Cai,C., Coleman,S.K., Niemi,K., and Keinanen,K. (2002). Selective binding of synapse-associated protein 97 to GluR-A alpha-amino-5-hydroxy-3-methyl-4-isoxazole propionate receptor subunit is determined by a novel sequence motif. J. Biol. Chem. *277*, 31484-31490.

Calikoglu,A.S., Gutierrez-Ospina,G., and D'Ercole,A.J. (1996). Congenital hypothyroidism delays the formation and retards the growth of the mouse primary somatic sensory cortex (S1). Neurosci. Lett. *213*, 132-136.

Cancedda,L., Putignano,E., Impey,S., Maffei,L., Ratto,G.M., and Pizzorusso,T. (2003a). Patterned vision causes CRE-mediated gene expression in the visual cortex through PKA and ERK. J. Neurosci. *23*, 7012-7020.

Cancedda,L., Putignano,E., Impey,S., Maffei,L., Ratto,G.M., and Pizzorusso,T. (2003b). Patterned vision causes CRE-mediated gene expression in the visual cortex through PKA and ERK. J. Neurosci *23*, 7012-7020.

Cases,O., Vitalis,T., Seif,I., De,M.E., Sotelo,C., and Gaspar,P. (1996). Lack of barrels in the somatosensory cortex of monoamine oxidase A-deficient mice: role of a serotonin excess during the critical period. Neuron *16*, 297-307.

Caviness, Jr. VS. Architecture and development of the thalamocortical projection in the mouse. Cellular thalamic mechanisms (Bentivoglio, M., Spereafico, R., eds) , 488-499. 1988. New York, Excerpta Medica.
Ref Type: Generic

Caviness,V.S., Jr. (1982). Development of neocortical afferent systems: studies in the reeler mouse. Neurosci Res. Program. Bull. *20*, 560-569.

Chae,J., Kim,M.J., Goo,J.H., Collier,S., Gubb,D., Charlton,J., Adler,P.N., and Park,W.J. (1999). The Drosophila tissue polarity gene starry night encodes a member of the protocadherin family. Development *126*, 5421-5429.

Chen,H.J., Rojas-Soto,M., Oguni,A., and Kennedy,M.B. (1998). A synaptic Ras-GTPase activating protein (p135 SynGAP) inhibited by CaM kinase II. Neuron *20*, 895-904.

Chen,L., Chetkovich,D.M., Petralia,R.S., Sweeney,N.T., Kawasaki,Y., Wenthold,R.J., Bredt,D.S., and Nicoll,R.A. (2000). Stargazin regulates synaptic targeting of AMPA receptors by two distinct mechanisms. Nature *408*, 936-943.

Chetkovich,D.M., Bunn,R.C., Kuo,S.H., Kawasaki,Y., Kohwi,M., and Bredt,D.S. (2002). Postsynaptic targeting of alternative postsynaptic density-95 isoforms by distinct mechanisms. J. Neurosci. *22*, 6415-6425.

Choe,E.S. and Wang,J.Q. (2001). Group I metabotropic glutamate receptor activation increases phosphorylation of cAMP response element-binding protein, Elk-1, and

extracellular signal-regulated kinases in rat dorsal striatum. Brain Res. Mol. Brain Res. *%19;94*, 75-84.

Choi,J., Ko,J., Park,E., Lee,J.R., Yoon,J., Lim,S., and Kim,E. (2002). Phosphorylation of stargazin by protein kinase A regulates its interaction with PSD-95. J. Biol. Chem. *277*, 12359-12363.

Chun,J.J. and Shatz,C.J. (1989). The earliest-generated neurons of the cat cerebral cortex: characterization by MAP2 and neurotransmitter immunohistochemistry during fetal life. J. Neurosci. *9*, 1648-1667.

Ciani,L., Krylova,O., Smalley,M.J., Dale,T.C., and Salinas,P.C. (2004). A divergent canonical WNT-signaling pathway regulates microtubule dynamics: dishevelled signals locally to stabilize microtubules. J. Cell Biol. *19;164*, 243-253.

Ciani,L. and Salinas,P.C. (2005). WNTs in the vertebrate nervous system: from patterning to neuronal connectivity. Nat. Rev Neurosci. *6*, 351-362.

Clements,J.D. and Westbrook,G.L. (1991). Activation kinetics reveal the number of glutamate and glycine binding sites on the N-methyl-D-aspartate receptor. Neuron *7*, 605-613.

Colledge,M., Dean,R.A., Scott,G.K., Langeberg,L.K., Huganir,R.L., and Scott,J.D. (2000). Targeting of PKA to glutamate receptors through a MAGUK-AKAP complex. Neuron *27*, 107-119.

Collingridge,G. (1987). Synaptic plasticity. The role of NMDA receptors in learning and memory. Nature *330*, 604-605.

Cotter,D., Kerwin,R., al-Sarraji,S., Brion,J.P., Chadwich,A., Lovestone,S., Anderton,B., and Everall,I. (1998). Abnormalities of Wnt signalling in schizophrenia--evidence for neurodevelopmental abnormality. Neuroreport *9*, 1379-1383.

Crair,M.C. and Malenka,R.C. (1995). A critical period for long-term potentiation at thalamocortical synapses. Nature *375*, 325-328.

D'Amato,R.J., Blue,M.E., Largent,B.L., Lynch,D.R., Ledbetter,D.J., Molliver,M.E., and Snyder,S.H. (1987). Ontogeny of the serotonergic projection to rat neocortex: transient expression of a dense innervation to primary sensory areas. Proc. Natl. Acad. Sci. U. S. A *84*, 4322-4326.

Dabdoub,A., Donohue,M.J., Brennan,A., Wolf,V., Montcouquiol,M., Sassoon,D.A., Hseih,J.C., Rubin,J.S., Salinas,P.C., and Kelley,M.W. (2003). Wnt signaling mediates reorientation of outer hair cell stereociliary bundles in the mammalian cochlea. Development *130*, 2375-2384.

Datwani,A., Iwasato,T., Itohara,S., and Erzurumlu,R.S. (2002a). Lesion-induced thalamocortical axonal plasticity in the S1 cortex is independent of NMDA receptor function in excitatory cortical neurons. J. Neurosci. *22*, 9171-9175.

Datwani,A., Iwasato,T., Itohara,S., and Erzurumlu,R.S. (2002b). NMDA receptor-dependent pattern transfer from afferents to postsynaptic cells and dendritic differentiation in the barrel cortex. Mol. Cell Neurosci. *21*, 477-492.

Daw,N.W., Reid,S.N., Wang,X.F., and Flavin,H.J. (1995). Factors that are critical for plasticity in the visual cortex. Ciba Found. Symp. *193*, 258-276.

De Paola,V., Holtmaat,A., Knott,G., Song,S., Wilbrecht,L., Caroni,P., and Svoboda,K. (2006). Cell type-specific structural plasticity of axonal branches and boutons in the adult neocortex. Neuron. *49*, 861-875.

DeBiasi,S., Minelli,A., Melone,M., and Conti,F. (1996). Presynaptic NMDA receptors in the neocortex are both auto- and heteroreceptors. Neuroreport 7, 2773-2776.

Deguchi,M., Hata,Y., Takeuchi,M., Ide,N., Hirao,K., Yao,I., Irie,M., Toyoda,A., and Takai,Y. (1998). BEGAIN (brain-enriched guanylate kinase-associated protein), a novel neuronal PSD-95/SAP90-binding protein. J. Biol. Chem. *273*, 26269-26272.

DeMarco,S.J. and Strehler,E.E. (2001). Plasma membrane Ca2+-atpase isoforms 2b and 4b interact promiscuously and selectively with members of the membrane-associated guanylate kinase family of PDZ (PSD95/Dlg/ZO-1) domain-containing proteins. J. Biol. Chem. *276*, 21594-21600.

Desai,A. and Mitchison,T.J. (1997). Microtubule polymerization dynamics. Annu. Rev. Cell Dev. Biol. *13*, 83-117.

Dheda,K., Huggett,J.F., Bustin,S.A., Johnson,M.A., Rook,G., and Zumla,A. (2004). Validation of housekeeping genes for normalizing RNA expression in real-time PCR. Biotechniques *37*, 112-119.

Di Cristo,G., Berardi,N., Cancedda,L., Pizzorusso,T., Putignano,E., Ratto,G.M., and Maffei,L. (2001). Requirement of ERK activation for visual cortical plasticity. Science *292*, 2337-2340.

Dickson,K.S. and Kind,P.C. (2003). NMDA receptors: neural map designers and refiners? Curr. Biol. *13*, R920-R922.

Dingledine,R., Borges,K., Bowie,D., and Traynelis,S.F. (1999). The Glutamate Receptor Ion Channels. Pharmacol Rev *51*, 7-61.

Drewes,G., Ebneth,A., and Mandelkow,E.M. (1998). MAPs, MARKs and microtubule dynamics. Trends Biochem. Sci. *23*, 307-311.

Eastwood,S.L. (2004). The synaptic pathology of schizophrenia: is aberrant neurodevelopment and plasticity to blame? Int. Rev Neurobiol. *59:47-72.*, 47-72.

Ebrahimi-Gaillard,A. and Roger,M. (1996). Development of spinal cord projections from neocortical transplants heterotopically placed in the neocortex of newborn hosts is highly dependent on the embryonic locus of origin of the graft. J. Comp Neurol. *365*, 129-140.

Egea,J., Nissen,U.V., Dufour,A., Sahin,M., Greer,P., Kullander,K., Mrsic-Flogel,T.D., Greenberg,M.E., Kiehn,O., Vanderhaeghen,P., and Klein,R. (2005). Regulation of EphA 4 kinase activity is required for a subset of axon guidance decisions suggesting a key role for receptor clustering in Eph function. Neuron *47*, 515-528.

Eldstrom,J., Doerksen,K.W., Steele,D.F., and Fedida,D. (2002). N-terminal PDZ-binding domain in Kv1 potassium channels. FEBS Lett. *%20;531*, 529-537.

Elwood, A, Hillen, M. J. P., Wijetunge, L. S., Watson, R. F., Porter, K., Cuthbert, P., and Grant, S. G. N. Role of MAGUK PROTEINS, PSD-95 and SAP-102, in Barrel Cortex development. Soc.Neurosci.Abstr. 716.7. 2005.
Ref Type: Abstract

Erzurumlu,R.S. and Jhaveri,S. (1992). Trigeminal ganglion cell processes are spatially ordered prior to the differentiation of the vibrissa pad. J. Neurosci. *12*, 3946-3955.

Erzurumlu,R.S., Jhaveri,S., and Benowitz,L.I. (1990). Transient patterns of GAP-43 expression during the formation of barrels in the rat somatosensory cortex. J. Comp Neurol. *292*, 443-456.

Erzurumlu,R.S. and Kind,P.C. (2001). Neural activity: sculptor of 'barrels' in the neocortex. Trends Neurosci. *24*, 589-595.

Fagiolini,M., Katagiri,H., Miyamoto,H., Mori,H., Grant,S.G., Mishina,M., and Hensch,T.K. (2003). Separable features of visual cortical plasticity revealed by N-methyl-D-aspartate receptor 2A signaling. Proc. Natl. Acad. Sci. U. S. A *100*, 2854-2859.

Fielding,R.T. and Kaiser,G. (1997). The Apache HTTP Server Project. Internet Computing, IEEE *1*, 88-90.

Forrest,D., Yuzaki,M., Soares,H.D., Ng,L., Luk,D.C., Sheng,M., Stewart,C.L., Morgan,J.I., Connor,J.A., and Curran,T. (1994). Targeted disruption of NMDA receptor 1 gene abolishes NMDA response and results in neonatal death. Neuron *13*, 325-338.

Fox,K. (1994). The cortical component of experience-dependent synaptic plasticity in the rat barrel cortex. J. Neurosci. *14*, 7665-7679.

Fox,K. (1992). A critical period for experience-dependent synaptic plasticity in rat barrel cortex. J. Neurosci. *12*, 1826-1838.

Fox,K. (2002). Anatomical pathways and molecular mechanisms for plasticity in the barrel cortex. Neuroscience *111*, 799-814.

Fox,K., Schlaggar,B.L., Glazewski,S., and O'Leary,D.D. (1996). Glutamate receptor blockade at cortical synapses disrupts development of thalamocortical and columnar organization in somatosensory cortex. Proc. Natl. Acad. Sci. U. S. A *93*, 5584-5589.

Frappe,I., Gaillard,A., and Roger,M. (2001). Attraction exerted in vivo by grafts of embryonic neocortex on developing thalamic axons. Exp. Neurol. *169*, 264-275.

Frappe,I., Roger,M., and Gaillard,A. (1999). Transplants of fetal frontal cortex grafted into the occipital cortex of newborn rats receive a substantial thalamic input from nuclei normally projecting to the frontal cortex. Neuroscience *89*, 409-421.

Frawley,W., Piatetsky-Shapiro,G., and Matheus,C. (1992). Knowledge Discovery in Databases: An Overview. AI Magazine *Fall 1992*, 213-228.

Freeman,T.C., Dixon,A.K., Campbell,E.A., Tait,T.M., Richardson,P.J., Rice,K.M., Maslen,G.L., Metcalfe,A.D., Streuli,C.H., and Bentley,D.R. (1998). Expression Mapping of Mouse Genes. MGI Direct Data Submission.

Fujimiya,M., Kimura,H., and Maeda,T. (1986). Postnatal development of serotonin nerve fibers in the somatosensory cortex of mice studied by immunohistochemistry. J. Comp Neurol. *246*, 191-201.

Fujiyama,F. and Masuko,S. (1996). Association of dopaminergic terminals and neurons releasing nitric oxide in the rat striatum: an electron microscopic study using NADPH-

diaphorase histochemistry and tyrosine hydroxylase immunohistochemistry. Brain Res. Bull. *40*, 121-127.

Fukaya,M. and Watanabe,M. (2000). Improved immunohistochemical detection of postsynaptically located PSD-95/SAP90 protein family by protease section pretreatment: a study in the adult mouse brain. J. Comp Neurol. *426*, 572-586.

Fukuchi-Shimogori,T. and Grove,E.A. (2003). Emx2 patterns the neocortex by regulating FGF positional signaling. Nat. Neurosci. *6*, 825-831.

Fukuchi-Shimogori,T. and Grove,E.A. (2001). Neocortex patterning by the secreted signaling molecule FGF8. Science *294*, 1071-1074.

Gaillard,A., Nasarre,C., and Roger,M. (2003). Early (E12) cortical progenitors can change their fate upon heterotopic transplantation. Eur. J. Neurosci. *17*, 1375-1383.

Gaillard,A. and Roger,M. (2000). Early commitment of embryonic neocortical cells to develop area-specific thalamic connections. Cereb. Cortex *10*, 443-453.

Galceran,J., Miyashita-Lin,E.M., Devaney,E., Rubenstein,J.L., and Grosschedl,R. (2000). Hippocampus development and generation of dentate gyrus granule cells is regulated by LEF1. Development *127*, 469-482.

Gallagher,S.M., Daly,C.A., Bear,M.F., and Huber,K.M. (2004). Extracellular signal-regulated protein kinase activation is required for metabotropic glutamate receptor-dependent long-term depression in hippocampal area CA1. J. Neurosci. *%19;24*, 4859-4864.

Galuske,R.A., Kim,D.S., Castren,E., Thoenen,H., and Singer,W. (1996). Brain-derived neurotrophic factor reversed experience-dependent synaptic modifications in kitten visual cortex. Eur. J. Neurosci. *8*, 1554-1559.

Garcia,R.A., Vasudevan,K., and Buonanno,A. (2000). The neuregulin receptor ErbB-4 interacts with PDZ-containing proteins at neuronal synapses. Proc. Natl. Acad. Sci. U. S. A *97*, 3596-3601.

Garel,S., Huffman,K.J., and Rubenstein,J.L. (2003). Molecular regionalization of the neocortex is disrupted in Fgf8 hypomorphic mutants. Development *130*, 1903-1914.

Garnier,C., Arnault,P., Ebrahimi-Gaillard,A., Letang,J., and Roger,M. (1995). The topographic distribution of the efferents from neocortical neurons is not only dependent upon where in the neocortex the cells develop. A transplantation study within one single neocortical region. Brain Res. Dev. Brain Res. *89*, 1-10.

Gaspar,P., Cases,O., and Maroteaux,L. (2003). The developmental role of serotonin: news from mouse molecular genetics. Nat. Rev Neurosci. *4*, 1002-1012.

Gavin,B.J., McMahon,J.A., and McMahon,A.P. (1990). Expression of multiple novel Wnt-1/int-1-related genes during fetal and adult mouse development. Genes Dev. *4*, 2319-2332.

Gibson,U.E., Heid,C.A., and Williams,P.M. (1996). A novel method for real time quantitative RT-PCR. Genome Res. *6*, 995-1001.

Giehl,K.M., Rohrig,S., Bonatz,H., Gutjahr,M., Leiner,B., Bartke,I., Yan,Q., Reichardt,L.F., Backus,C., Welcher,A.A., Dethleffsen,K., Mestres,P., and Meyer,M. (2001). Endogenous

brain-derived neurotrophic factor and neurotrophin-3 antagonistically regulate survival of axotomized corticospinal neurons in vivo. J. Neurosci. *21*, 3492-3502.

Gil,O.D., Needleman,L., and Huntley,G.W. (2002). Developmental patterns of cadherin expression and localization in relation to compartmentalized thalamocortical terminations in rat barrel cortex. J. Comp Neurol. *453*, 372-388.

Glazewski,S., Chen,C.M., Silva,A., and Fox,K. (1996). Requirement for alpha-CaMKII in experience-dependent plasticity of the barrel cortex. Science *272*, 421-423.

Goold,R.G., Owen,R., and Gordon-Weeks,P.R. (1999). Glycogen synthase kinase 3beta phosphorylation of microtubule-associated protein 1B regulates the stability of microtubules in growth cones. J. Cell Sci. *112 (Pt 19)*, 3373-3384.

Gordon-Weeks,P.R. and Fischer,I. (2000). MAP1B expression and microtubule stability in growing and regenerating axons. Microsc. Res. Tech. *48*, 63-74.

Gotthardt,M., Trommsdorff,M., Nevitt,M.F., Shelton,J., Richardson,J.A., Stockinger,W., Nimpf,J., and Herz,J. (2000). Interactions of the low density lipoprotein receptor gene family with cytosolic adaptor and scaffold proteins suggest diverse biological functions in cellular communication and signal transduction. J. Biol. Chem. *275*, 25616-25624.

Grant,S.G. and O'Dell,T.J. (2001). Multiprotein complex signaling and the plasticity problem. Curr. Opin. Neurobiol. *11*, 363-368.

Greco,T.L., Sussman,D.J., and Camper,S.A. (1996). Dishevelled-2 maps to human chromosome 17 and distal to Wnt3a and vestigial tail (vt) on mouse chromosome 11. Mamm. Genome *7*, 475-476.

Greenough,W.T. and Chang,F.L. (1988). Dendritic pattern formation involves both oriented regression and oriented growth in the barrels of mouse somatosensory cortex. Brain Res. *471*, 148-152.

Grove,E.A. and Fukuchi-Shimogori,T. (2003). Generating the cerebral cortical area map. Annu. Rev Neurosci. *26:355-80.*, 355-380.

Grove,E.A., Tole,S., Limon,J., Yip,L., and Ragsdale,C.W. (1998). The hem of the embryonic cerebral cortex is defined by the expression of multiple Wnt genes and is compromised in Gli3-deficient mice. Development *125*, 2315-2325.

Guidato,S., Tsai,L.H., Woodgett,J., and Miller,C.C. (1996). Differential cellular phosphorylation of neurofilament heavy side-arms by glycogen synthase kinase-3 and cyclin-dependent kinase-5. J. Neurochem. *66*, 1698-1706.

Gulisano,M., Broccoli,V., Pardini,C., and Boncinelli,E. (1996). Emx1 and Emx2 show different patterns of expression during proliferation and differentiation of the developing cerebral cortex in the mouse. Eur. J. Neurosci. *8*, 1037-1050.

Habas,R., Dawid,I.B., and He,X. (2003). Coactivation of Rac and Rho by Wnt/Frizzled signaling is required for vertebrate gastrulation. Genes Dev. *17*, 295-309.

Hall,A.C., Brennan,A., Goold,R.G., Cleverley,K., Lucas,F.R., Gordon-Weeks,P.R., and Salinas,P.C. (2002). Valproate regulates GSK-3-mediated axonal remodeling and synapsin I clustering in developing neurons. Mol. Cell Neurosci. *20*, 257-270.

Hall,A.C., Lucas,F.R., and Salinas,P.C. (2000). Axonal remodeling and synaptic differentiation in the cerebellum is regulated by WNT-7a signaling. Cell *100*, 525-535.

Hamasaki,T., Leingartner,A., Ringstedt,T., and O'Leary,D.D. (2004). EMX2 regulates sizes and positioning of the primary sensory and motor areas in neocortex by direct specification of cortical progenitors. Neuron *43*, 359-372.

Hamblet,N.S., Lijam,N., Ruiz-Lozano,P., Wang,J., Yang,Y., Luo,Z., Mei,L., Chien,K.R., Sussman,D.J., and Wynshaw-Boris,A. (2002). Dishevelled 2 is essential for cardiac outflow tract development, somite segmentation and neural tube closure. Development *129*, 5827-5838.

Hanada,N., Makino,K., Koga,H., Morisaki,T., Kuwahara,H., Masuko,N., Tabira,Y., Hiraoka,T., Kitamura,N., Kikuchi,A., and Saya,H. (2000). NE-dlg, a mammalian homolog of Drosophila dlg tumor suppressor, induces growth suppression and impairment of cell adhesion: possible involvement of down-regulation of beta-catenin by NE-dlg expression. Int. J. Cancer *86*, 480-488.

Hand,D., Manilla,H., and Smyth,P. (2001). Principles of Data Mining. MIT Press).

Hannan,A.J., Blakemore,C., Katsnelson,A., Vitalis,T., Huber,K.M., Bear,M., Roder,J., Kim,D., Shin,H.S., and Kind,P.C. (2001). PLC-beta1, activated via mGluRs, mediates activity-dependent differentiation in cerebral cortex. Nat. Neurosci. *4*, 282-288.

Hannan,A.J., Kind,P.C., and Blakemore,C. (1998). Phospholipase C-beta1 expression correlates with neuronal differentiation and synaptic plasticity in rat somatosensory cortex. Neuropharmacology *37*, 593-605.

Hanover,J.L., Huang,Z.J., Tonegawa,S., and Stryker,M.P. (1999). Brain-derived neurotrophic factor overexpression induces precocious critical period in mouse visual cortex. J. Neurosci. *19*, RC40.

Hardingham,N., Glazewski,S., Pakhotin,P., Mizuno,K., Chapman,P.F., Giese,K.P., and Fox,K. (2003). Neocortical long-term potentiation and experience-dependent synaptic plasticity require alpha-calcium/calmodulin-dependent protein kinase II autophosphorylation. J. Neurosci. *23*, 4428-4436.

Harrison,P.J. (1997). Schizophrenia: a disorder of neurodevelopment? Curr. Opin. Neurobiol. *7*, 285-289.

Hebb,D.O. (1949). The organization of behavior. (New York: Wiley).

Heikkila,M., Peltoketo,H., Leppaluoto,J., Ilves,M., Vuolteenaho,O., and Vainio,S. (2002). Wnt-4 deficiency alters mouse adrenal cortex function, reducing aldosterone production. Endocrinology *143*, 4358-4365.

Heimer,L. (1994). The Human Brain and Spinal Cord: Functional Neuroanatomy and Dissection Guide. (New York: Springer).

Heisenberg,C.P., Houart,C., Take-Uchi,M., Rauch,G.J., Young,N., Coutinho,P., Masai,I., Caneparo,L., Concha,M.L., Geisler,R., Dale,T.C., Wilson,S.W., and Stemple,D.L. (2001). A mutation in the Gsk3-binding domain of zebrafish Masterblind/Axin1 leads to a fate transformation of telencephalon and eyes to diencephalon. Genes Dev. *15*, 1427-1434.

Hensch,T.K. and Fagiolini,M. (2005). Excitatory-inhibitory balance and critical period plasticity in developing visual cortex. Prog. Brain Res. *147*, 115-124.

Hensch,T.K., Fagiolini,M., Mataga,N., Stryker,M.P., Baekkeskov,S., and Kash,S.F. (1998). Local GABA circuit control of experience-dependent plasticity in developing visual cortex. Science *282*, 1504-1508.

Hering,H. and Sheng,M. (2002). Direct interaction of Frizzled-1, -2, -4, and -7 with PDZ domains of PSD-95. FEBS Lett. *19;521*, 185-189.

Hevner,R.F., Miyashita-Lin,E., and Rubenstein,J.L. (2002). Cortical and thalamic axon pathfinding defects in Tbr1, Gbx2, and Pax6 mutant mice: evidence that cortical and thalamic axons interact and guide each other. J. Comp Neurol. *447*, 8-17.

Hilfiker,S., Pieribone,V.A., Czernik,A.J., Kao,H.T., Augustine,G.J., and Greengard,P. (1999). Synapsins as regulators of neurotransmitter release. Philos. Trans. R. Soc. Lond B Biol. Sci. *354*, 269-279.

Hirbec,H., Francis,J.C., Lauri,S.E., Braithwaite,S.P., Coussen,F., Mulle,C., Dev,K.K., Coutinho,V., Meyer,G., Isaac,J.T., Collingridge,G.L., and Henley,J.M. (2003). Rapid and differential regulation of AMPA and kainate receptors at hippocampal mossy fibre synapses by PICK1 and GRIP. Neuron *%20:37*, 625-638.

Hollmann,M. and Heinemann,S. (1994). Cloned glutamate receptors. Annu. Rev. Neurosci. *17*, 31-108.

Holtmaat,A., Wilbrecht,L., Knott,G.W., Welker,E., and Svoboda,K. (2006). Experience-dependent and cell-type-specific spine growth in the neocortex. Nature. *441*, 979-983.

Horio,Y., Hibino,H., Inanobe,A., Yamada,M., Ishii,M., Tada,Y., Satoh,E., Hata,Y., Takai,Y., and Kurachi,Y. (1997). Clustering and enhanced activity of an inwardly rectifying potassium channel, Kir4.1, by an anchoring protein, PSD-95/SAP90. J. Biol. Chem. *272*, 12885-12888.

Hou,X.Y., Zhang,G.Y., Yan,J.Z., Chen,M., and Liu,Y. (2002). Activation of NMDA receptors and L-type voltage-gated calcium channels mediates enhanced formation of Fyn-PSD95-NR2A complex after transient brain ischemia. Brain Res. *955*, 123-132.

Houart,C., Caneparo,L., Heisenberg,C., Barth,K., Take-Uchi,M., and Wilson,S. (2002). Establishment of the telencephalon during gastrulation by local antagonism of Wnt signaling. Neuron *35*, 255-265.

Howard,J.S. (1996). Herpes encephalitis, schizophrenia and the crossroads of psychiatry. Integr. Physiol Behav. Sci. *31*, 219-223.

Hruska-Hageman,A.M., Benson,C.J., Leonard,A.S., Price,M.P., and Welsh,M.J. (2004). PSD-95 and Lin-7b interact with acid-sensing ion channel-3 and have opposite effects on H+-gated current. J. Biol. Chem. *279*, 46962-46968.

Hsieh,J.C., Kodjabachian,L., Rebbert,M.L., Rattner,A., Smallwood,P.M., Samos,C.H., Nusse,R., Dawid,I.B., and Nathans,J. (1999a). A new secreted protein that binds to Wnt proteins and inhibits their activities. Nature *398*, 431-436.

Hsieh,J.C., Rattner,A., Smallwood,P.M., and Nathans,J. (1999b). Biochemical characterization of Wnt-frizzled interactions using a soluble, biologically active vertebrate Wnt protein. Proc. Natl. Acad. Sci. U. S. A *96*, 3546-3551.

Hsueh,Y.P., Kim,E., and Sheng,M. (1997). Disulfide-linked head-to-head multimerization in the mechanism of ion channel clustering by PSD-95. Neuron *18*, 803-814.

Hu,L.A., Tang,Y., Miller,W.E., Cong,M., Lau,A.G., Lefkowitz,R.J., and Hall,R.A. (2000). beta 1-adrenergic receptor association with PSD-95. Inhibition of receptor internalization and facilitation of beta 1-adrenergic receptor interaction with N-methyl-D-aspartate receptors. J. Biol. Chem. *275*, 38659-38666.

Hua,J.Y. and Smith,S.J. (2004). Neural activity and the dynamics of central nervous system development. Nat. Neurosci *7*, 327-332.

Huang,H.C. and Klein,P.S. (2004). The Frizzled family: receptors for multiple signal transduction pathways. Genome Biol. *5*, 234.

Huang,Y.Z., Wang,Q., Won,S., Luo,Z.G., Xiong,W.C., and Mei,L. (2002). Compartmentalized NRG signaling and PDZ domain-containing proteins in synapse structure and function. Int. J. Dev. Neurosci. *20*, 173-185.

Huang,Y.Z., Won,S., Ali,D.W., Wang,Q., Tanowitz,M., Du,Q.S., Pelkey,K.A., Yang,D.J., Xiong,W.C., Salter,M.W., and Mei,L. (2000). Regulation of neuregulin signaling by PSD-95 interacting with ErbB4 at CNS synapses. Neuron *26*, 443-455.

Huang,Z.J., Kirkwood,A., Pizzorusso,T., Porciatti,V., Morales,B., Bear,M.F., Maffei,L., and Tonegawa,S. (1999). BDNF regulates the maturation of inhibition and the critical period of plasticity in mouse visual cortex. Cell. *98*, 739-755.

Hubel,D.H., Wiesel,T.N., and LeVay,S. (1977). Plasticity of ocular dominance columns in monkey striate cortex. Philos. Trans. R. Soc. Lond B Biol. Sci. *278*, 377-409.

Huber,K.M., Kayser,M.S., and Bear,M.F. (2000). Role for rapid dendritic protein synthesis in hippocampal mGluR-dependent long-term depression. Science *288*, 1254-1257.

Huelsken,J. and Behrens,J. (2002). The Wnt signalling pathway. J. Cell Sci. *115*, 3977-3978.

Huffman,K.J., Garel,S., and Rubenstein,J.L. (2004). Fgf8 regulates the development of intra-neocortical projections. J. Neurosci. *24*, 8917-8923.

Hughes,P.D., Wilson,W.R., and Leslie,S.W. (2001). Effect of gestational ethanol exposure on the NMDA receptor complex in rat forebrain: from gene transcription to cell surface. Brain Res. Dev. Brain Res. *129*, 135-145.

Husi, H. NRC components. 2005.
Ref Type: Personal Communication

Husi,H., Ward,M.A., Choudhary,J.S., Blackstock,W.P., and Grant,S.G. (2000). Proteomic analysis of NMDA receptor-adhesion protein signaling complexes. Nat. Neurosci. *3*, 661-669.

Ikeda,K., Araki,K., Takayama,C., Inoue,Y., Yagi,T., Aizawa,S., and Mishina,M. (1995). Reduced spontaneous activity of mice defective in the epsilon 4 subunit of the NMDA receptor channel. Brain Res. Mol. Brain Res. *33*, 61-71.

Imamura,K., Morii,H., Nakadate,K., Yamada,T., Mataga,N., Watanabe,Y., and Mori,N. (2006). Brain-derived neurotrophic factor enhances expression of superior cervical ganglia clone 10 in lateral geniculate nucleus and visual cortex of developing kittens. Eur. J. Neurosci. *23*, 637-648.

Inagaki,S., Ohoka,Y., Sugimoto,H., Fujioka,S., Amazaki,M., Kurinami,H., Miyazaki,N., Tohyama,M., and Furuyama,T. (2001). Sema4c, a transmembrane semaphorin, interacts with a post-synaptic density protein, PSD-95. J. Biol. Chem. *276*, 9174-9181.

Inan,M., Lu,H.C., Albright,M.J., She,W.C., and Crair,M.C. (2006). Barrel map development relies on protein kinase A regulatory subunit IIbeta-mediated cAMP signaling. J. Neurosci. *26*, 4338-4349.

Inan, M., Lu, W., She, W., and Crair, M. C. Barrel map development in PKARIIβ knock-out mice. Soc.Neurosci.Abstr. 26.5. 2005.
Ref Type: Abstract

Inoue,T., Oz,H.S., Wiland,D., Gharib,S., Deshpande,R., Hill,R.J., Katz,W.S., and Sternberg,P.W. (2004). C. elegans LIN-18 is a Ryk ortholog and functions in parallel to LIN-17/Frizzled in Wnt signaling. Cell *118*, 795-806.

Irie,M., Hata,Y., Takeuchi,M., Ichtchenko,K., Toyoda,A., Hirao,K., Takai,Y., Rosahl,T.W., and Sudhof,T.C. (1997). Binding of neuroligins to PSD-95. Science *277*, 1511-1515.

Ishitani,T., Kishida,S., Hyodo-Miura,J., Ueno,N., Yasuda,J., Waterman,M., Shibuya,H., Moon,R.T., Ninomiya-Tsuji,J., and Matsumoto,K. (2003). The TAK1-NLK mitogen-activated protein kinase cascade functions in the Wnt-5a/Ca(2+) pathway to antagonize Wnt/beta-catenin signaling. Mol. Cell Biol. *23*, 131-139.

Iwasato,T., Datwani,A., Wolf,A.M., Nishiyama,H., Taguchi,Y., Tonegawa,S., Knopfel,T., Erzurumlu,R.S., and Itohara,S. (2000). Cortex-restricted disruption of NMDAR1 impairs neuronal patterns in the barrel cortex. Nature *406*, 726-731.

Iwasato,T., Erzurumlu,R.S., Huerta,P.T., Chen,D.F., Sasaoka,T., Ulupinar,E., and Tonegawa,S. (1997). NMDA receptor-dependent refinement of somatotopic maps. Neuron *19*, 1201-1210.

Izzo,P.N., Graybiel,A.M., and Bolam,J.P. (1987). Characterization of substance P- and [Met]enkephalin-immunoreactive neurons in the caudate nucleus of cat and ferret by a single section Golgi procedure. Neuroscience *20*, 577-587.

Jablensky,A. (1997). The 100-year epidemiology of schizophrenia. Schizophr. Res. *28*, 111-125.

Jackson Laboratories Mouse Genome Informatics direct submission. Deltagen Data Submission to MGI via the NIH Knockout Project. Jackson Laboratories Mouse Genome Informatics Database . 2005.
Ref Type: Electronic Citation

Jeanmonod,D., Rice,F.L., and Van der Loos,H. (1981). Mouse somatosensory cortex: alterations in the barrelfield following receptor injury at different early postnatal ages. Neuroscience *6*, 1503-1535.

Jensen,K.F. and Killackey,H.P. (1987). Terminal arbors of axons projecting to the somatosensory cortex of the adult rat. II. The altered morphology of thalamocortical afferents following neonatal infraorbital nerve cut. J. Neurosci. *7*, 3544-3553.

Jhaveri,S., Erzurumlu,R.S., and Crossin,K. (1991). Barrel construction in rodent neocortex: role of thalamic afferents versus extracellular matrix molecules. Proc. Natl. Acad. Sci. U. S. A *88*, 4489-4493.

Jo,K., Derin,R., Li,M., and Bredt,D.S. (1999). Characterization of MALS/Velis-1, -2, and -3: a family of mammalian LIN-7 homologs enriched at brain synapses in association with the postsynaptic density-95/NMDA receptor postsynaptic complex. J. Neurosci. *19*, 4189-4199.

Kandel,E.R., Schwartz,J.H., and Jessel,T.M. (2000). The Anatomical Organisation of the Central Nervous System. In Principles of neural science, (New York: McGraw-Hill, Health Professions Division), pp. 317-336.

Kanegae,Y., Lee,G., Sato,Y., Tanaka,M., Nakai,M., Sakaki,T., Sugano,S., and Saito,I. (1995). Efficient gene activation in mammalian cells by using recombinant adenovirus expressing site-specific Cre recombinase. Nucleic Acids Res. *23*, 3816-3821.

Karnak,D., Lee,S., and Margolis,B. (2002). Identification of multiple binding partners for the amino-terminal domain of synapse-associated protein 97. J. Biol. Chem. *277*, 46730-46735.

Katanaev,V.L., Ponzielli,R., Semeriva,M., and Tomlinson,A. (2005). Trimeric G protein-dependent frizzled signaling in Drosophila. Cell *120*, 111-122.

Katoh,M. (2002). Molecular cloning and expression of mouse Wnt14, and structural comparison between mouse Wnt14-Wnt3a gene cluster and human WNT14-WNT3A gene cluster. Int. J. Mol. Med. *9*, 221-227.

Katsnelson, A. Genetic and Epigenetic factors in the Development of the Somatosensory Cortex. 2002. Oxford University.
Ref Type: Thesis/Dissertation

Kawachi,H., Tamura,H., Watakabe,I., Shintani,T., Maeda,N., and Noda,M. (1999). Protein tyrosine phosphatase zeta/RPTPbeta interacts with PSD-95/SAP90 family. Brain Res. Mol. Brain Res. *72*, 47-54.

Kennedy,M.B. (1997). The postsynaptic density at glutamatergic synapses. Trends Neurosci. *20*, 264-268.

Kido,M., Obata,S., Tanihara,H., Rochelle,J.M., Seldin,M.F., Taketani,S., and Suzuki,S.T. (1998). Molecular properties and chromosomal location of cadherin-8. Genomics *48*, 186-194.

Killackey,H.P. (1973). Anatomical evidence for cortical subdivisions based on vertically discrete thalamic projections from the ventral posterior nucleus to cortical barrels in the rat. Brain Res. *51*, 326-331.

Killackey,H.P., Belford,G., Ryugo,R., and Ryugo,D.K. (1976). Anomalous organization of thalamocortical projections consequent to vibrissae removal in the newborn rat and mouse. Brain Res. *104*, 309-315.

Killackey,H.P. and Belford,G.R. (1979). The formation of afferent patterns in the somatosensory cortex of the neonatal rat. J. Comp Neurol. *183*, 285-303.

Killackey,H.P. and Leshin,S. (1975). The organization of specific thalamocortical projections to the posteromedial barrel subfield of the rat somatic sensory cortex. Brain Res. *86*, 469-472.

Killackey,H.P., Rhoades,R.W., and nett-Clarke,C.A. (1995). The formation of a cortical somatotopic map. Trends Neurosci. *18*, 402-407.

Kim,E., Naisbitt,S., Hsueh,Y.P., Rao,A., Rothschild,A., Craig,A.M., and Sheng,M. (1997). GKAP, a novel synaptic protein that interacts with the guanylate kinase-like domain of the PSD-95/SAP90 family of channel clustering molecules. J. Cell Biol. *136*, 669-678.

Kim,E., Niethammer,M., Rothschild,A., Jan,Y.N., and Sheng,M. (1995). Clustering of Shaker-type K+ channels by interaction with a family of membrane-associated guanylate kinases. Nature *378*, 85-88.

Kim,E. and Sheng,M. (1996). Differential K+ channel clustering activity of PSD-95 and SAP97, two related membrane-associated putative guanylate kinases. Neuropharmacology *35*, 993-1000.

Kim,J.H., Lee,H.K., Takamiya,K., and Huganir,R.L. (2003a). The role of synaptic GTPase-activating protein in neuronal development and synaptic plasticity. J. Neurosci. *23*, 1119-1124.

Kim,J.H., Lee,H.K., Takamiya,K., and Huganir,R.L. (2003b). The role of synaptic GTPase-activating protein in neuronal development and synaptic plasticity. J. Neurosci *23*, 1119-1124.

Kim,J.H., Liao,D., Lau,L.F., and Huganir,R.L. (1998). SynGAP: a synaptic RasGAP that associates with the PSD-95/SAP90 protein family. Neuron *20*, 683-691.

Kim,M.J., Dunah,A.W., Wang,Y.T., and Sheng,M. (2005). Differential roles of NR2A- and NR2B-containing NMDA receptors in Ras-ERK signaling and AMPA receptor trafficking. Neuron *46*, 745-760.

Kimura-Yoshida,C., Nakano,H., Okamura,D., Nakao,K., Yonemura,S., Belo,J.A., Aizawa,S., Matsui,Y., and Matsuo,I. (2005). Canonical Wnt signaling and its antagonist regulate anterior-posterior axis polarization by guiding cell migration in mouse visceral endoderm. Dev. Cell *9*, 639-650.

Kitano,J., Yamazaki,Y., Kimura,K., Masukado,T., Nakajima,Y., and Nakanishi,S. (2003). Tamalin is a scaffold protein that interacts with multiple neuronal proteins in distinct modes of protein-protein association. J. Biol. Chem. *278*, 14762-14768.

Kiyono,T., Hiraiwa,A., Fujita,M., Hayashi,Y., Akiyama,T., and Ishibashi,M. (1997). Binding of high-risk human papillomavirus E6 oncoproteins to the human homologue of the Drosophila discs large tumor suppressor protein. Proc. Natl. Acad. Sci. U. S. A *94*, 11612-11616.

Kleckner,N.W. and Dingledine,R. (1991). Regulation of hippocampal NMDA receptors by magnesium and glycine during development. Brain Res. Mol. Brain Res. *11*, 151-159.

Kleinschmidt,A., Bear,M.F., and Singer,W. (1987). Blockade of "NMDA" receptors disrupts experience-dependent plasticity of kitten striate cortex. Science *238*, 355-358.

Komiyama,N.H., Watabe,A.M., Carlisle,H.J., Porter,K., Charlesworth,P., Monti,J., Strathdee,D.J., O'Carroll,C.M., Martin,S.J., Morris,R.G., O'Dell,T.J., and Grant,S.G. (2002). SynGAP regulates ERK/MAPK signaling, synaptic plasticity, and learning in the complex with postsynaptic density 95 and NMDA receptor. J. Neurosci. *22*, 9721-9732.

Kornau,H.C., Schenker,L.T., Kennedy,M.B., and Seeburg,P.H. (1995). Domain interaction between NMDA receptor subunits and the postsynaptic density protein PSD-95. Science *269*, 1737-1740.

Kozlovsky,N., Belmaker,R.H., and Agam,G. (2001). Low GSK-3 activity in frontal cortex of schizophrenic patients. Schizophr. Res. *52*, 101-105.

Kozlovsky,N., Nadri,C., and Agam,G. (2005). Low GSK-3beta in schizophrenia as a consequence of neurodevelopmental insult. Eur. Neuropsychopharmacol. *15*, 1-11.

Krapivinsky,G., Medina,I., Krapivinsky,L., Gapon,S., and Clapham,D.E. (2004). SynGAP-MUPP1-CaMKII synaptic complexes regulate p38 MAP kinase activity and NMDA receptor-dependent synaptic AMPA receptor potentiation. Neuron *%19;43*, 563-574.

Krettek,J.E. and Price,J.L. (1977a). Projections from the amygdaloid complex and adjacent olfactory structures to the entorhinal cortex and to the subiculum in the rat and cat. J Comp Neurol. *172*, 723-752.

Krettek,J.E. and Price,J.L. (1977b). Projections from the amygdaloid complex to the cerebral cortex and thalamus in the rat and cat. J Comp Neurol. *172*, 687-722.

Kroemer,G. and Reed,J.C. (2000). Mitochondrial control of cell death. Nat. Med. *6*, 513-519.

Krylova,O., Herreros,J., Cleverley,K.E., Ehler,E., Henriquez,J.P., Hughes,S.M., and Salinas,P.C. (2002). WNT-3, expressed by motoneurons, regulates terminal arborization of neurotrophin-3-responsive spinal sensory neurons. Neuron *35*, 1043-1056.

Krylova,O., Messenger,M.J., and Salinas,P.C. (2000). Dishevelled-1 regulates microtubule stability: a new function mediated by glycogen synthase kinase-3beta. J. Cell Biol. *151*, 83-94.

Kuhl,M., Sheldahl,L.C., Malbon,C.C., and Moon,R.T. (2000a). Ca(2+)/calmodulin-dependent protein kinase II is stimulated by Wnt and Frizzled homologs and promotes ventral cell fates in Xenopus. J. Biol. Chem. *275*, 12701-12711.

Kuhl,M., Sheldahl,L.C., Park,M., Miller,J.R., and Moon,R.T. (2000b). The Wnt/Ca2+ pathway: a new vertebrate Wnt signaling pathway takes shape. Trends Genet. *16*, 279-283.

Kutsuwada,T., Sakimura,K., Manabe,T., Takayama,C., Katakura,N., Kushiya,E., Natsume,R., Watanabe,M., Inoue,Y., Yagi,T., Aizawa,S., Arakawa,M., Takahashi,T., Nakamura,Y., Mori,H., and Mishina,M. (1996). Impairment of suckling response, trigeminal neuronal pattern formation, and hippocampal LTD in NMDA receptor epsilon 2 subunit mutant mice. Neuron *16*, 333-344.

Kuwahara,H., Araki,N., Makino,K., Masuko,N., Honda,S., Kaibuchi,K., Fukunaga,K., Miyamoto,E., Ogawa,M., and Saya,H. (1999). A novel NE-dlg/SAP102-associated protein, p51-nedasin, related to the amidohydrolase superfamily, interferes with the association between NE-dlg/SAP102 and N-methyl-D-aspartate receptor. J. Biol. Chem. *274*, 32204-32214.

Lachance,P.E. and Chaudhuri,A. (2004). Microarray analysis of developmental plasticity in monkey primary visual cortex. J. Neurochem. *88*, 1455-1469.

Lako,M., Lindsay,S., Lincoln,J., Cairns,P.M., Armstrong,L., and Hole,N. (2001). Characterisation of Wnt gene expression during the differentiation of murine embryonic stem cells in vitro: role of Wnt3 in enhancing haematopoietic differentiation. Mech. Dev. *103*, 49-59.

Lanzetti,L., Palamidessi,A., Areces,L., Scita,G., and Di Fiore,P.P. (2004). Rab5 is a signalling GTPase involved in actin remodelling by receptor tyrosine kinases. Nature *%20;429*, 309-314.

Larsson,M., Hjalm,G., Sakwe,A.M., Engstrom,A., Hoglund,A.S., Larsson,E., Robinson,R.C., Sundberg,C., and Rask,L. (2003). Selective interaction of megalin with postsynaptic density-95 (PSD-95)-like membrane-associated guanylate kinase (MAGUK) proteins. Biochem. J. *373*, 381-391.

Lau,L.F., Mammen,A., Ehlers,M.D., Kindler,S., Chung,W.J., Garner,C.C., and Huganir,R.L. (1996). Interaction of the N-methyl-D-aspartate receptor complex with a novel synapse-associated protein, SAP102. J. Biol. Chem. *271*, 21622-21628.

Lebrand,C., Cases,O., Adelbrecht,C., Doye,A., Alvarez,C., El,M.S., Seif,I., and Gaspar,P. (1996). Transient uptake and storage of serotonin in developing thalamic neurons. Neuron *17*, 823-835.

Lee,S.M., Tole,S., Grove,E., and McMahon,A.P. (2000a). A local Wnt-3a signal is required for development of the mammalian hippocampus. Development *127*, 457-467.

Lee,T., Winter,C., Marticke,S.S., Lee,A., and Luo,L. (2000b). Essential roles of Drosophila RhoA in the regulation of neuroblast proliferation and dendritic but not axonal morphogenesis. Neuron *25*, 307-316.

Leighton,P.A., Mitchell,K.J., Goodrich,L.V., Lu,X., Pinson,K., Scherz,P., Skarnes,W.C., and Tessier-Lavigne,M. (2001). Defining brain wiring patterns and mechanisms through gene trapping in mice. Nature *410*, 174-179.

Lendvai,B., Stern,E.A., Chen,B., and Svoboda,K. (2000). Experience-dependent plasticity of dendritic spines in the developing rat barrel cortex in vivo. Nature. *%20;404*, 876-881.

Letang,J., Gaillard,A., and Roger,M. (1998). Specific invasion of occipital-to-frontal neocortical grafts by axons from the lateral posterior thalamic nucleus consecutive to neonatal lesion of the rat occipital cortex. Exp. Neurol. *152*, 64-73.

Li,L., Chin,L.S., Shupliakov,O., Brodin,L., Sihra,T.S., Hvalby,O., Jensen,V., Zheng,D., McNamara,J.O., Greengard,P., and . (1995). Impairment of synaptic vesicle clustering and of synaptic transmission, and increased seizure propensity, in synapsin I-deficient mice. Proc. Natl. Acad. Sci. U. S. A *92*, 9235-9239.

Li,W., Okano,A., Tian,Q.B., Nakayama,K., Furihata,T., Nawa,H., and Suzuki,T. (2001). Characterization of a novel synGAP isoform, synGAP-beta. J. Biol. Chem. *276*, 21417-21424.

Li,Y., Erzurumlu,R.S., Chen,C., Jhaveri,S., and Tonegawa,S. (1994). Whisker-related neuronal patterns fail to develop in the trigeminal brainstem nuclei of NMDAR1 knockout mice. Cell *76*, 427-437.

Li,Z., Van,A.L., and Cline,H.T. (2000). Rho GTPases regulate distinct aspects of dendritic arbor growth in Xenopus central neurons in vivo. Nat. Neurosci. *3*, 217-225.

Lijam,N., Paylor,R., McDonald,M.P., Crawley,J.N., Deng,C.X., Herrup,K., Stevens,K.E., Maccaferri,G., McBain,C.J., Sussman,D.J., and Wynshaw-Boris,A. (1997). Social interaction and sensorimotor gating abnormalities in mice lacking Dvl1. Cell *90*, 895-905.

Lim,I.A., Hall,D.D., and Hell,J.W. (2002). Selectivity and promiscuity of the first and second PDZ domains of PSD-95 and synapse-associated protein 102. J. Biol. Chem. *277*, 21697-21711.

Liu,P., Wakamiya,M., Shea,M.J., Albrecht,U., Behringer,R.R., and Bradley,A. (1999a). Requirement for Wnt3 in vertebrate axis formation. Nat. Genet. *22*, 361-365.

Liu,S., Rao,Y., and Daw,N. (2003). Roles of protein kinase A and protein kinase G in synaptic plasticity in the visual cortex. Cereb. Cortex *13*, 864-869.

Liu,T., DeCostanzo,A.J., Liu,X., Wang,H., Hallagan,S., Moon,R.T., and Malbon,C.C. (2001). G protein signaling from activated rat frizzled-1 to the beta-catenin-Lef-Tcf pathway. Science *292*, 1718-1722.

Liu,X., Liu,T., Slusarski,D.C., Yang-Snyder,J., Malbon,C.C., Moon,R.T., and Wang,H. (1999b). Activation of a frizzled-2/beta-adrenergic receptor chimera promotes Wnt signaling and differentiation of mouse F9 teratocarcinoma cells via Galphao and Galphat. Proc. Natl. Acad. Sci. U. S. A *96*, 14383-14388.

Logan,C.Y. and Nusse,R. (2004). The Wnt signaling pathway in development and disease. Annu. Rev Cell Dev. Biol. *20:781-810.*, 781-810.

Lu,H.C., Gonzalez,E., and Crair,M.C. (2001). Barrel cortex critical period plasticity is independent of changes in NMDA receptor subunit composition. Neuron *32*, 619-634.

Lu,H.C., She,W.C., Plas,D.T., Neumann,P.E., Janz,R., and Crair,M.C. (2003). Adenylyl cyclase I regulates AMPA receptor trafficking during mouse cortical 'barrel' map development. Nat. Neurosci. *6*, 939-947.

Lu,W., Yamamoto,V., Ortega,B., and Baltimore,D. (2004). Mammalian Ryk is a Wnt coreceptor required for stimulation of neurite outgrowth. Cell *119*, 97-108.

Lucas,F.R., Goold,R.G., Gordon-Weeks,P.R., and Salinas,P.C. (1998). Inhibition of GSK-3beta leading to the loss of phosphorylated MAP-1B is an early event in axonal remodelling induced by WNT-7a or lithium. J. Cell Sci. *111*, 1351-1361.

Lucas,F.R. and Salinas,P.C. (1997). WNT-7a induces axonal remodeling and increases synapsin I levels in cerebellar neurons. Dev. Biol. *192*, 31-44.

Ludford-Menting,M.J., Thomas,S.J., Crimeen,B., Harris,L.J., Loveland,B.E., Bills,M., Ellis,S., and Russell,S.M. (2002). A functional interaction between CD46 and DLG4: a role for DLG4 in epithelial polarization. J. Biol. Chem. *277*, 4477-4484.

Luo,L. (2000). Rho GTPases in neuronal morphogenesis. Nat. Rev. Neurosci. *1*, 173-180.

Luo,Z.G., Wang,Q., Zhou,J.Z., Wang,J., Luo,Z., Liu,M., He,X., Wynshaw-Boris,A., Xiong,W.C., Lu,B., and Mei,L. (2002). Regulation of AChR clustering by Dishevelled interacting with MuSK and PAK1. Neuron *35*, 489-505.

Lyuksyutova,A.I., Lu,C.C., Milanesio,N., King,L.A., Guo,N., Wang,Y., Nathans,J., Tessier-Lavigne,M., and Zou,Y. (2003). Anterior-posterior guidance of commissural axons by Wnt-frizzled signaling. Science *302*, 1984-1988.

Ma,P.M. (1991). The barrelettes--architectonic vibrissal representations in the brainstem trigeminal complex of the mouse. I. Normal structural organization. J. Comp Neurol. *309*, 161-199.

Ma,P.M. (1993). Barrelettes--architectonic vibrissal representations in the brainstem trigeminal complex of the mouse. II. Normal post-natal development. J. Comp Neurol. *327*, 376-397.

MacDermott,A.B., Mayer,M.L., Westbrook,G.L., Smith,S.J., and Barker,J.L. (1986). NMDA-receptor activation increases cytoplasmic calcium concentration in cultured spinal cord neurones. Nature *321*, 519-522.

Machon,O., van den Bout,C.J., Backman,M., Kemler,R., and Krauss,S. (2003). Role of beta-catenin in the developing cortical and hippocampal neuroepithelium. Neuroscience *122*, 129-143.

Maffei,L. (2002). Plasticity in the visual system: role of neurotrophins and electrical activity. Arch. Ital. Biol. *140*, 341-346.

Maier,D.L., Mani,S., Donovan,S.L., Soppet,D., Tessarollo,L., McCasland,J.S., and Meiri,K.F. (1999). Disrupted cortical map and absence of cortical barrels in growth-associated protein (GAP)-43 knockout mice. Proc. Natl. Acad. Sci. U. S. A *96*, 9397-9402.

Majdan,M. and Shatz,C.J. (2006). Effects of visual experience on activity-dependent gene regulation in cortex. Nat. Neurosci *9*, 650-659.

Makino,K., Kuwahara,H., Masuko,N., Nishiyama,Y., Morisaki,T., Sasaki,J., Nakao,M., Kuwano,A., Nakata,M., Ushio,Y., and Saya,H. (1997). Cloning and characterization of NE-dlg: a novel human homolog of the Drosophila discs large (dlg) tumor suppressor protein interacts with the APC protein. Oncogene *14*, 2425-2433.

Malenka,R.C. and Bear,M.F. (2004). LTP and LTD: an embarrassment of riches. Neuron *44*, 5-21.

Malenka,R.C. and Nicoll,R.A. (1999). Long-term potentiation--a decade of progress? Science *285*, 1870-1874.

Malenka,R.C. and Nicoll,R.A. (1993). NMDA-receptor-dependent synaptic plasticity: multiple forms and mechanisms. Trends Neurosci. *16*, 521-527.

Mandelkow,E.M., Drewes,G., Biernat,J., Gustke,N., Van,L.J., Vandenheede,J.R., and Mandelkow,E. (1992). Glycogen synthase kinase-3 and the Alzheimer-like state of microtubule-associated protein tau. FEBS Lett *314*, 315-321.

Mao,B., Wu,W., Davidson,G., Marhold,J., Li,M., Mechler,B.M., Delius,H., Hoppe,D., Stannek,P., Walter,C., Glinka,A., and Niehrs,C. (2002). Kremen proteins are Dickkopf receptors that regulate Wnt/beta-catenin signalling. Nature *417*, 664-667.

Mao,J., Wang,J., Liu,B., Pan,W., Farr,G.H., III, Flynn,C., Yuan,H., Takada,S., Kimelman,D., Li,L., and Wu,D. (2001). Low-density lipoprotein receptor-related protein-5 binds to Axin and regulates the canonical Wnt signaling pathway. Mol. Cell *7*, 801-809.

Maretto,S., Cordenonsi,M., Dupont,S., Braghetta,P., Broccoli,V., Hassan,A.B., Volpin,D., Bressan,G.M., and Piccolo,S. (2003). Mapping Wnt/beta-catenin signaling during mouse development and in colorectal tumors. Proc. Natl. Acad. Sci. U. S. A *100*, 3299-3304.

Marsden,M. and DeSimone,D.W. (2001). Regulation of cell polarity, radial intercalation and epiboly in Xenopus: novel roles for integrin and fibronectin. Development *128*, 3635-3647.

Masuko,N., Makino,K., Kuwahara,H., Fukunaga,K., Sudo,T., Araki,N., Yamamoto,H., Yamada,Y., Miyamoto,E., and Saya,H. (1999). Interaction of NE-dlg/SAP102, a neuronal and endocrine tissue-specific membrane-associated guanylate kinase protein, with calmodulin and PSD-95/SAP90. A possible regulatory role in molecular clustering at synaptic sites. J. Biol. Chem. *274*, 5782-5790.

McAllister,A.K., Katz,L.C., and Lo,D.C. (1996). Neurotrophin regulation of cortical dendritic growth requires activity. Neuron *17*, 1057-1064.

McAllister,A.K., Katz,L.C., and Lo,D.C. (1997). Opposing roles for endogenous BDNF and NT-3 in regulating cortical dendritic growth. Neuron *18*, 767-778.

McBain, C. and Mayer, M L. N-methyl-D-aspartic acid receptor structure and function. Physiol Rev. 74, 723-760. 1994.
Ref Type: Abstract

McIlvain,V. and McCasland,J.S. (2006). GAP-43 heterozygous mice show delayed barrel patterning, differentiation of radial glia, and downregulation of GAP-43. Anat. Rec. A Discov. Mol. Cell Evol. Biol. *288*, 143-157.

McIlvain,V.A., Robertson,D.R., Maimone,M.M., and McCasland,J.S. (2003). Abnormal thalamocortical pathfinding and terminal arbors lead to enlarged barrels in neonatal GAP-43 heterozygous mice. J. Comp Neurol. *462*, 252-264.

Mehta,S., Wu,H., Garner,C.C., and Marshall,J. (2001). Molecular mechanisms regulating the differential association of kainate receptor subunits with SAP90/PSD-95 and SAP97. J. Biol. Chem. *276*, 16092-16099.

Miaczynska,M., Christoforidis,S., Giner,A., Shevchenko,A., Uttenweiler-Joseph,S., Habermann,B., Wilm,M., Parton,R.G., and Zerial,M. (2004). APPL proteins link Rab5 to nuclear signal transduction via an endosomal compartment. Cell *116*, 445-456.

Migaud,M., Charlesworth,P., Dempster,M., Webster,L.C., Watabe,A.M., Makhinson,M., He,Y., Ramsay,M.F., Morris,R.G., Morrison,J.H., O'Dell,T.J., and Grant,S.G. (1998). Enhanced long-term potentiation and impaired learning in mice with mutant postsynaptic density-95 protein. Nature *396*, 433-439.

Miller,J.R. (2002). The Wnts. Genome Biol. *3*, 3001-3015.

Miller,J.R., Hocking,A.M., Brown,J.D., and Moon,R.T. (1999). Mechanism and function of signal transduction by the Wnt/beta-catenin and Wnt/Ca2+ pathways. Oncogene *18*, 7860-7872.

Miller,M.W. (1995). Relationship of the time of origin and death of neurons in rat somatosensory cortex: barrel versus septal cortex and projection versus local circuit neurons. J. Comp Neurol. *355*, 6-14.

Mitrovic,N., Mohajeri,H., and Schachner,M. (1996). Effects of NMDA receptor blockade in the developing rat somatosensory cortex on the expression of the glia-derived extracellular matrix glycoprotein tenascin-C. Eur. J. Neurosci. *8*, 1793-1802.

Miyaoka,T., Seno,H., and Ishino,H. (1999). Increased expression of Wnt-1 in schizophrenic brains. Schizophr. Res. *38*, 1-6.

Mok,H., Shin,H., Kim,S., Lee,J.R., Yoon,J., and Kim,E. (2002). Association of the kinesin superfamily motor protein KIF1Balpha with postsynaptic density-95 (PSD-95), synapse-associated protein-97, and synaptic scaffolding molecule PSD-95/discs large/zona occludens-1 proteins. J. Neurosci. *22*, 5253-5258.

Molnár,Z., Adams,R., and Blakemore,C. (1998). Mechanisms underlying the early establishment of thalamocortical connections in the rat. J. Neurosci. *18*, 5723-5745.

Molnar,Z. and Hannan,A.J. (2000). Development of thalamocortical projections in normal and mutant mice. Results Probl. Cell Differ. *30:293-332.*, 293-332.

Moon,R.T., DeMarais,A., and Olson,D.J. (1993). Responses to Wnt signals in vertebrate embryos may involve changes in cell adhesion and cell movement. J. Cell Sci. Suppl. *17:183-8.*, 183-188.

Morris,R. (1984). Developments of a water-maze procedure for studying spatial learning in the rat. J. Neurosci. Methods *11*, 47-60.

Morris,R.G., Moser,E.I., Riedel,G., Martin,S.J., Sandin,J., Day,M., and O'Carroll,C. (2003). Elements of a neurobiological theory of the hippocampus: the role of activity-dependent synaptic plasticity in memory. Philos. Trans. R. Soc. Lond B Biol. Sci. *358*, 773-786.

Morrison,T.B., Weis,J.J., and Wittwer,C.T. (1998). Quantification of low-copy transcripts by continuous SYBR Green I monitoring during amplification. Biotechniques *24*, 954-8, 960, 962.

Mount,H.T., Dreyfus,C.F., and Black,I.B. (1994). Neurotrophin-3 selectively increases cultured Purkinje cell survival. Neuroreport *5*, 2497-2500.

Mouse Genome Informatics. Deltagen Data Submission to MGI via the NIH Knockout Project. NIH Knockout Project . 2006.
Ref Type: Electronic Citation

Moyner,H., Jonas,P., and Rossier,J. (1999). Molecular determinants controlling functional properties of AMPARs and NMDARs in the mammalian CNS. In Ionotropic Glutamate receptors in the CNS., P.Jonas and H.Moyner, eds. Springer), pp. 309-339.

Muller,B.M., Kistner,U., Kindler,S., Chung,W.J., Kuhlendahl,S., Fenster,S.D., Lau,L.F., Veh,R.W., Huganir,R.L., Gundelfinger,E.D., and Garner,C.C. (1996). SAP102, a novel postsynaptic protein that interacts with NMDA receptor complexes in vivo. Neuron *17*, 255-265.

Mulroy,T., McMahon,J.A., Burakoff,S.J., McMahon,A.P., and Sen,J. (2002). Wnt-1 and Wnt-4 regulate thymic cellularity. Eur. J. Immunol. *32*, 967-971.

Munoz,A., Liu,X.B., and Jones,E.G. (1999). Development of metabotropic glutamate receptors from trigeminal nuclei to barrel cortex in postnatal mouse. J. Comp Neurol. *409*, 549-566.

Murray,R.M., Sham,P., Van,O.J., Zanelli,J., Cannon,M., and McDonald,C. (2004). A developmental model for similarities and dissimilarities between schizophrenia and bipolar disorder. Schizophr. Res. *71*, 405-416.

Naisbitt,S., Kim,E., Tu,J.C., Xiao,B., Sala,C., Valtschanoff,J., Weinberg,R.J., Worley,P.F., and Sheng,M. (1999). Shank, a novel family of postsynaptic density proteins that binds to the NMDA receptor/PSD-95/GKAP complex and cortactin. Neuron *23*, 569-582.

Naisbitt,S., Valtschanoff,J., Allison,D.W., Sala,C., Kim,E., Craig,A.M., Weinberg,R.J., and Sheng,M. (2000). Interaction of the postsynaptic density-95/guanylate kinase domain-associated protein complex with a light chain of myosin-V and dynein. J. Neurosci. *20*, 4524-4534.

Nakamura,T. and Akiyama,T. (2005). Role of the Wnt signaling network in embryogenesis and tumorigenesis. Seikagaku. *77*, 5-19.

Nakayama,A.Y., Harms,M.B., and Luo,L. (2000). Small GTPases Rac and Rho in the maintenance of dendritic spines and branches in hippocampal pyramidal neurons. J. Neurosci. *20*, 5329-5338.

Nam,J.S., Turcotte,T.J., Smith,P.F., Choi,S., and Yoon,J.K. (2006). Mouse cristin/R-spondin family proteins are novel ligands for the Frizzled 8 and LRP6 receptors and activate beta-catenin-dependent gene expression. J. Biol. Chem. *281*, 13247-13257.

Navarro-Lerida,I., Martinez,M.M., Roncal,F., Gavilanes,F., Albar,J.P., and Rodriguez-Crespo,I. (2004). Proteomic identification of brain proteins that interact with dynein light chain LC8. Proteomics. *4*, 339-346.

Nehring,R.B., Wischmeyer,E., Doring,F., Veh,R.W., Sheng,M., and Karschin,A. (2000). Neuronal inwardly rectifying K(+) channels differentially couple to PDZ proteins of the PSD-95/SAP90 family. J. Neurosci. *20*, 156-162.

Nicol,X., Muzerelle,A., Bachy,I., Ravary,A., and Gaspar,P. (2005). Spatiotemporal localization of the calcium-stimulated adenylate cyclases, AC1 and AC8, during mouse brain development. J. Comp Neurol. *486*, 281-294.

Nicol,X., Muzerelle,A., Rio,J.P., Metin,C., and Gaspar,P. (2006). Requirement of adenylate cyclase 1 for the ephrin-A5-dependent retraction of exuberant retinal axons. J. Neurosci. *26*, 862-872.

Niethammer,M., Kim,E., and Sheng,M. (1996). Interaction between the C terminus of NMDA receptor subunits and multiple members of the PSD-95 family of membrane-associated guanylate kinases. J. Neurosci. *16*, 2157-2163.

Niethammer,M., Valtschanoff,J.G., Kapoor,T.M., Allison,D.W., Weinberg,T.M., Craig,A.M., and Sheng,M. (1998). CRIPT, a novel postsynaptic protein that binds to the third PDZ domain of PSD-95/SAP90. Neuron *20*, 693-707.

Nollet,F., Kools,P., and van,R.F. (2000). Phylogenetic analysis of the cadherin superfamily allows identification of six major subfamilies besides several solitary members. J. Mol. Biol. *299*, 551-572.

Nose,A., Nagafuchi,A., and Takeichi,M. (1988). Expressed recombinant cadherins mediate cell sorting in model systems. Cell *54*, 993-1001.

Nowak,L., Bregestovski,P., Ascher,P., Herbet,A., and Prochiantz,A. (1984). Magnesium gates glutamate-activated channels in mouse central neurones. Nature *307*, 462-465.

Nusse,R. (2005). Wnt signaling in disease and in development. Cell Res. *15*, 28-32.

O'Brien,T.F., Steindler,D.A., and Cooper,N.G. (1987). Abnormal glial and glycoconjugate dispositions in the somatosensory cortical barrel field of the early postnatal reeler mutant mouse. Brain Res. *429*, 309-317.

O'Leary,D.D. (1989). Do cortical areas emerge from a protocortex? Trends Neurosci. *12*, 400-406.

O'Leary,D.D., Schlaggar,B.L., and Tuttle,R. (1994). Specification of neocortical areas and thalamocortical connections. Annu. Rev. Neurosci. *17*, 419-439.

Oh,J.S., Manzerra,P., and Kennedy,M.B. (2004). Regulation of the neuron-specific Ras GTPase-activating protein, synGAP, by Ca2+/calmodulin-dependent protein kinase II. J. Biol. Chem. *279*, 17980-17988.

Okabe,T., Nakamura,T., Nishimura,Y.N., Kohu,K., Ohwada,S., Morishita,Y., and Akiyama,T. (2003). RICS, a novel GTPase-activating protein for Cdc42 and Rac1, is involved in the beta-catenin-N-cadherin and N-methyl-D-aspartate receptor signaling. J. Biol. Chem. *278*, 9920-9927.

Orrenius,S., Zhivotovsky,B., and Nicotera,P. (2003). Regulation of cell death: the calcium-apoptosis link. Nat. Rev. Mol. Cell Biol. *4*, 552-565.

Ossipow,V., Pellissier,F., Schaad,O., and Ballivet,M. (2004). Gene expression analysis of the critical period in the visual cortex. Mol. Cell Neurosci *27*, 70-83.

Osterheld-Haas,M.C., Van der,L.H., and Hornung,J.P. (1994). Monoaminergic afferents to cortex modulate structural plasticity in the barrelfield of the mouse. Brain Res. Dev. Brain Res. *77*, 189-202.

Ottersen,O.P. and Storm-Mathisen,J. (1984). Glutamate- and GABA-containing neurons in the mouse and rat brain, as demonstrated with a new immunocytochemical technique. J. Comp Neurol. *229*, 374-392.

Pak,D.T., Yang,S., Rudolph-Correia,S., Kim,E., and Sheng,M. (2001). Regulation of dendritic spine morphology by SPAR, a PSD-95-associated RapGAP. Neuron *31*, 289-303.

Papadakis,M., Hawkins,L.M., and Stephenson,F.A. (2004). Appropriate NR1-NR1 disulfide-linked homodimer formation is requisite for efficient expression of functional, cell surface N-methyl-D-aspartate NR1/NR2 receptors. J. Biol. Chem. *279*, 14703-14712.

Parnavelas,J.G. (2000). The origin and migration of cortical neurones: new vistas. Trends Neurosci *23*, 126-131.

Parr,B.A., Cornish,V.A., Cybulsky,M.I., and McMahon,A.P. (2001). Wnt7b regulates placental development in mice. Dev. Biol. *237*, 324-332.

Parr,B.A. and McMahon,A.P. (1998). Sexually dimorphic development of the mammalian reproductive tract requires Wnt-7a. Nature *395*, 707-710.

Parr,B.A., Shea,M.J., Vassileva,G., and McMahon,A.P. (1993). Mouse Wnt genes exhibit discrete domains of expression in the early embryonic CNS and limb buds. Development *119*, 247-261.

Peifer,M. and Polakis,P. (2000). Wnt signaling in oncogenesis and embryogenesis--a look outside the nucleus. Science. *287*, 1606-1609.

Penfield,W. and Boldrey,E. (1937). Somatic motor and sensory representation in the cerebral cortex of man as studues by electrical stimulation. Brain *60*, 389-443.

Penfield,W. and Rasmussen,T. (1950). A clinical study of localisation of function. In The Cerebreal Cortex of Man, (New York: Macmillan).

Petralia,R.S., Sans,N., Wang,Y.X., and Wenthold,R.J. (2005). Ontogeny of postsynaptic density proteins at glutamatergic synapses. Mol. Cell Neurosci. *29*, 436-452.

Pfaffl,M.W. (2001). A new mathematical model for relative quantification in real-time RT-PCR. Nucl. Acids Res. *29*, e45.

Philpot,B.D., Sekhar,A.K., Shouval,H.Z., and Bear,M.F. (2001a). Visual experience and deprivation bidirectionally modify the composition and function of NMDA receptors in visual cortex. Neuron *29*, 157-169.

Philpot,B.D., Weisberg,M.P., Ramos,M.S., Sawtell,N.B., Tang,Y.P., Tsien,J.Z., and Bear,M.F. (2001b). Effect of transgenic overexpression of NR2B on NMDA receptor function and synaptic plasticity in visual cortex. Neuropharmacology *41*, 762-770.

Pilpel,Y. and Segal,M. (2004). Activation of PKC induces rapid morphological plasticity in dendrites of hippocampal neurons via Rac and Rho-dependent mechanisms. Eur. J. Neurosci. *19*, 3151-3164.

Pinson,K.I., Brennan,J., Monkley,S., Avery,B.J., and Skarnes,W.C. (2000). An LDL-receptor-related protein mediates Wnt signalling in mice. Nature. *407*, 535-538.

Plump,A.S., Erskine,L., Sabatier,C., Brose,K., Epstein,C.J., Goodman,C.S., Mason,C.A., and Tessier-Lavigne,M. (2002). Slit1 and Slit2 cooperate to prevent premature midline crossing of retinal axons in the mouse visual system. Neuron *33*, 219-232.

Polleux,F. (2004). Generation of the cortical area map; emx2 strikes back. Neuron *43*, 295-297.

Porter,K., Komiyama,N.H., Vitalis,T., Kind,P.C., and Grant,S.G. (2005). Differential expression of two NMDA receptor interacting proteins, PSD-95 and SynGAP during mouse development. Eur. J. Neurosci. *21*, 351-362.

Prasad,S.S., Kojic,L.Z., Li,P., Mitchell,D.E., Hachisuka,A., Sawada,J., Gu,Q., and Cynader,M.S. (2002). Gene expression patterns during enhanced periods of visual cortex plasticity. Neuroscience *111*, 35-45.

Pratt,T., Vitalis,T., Warren,N., Edgar,J.M., Mason,J.O., and Price,D.J. (2000). A role for Pax6 in the normal development of dorsal thalamus and its cortical connections. Development *127*, 5167-5178.

Price, D. J and Willshaw, D. J. Mechanisms of cortical development. Early Development of the Telencephalon. Monographs of the Physiological Society 48, 9-48. 1-1-2000. Oxford;New York, Oxford University Press.
Ref Type: Generic

Quinlan,E.M., Olstein,D.H., and Bear,M.F. (1999). Bidirectional, experience-dependent regulation of N-methyl-D-aspartate receptor subunit composition in the rat visual cortex during postnatal development. Proc. Natl. Acad. Sci. U. S. A *96*, 12876-12880.

Rakic,L. and Lyubimov,N.N. (1988). Use of animal models in study of recovery functions after brain lesions. Scand. J. Rehabil. Med. Suppl *17*, 15-23.

Rang,H., Dale,M., and Ritter,J. (1997). Pharmacology. (Edinburgh: Churchill Livingstone).

Ranheim,E.A., Kwan,H.C., Reya,T., Wang,Y.K., Weissman,I.L., and Francke,U. (2005). Frizzled 9 knock-out mice have abnormal B-cell development. Blood *105*, 2487-2494.

Ravary,A., Muzerelle,A., Herve,D., Pascoli,V., Ba-Charvet,K.N., Girault,J.A., Welker,E., and Gaspar,P. (2003). Adenylate cyclase 1 as a key actor in the refinement of retinal projection maps. J. Neurosci. *23*, 2228-2238.

Rebsam,A., Seif,I., and Gaspar,P. (2002). Refinement of thalamocortical arbors and emergence of barrel domains in the primary somatosensory cortex: a study of normal and monoamine oxidase a knock-out mice. J. Neurosci. *22*, 8541-8552.

Rebsam,A., Seif,I., and Gaspar,P. (2005). Dissociating barrel development and lesion-induced plasticity in the mouse somatosensory cortex. J. Neurosci. *25*, 706-710.

Redmond,L. and Ghosh,A. (2001). The role of Notch and Rho GTPase signaling in the control of dendritic development. Curr. Opin. Neurobiol. *11*, 111-117.

Redmond,L., Oh,S.R., Hicks,C., Weinmaster,G., and Ghosh,A. (2000). Nuclear Notch1 signaling and the regulation of dendritic development. Nat. Neurosci. *3*, 30-40.

Reid,S.N., Romano,C., Hughes,T., and Daw,N.W. (1995). Immunohistochemical study of two phosphoinositide-linked metabotropic glutamate receptors (mGluR1 alpha and mGluR5) in the cat visual cortex before, during, and after the peak of the critical period for eye-specific connections. J. Comp Neurol. *355*, 470-477.

Reznikov,K.Y., Fulop,Z., and Hajos,F. (1984). Mosaicism of the ventricular layer as the developmental basis of neocortical columnar organization. A 3H-thymidine autoradiographic study in newborn mice. Anat. Embryol. (Berl) *170*, 99-105.

Rhoades,R.W., Chiaia,N.L., and Macdonald,G.J. (1990). Topographic organization of the peripheral projections of the trigeminal ganglion in the fetal rat. Somatosens. Mot. Res. *7*, 67-84.

Rhoades,R.W., Strang,V., nett-Clarke,C.A., Killackey,H.P., and Chiaia,N.L. (1997). Sensitive period for lesion-induced reorganization of intracortical projections within the vibrissae representation of rat's primary somatosensory cortex. J. Comp Neurol. *389*, 185-192.

Rice,F.L. and Van der Loos,H. (1977). Development of the barrels and barrel field in the somatosensory cortex of the mouse. J. Comp Neurol. *171*, 545-560.

Roelink,H. and Nusse,R. (1991). Expression of two members of the Wnt family during mouse development--restricted temporal and spatial patterns in the developing neural tube. Genes Dev. *5*, 381-388.

Roman-Roman,S., Shi,D.L., Stiot,V., Hay,E., Vayssiere,B., Garcia,T., Baron,R., and Rawadi,G. (2004). Murine Frizzled-1 behaves as an antagonist of the canonical Wnt/beta-catenin signaling. J. Biol. Chem. *279*, 5725-5733.

Romano,C., van den Pol,A.N., and O'Malley,K.L. (1996). Enhanced early developmental expression of the metabotropic glutamate receptor mGluR5 in rat brain: protein, mRNA splice variants, and regional distribution. J. Comp Neurol. *367*, 403-412.

Rosahl,T.W., Spillane,D., Missler,M., Herz,J., Selig,D.K., Wolff,J.R., Hammer,R.E., Malenka,R.C., and Sudhof,T.C. (1995). Essential functions of synapsins I and II in synaptic vesicle regulation. Nature *375*, 488-493.

Rosso,S.B., Sussman,D., Wynshaw-Boris,A., and Salinas,P.C. (2005). Wnt signaling through Dishevelled, Rac and JNK regulates dendritic development. Nat. Neurosci. *8*, 34-42.

Rothemund,Y., Schaefer,M., Grusser,S.M., and Flor,H. (2005). Localization of the human female breast in primary somatosensory cortex. Exp. Brain Res. *164*, 357-364.

Rubenstein,J.L., Anderson,S., Shi,L., Miyashita-Lin,E., Bulfone,A., and Hevner,R. (1999). Genetic control of cortical regionalization and connectivity. Cereb. Cortex *9*, 524-532.

Rubio,M.E., Curcio,C., Chauvet,N., and Bruses,J.L. (2005). Assembly of the N-cadherin complex during synapse formation involves uncoupling of p120-catenin and association with presenilin 1. Mol. Cell Neurosci *30*, 611-623.

Ruchhoeft,M.L., Ohnuma,S., McNeill,L., Holt,C.E., and Harris,W.A. (1999). The neuronal architecture of Xenopus retinal ganglion cells is sculpted by rho-family GTPases in vivo. J. Neurosci. *19*, 8454-8463.

Rudhard,Y., Kneussel,M., Nassar,M.A., Rast,G.F., Annala,A.J., Chen,P.E., Tigaret,C.M., Dean,I., Roes,J., Gibb,A.J., Hunt,S.P., and Schoepfer,R. (2003b). Absence of Whisker-related pattern formation in mice with NMDA receptors lacking coincidence detection properties and calcium signaling. J. Neurosci *23*, 2323-2332.

Rudhard,Y., Kneussel,M., Nassar,M.A., Rast,G.F., Annala,A.J., Chen,P.E., Tigaret,C.M., Dean,I., Roes,J., Gibb,A.J., Hunt,S.P., and Schoepfer,R. (2003a). Absence of Whisker-related pattern formation in mice with NMDA receptors lacking coincidence detection properties and calcium signaling. J. Neurosci. *23*, 2323-2332.

Russwurm,M., Wittau,N., and Koesling,D. (2001). Guanylyl cyclase/PSD-95 interaction: targeting of the nitric oxide-sensitive alpha2beta1 guanylyl cyclase to synaptic membranes. J. Biol. Chem. *276*, 44647-44652.

Rutter,A.R., Freeman,F.M., and Stephenson,F.A. (2002). Further characterization of the molecular interaction between PSD-95 and NMDA receptors: the effect of the NR1 splice variant and evidence for modulation of channel gating. J. Neurochem. *81*, 1298-1307.

Saito,H., Santoni,M.J., Arsanto,J.P., Jaulin-Bastard,F., Le,B.A., Marchetto,S., Audebert,S., Isnardon,D., Adelaide,J., Birnbaum,D., and Borg,J.P. (2001). Lano, a novel LAP protein directly connected to MAGUK proteins in epithelial cells. J. Biol. Chem. *276*, 32051-32055.

Sala,C., Futai,K., Yamamoto,K., Worley,P.F., Hayashi,Y., and Sheng,M. (2003). Inhibition of dendritic spine morphogenesis and synaptic transmission by activity-inducible protein Homer1a. J. Neurosci. *23*, 6327-6337.

Salinas,P.C. (2005). Retrograde signalling at the synapse: a role for Wnt proteins. Biochem. Soc. Trans. *33*, 1295-1298.

Salinas,P.C. and Price,S.R. (2005). Cadherins and catenins in synapse development. Curr. Opin. Neurobiol. *15*, 73-80.

Sanchez-Prieto,J., Budd,D.C., Herrero,I., Vazquez,E., and Nicholls,D.G. (1996). Presynaptic receptors and the control of glutamate exocytosis. Trends Neurosci. *19*, 235-239.

Saneyoshi,T., Kume,S., Amasaki,Y., and Mikoshiba,K. (2002). The Wnt/calcium pathway activates NF-AT and promotes ventral cell fate in Xenopus embryos. Nature *417*, 295-299.

Sans,N., Petralia,R.S., Wang,Y.X., Blahos,J., Hell,J.W., and Wenthold,R.J. (2000). A developmental change in NMDA receptor-associated proteins at hippocampal synapses. J. Neurosci. *20*, 1260-1271.

Sans,N., Prybylowski,K., Petralia,R.S., Chang,K., Wang,Y.X., Racca,C., Vicini,S., and Wenthold,R.J. (2003). NMDA receptor trafficking through an interaction between PDZ proteins and the exocyst complex. Nat. Cell Biol. *5*, 520-530.

Sanson, B. **At the edge of developmental biology: advances and mysteries about the *wnt* genes**. The annals of the MCFA I. 2000.
Ref Type: Electronic Citation

Satoh,K., Yanai,H., Senda,T., Kohu,K., Nakamura,T., Okumura,N., Matsumine,A., Kobayashi,S., Toyoshima,K., and Akiyama,T. (1997). DAP-1, a novel protein that interacts with the guanylate kinase-like domains of hDLG and PSD-95. Genes Cells *2*, 415-424.

Sauer,B. and Henderson,N. (1988). Site-specific DNA recombination in mammalian cells by the Cre recombinase of bacteriophage P1. Proc. Natl. Acad. Sci. U. S. A *85*, 5166-5170.

Savinainen,A., Garcia,E.P., Dorow,D., Marshall,J., and Liu,Y.F. (2001). Kainate receptor activation induces mixed lineage kinase-mediated cellular signaling cascades via post-synaptic density protein 95. J. Biol. Chem. *276*, 11382-11386.

Schanne,F.A., Kane,A.B., Young,E.E., and Farber,J.L. (1979). Calcium dependence of toxic cell death: a final common pathway. Science *206*, 700-702.

Schlaggar,B.L. and O'Leary,D.D. (1991). Potential of visual cortex to develop an array of functional units unique to somatosensory cortex. Science *252*, 1556-1560.

Schlitt,M., Lakeman,F.D., and Whitley,R.J. (1985). Psychosis and herpes simplex encephalitis. South. Med. J *78*, 1347-1350.

Schmidt,C. and Patel,K. (2005). Wnts and the neural crest. Anat. Embryol. (Berl). *209*, 349-355.

Schmitt,A.M., Shi,J., Wolf,A.M., Lu,C.C., King,L.A., and Zou,Y. (2006). Wnt-Ryk signalling mediates medial-lateral retinotectal topographic mapping. Nature. *439*, 31-37.

Schnell,E., Sizemore,M., Karimzadegan,S., Chen,L., Bredt,D.S., and Nicoll,R.A. (2002). Direct interactions between PSD-95 and stargazin control synaptic AMPA receptor number. Proc. Natl. Acad. Sci. U. S. A *99*, 13902-13907.

Schultze,W., Eulenburg,V., Lessmann,V., Herrmann,L., Dittmar,T., Gundelfinger,E.D., Heumann,R., and Erdmann,K.S. (2001). Semaphorin4F interacts with the synapse-associated protein SAP90/PSD-95. J. Neurochem. *78*, 482-489.

Scott,E.K. and Luo,L. (2001). How do dendrites take their shape? Nat. Neurosci. *4*, 359-365.

Seabold,G.K., Burette,A., Lim,I.A., Weinberg,R.J., and Hell,J.W. (2003). Interaction of the tyrosine kinase Pyk2 with the N-methyl-D-aspartate receptor complex via the Src homology 3 domains of PSD-95 and SAP102. J. Biol. Chem. *278*, 15040-15048.

Senft,S.L. and Woolsey,T.A. (1991). Growth of thalamic afferents into mouse barrel cortex. Cereb. Cortex *1*, 308-335.

Sestan,N., rtavanis-Tsakonas,S., and Rakic,P. (1999). Contact-dependent inhibition of cortical neurite growth mediated by notch signaling. Science. *286*, 741-746.

Seto,E.S. and Bellen,H.J. (2004). The ins and outs of Wingless signaling. Trends Cell Biol. *14*, 45-53.

Shapiro,L. and Colman,D.R. (1999). The diversity of cadherins and implications for a synaptic adhesive code in the CNS. Neuron *23*, 427-430.

Shapiro,L., Fannon,A.M., Kwong,P.D., Thompson,A., Lehmann,M.S., Grubel,G., Legrand,J.F., ls-Nielsen,J., Colman,D.R., and Hendrickson,W.A. (1995). Structural basis of cell-cell adhesion by cadherins. Nature *374*, 327-337.

Sharp,F.R., Gonzalez,M.F., Morgan,C.W., Morton,M.T., and Sharp,J.W. (1988). Common fur and mystacial vibrissae parallel sensory pathways: 14 C 2-deoxyglucose and WGA-HRP studies in the rat. J. Comp Neurol. *270*, 446-469.

Sheldahl,L.C., Park,M., Malbon,C.C., and Moon,R.T. (1999). Protein kinase C is differentially stimulated by Wnt and Frizzled homologs in a G-protein-dependent manner. Curr. Biol. *9*, 695-698.

Sheldahl,L.C., Slusarski,D.C., Pandur,P., Miller,J.R., Kuhl,M., and Moon,R.T. (2003). Dishevelled activates Ca2+ flux, PKC, and CamKII in vertebrate embryos. J. Cell Biol. *161*, 769-777.

Sheng,M. (2001). Molecular organization of the postsynaptic specialization. Proc. Natl. Acad. Sci. U. S. A *98*, 7058-7061.

Shi,J., Aamodt,S.M., and Constantine-Paton,M. (1997). Temporal correlations between functional and molecular changes in NMDA receptors and GABA neurotransmission in the superior colliculus. J. Neurosci. *17*, 6264-6276.

Shimamura,K. and Rubenstein,J.L. (1997). Inductive interactions direct early regionalization of the mouse forebrain. Development *124*, 2709-2718.

Shimogori,T. and Grove,E.A. (2005). Fibroblast growth factor 8 regulates neocortical guidance of area-specific thalamic innervation. J. Neurosci. *25*, 6550-6560.

Shimogori,T., VanSant,J., Paik,E., and Grove,E.A. (2004). Members of the Wnt, Fz, and Frp gene families expressed in postnatal mouse cerebral cortex. J. Comp Neurol. *473*, 496-510.

Sin,W.C., Haas,K., Ruthazer,E.S., and Cline,H.T. (2002). Dendrite growth increased by visual activity requires NMDA receptor and Rho GTPases. Nature *419*, 475-480.

Single,F.N., Rozov,A., Burnashev,N., Zimmermann,F., Hanley,D.F., Forrest,D., Curran,T., Jensen,V., Hvalby,O., Sprengel,R., and Seeburg,P.H. (2000). Dysfunctions in mice by NMDA receptor point mutations NR1(N598Q) and NR1(N598R). J. Neurosci. *20*, 2558-2566.

Snyder,E.M., Colledge,M., Crozier,R.A., Chen,W.S., Scott,J.D., and Bear,M.F. (2005). Role for A kinase-anchoring proteins (AKAPS) in glutamate receptor trafficking and long term synaptic depression. J. Biol. Chem. *280*, 16962-16968.

Spires,T.L., Molnar,Z., Kind,P.C., Cordery,P.M., Upton,A.L., Blakemore,C., and Hannan,A.J. (2005). Activity-dependent regulation of synapse and dendritic spine morphology in developing barrel cortex requires phospholipase C-beta1 signalling. Cereb. Cortex *15*, 385-393.

Spires,T.L., Molnar,Z., Kind,P.C., Cordery,P.M., Upton,A.L., Blakemore,C., and Hannan,A.J. (2004). Activity-dependent Regulation of Synapse and Dendritic Spine Morphology in Developing Barrel Cortex Requires Phospholipase C-{beta}1 Signalling. Cereb. Cortex ..

Stark,K., Vainio,S., Vassileva,G., and McMahon,A.P. (1994). Epithelial transformation of metanephric mesenchyme in the developing kidney regulated by Wnt-4. Nature *372*, 679-683.

Strutt,D. (2001). Planar polarity: getting ready to ROCK. Curr. Biol. *11*, R506-R509.

Strutt,D.I., Weber,U., and Mlodzik,M. (1997). The role of RhoA in tissue polarity and Frizzled signalling. Nature *387*, 292-295.

Stryer,L. (1995). Biochemistry. (New York: W.H. Freeman and Company).

Suzuki,T., Higgins,P.J., and Crawford,D.R. (2000). Control selection for RNA quantitation. Biotechniques *29*, 332-337.

Suzuki,T., Li,W., Zhang,J.P., Tian,Q.B., Sakagami,H., Usuda,N., Kondo,H., Fujii,T., and Endo,S. (2005). A novel scaffold protein, TANC, possibly a rat homolog of Drosophila rolling pebbles (rols), forms a multiprotein complex with various postsynaptic density proteins. Eur. J. Neurosci. *21*, 339-350.

Sweatt,J.D. (2001). The neuronal MAP kinase cascade: a biochemical signal integration system subserving synaptic plasticity and memory. J. Neurochem. *76*, 1-10.

Sweatt,J.D. (2004). Mitogen-activated protein kinases in synaptic plasticity and memory. Curr. Opin. Neurobiol. *14*, 311-317.

Tada,M. and Smith,J.C. (2000). Xwnt11 is a target of Xenopus Brachyury: regulation of gastrulation movements via Dishevelled, but not through the canonical Wnt pathway. Development *127*, 2227-2238.

Taha,S., Hanover,J.L., Silva,A.J., and Stryker,M.P. (2002). Autophosphorylation of alphaCaMKII is required for ocular dominance plasticity. Neuron *36*, 483-491.

Takada,R., Hijikata,H., Kondoh,H., and Takada,S. (2005). Analysis of combinatorial effects of Wnts and Frizzleds on beta-catenin/armadillo stabilization and Dishevelled phosphorylation. Genes Cells *10*, 919-928.

Takeuchi,M., Hata,Y., Hirao,K., Toyoda,A., Irie,M., and Takai,Y. (1997). SAPAPs. A family of PSD-95/SAP90-associated proteins localized at postsynaptic density. J. Biol. Chem. *272*, 11943-11951.

Talamillo,A., Quinn,J.C., Collinson,J.M., Caric,D., Price,D.J., West,J.D., and Hill,R.E. (2003). Pax6 regulates regional development and neuronal migration in the cerebral cortex. Dev. Biol. *255*, 151-163.

Tamai,K., Semenov,M., Kato,Y., Spokony,R., Liu,C., Katsuyama,Y., Hess,F., Saint-Jeannet,J.P., and He,X. (2000a). LDL-receptor-related proteins in Wnt signal transduction. Nature. *407*, 530-535.

Tamai,K., Semenov,M., Kato,Y., Spokony,R., Liu,C., Katsuyama,Y., Hess,F., Saint-Jeannet,J.P., and He,X. (2000b). LDL-receptor-related proteins in Wnt signal transduction. Nature *407*, 530-535.

Tamura,K., Shan,W.S., Hendrickson,W.A., Colman,D.R., and Shapiro,L. (1998). Structure-function analysis of cell adhesion by neural (N-) cadherin. Neuron *20*, 1153-1163.

Terada,Y., Tanaka,H., Okado,T., Shimamura,H., Inoshita,S., Kuwahara,M., and Sasaki,S. (2003). Expression and Function of the Developmental Gene Wnt-4 during Experimental Acute Renal Failure in Rats. J Am Soc Nephrol *14*, 1223-1233.

Tezuka,T., Umemori,H., Akiyama,T., Nakanishi,S., and Yamamoto,T. (1999). PSD-95 promotes Fyn-mediated tyrosine phosphorylation of the N-methyl-D-aspartate receptor subunit NR2A. Proc. Natl. Acad. Sci. U. S. A *%19;96*, 435-440.

Threadgill,R., Bobb,K., and Ghosh,A. (1997). Regulation of dendritic growth and remodeling by Rho, Rac, and Cdc42. Neuron. *19*, 625-634.

Tissir,F., Bar,I., Jossin,Y., De,B.O., and Goffinet,A.M. (2005). Protocadherin Celsr3 is crucial in axonal tract development. Nat. Neurosci. *8*, 451-457.

Tissir,F., De-Backer,O., Goffinet,A.M., and Lambert de,R.C. (2002). Developmental expression profiles of Celsr (Flamingo) genes in the mouse. Mech. Dev. *112*, 157-160.

Tissir,F. and Goffinet,A.M. (2006). Expression of planar cell polarity genes during development of the mouse CNS. Eur. J. Neurosci. *23*, 597-607.

Togashi,H., Abe,K., Mizoguchi,A., Takaoka,K., Chisaka,O., and Takeichi,M. (2002). Cadherin regulates dendritic spine morphogenesis. Neuron *35*, 77-89.

Tomoda,T., Kim,J.H., Zhan,C., and Hatten,M.E. (2004). Role of Unc51.1 and its binding partners in CNS axon outgrowth. Genes Dev. *18*, 541-558.

Topol,L., Jiang,X., Choi,H., Garrett-Beal,L., Carolan,P.J., and Yang,Y. (2003). Wnt-5a inhibits the canonical Wnt pathway by promoting GSK-3-independent beta-catenin degradation. J. Cell Biol. *162*, 899-908.

Torres,M.A., Yang-Snyder,J.A., Purcell,S.M., DeMarais,A.A., McGrew,L.L., and Moon,R.T. (1996). Activities of the Wnt-1 class of secreted signaling factors are antagonized by the Wnt-5A class and by a dominant negative cadherin in early Xenopus development. J. Cell Biol. *133*, 1123-1137.

Trachtenberg,J.T., Chen,B.E., Knott,G.W., Feng,G., Sanes,J.R., Welker,E., and Svoboda,K. (2002). Long-term in vivo imaging of experience-dependent synaptic plasticity in adult cortex. Nature *420*, 788-794.

Trump,B.F. and Berezesky,I.K. (1995). Calcium-mediated cell injury and cell death. FASEB J. *9*, 219-228.

Tsang,M., Lijam,N., Yang,Y., Beier,D.R., Wynshaw-Boris,A., and Sussman,D.J. (1996). Isolation and characterization of mouse dishevelled-3. Dev. Dyn. *207*, 253-262.

Tsien,J.Z., Huerta,P.T., and Tonegawa,S. (1996). The essential role of hippocampal CA1 NMDA receptor-dependent synaptic plasticity in spatial memory. Cell *87*, 1327-1338.

Tu,J.C., Xiao,B., Naisbitt,S., Yuan,J.P., Petralia,R.S., Brakeman,P., Doan,A., Aakalu,V.K., Lanahan,A.A., Sheng,M., and Worley,P.F. (1999). Coupling of mGluR/Homer and PSD-95 complexes by the Shank family of postsynaptic density proteins. Neuron *23*, 583-592.

Uchida,N., Honjo,Y., Johnson,K.R., Wheelock,M.J., and Takeichi,M. (1996). The catenin/cadherin adhesion system is localized in synaptic junctions bordering transmitter release zones. J. Cell Biol. *135*, 767-779.

Ule,J. and Darnell,R.B. (2006). RNA binding proteins and the regulation of neuronal synaptic plasticity. Curr. Opin. Neurobiol. *16*, 102-110.

Umbhauer,M., Djiane,A., Goisset,C., Penzo-Mendez,A., Riou,J.F., Boucaut,J.C., and Shi,D.L. (2000). The C-terminal cytoplasmic Lys-thr-X-X-X-Trp motif in frizzled receptors mediates Wnt/beta-catenin signalling. EMBO J. *19*, 4944-4954.

Upton, A. L, Katsnelson, A, Cordery, P. M., Ellender, T. J., Blakemore, C, Hannan, A. J., and Kind, P. C. Axonal segregation, cellular redistribution and dendritic growth are independently regulated during barrel formation in mouse primary somatosensory cortex. J.Neurosci. 2005. Ref Type: In Press

Upton, A. L, Katsnelson, A, Cordery, P. M., Ellender, T. J., Blakemore, C, Hannan, A. J., and Kind, P. C. Axonal segregation, cellular redistribution and dendritic growth are independently regulated during barrel formation in mouse primary somatosensory cortex. J.Neurosci. 2006. Ref Type: In Press

Usui,T., Shima,Y., Shimada,Y., Hirano,S., Burgess,R.W., Schwarz,T.L., Takeichi,M., and Uemura,T. (1999). Flamingo, a seven-pass transmembrane cadherin, regulates planar cell polarity under the control of Frizzled. Cell *98*, 585-595.

Valencia-Sanchez,M.A., Liu,J., Hannon,G.J., and Parker,R. (2006). Control of translation and mRNA degradation by miRNAs and siRNAs. Genes Dev. *20*, 515-524.

Van Aelst,L. and Cline,H.T. (2004). Rho GTPases and activity-dependent dendrite development. Curr. Opin. Neurobiol. *14*, 297-304.

Van der Loos H. and Woolsey,T.A. (1973). Somatosensory cortex: structural alterations following early injury to sense organs. Science *179*, 395-398.

Van der Loos,H. (1976). Neuronal circuitry and its development. Prog. Brain Res. *45*, 259-278.

Van der Loos,H. and Dörfl,J. (1978). Does the skin tell the somatosensory cortex how to construct a map of the periphery? Neurosci. Lett *7*, 23-30.

Van der Loos,H. and Woolsey,T.A. (1973a). Somatosensory cortex: structural alterations following early injury to sense organs. Science *179*, 395-398.

Van der Loos,H. and Woolsey,T.A. (1973b). Somatosensory cortex: structural alterations following early injury to sense organs. Science *179*, 395-398.

van Zundert,B., Yoshii,A., and Constantine-Paton,M. (2004). Receptor compartmentalization and trafficking at glutamate synapses: a developmental proposal. Trends Neurosci. *27*, 428-437.

Vanderhaeghen,P., Lu,Q., Prakash,N., Frisen,J., Walsh,C.A., Frostig,R.D., and Flanagan,J.G. (2000). A mapping label required for normal scale of body representation in the cortex. Nat. Neurosci *3*, 358-365.

Vanderklish,P.W. and Edelman,G.M. (2002). Dendritic spines elongate after stimulation of group 1 metabotropic glutamate receptors in cultured hippocampal neurons. Proc. Natl. Acad. Sci. U. S. A *99*, 1639-1644.

Veeman,M.T., Slusarski,D.C., Kaykas,A., Louie,S.H., and Moon,R.T. (2003). Zebrafish prickle, a modulator of noncanonical Wnt/Fz signaling, regulates gastrulation movements. Curr. Biol. *13*, 680-685.

Vitalis,T., Cases,O., Gillies,K., Hanoun,N., Hamon,M., Seif,I., Gaspar,P., Kind,P., and Price,D.J. (2002). Interactions between TrkB signaling and serotonin excess in the developing murine somatosensory cortex: a role in tangential and radial organization of thalamocortical axons. J. Neurosci. *22*, 4987-5000.

Wagner,U., Utton,M., Gallo,J.M., and Miller,C.C. (1996). Cellular phosphorylation of tau by GSK-3 beta influences tau binding to microtubules and microtubule organisation. J. Cell Sci. *109 (Pt 6)*, 1537-1543.

Walikonis,R.S., Jensen,O.N., Mann,M., Provance,D.W., Jr., Mercer,J.A., and Kennedy,M.B. (2000). Identification of proteins in the postsynaptic density fraction by mass spectrometry. J. Neurosci. *20*, 4069-4080.

Wallingford,J.B. and Habas,R. (2005). The developmental biology of Dishevelled: an enigmatic protein governing cell fate and cell polarity. Development *132*, 4421-4436.

Wallingford,J.B. and Harland,R.M. (2001). Xenopus Dishevelled signaling regulates both neural and mesodermal convergent extension: parallel forces elongating the body axis. Development *128*, 2581-2592.

Wallingford,J.B., Rowning,B.A., Vogeli,K.M., Rothbacher,U., Fraser,S.E., and Harland,R.M. (2000). Dishevelled controls cell polarity during Xenopus gastrulation. Nature *405*, 81-85.

Wang,Y., Huso,D., Cahill,H., Ryugo,D., and Nathans,J. (2001). Progressive cerebellar, auditory, and esophageal dysfunction caused by targeted disruption of the frizzled-4 gene. J. Neurosci. *21*, 4761-4771.

Wang,Y., Thekdi,N., Smallwood,P.M., Macke,J.P., and Nathans,J. (2002). Frizzled-3 is required for the development of major fiber tracts in the rostral CNS. J. Neurosci. *22*, 8563-8573.

Wang,Z., Shu,W., Lu,M.M., and Morrisey,E.E. (2005). Wnt7b activates canonical signaling in epithelial and vascular smooth muscle cells through interactions with Fzd1, Fzd10, and LRP5. Mol. Cell Biol. *25*, 5022-5030.

Warren,N., Caric,D., Pratt,T., Clausen,J.A., Asavaritikrai,P., Mason,J.O., Hill,R.E., and Price,D.J. (1999). The transcription factor, Pax6, is required for cell proliferation and differentiation in the developing cerebral cortex. Cereb. Cortex *9*, 627-635.

Warren,N. and Price,D.J. (1997). Roles of Pax-6 in murine diencephalic development. Development *124*, 1573-1582.

Wassarman,K.M., Lewandoski,M., Campbell,K., Joyner,A.L., Rubenstein,J.L., Martinez,S., and Martin,G.R. (1997). Specification of the anterior hindbrain and establishment of a normal mid/hindbrain organizer is dependent on Gbx2 gene function. Development *124*, 2923-2934.

Watanabe,M., Nakamura,M., Sato,K., Kano,M., Simon,M.I., and Inoue,Y. (1998). Patterns of expression for the mRNA corresponding to the four isoforms of phospholipase Cbeta in mouse brain. Eur. J. Neurosci *10*, 2016-2025.

Watson, R. F., Abdel-Majid, R. M., Barnett, M. W., Willis, B. S., Katsnelson, A. K., Gillingwater, T. G., McKnight, G. S, Kind, P. C, and Neumann, P. E. Involvement of Protein Kinase A in Patterning of the Mouse Somatosensory Cortex. J.Neurosci. 20-5-2006a.
Ref Type: In Press

Watson,R.F., bdel-Majid,R.M., Barnett,M.W., Willis,B.S., Katsnelson,A., Gillingwater,T.H., McKnight,G.S., Kind,P.C., and Neumann,P.E. (2006b). Involvement of protein kinase A in patterning of the mouse somatosensory cortex. J. Neurosci *26*, 5393-5401.

Watson, R. F., Konkel, J., Barnett, M. W., and Kind, P. C. The role of PKARIIβ in somatosensory cortex development. Soc.Neurosci.Abstr. 716.9. 2005.
Ref Type: Abstract

Wayman,G.A., Impey,S., Marks,D., Saneyoshi,T., Grant,W.F., Derkach,V., and Soderling,T.R. (2006). Activity-dependent dendritic arborization mediated by CaM-kinase I activation and enhanced CREB-dependent transcription of Wnt-2. Neuron *50*, 897-909.

Wehrli,M., Dougan,S.T., Caldwell,K., O'Keefe,L., Schwartz,S., Vaizel-Ohayon,D., Schejter,E., Tomlinson,A., and DiNardo,S. (2000). arrow encodes an LDL-receptor-related protein essential for Wingless signalling. Nature. *407*, 527-530.

Wei,J.Y., Roy,D.S., Leconte,L., and Barnstable,C.J. (1998). Molecular and pharmacological analysis of cyclic nucleotide-gated channel function in the central nervous system. Prog. Neurobiol. *56*, 37-64.

Weidinger,G. and Moon,R.T. (2003). When Wnts antagonize Wnts. J. Cell Biol. *162*, 753-755.

Welker,C. and Woolsey,T.A. (1974). Structure of layer IV in the somatosensory neocortex of the rat: description and comparison with the mouse. J. Comp Neurol. *158*, 437-453.

Welker,E., Armstrong-James,M., Bronchti,G., Ourednik,W., Gheorghita-Baechler,F., Dubois,R., Guernsey,D.L., Van der Loos,H., and Neumann,P.E. (1996). Altered sensory processing in the somatosensory cortex of the mouse mutant barrelless. Science *271*, 1864-1867.

Wenthold,R.J., Prybylowski,K., Standley,S., Sans,N., and Petralia,R.S. (2003). Trafficking of NMDA receptors. Annu. Rev. Pharmacol. Toxicol. *43*, 335-358.

Wharton,K.A., Jr. (2003). Runnin' with the Dvl: proteins that associate with Dsh/Dvl and their significance to Wnt signal transduction. Dev. Biol. *253*, 1-17.

Whitford,K.L., Dijkhuizen,P., Polleux,F., and Ghosh,A. (2002a). Molecular control of cortical dendrite development. Annu. Rev. Neurosci. *25*, 127-149.

Whitford,K.L., Marillat,V., Stein,E., Goodman,C.S., Tessier-Lavigne,M., Chedotal,A., and Ghosh,A. (2002b). Regulation of cortical dendrite development by Slit-Robo interactions. Neuron *33*, 47-61.

Wilson,D.A. and Racine,R.J. (1983). The postnatal development of post-activation potentiation in the rat neocortex. Brain Res. *283*, 271-276.

Wilson,S.I., Rydstrom,A., Trimborn,T., Willert,K., Nusse,R., Jessell,T.M., and Edlund,T. (2001). The status of Wnt signalling regulates neural and epidermal fates in the chick embryo. Nature *411*, 325-330.

Wilson,S.W. and Houart,C. (2004). Early steps in the development of the forebrain. Dev. Cell *6*, 167-181.

Wise,S.P. and Jones,E.G. (1978). Developmental studies of thalamocortical and commissural connections in the rat somatic sensory cortex. J. Comp Neurol. *178*, 187-208.

Wong,M.L. and Medrano,J.F. (2005). Real-time PCR for mRNA quantitation. Biotechniques *39*, 75-85.

Wong,R.O. and Ghosh,A. (2002). Activity-dependent regulation of dendritic growth and patterning. Nat. Rev. Neurosci. *3*, 803-812.

Woodgett,J.R. (2001). Judging a protein by more than its name: GSK-3. Sci. STKE. *2001*, RE12.

Woolsey,T.A., Dierker,M.L., and Wann,D.F. (1975). Mouse SmI cortex: qualitative and quantitative classification of golgi-impregnated barrel neurons. Proc. Natl. Acad. Sci. U. S. A *72*, 2165-2169.

Woolsey,T.A. and Van der Loos,H. (1970). The structural organization of layer IV in the somatosensory region (SI) of mouse cerebral cortex. The description of a cortical field composed of discrete cytoarchitectonic units. Brain Res. *17*, 205-242.

Woolsey,T.A. and Wann,J.R. (1976). Areal changes in mouse cortical barrels following vibrissal damage at different postnatal ages. J. Comp Neurol. *170*, 53-66.

Wyszynski,M., Lin,J., Rao,A., Nigh,E., Beggs,A.H., Craig,A.M., and Sheng,M. (1997). Competitive binding of alpha-actinin and calmodulin to the NMDA receptor. Nature *385*, 439-442.

Xia,Z., Dudek,H., Miranti,C.K., and Greenberg,M.E. (1996). Calcium influx via the NMDA receptor induces immediate early gene transcription by a MAP kinase/ERK-dependent mechanism. J. Neurosci. *16*, 5425-5436.

Xia,Z., Gray,J.A., Compton-Toth,B.A., and Roth,B.L. (2003). A direct interaction of PSD-95 with 5-HT2A serotonin receptors regulates receptor trafficking and signal transduction. J. Biol. Chem. *278*, 21901-21908.

Xia,Z. and Storm,D.R. (2005). The role of calmodulin as a signal integrator for synaptic plasticity. Nat. Rev Neurosci. *6*, 267-276.

Yamakado,M. (1985). [Postnatal development of barreloid neuropils in the ventrobasal complex of mouse thalamus: a histochemical study for cytochrome oxidase]. No To Shinkei *37*, 497-506.

Yanai,H., Satoh,K., Matsumine,A., and Akiyama,T. (2000). The colorectal tumour suppressor APC is present in the NMDA-receptor-PSD-95 complex in the brain. Genes Cells *5*, 815-822.

Yang,Y., Fischer,Q.S., Zhang,Y., Baumgartel,K., Mansuy,I.M., and Daw,N.W. (2005). Reversible blockade of experience-dependent plasticity by calcineurin in mouse visual cortex. Nat. Neurosci. *8*, 791-796.

Yao,I., Hata,Y., Ide,N., Hirao,K., Deguchi,M., Nishioka,H., Mizoguchi,A., and Takai,Y. (1999). MAGUIN, a novel neuronal membrane-associated guanylate kinase-interacting protein. J. Biol. Chem. *274*, 11889-11896.

Ying,Z., Bingaman,W., and Najm,I.M. (2004). Increased numbers of coassembled PSD-95 to NMDA-receptor subunits NR2B and NR1 in human epileptic cortical dysplasia. Epilepsia *45*, 314-321.

Yoshii,A., Sheng,M.H., and Constantine-Paton,M. (2003). Eye opening induces a rapid dendritic localization of PSD-95 in central visual neurons. Proc. Natl. Acad. Sci. U. S. A *100*, 1334-1339.

Yoshikawa,S., McKinnon,R.D., Kokel,M., and Thomas,J.B. (2003). Wnt-mediated axon guidance via the Drosophila Derailed receptor. Nature *422*, 583-588.

Yu,X. and Malenka,R.C. (2003). Beta-catenin is critical for dendritic morphogenesis. Nat. Neurosci. *6*, 1169-1177.

Yu,X. and Malenka,R.C. (2004). Multiple functions for the cadherin/catenin complex during neuronal development. Neuropharmacology *47*, 779-786.

Zakin,L.D., Mazan,S., Maury,M., Martin,N., Guenet,J.L., and Brulet,P. (1998). Structure and expression of Wnt13, a novel mouse Wnt2 related gene. Mech. Dev. *73*, 107-116.

Zhang,S., Ehlers,M.D., Bernhardt,J.P., Su,C.T., and Huganir,R.L. (1998). Calmodulin mediates calcium-dependent inactivation of N-methyl-D-aspartate receptors. Neuron *21*, 443-453.

Zhang,W., Vazquez,L., Apperson,M., and Kennedy,M.B. (1999). Citron binds to PSD-95 at glutamatergic synapses on inhibitory neurons in the hippocampus. J. Neurosci. *19*, 96-108.

Zhao,C., Aviles,C., Abel,R.A., Almli,C.R., McQuillen,P., and Pleasure,S.J. (2005). Hippocampal and visuospatial learning defects in mice with a deletion of frizzled 9, a gene in the Williams syndrome deletion interval. Development *132*, 2917-2927.